National University of Science and Technology
POLITEHNICA Bucharest

Faculty of Industrial Engineering and Robotics

Journal of Industrial Engineering and Robotics

2025, Volume 9, Issue 3

AUTOMATIC CNC SYSTEM FOR METAL INSERTS IN 3D PRINTED PARTS

HANGA Mihail, DRĂGUȚU Matei, NAȘU Teodor-Cristian, CAZACU Carmen-Cristiana (Conducător științific)

Faculty of Industrial Engineering and Robotics, Specialization: Applied Computer Science in Industrial Engineering, Year: IV, e-mail: mihailhanga@gmail.com

ABSTRACT: This paper presents the development of an automated routing system designed for embedding metal threaded inserts into 3D-printed parts. The system is composed of two primary modules: a motion base that accurately positions the end-effector at insertion locations, and an insertion unit that automates both the loading and embedding of the inserts. The mechanical design utilizes an H-belt drive mechanism powered by two MOONS MS17HD2P4100 stepper motors. These motors are configured to drive a single belt in synchronization, enabling smooth and precise bidirectional movement along the X and Y axes. By eliminating the need for linear rods or leadscrews, the system achieves a more compact, rigid, and maintenance-friendly structure. The stepper motors, widely used in 3D printing, were selected for their proven reliability and step accuracy.

KEY WORDS: CAD, CNC, 3D Print.

1. Introduction

The automation of processes in additive manufacturing has led to the development of complementary systems that can extend the functionalities of 3D printers beyond the simple deposit of the material [1]. In particular, the need to improve the mechanical characteristics of the products obtained has led to the emergence of solutions dedicated to the insertion of metal components, such as threaded inserts [7]. In the absence of such systems, the integration of these elements remains a manual process, susceptible to positioning errors or damage to the parts. The present project proposes an integrated approach, in which the principles of precision mechanics are combined with digital control to achieve an automated system capable of accurately inserting threaded inserts [7] into 3D printed objects. By using components taken from the area of CNC systems [6] and adapted for desktop applications, the solution aims to provide a balance between reliability, cost and ease of use. Thus, the way is opened to the standardization of post-processing processes in 3D printing, with direct applicability in prototyping, mechatronics and small series production.

2. State of the art

Conventional systems for inserting threaded inserts [7] into 3D printed parts have significant limitations that affect both process quality and productivity. Manual or semi-automatic insertion, carried out with screwdrivers or improvised heaters, introduces positioning errors due to the lack of a precise guidance system and the dependence on the operator's skills. These inaccuracies are manifested by unwanted inclinations of the inserts [7] or lateral displacements, resulting in uncentered threads that compromise the functionality of the assembly and cause thermal deformations of the material, especially in sensitive polymers such as PLA [1].

Another major problem is the lack of repeatability, with manual processes unable to guarantee consistency between parts, even within the same production batch. For example, the insertion depth can vary by ±1 mm, which requires frequent recalibration and reduces the reliability of the final product. Operational inefficiency is another significant disadvantage, with processing times reaching up to 5-10 minutes per part due to the manual insertion stage, which creates an obvious economical bottleneck in small or medium series production. The proposed system addresses these deficiencies through an integrated architecture that combines precision mechanics with digital control and CAD interoperability. While conventional systems offer an accuracy of only ±2 mm, the presented solution achieves a precision of ±0.05 mm thanks to the implementation of micro-stepping and advanced kinematic corrections. Repeatability is ensured through algorithmically calculated trajectories, eliminating part-to-part variations and guaranteeing 100% consistency, while processing time is reduced to under 1 minute per piece by using parallel movement along the XY axes and automatic insertion.

The system also integrates active force control mechanisms, such as springs and cams, which protect the part from cracking or deformation. A distinctive advantage is the direct integration with CAD platforms, allowing the use of coordinates extracted from Onshape[2], thus eliminating human errors associated with traditional methods based on physical markings or trial-and-error approaches. These improvements make the proposed solution a superior alternative in terms of accuracy, reliability, and economic efficiency.

3. Development of the current system

3.1 Design

During the system design phase, the essential components for supporting and operating the printer were created. Two frames [Fig. 1] were designed, covering an operating area of 260×300 mm, sized to ensure precise and stable movement during operation. These frames constitute the base on which the drive system and the work platform are mounted. In addition, dedicated supports were created for the two motors, with the role of fixing and correctly aligning the motors in the system, so as to allow efficient transmission of movement to the moving elements.

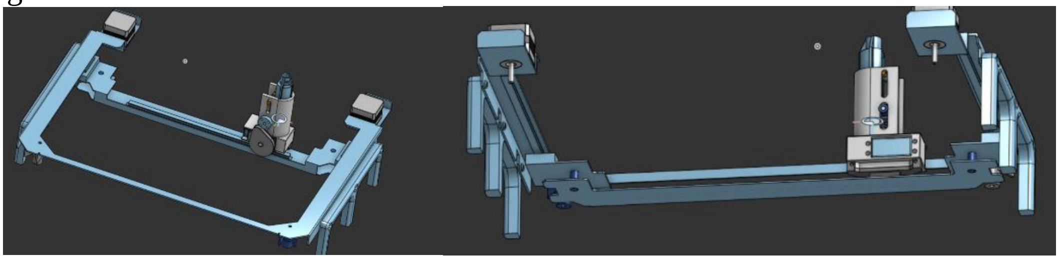

a) b)

Fig. 1 Frame design

The mechanical system is built on an H-type structure, where two stepper motors control a closed belt that allows the movement of a mobile subassembly at any point on the XY plane, corresponding to the location of the insertion of the metal elements. The subassembly responsible for the actual insertion of the insert is made up of a cam mechanism [Fig. 2], above which the effector that supports the insert is mounted. When activated by the servo motor at the base, a vertical rod is pushed upwards, guided by two lateral axes that allow exclusively translational movement, thus ensuring the stability of the assembly [Fig. 3]. A spring with a damping role is mounted on the rod, which takes over part of the insertion force and prevents damage to the printed part. The effector is supported by a linear guide system fixed to the walls of the internal structure, thus maintaining precise alignment during the insertion process. The operation of the assembly is started to balance the applied force and the positioning accuracy, avoiding deformation or cracking of the final product.

The design of the mechanical components of the system was carried out using the Onshape [2] CAD platform, which allowed the individual modeling of each part and their integration into a coherent assembly. The use of the Onshape [2] parametric environment facilitated the rapid adjustment of the geometry of the parts according to the functional and spatial requirements of the entire system.

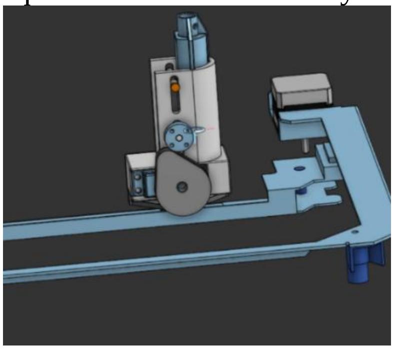

Fig. 2 - Cam Mechanism Driving the Insertion Process

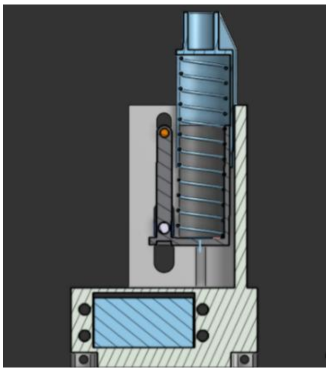

Fig. 3 - Guided Translational Rod with Spring Damping System

3.2 Programming

The code implements a control system for a two-dimensional (XY) motion mechanism based on two MOONS MS17HD2P4100 stepper motors, designed to operate on a Raspberry Pi [4] platform [3]. The system uses a modular approach, separating the motor control logic (Motor and Motor_threaded classes) from the kinematics management (MotionController and MotionController_angled classes). The main functionality consists of converting high-level motion commands – either discrete directions or arbitrary angles – into synchronized step signals for the two motors, considering the configured micro-steps and the corrections required due to the geometry of the physical system [5]. The MotionController_angled class solves the inverse kinematics of the mechanism by vectorizing the motion into individual components for each motor, applying an empirical correction factor to compensate for mechanical non-idealities. Thread support allows concurrent execution of motor movements, optimizing travel time. The additional Onshape [2] integration module provides precise spatial localization capabilities by referencing CAD points, facilitating automated positioning applications. The implementation demonstrates a robust approach for position control in mechatronic systems with distributed actuation.

3.3. Data Retrieval and Processing from Onshape

The code uses the OnshapeConnector class to extract the coordinates of mate connectors from a cloud-based CAD model. It accesses the Onshape [2] API via HTTP requests, obtaining the geometric transformations of each point. [Fig. 4]

```
def fetch_mate_coords(self, round_coordinates=False):
    url = f"/api/assemblies/d/{self._did}/w/{self._wid}/e/{self._eid}"
    params = {"includeMateConnectors": "true"}
    response = self.client.api_client.request("GET", self._onshape_base_url + url,
paradatparajson.loads(response.data)
```

Fig. 4. API-Based Extraction of Geometric Transformations in Onshape

The data is converted from meters to millimeters (pos_m*1000.0) and stored in a dictionary in the form {"connector_name": [x, y, z]}.

3.4. Calculating Relative Positions

To determine the relative distances between connectors, the code applies inverse matrix transformations. If a reference connector has coordinates ref_mm, the position of any other connector is calculated through 2 logical sequences:

- Constructing the inverse transformation matrix [Fig. 5]
- Applying the inverse transformation [Fig.6]

```
T_ref = np.eye(4); T_ref[:3,3] = ref_m / 1000.0  # Conversie în
T_ref_inv = self._invert_transform(T_ref)  # Inversare matriceală
```

Fig. 5. Constructing the inverse transformation matrix

```
p_rel_m = T_ref_inv.dot(np.hstack([p_m, 1.0]))[:3]  # [dx, dy, dz] în
rel_mm = p_rel_m * 1000.0  # Conversie în mm
```

Fig. 6. Applying the inverse transformation

This approach ensures submillimetre accuracy (np.round(rel_mm, 2)), essential for precise positioning applications.

3.5. Controlling the XY Mechanism with Stepper Motors

The MotionController_angled class converts angles and distances into commands for the two motors, using kinematic equations derived from the geometry of the belts:

Table 1: Kinematic equations

Equation	**Implementation**
X-Displacement: *s_left + s_right*	*dx = math.cos(rad) * mm*
Y-Displacement: *s_right - s_left*	*dy = math.sin(rad) * mm*
Left motor steps: *(dx - dy)/2*	*s_left_mm = (dx - dy) / 2.0*
Right motor steps: *(dx + dy)/2*	*s_right_mm = (dx + dy) / 2.0*

An empirical correction factor (mm *= 2.03) compensates for mechanical errors such as belt slippage. The motors are configured for micro-stepping, increasing resolution [Fig. 7]:

```
motor_dr.set_mode('1/16')  # 3200 de micropași/rotație (200 pași × 16)
motor_dr.set_speed_factor(500)  # Ajustare viteză
```

Fig. 7 Motor Setup with Micro-Stepping for Increased Precision

Accuracy is determined by:
- Pulley diameter (RADIUS = 5.73 mm in Motor_threaded).
- Step displacement calculation formula

$$mm/step = \frac{2 \times \pi \times RADIUS}{SPR \times microstep\_factor} \tag{1}$$

3.6. Parallel Execution with Threading

Motor movements are run concurrently to reduce overall time, but also to ensure that movements can be performed as required. This optimization allows for diagonal movements without delays between axes. [Fig. 8]

```
t_left = self.left.rotate(steps_left, dir_left, asynchronous=True)  # Thread separat
t_right = self.right.rotate(steps_right, dir_right, asynchronous=True)
t_left.join(); t_right.join()  # Așteptare finalizare
```

Fig. 8. Concurrent Motor Movements for Optimized Multi-Axis Control

4. Innovations

1. XY Positioning System with Optimized Kinematics [8]
    a. Uses matrix equations to convert CAD coordinates into motor commands:

$$\begin{cases} \Delta X = S_{right} + S_{left} \\ \Delta Y = S_{right} - S_{left} \end{cases} \quad (2)$$

    b. Empirical correction factor (mm × 2.03) compensates for belt stretch
2. Insertion mechanism with passive feedback
    a. Damping spring ensures constant force, regardless of material density.
    b. Linear guides eliminate tilting.
3. Digital Flow from CAD to Production

Extracts coordinate from mate connectors and converts them into movement commands:

```
relative_pos = onshape.relative_distance_from_ref("PunctReferință")
```

Fig. 9. Conversion of Mate Connector Coordinates into Movement Commands

5. System versatility

In addition to the insertion of threaded components, the system can be quickly adapted for other machining operations, thanks to its modular architecture and high precision [1]. By replacing the end effector with a dedicated tool (e.g. chisel for engraving, drill for drilling), the XY platform can perform:

- Detailed engraving on flat surfaces (e.g. texts, QR codes), with resolution below 0.1 mm thanks to micro-steps.
- Precise drilling for mounting holes or ventilation channels, avoiding material cracking by controlling speed and depth.
- Rotary blade cutting for trimming or finishing the edges of printed parts.

6. Future plans

To extend the applicability of the system to parts with heights, an automatic height adjustment mechanism for the effector will be developed. This will include:

- Distance sensors (e.g. laser or ultrasonic) for detecting the height of the part.
- Z-axis motorization with trapezoidal screw, synchronized with the XY system [8], for fine adjustment of the insertion position.
- Calibration software to correlate the height with the applied pressure, avoiding material overload.

Benefits:

- Dynamic adaptation to complex geometries (e.g. parts with inclined surfaces).
- Compatibility with materials of different stiffness (from flexible PLA to rigid ABS).
- Reduced setup time by eliminating manual adjustments.

This improvement will transform the system into a complete multifunctional platform, capable of automating not only the insertion, but also the finishing or assembly of 3D printed parts.

7. Conclusion

The presented system represents [Fig.10] a significant advance in the automation of post-processing of 3D printed parts, offering an accurate, fast and cost-effective alternative to existing manual or semi-automatic methods. By integrating an XY positioning mechanism [8] with advanced kinematic control, an adaptive vertical insertion system and direct connectivity with CAD platforms, this solution addresses the most common problems of current processes: imprecision, lack of repeatability, risk of part damage and operational inefficiency.

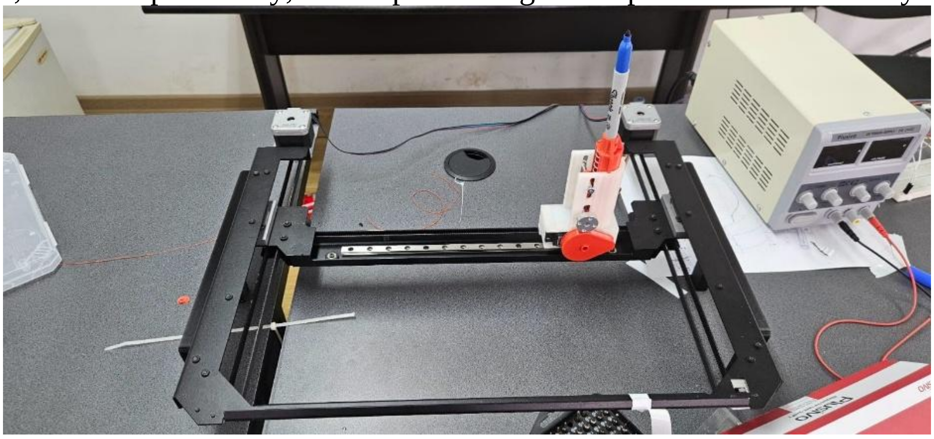

Fig. 10. The presented system with a pen as a proof of concept

Future improvements, such as automatic height adjustment and real-time monitoring of insertion force, will strengthen the position of this system as an indispensable multifunctional platform in both rapid prototyping and small series production.

In conclusion, this approach not only solves the shortcomings of conventional systems but also opens new possibilities in standardizing and optimizing post-processing processes in additive manufacturing, making precision technologies available at affordable costs. Therefore, it represents an important step towards a new generation of fully automated and interoperable digital manufacturing workshops.

8. Bibliography

[1]. Gibson, I., Rosen, D., Stucker, B., Khorasani, M. (2021), *Additive Manufacturing Technologies: 3D Printing, Rapid Prototyping, and Direct Digital Manufacturing* (ediția a 3-a), Springer, eBook ISBN 978-3-030-56127-7.
[2] PTC (Onshape), "Onshape Product Development Platform," onshape.com, 2025. [Online]. Available: https://www.onshape.com.
[3] MOONS Industries, *MS17HD2P4100 NEMA 17 Stepper Motor*, Moons Industries Website, 2025. [Online]. Available: https://www.moonsindustries.com/p/nema-17-standard-hybrid-stepper-motors/ms17hd2p4100-000004611110008899
[4] Raspberry Pi Foundation, "Raspberry Pi (single-board computer)," raspberrypi.com, 2025. [Online]. Available: https://www.raspberrypi.com
[5] C. Chang and T. Tran, *Mastering Precision: Understanding Microstepping in Motion Control*, *Analog Dialogue*, vol. 59, Mar. 2025. [Online]. Available:

https://www.analog.com/en/resources/analog-dialogue/articles/mastering-precision-understanding-microstepping.html
[6] X. Peng, L. Kong, J. Y. H. Fuh, and H. Wang, *A Review of Post-Processing Technologies in Additive Manufacturing*, *Journal of Manufacturing and Materials Processing*, vol. 5, no. 2, 2021. [Online]. Available: https://www.mdpi.com/2504-4494/5/2/38
[7] C. M. A. Silva *et al.*, *A New Methodology to Fabricate Polymer–Metal Parts Through Hybrid Fused Filament Fabrication*, *Sustainability*, vol. 17, no. 10, 2025. [Online]. Available: https://www.mdpi.com/2071-1050/17/10/4254
[8] Physik Instrumente (PI) L.P., *XY Stages – Motorized 2-Axis Positioning Tables*, PI USA, 2025. [Online]. Available: https://www.pi-usa.us/en/products/precision-motorized-linear-stages/integrated-xy-precision-motorized-stages-planar-xy-stages

DIGITAL SYSTEM FOR ENVIRONMENTAL CONTROL IN INDUSTRIAL AND AGRICULTURAL SECTORS

BĂLAN Silvian Ștefan, MINCU Eduard Mihai, ROTARIU Ștefan Lucian,CAZACU Carmen-Cristiana(Conducător științific)

Faculty: Industrial Engineering and Robotics, Specialization: Digital Manufacturing Systems, Year: I, e-mail: stefantytan19@gmail.com

ABSTRACT: This project presents a scalable and cost-effective IoT-based solution for environmental control, demonstrated through a smart automated flowerpot. Designed using an ESP32 microcontroller, humidity and temperature sensors, and a transistor-controlled water pump, the system monitors environmental conditions and autonomously irrigates plants as needed. Integrated with the Home Assistant platform via ESPHome, it enables remote monitoring, automation, and data logging within a smart ecosystem.
Though initially developed as a household prototype, this proof of concept serves as a foundational model for broader applications in industrial and agricultural settings. It illustrates the feasibility of using modular, low-cost technologies to implement precision irrigation and environmental monitoring at scale. By bridging smart home automation with modern agricultural practices, the project contributes to sustainability, resource optimization, and the advancement of digital environmental control systems.

Keywords: Home Assistant, monitoring, agriculture.

1.Introduction

The growing integration of technology into our everyday lives highlights the increasing relevance of automating routine tasks, particularly in plant care. This is especially true in urban settings where time constraints and environmental factors can make traditional gardening challenging. This endeavour introduces a proof of concept: a clever flowerpot. This self-contained system leverages internet connectivity to keep tabs on environmental conditions and automatically water a plant as needed.

Employing a small but powerful microcontroller, sensors for soil moisture and air conditions, and a water pump activated by an electronic switch, this device ensures plants receive optimal care with minimal human involvement. Its seamless connection with the Home Assistant platform, facilitated by specialized software, enables not only real-time observation but also remote automation and control through an intuitive interface. While this smart flowerpot is a small-scale example, it acts as a foundation that demonstrates the core ideas behind a larger vision. The same approach of using connected devices for monitoring and automation can be expanded to bigger applications, such as greenhouses, indoor vertical farms, and intelligent watering systems. This illustrates how affordable, adaptable technologies can significantly change precision agriculture and environmental management in industrial settings.

By starting with a practical and easily constructed device, this project sets the stage for more advanced and widespread environmental control systems, blending affordability, flexibility, and technological ingenuity.

2.State of the art

The increasing need for sustainable agriculture and intelligent environmental management has spurred the rapid advancement of connected, automated solutions for monitoring and control. Traditional plant care, whether at home or on a farm, often grapples with issues like inconsistent watering, delayed responses to plant needs, and inefficient use of resources. In cities, limited time and space can make it hard for individuals to maintain healthy plants. Meanwhile, in large-scale agriculture, the complexity of overseeing vast operations frequently leads to either over- or under-utilization of water and other vital inputs.

Sophisticated commercial watering systems do exist, often relying on central control units, weather-based scheduling, or satellite imagery. However, these solutions are typically expensive, require specialized installation, and are not easily adjusted for smaller growers or individual users. Furthermore, many older systems lack the ability to connect with modern internet-based ecosystems, limiting their ability to grow and work with other smart devices. Recent advancements in smart agriculture research and development have focused on distributed networks of sensors, local data processing, and automation platforms like Home Assistant. These enable systems that are modular, customizable, and can be controlled remotely. The use of open-source software like ESPHome, along with affordable microcontrollers such as the ESP32, has made advanced environmental control technologies more accessible to a wider range of users.

This project aligns with this trend by presenting a cost-effective, straightforward solution that combines environmental sensing and automated watering into a unified system. Its significance extends beyond just household plant care; it has the potential to be adapted and scaled for precision agriculture, greenhouse automation, and even environmentally conscious urban infrastructure. By serving as a working model, the smart flowerpot bridges the gap between individual experimentation and industrial application, showcasing how modern connected technologies can contribute to efficient and sustainable environmental management.

3. Components used in Proof of Concept

-Plusivo development board with ESP32 and BLE
-Soil moisture sensor (analog)
-DHT22 temperature and humidity sensor
-Mini submersible water pump (3-6V)
-S8050 NPN transistor
-2kΩ resistor
-Connection wires

4. Component selection criteria

Each component chosen in this project was strategically selected based on functionality, compatibility and efficiency:

-ESP32 (Plusivo board): It is a powerful microcontroller with Wi-Fi and Bluetooth connectivity, ideal for IoT applications. It has multiple digital and analog inputs/outputs, supports Over-The-Air updates and integrates perfectly with Home Assistant via ESPHome.

-Soil moisture sensor (analog): Allows precise monitoring of soil moisture. Analog sensors offer more granularity than digital ones, making them ideal for automation based on dynamic thresholds.

-DHT22 sensor: Measures air temperature and humidity with high precision. It is natively supported by ESPHome, which makes it easy to integrate and read values.

-Mini submersible water pump (3–6V): Compact, quiet and efficient, this pump is enough to irrigate one plant or a small group of plants. The low operating voltage makes it safe for domestic applications.

-S8050 NPN transistor and 2kΩ resistor: Use to create an electronic switch that allows the ESP32 to control the pump, without overloading the microcontroller output.

-Wire, power supply and breadboard: Essential auxiliary elements for making connections and correctly powering the components.

This combination of components provides an optimal balance between cost, performance and ease of use, making it ideal for both educational prototypes and real functional applications.

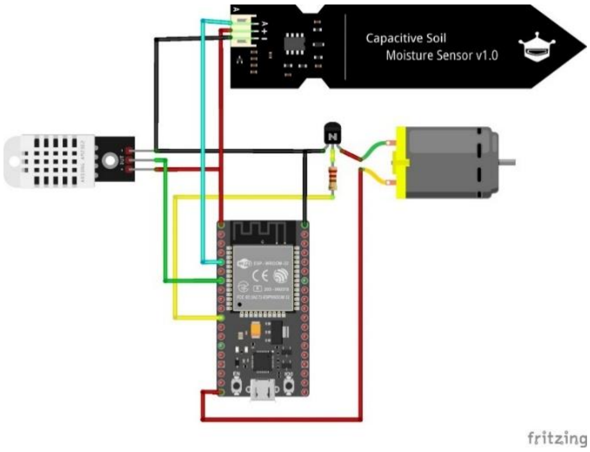

Fig.1 Electrical Diagram

5. Functional Description

The project works on the principle of automatic detection of soil moisture. When it drops below a certain threshold, a pump is activated to water the plant. In addition, the DHT22 sensor collects data on air temperature and humidity, providing a complete picture of the microclimate. All this information can be stored or displayed through a web interface developed using the Wi-Fi connectivity of the ESP32 module. This architecture allows remote control and monitoring of the plant's condition.

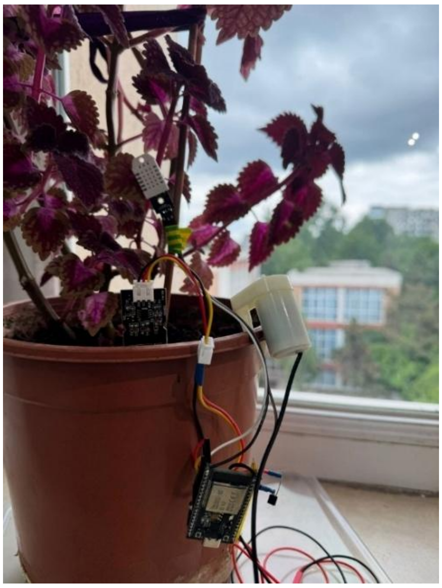

Fig. 2. The applied system

6. IoT and Home Assistant Integration

To achieve complete automation and remote control, the project was integrated into an IoT ecosystem through the Home Assistant platform. The ESPHome addon was used, which allows programming and controlling the ESP32 microcontroller directly from the Home Assistant interface. Automations are performed using the "Automations and Scenes" section of Home Assistant, where the operating logic can be set. For example: if the soil humidity drops below 50%, the pump starts automatically for 5 seconds; continuous humidity check until it reaches a minimum of 70%; notification sent to the user's phone if the Home Assistant application is installed.

Through Home Assistant, you can view the values read by the sensors in real time, and in the "Logbook" you can track all the automatic actions performed by the device.

The ESPHome configuration used includes the following components:

- Soil moisture sensor calibrated by calibrate_linear (analog value converted to percentage)
- Temperature and humidity sensor (DHT22)
- Wi-Fi signal measurement for diagnostics
- OTA (Over-the-Air updates) for firmware update via the network
- Wi-Fi fallback mode (Access Point) for cases where the main network is unavailable

This configuration transforms the device from a simple automated pot into a smart node in a truly functional IoT network.

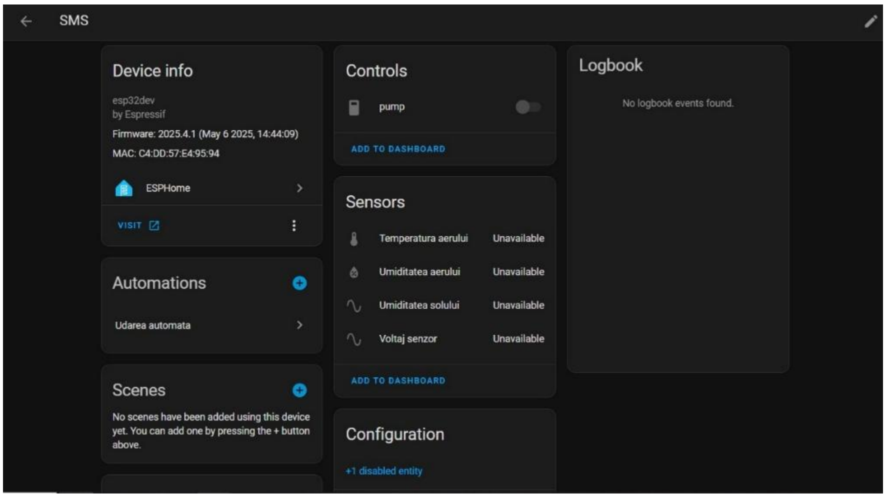

Fig. 3. Application interface

1. Device Identification

```
name: sms
friendly_name: SMS
```

2. ESP32 Board Configuration

```
esp32:
  board: esp32dev
  framework:
    type: arduino
```

3. Enable Logging

```
logger:
```

4. Home Assistant API Integration

```
api:
  encryption:
```

```
    key: "……………"
```

5. Over-the-Air (OTA) Updates

```
ota:
  - platform: esphome
    password: "………..."
```

6. Wi-Fi Setup and Fallback Hotspot

```
wifi:
  ssid: !secret wifi_ssid
  password: !secret wifi_password
  # Enable fallback hotspot (captive portal) in case wifi connection fails
  ap:
    ssid: "Sms Fallback Hotspot"
    password: "……………………"
```

7. Captive Portal

```
captive_portal:
```

8. Water Pump Control via GPIO

```
switch:
  - platform: gpio
    pin: GPIO27
    name: "pump"
    id: my_relay
```

9. Soil Moisture Sensor (Analog)

```
sensor:
- platform: adc
  attenuation: 11db
  pin:
    number: GPIO34
    allow_other_uses: true
  id: "adcMoisture"
  accuracy_decimals: 5
  unit_of_measurement: '%'
  filters:
    - calibrate_linear:
      - 1.171  -> 100.0
      - 2.641 -> 0
```

10. Raw Sensor Voltage (Optional Diagnostic)

```
  - platform: adc
    id: "adcRaw_Sensor_Data"
```

11. Wi-Fi Signal Strength

```
- platform: wifi_signal
  name: "Calitate WIFI"
```

12. Air Temperature and Humidity (DHT22)

```
- platform: dht
  pin:
    number: GPIO32
  temperature:
    name: "Temperatura aerului"
  humidity:
    name: "Umiditatea aerului"
```

7. Degree of Applicability

The implemented system showcases broad utility, spanning both home and industrial uses. Initially conceived as a clever flowerpot demonstration, this project illustrates how affordable connected technology can automate key environmental management tasks, such as tracking soil moisture and controlling watering with little need for user interaction. For home users, the system offers a useful solution for those with limited time, gardening expertise, or access to traditional gardening spaces. It's well-suited for apartments, houses, schools, and offices, providing an engaging and practical way to learn about connected devices, automation, and sustainable plant care. Beyond its role as a user-friendly gadget, this initial design acts as a stepping stone for more extensive applications. The same fundamental structure, built around adaptable sensors, automated decision-making, and central oversight through platforms like Home Assistant, can be scaled up to manage environmental conditions in greenhouses, vertical farms, and conventional agriculture. This enables more efficient water use, reduces manual labor, and improves crop yield management. Furthermore, the system's open design and networking capabilities make it suitable for integration into smart city frameworks, environmental monitoring networks, and data-driven precision agriculture initiatives. With minor adjustments, numerous units can be deployed and managed remotely, providing real-time environmental information and facilitating proactive maintenance or intelligent watering approaches driven by artificial intelligence. In this manner, the project effectively connects a straightforward initial concept with its potential to function as a component within sophisticated, large-scale environmental control systems, highlighting its flexibility, adaptability, and significance in both personal and industrial settings.

8. Conclusion

The creation of an automated smart flowerpot, built on the principles of the Internet of Things, vividly demonstrates how practical it is to integrate environmental monitoring and control into both home and professional environments. By bringing together an ESP32 microcontroller, sensors for soil moisture and air quality, and an automated watering system driven by a pump, this setup offers a compact yet powerful solution for maintaining ideal growing conditions with minimal human effort. Far more than just a convenient gadget for the home, this project acts as a foundational concept for a grander vision: a comprehensive digital system for environmental management across industrial and agricultural sectors. Its adaptable design, affordable manufacturing, and seamless integration with open-source platforms like ESPHome and Home Assistant mean it can be scaled up well beyond a single use. The underlying structure can readily be expanded into widespread sensor networks for intelligent greenhouses, data-informed irrigation systems for farms, and environmental tracking points within smart urban infrastructure. This approach directly supports the objectives of modern precision agriculture, which aims to boost resource efficiency, cut down on waste, and improve crop yields through precise interventions guided by live data. What's more, by making these technologies available to students, enthusiasts, and small-scale growers, the project fosters wider engagement in the digital evolution of farming and environmental care.

Ultimately, this smart flowerpot isn't merely a device; it's an entry point to deploying intelligent, sustainable, and flexible environmental control systems that can benefit both individuals and large-scale operations in the ever-changing world of smart technology.

9. Bibliography

[1] ESPHome, “ESPHome: Home Automation for ESP8266/ESP32,” [Online]. Available: https://esphome.io/. [Accessed: May 2025].

[2] Home Assistant, “Open Source Home Automation that puts local control and privacy first,” [Online]. Available: https://www.home-assistant.io/. [Accessed: May 2025].
[3] Espressif Systems, “ESP32 Series Datasheet,” 2022. [Online]. Available: https://www.espressif.com/en/products/socs/esp32/resources. [Accessed: May 2025].
[4] Aosong Electronics, “DHT22 Temperature and Humidity Sensor Datasheet,” [Online]. Available: https://www.aosong.com/en/products-37.html. [Accessed: May 2025].
[5] A. Kumar, S. Roy, “Smart irrigation system using IoT,” ***International Journal of Scientific Research in Computer Science***, vol. 6, no. 1, pp. 45–49, 2021.

AUTOMATED PET FEEDING SYSTEM

ALEXANDRU David-Andrei, MORARIU Diana-Elena, IVAN Andrei Mario(Conducător științific)

Faculty: Industrial Engineering and Robotics, Specialization: Robotics, Year of Study: I , e-mail: dianamorariu04@gmail.com

SUMMARY: This article presents the development of an automated pet feeding system designed to dispense regular and precise food portions in the owner's absence. The device integrates mechanical design, electronics and programming through an Arduino-based controller. It features a 3D-printed structure with a screw-driven dispenser powered by a stepper motor and triggered by an ultrasonic sensor. The user interface includes LED indicators and manual buttons for maintenance and reset. Developed with sustainability, efficiency and accessibility in mind, the system supports autonomous operation and easy interaction. Potential future upgrades include mobile connectivity, weight monitoring, and pet identification features. The project shows how embedded systems can be used to create useful and easy-to-expand solutions for smart homes.

KEY WORDS: automation, arduino, feeder, sensor, pets

1. Introduction

Automated solutions in daily life are increasingly valued for their ability to save time and improve efficiency. In the context of pet care, feeding systems that operate without constant human supervision are becoming a necessity. This project was initiated to explore how embedded systems and low-cost technologies can address such a need [1].

The main goal was to create a reliable and accessible automated feeder by applying principles from electronics, mechanics and software development. The system was developed by designing the structure in 3D, integrating sensors and programming its functions. This multidisciplinary approach allowed us to design a product that balances technical performance with practical everyday use. Our goal was to create a device that solves a real need and can be improved further in the future.

2. Current State

In response to the increasing need for convenient pet care, automated pet feeders have gained significant popularity. Many commercial systems now offer features such as timed dispensing, portion control and mobile app connectivity. Devices like PetSafe Smart Feed and WOPET feeders rely on embedded electronics, integrating components such as Wi-Fi modules and sensors to automate the feeding process. Despite their advantages, these systems are often expensive and offer limited flexibility for user customization.

At the same time, numerous DIY approaches have emerged in the maker community, particularly using platforms like Arduino and Raspberry Pi. These solutions typically involve stepper motors, ultrasonic sensors and simple control logic to create functional and affordable feeders [4]. Although effective, such systems may lack modular construction, remote access, or user-friendly interfaces, leaving room for further development in the field. This highlights the ongoing demand for customizable, low-cost solutions that can adapt to diverse household needs.

3. Structural Design

At this stage of development, the automated pet feeding system (see in figure 1) is fully functional and structurally complete. The system is built around a 3D-printed modular casing that provides mechanical stability and ensures the protection of all internal components [2]. The detachable vertical tube is mounted using a custom rail system (see in figure 2), allowing it to slide out easily for cleaning or replacement. A protective lid is placed on top to maintain hygiene, while a removable bowl at the bottom collects the food in a clean and practical manner.

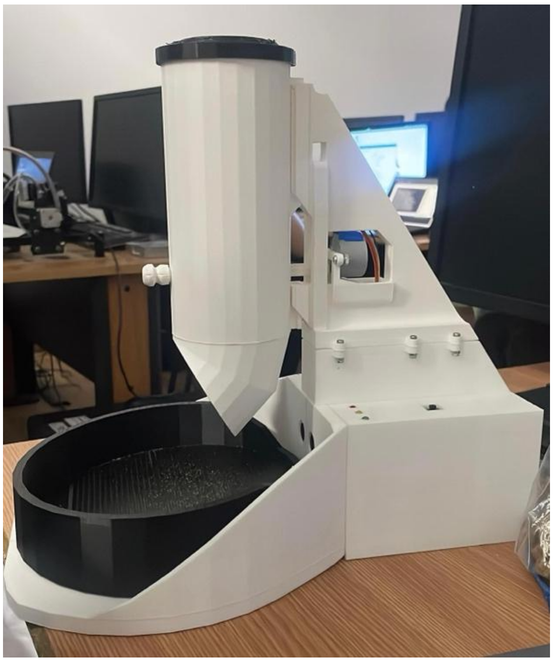

Fig. 1. The automated pet feeding system

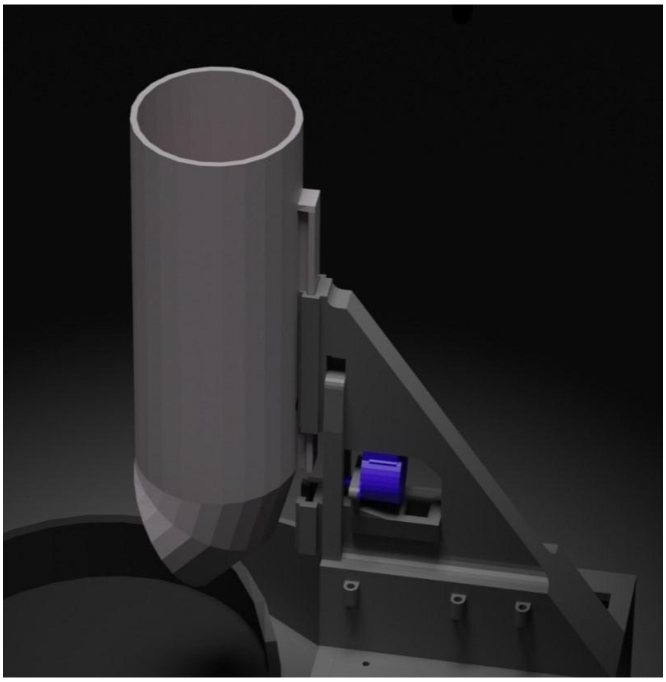

Fig. 2. Rail system

4. Feeding and Control System

The food dispensing mechanism is based on a vertical tube containing a screw-like shaft, which rotates to release precise food portions. This motion is powered by a stepper motor (model 28BYJ-48) operating at 5V, providing consistent and accurate control during each feeding cycle.

The system's logic and control are handled by an Arduino Uno R3 microcontroller, which receives input from an HC-SR04 ultrasonic sensor. This sensor detects the pet's presence within a predefined range [4] and when activated, triggers the motor to dispense food. All electronic components (see in figure 3), including the sensor, motor driver, LEDs, control buttons and power connector—are connected via jumper wires and securely housed inside the structure. The system is powered through a standard 5V connector [3], [5], ensuring safety, reliability and ease of maintenance.

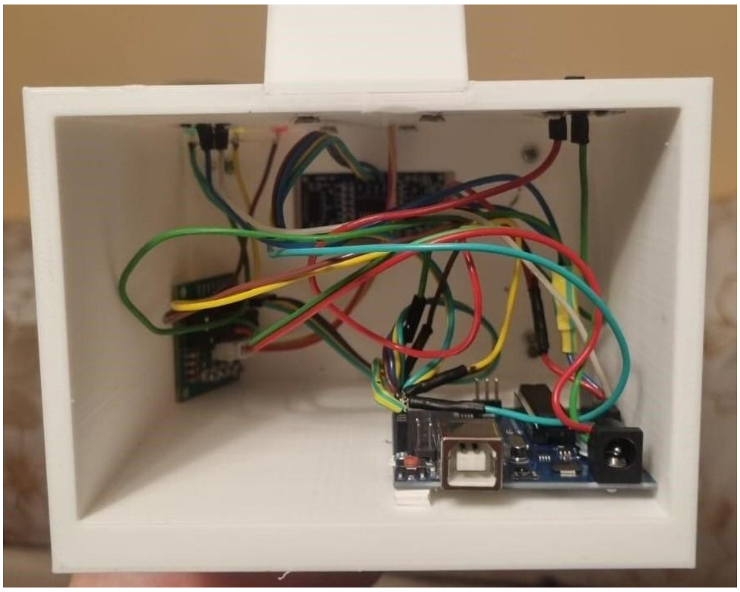

Fig. 3. Electronic components

5. User Interface

The system features a straightforward yet effective interface that combines real-time visual feedback with manual control. It includes three LED indicators—green, yellow and red—and two buttons. At startup, the LEDs flash in a specific sequence to confirm the initialization was successful. Once complete, the green LED stays on, showing that the system is ready and waiting for the pet to approach. When motion is detected by the ultrasonic sensor, the yellow LED lights up, indicating that the motor is spinning and food is being dispensed. Afterward, the red LED signals a cooldown period during which the system is inactive to avoid repeated triggers.

The two buttons offer manual interaction. The maintenance button disables the sensor so the user can safely clean or refill the feeder. If pressed with less than three seconds left on the cooldown, the system waits an extra three seconds before becoming operational, in order for the user to back away from the sensor. The reset button stops the system briefly and reactivates it, even if the motor is running. It also allows users to skip the cooldown by triggering a new startup cycle with the LED animation.

6. Software Component

The software of the automated pet feeder was developed using the Arduino IDE and uploaded directly to the Arduino Uno board. It manages the entire system by integrating sensor input, controlling the motor and enabling user interaction. The program continuously reads data from the ultrasonic sensor to detect the pet's presence and based on this input, it activates the stepper motor to dispense food.

At the same time, it controls the LED indicators—green, yellow and red—to provide visual feedback throughout all phases of operation. To prevent repeated activations in a short period, the software includes a cooldown timer that temporarily disables dispensing after each feeding. It also manages the input from the maintenance button (see in figure 4), implementing a toggle function for the button (see in figure 5), that temporarily deactivates the sensor, allowing safe cleaning or refilling. All functions are synchronized to ensure the feeder operates autonomously, safely and in a user-friendly manner.

```
// ==> se intra in modul mentenanta

  lbs=cbs;
  cbs=digitalRead(button);

  if(lbs== HIGH and cbs ==LOW)
  {
    if(yelledstate == 0) // se aprinde galbenul impreuna cu rosu
    {
      redledstate=50;
      yelledstate=50;
      grenledstate=0;
    }
    else // alta apasare de buton
    {
      redledstate = 50;
      yelledstate=0;
      grenledstate = 0;
      timer=0;
      if(event-ver<3000) /// daca cooldown-ul mai este activ pt mai putin de 3 secunde dupa oprirea mentenantei:
        ver=event-3000; /// se seteaza cooldown-ul sa mai fie activ pt 3 secunde
    }
  }
  analogWrite(redled, redledstate);
  analogWrite(yelled, yelledstate);
  analogWrite(grenled, grenledstate);
  lbs=cbs; /// actualizarea lbs
```

Fig. 4. Maintenance button code

```
// button toggle below
  lbs=cbs; // lbs = last button state; cbs= current button state
  cbs=digitalRead(button);

  if(lbs== HIGH and cbs ==LOW)
  {
    if(redledstate == 0)
    {
      redledstate=50;
      ///digitalWrite(led,HIGH);
      yelledstate=50;
      grenledstate=0;
    }
    else
    {
      redledstate = 0;
      ///digitalWrite(led,LOW);
      yelledstate=0;
      grenledstate = 30;
    }
  }
  analogWrite(redled, redledstate);
  analogWrite(yelled, yelledstate);
  analogWrite(grenled, grenledstate);
```

Fig. 5. Toggle function code

7. The 3D Printing

The structural design of the feeder was developed in Blender, with a focus on modular geometry, symmetry and ease of assembly. The layout was optimized to ensure stability on flat surfaces and to provide unhindered access to internal components for maintenance or upgrades.

All mechanical parts were fabricated using Fused Deposition Modeling (FDM), a reliable additive manufacturing technique. PLA filament was selected due to its print quality and mechanical stability, suitable for precise prototyping. Key printed parts (see in figure 6) include the vertical tube, screw housing, enclosure walls and a detachable food bowl.

The design incorporates dedicated spaces for all electronic modules—such as sensors, LEDs, control buttons and power input—ensuring a compact and coherent structure. The result is a lightweight and streamlined casing that supports both performance and aesthetics, while minimizing the need for extensive post-processing [2].

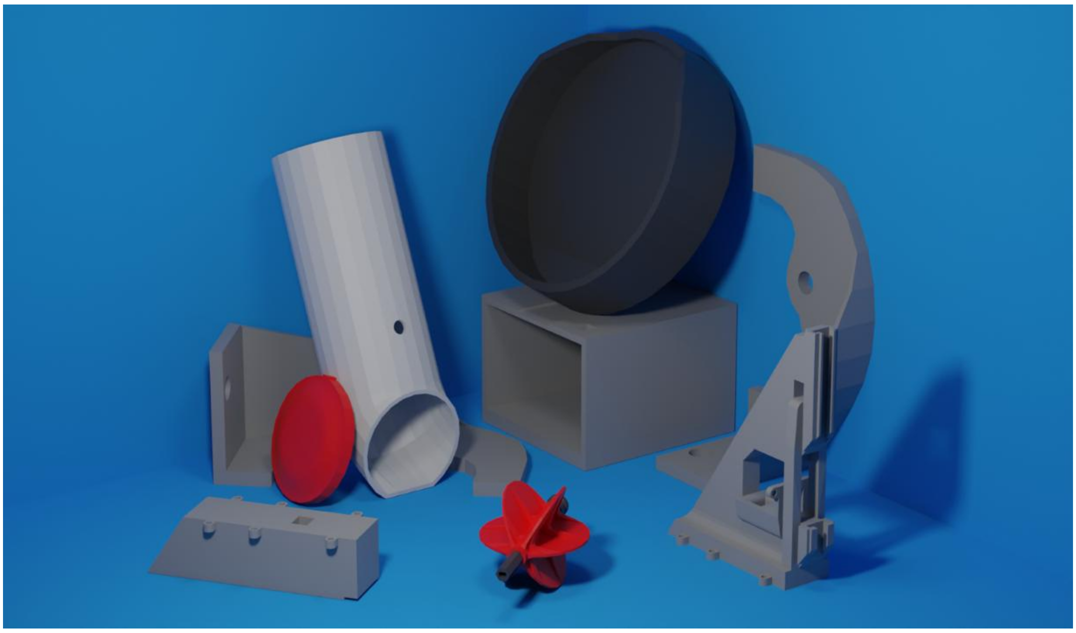

Fig. 6. Printed parts

8. Project Objectives

The project was shaped by three core objectives: sustainability, efficiency and accessibility—each contributing to both functional and conceptual decisions.

Sustainability focused on material choices and energy usage. Components were selected for durability and low power consumption, promoting long-term, environmentally responsible operation.

Efficiency targeted autonomous functionality. The system was designed to dispense food reliably using sensor feedback and controlled motor actuation, without requiring constant user input.

Accessibility ensured ease of use for a broad audience. From intuitive LED signaling to straightforward button controls, the interface was built to be simple and inclusive. Additionally, the system’s modular design supports easy maintenance and potential future upgrades.

9. System Improvements

The system can be improved with smart upgrades. Mobile app control, enabled by integrating a Wi-Fi or Bluetooth module, allows users to manage feeding schedules and dispense food remotely via smartphone. A weight sensor placed under the food bowl measures the exact amount of food served and eaten, helping regulate the pet's diet and prevent overfeeding. A battery backup keeps the device running during power outages. Pet recognition using a camera or RFID tag identifies each animal and enables personalized feeding, ideal for households with multiple pets.

10. Conclusions

This project gave us valuable hands-on experience and helped us better understand how technical ideas can be applied in real life. It taught us to work step by step—from planning and designing to coding and testing. Working as a team also improved our communication, decision-making and problem-solving when challenges came up. Besides being functional, the feeder shows how simple ideas can be turned into useful tools that make everyday life easier. The project encouraged us to think creatively and sparked our interest in future improvements and smart technologies.

11. Bibliography

[1]. Barr, M. & Massa, A. (2006). Programming Embedded Systems: With C and GNU Development Tools. O'Reilly Media, Sebastopol.
[2]. Gibson, I., Rosen, D.W. & Stucker, B. (2015). Additive Manufacturing Technologies: 3D Printing, Rapid Prototyping and Direct Digital Manufacturing. Springer.
[3]. Monk, S. (2012). Programming Arduino: Getting Started with Sketches. McGraw-Hill Education, New York.
[4]. Mishra, R. & Waghmare, L.M. (2016). "Design and Development of Smart Pet Feeder Using IoT." Proceedings, 2nd International Conference on Computing, Communication, Control and Automation (ICCUBEA), IEEE.
[5]. Banzi, M. & Shiloh, M. (2014). Getting Started with Arduino, 3rd Edition. Maker Media, San Francisco.

THE DEVELOPMENT OF A HUMANOID ROBOT

ROȘIORU Gabriel-Sebastian, IVAN Andrei Mario (Conducător științific)

Faculty: Industrial Engineering and Robotics, Specialization: Mechatronics and Robotics, Year of study: I, email: sebirosioru12@gmail.com

ABSTRACT: This paper presents the process of making a small humanoid robot that is able to participate in various kinds of competitions like sumo, weightlifting, obstacle course race.

KEY WORDS: Humanoid robot, Raspberry Pi, ESP32, autonomous, 3D, PyBullet.

1. Introduction

Humanoid robots are not a new topic in the robotics world, but with the rise of AI and technology, they have become more prevalent in our lives. I wanted to create a small scale robot with a design similar to Kondo's KHR-3HV but with the complex capabilities of another small-scale robot, the AiNex from Hiwonder. The robot is equipped with a Raspberry Pi 5, 22 smart serial servos, an ESP32 board that serves as the servo driver and also has an integrated IMU, and a TOF camera from Arducam.

To leverage the processing capabilities of the Raspberry Pi, the robot runs a lightweight simulator without a graphical interface, which calculates inverse kinematics (IK) for the walking cycle. The output from the simulator is then normalized, converted to appropriate control values, and transmitted via serial communication to the ESP32, which manages servo actuation.

Additionally, a graphical user interface is implemented to create custom animations by saving each robot pose, allowing for versatile control and movement programming.

The goal of the robot is to be able to participate in 3 major types of competitions: sumo, weightlifting and obstacle race.

2. Current status

Small-form-factor humanoid robots such as AiNex and KHR-3HV have seen significant advancements in recent years, particularly in motion control, modularity, and autonomy. These robots are now commonly used in research, education, and competitions due to their compact design and versatility. Many models feature advanced servo coordination, IMU integration, and basic computer vision systems. Cross-platform software support, especially under Linux environments, allows for robust development workflows.

Despite these improvements, challenges remain in achieving stable, adaptive walking in dynamic environments. Most small humanoid robots still rely on pre-scripted gaits, with limited real-time adjustment based on sensor input. Research continues into integrating IMU feedback and machine learning techniques to enable more responsive, terrain-adaptive locomotion.

3. Project implementation

3.1 The design

The design of the robot was heavily inspired by the KHR-3HV from Kondo. I chose this particular robot because of its leg structure and the presence of a waist servo that can aid the walking cycle. After finishing the design of the robot, I needed to convert the CAD into a specific format to help me use my robot model in the simulator, so I needed to convert my design to URD (a specific file type used by a lot of simulators). The final design of the robot can be seen in the picture below (Fig. 1).

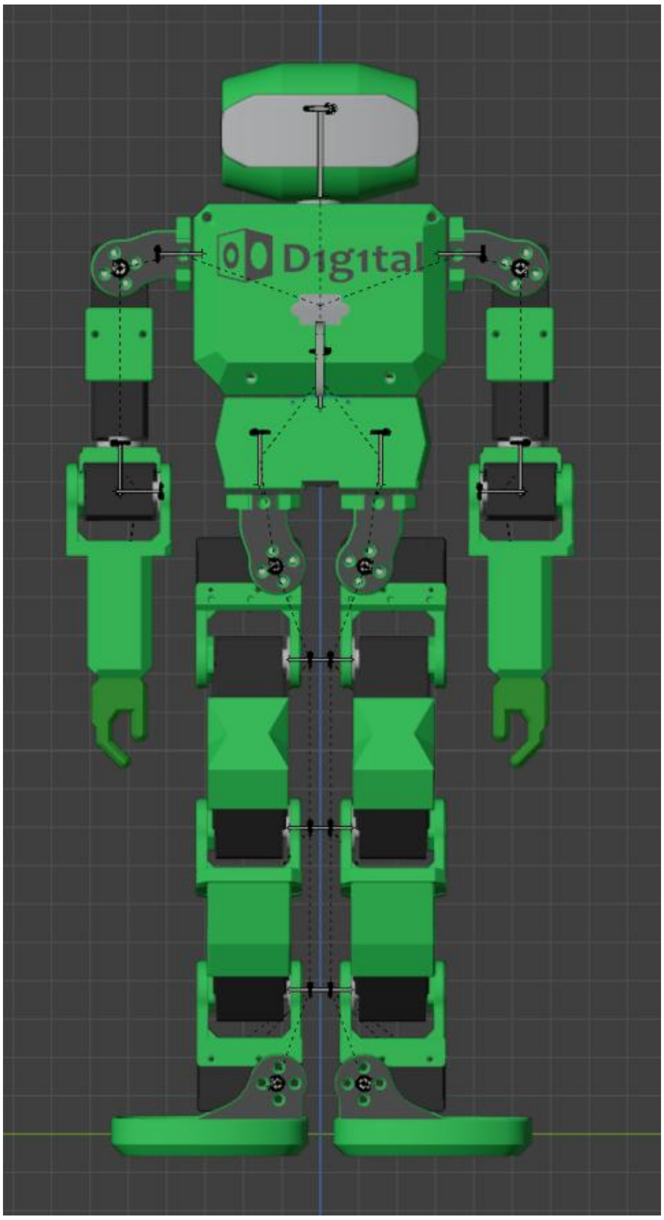

Fig. 1. Final design

3.2 Auxiliary Software

One of the most important tasks in building this robot was developing auxiliary software for generating servo animations. The goal was to create a program compatible with all operating systems that could run natively on Linux, leading to the selection of the Avalonia UI framework. Inspired by existing software used in programming other humanoid robots, the application runs on the Raspberry Pi and communicates via serial with the ESP32.

The interface is intuitive, featuring sliders that represent the robot's physical joints, allowing for easy pose configuration. The software operates in two modes: offline mode and live mode. In offline mode, the robot remains stationary until commanded to move to a specific position. In live mode, the robot moves in real-time according to the slider adjustments.

After positioning the robot as desired, the user can add that pose to a timeline, specifying the speed at which each servo moves to that position and the delay between poses. Once the desired sequence of poses is created, the user can save the animation data as a text file.

The interface can be seen in the image below (Fig. 2)

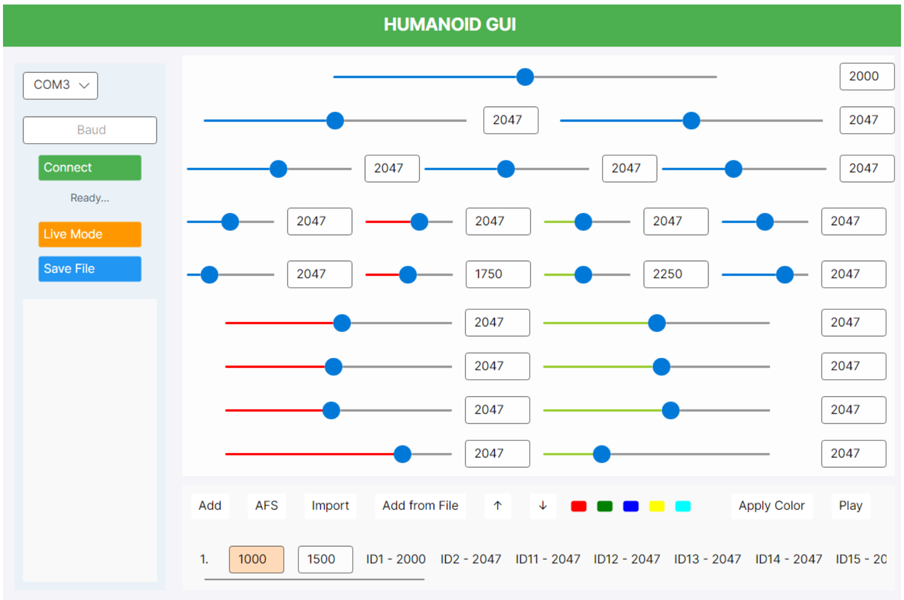

Fig. 2. Humanoid GUI

3.3 Main Software

As stated earlier, the robot runs a simulator that actually is a Python library called PyBullet. This enhances the robot's functionality through precise IK calculations based on the URDF model. In the following photos there will be an example trajectory [1] for the hip and the feet of one of the legs (Fig. 3 & Fig. 4).

```
if (t < t1):
    x2 = xi + 3 * (x0 / 4) * ((t) ** 2) / ((t1) ** 2) - 2 * (x0 / 4) * ((t) ** 3) / ((t1) ** 3)
elif (t < t2):
    x2 = xi + x0 / 4
else:
    x2 = (xi + x0 / 4) + 3 * (x0 / 4) * ((t - t2) ** 2) / ((t1) ** 2) - 2 * (x0 / 4) * ((t - t2) ** 3) / (
            (t1) ** 3)
y2 = (yi - l0 / 2) + (temp) * np.sqrt(abs(1 - ((x2 - (xi + x0 / 4)) / (x0 / 4)) ** 2))
```

Fig. 3. Sample trajectory for hip

```
if (t < t3):
    x1 = xi - x0 / 4
elif (t < t4):
    x1 = xi - x0 / 4 + 3 * (x0) * ((t - t3) ** 2) / ((t0 - 2 * t3) ** 2) - 2 * (x0) * ((t - t3) ** 3) / (
            (t0 - 2 * t3) ** 3)
else:
    x1 = xi + 3 * x0 / 4

y1 = yi - l0 / 2

z1_basic = (self.stepH) * np.sqrt(abs(1 - ((x1 - (xi + x0 / 4)) / (x0 / 2)) ** 2))
```

Fig. 4. Sample trajectory for foot

One problem that I encountered was that by using the default walking gait, the global starting Z position of the foot was not the same as the global end Z position of the foot, thus making the robot as if it were descending stairs.

The solution I implemented involved adding a time-based compensation to eliminate this error. The code below shows the solution found (Fig. 5).

```
nominal_sway = swayLength / 1000
K = 0.0358  # compensation gain
compensation = K * (swayLength - nominal_sway)

if t < t3:
    blend = 0.0
elif t < t4:
    phase_duration = t4 - t3
    phase_time = t - t4
    corect = abs(phase_time / phase_duration)
    blend = (np.pi / 2.3) * (1 - corect ** 2 )** np.sqrt(25)

    print("blend = ", blend)
else:
    blend = 1.3659098493868667

z1 = z1_basic + blend * compensation
```

Fig. 5. Fixing the Z position

The following image will contain 3 graphs, representing the position of each feet on the X,Y,Z axis over time (Fig. 6):

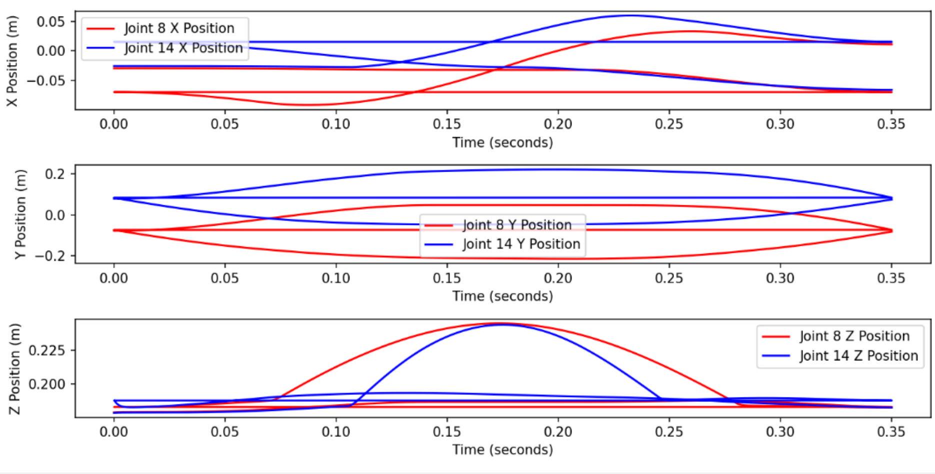

Fig. 6. Position of each foot over time

For the code used in sumo competitions, I have trained a custom YOLOv11 object detection model. This allows the robot to determine the location of its opponent and taking full advantage of the TOF camera, how far his opponent is. The model processes a 250x250 image and generates a bounding box around the zone of interest — specifically, the opponent robot (Fig. 7).

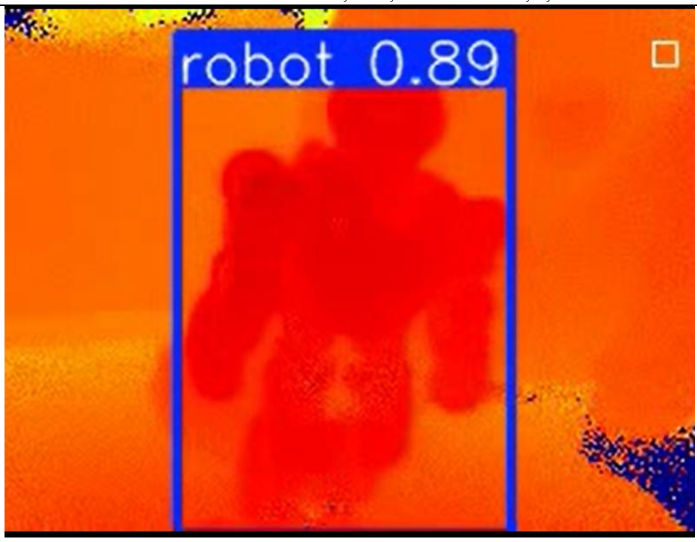

Fig. 7. Outputed image from the model

I have also implemented a universal opponent detection system for combat, without using any machine learning, by checking if an object in the middle of the screen is closer than a specific threshold value. If this condition is met, the robot executes a punching move (Fig.8 & Fig.9). If it does not detect any opponent, the robot starts scanning its surroundings by moving its waist servo. If it does not find any target after two scans (rotating twice), it takes two steps forward.

Fig. 8. Start of the punching move

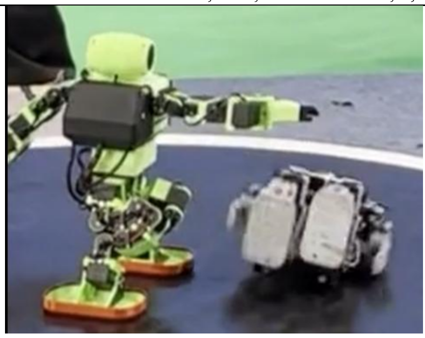

Fig. 9. End of the punching move

4. Conclusion

The robot is capable of competing in sumo, weightlifting, and obstacle race competitions, having a robust and versatile code structure that allows it to easily adjust its behavior for specific tasks.

In the future, I plan to redesign the robot to reduce its weight by replacing the 3D-printed materials with aluminum for the structure.

Another potential improvement involves implementing a technique called Zero Moment Point (ZMP)[2] to stabilize the walking cycle, although it is not typically recommended for small-scale humanoid robots because it involves mounting on each feet 4 presure sensors. Alternatively, I could use a method known as Upper Body Vertical Control, which leverages IMU data to stabilize the walking cycle in real time.

Additionally, to further enhance the walking gait, training a reinforcement learning (RL) agent to optimize the robot's movement could be a promising approach. NVIDIA's Isaac Sim provides a highly realistic simulation environment that can be leveraged to model the physical characteristics of the robot, including its joints, sensors, and contact points. By integrating Isaac Sim with Isaac Gym, a powerful RL training framework, the robot can undergo extensive training in a virtual environment to learn stable walking patterns and adaptive gaits.

Isaac Gym allows for rapid parallel training of RL agents, significantly reducing the time required to achieve optimal control policies. The trained agent can then be transferred to the physical robot, where fine-tuning using IMU data and other sensory inputs can further refine its walking cycle in real-world conditions. This approach not only accelerates the development of robust walking algorithms but also mitigates the risk of physical damage to the hardware during initial training phases.

5. Resources & Bibliography

[1]. https://github.com/puru2411/bipedal-robot.git

[2]. Kaymak, Ç., Uçar, A. și Güzeliş, C. (2023), "Development of a New Robust Stable Walking Algorithm for a Humanoid Robot Using Deep Reinforcement Learning with Multi-Sensor Data Fusion", Electronics, 12(3), 568, ISSN 2079-9292.

MANIPULATION APPLICATION WITH AUTOMATIC RECOGNITION SYSTEM OF OBJECTS

GHINEȚ Andreea-Diana, BUCUR Ianis-Nicolae, POSTELNICU Andrei, IVAN Andrei-Mario (Conducător științific)

Faculty of Industrial Engineering and Robotics, Specialization: Robotics, Years of study: III, II,
e-mail: ghinet.diana@yahoo.com

ABSTRACT

As part of this challenge, the goal is to program an intelligent robotic manipulator capable of identifying and sorting objects using visual data in a dynamic virtual environment. The manipulation environments used are simulated worlds in Gazebo, inspired by the documented example from MathWorks "Pick and Place Robot Manipulator." The competition takes place in a specially configured virtual machine for RoboCup, and installation instructions can be found on the dedicated GitHub repository. The robot used is the Universal UR5e model, equipped with an RGB camera and a depth camera, both of which can be used to solve the challenge.
KEYWORDS: Gazebo, MathWorks, RoboCup, UR5e

1.Introduction

In the context of advancing autonomous robotic systems, this project aims to develop an intelligent manipulator capable of object identification and sorting within a simulated, dynamic environment. The robotic platform utilized is the Universal Robots UR5e, integrated with both an RGB camera and a depth sensor to enable visual perception and spatial reasoning. Simulations are conducted in Gazebo, leveraging environments modeled after the MathWorks "Pick and Place Robot Manipulator" framework. The experimental setup is deployed within a custom-configured virtual machine tailored for the RoboCup competition. Comprehensive installation and configuration guidelines are provided through the associated GitHub repository, facilitating reproducibility and standardized evaluation.

2. Current status

The project is currently in a functional development stage, with the UR5e robotic arm and its visual sensors (RGB and depth cameras) successfully integrated into the Gazebo simulation environment. Initial testing is focused on visual perception, object detection, and manipulation capabilities, with ongoing efforts aimed at improving the accuracy and efficiency of these components. At this stage, all development and validation are being conducted exclusively within the simulation phase.

3. Robot Trajectories and Motion Planning

In this project, the control of the UR5e robotic arm was achieved using the Robot Operating System (ROS), with communication established via a static IP address between the host machine and the robot controller. Once the ROS session was initialized, action clients were configured for both joint trajectory control and gripper actuation.

The robotic gripper was controlled using a ROS action client for the follow_joint_trajectory interface. The gripper's opening width was adjusted according to the object to be grasped, starting from an open state and moving to a closed configuration to simulate the gripping action.

The robot's kinematic model was loaded in MATLAB using the UR5e configuration from the Robotics System Toolbox. Joint transformations were adjusted to align the model with the physical configuration of the robot used in the laboratory setup. An inverse kinematics solver was instantiated to compute the joint angles required to reach specific end-effector positions and orientations.

An initial joint configuration was chosen to move the robot to a safe home pose, ensuring that the arm avoided potential obstacles like the table. Subsequently, target poses were defined for various stages of the pick-and-place task: aligning with the object (a plastic bottle), approaching it from above, grasping it by closing the gripper, lifting it, transporting it above a disposal area (bin), and releasing it. *(Fig. 1)*

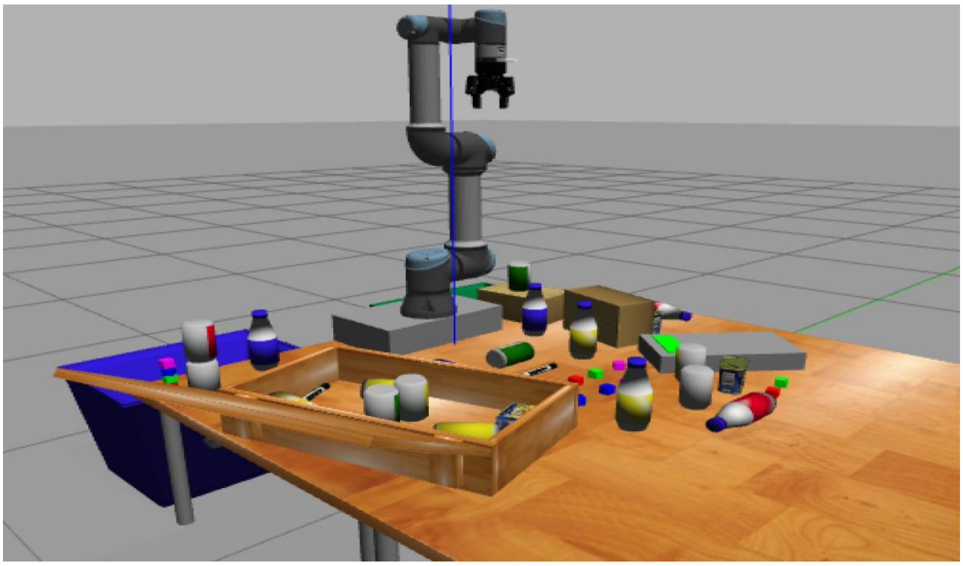

Fig. 1

Each target end-effector pose was specified as a combination of translation and orientation. These poses were transformed into joint configurations using inverse kinematics. A subscriber was also used to monitor the real-time joint states to ensure the robot accurately followed the planned trajectories.

This modular and robust sequence of motions enables autonomous object manipulation in a dynamic environment, integrating both motion planning and real-time feedback.

4. Visual Object Detection

Following the robot motion planning, a visual object detection system was implemented using an RGB-Depth camera integrated into the ROS network. A separate IP address and node configuration were used to initialize the connection to the camera and to subscribe to the appropriate image topics.

The intrinsic parameters of the camera, such as focal lengths and optical center, were extracted from the camera calibration data. These parameters are crucial for reconstructing the 3D positions of points from the depth image.

Both RGB and depth images were acquired from the camera using dedicated ROS subscribers. The depth image was converted and displayed to analyze its range and distribution. Key statistics such as minimum and maximum depth values, as well as the percentage of invalid data points, were computed. A binary mask was created to filter out invalid pixels, retaining only depth values within a useful range for manipulation tasks. *(Fig. 2, Fig. 3)*

For object segmentation, the RGB image was converted to HSV color space. A simple thresholding strategy was applied to isolate green objects, which were assumed to represent the item of interest. This resulted in a binary mask highlighting the object's location in the image.

Using the combined depth image and object mask, the mean 3D coordinates of the object were calculated. These coordinates represent the object's estimated position in the camera's coordinate frame and can later be transformed into the robot's base frame for manipulation.

This integration of visual feedback with robotic control allows for dynamic and adaptive pick-and-place tasks, enabling the robot to locate and interact with objects in real-time based on visual cues**.**

Fig. 2

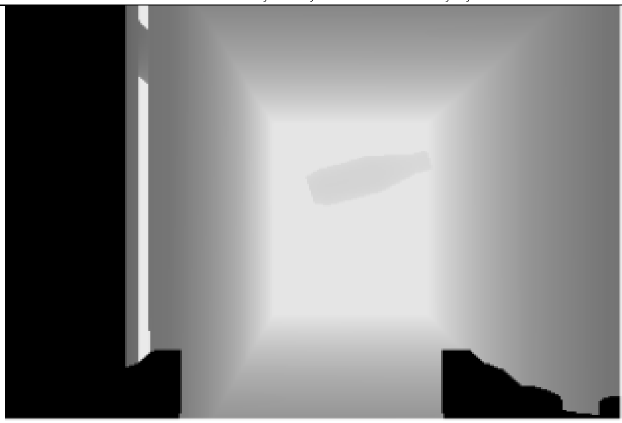

Fig. 3

5. System Implementation and Code Integration

The system was developed using MATLAB and ROS, with a strong focus on modularity, clarity, and the use of well-established ROS interfaces. The implementation was structured into two main components: robotic control (trajectory and gripper execution) and visual data processing.

Below is a snippet illustrating how the ROS connection is initialized and how the action clients are defined for the manipulator and gripper:

“rosIP = "192.168.78.128"; % IP address of the ROS master

rosshutdown;

rosinit(rosIP,11311); % Initialize ROS node

[gripAct, gripGoal] = rosactionclient('/gripper_controller/follow_joint_trajectory', ...

'control_msgs/FollowJointTrajectory','DataFormat','struct');”

Once initialized, the UR5e robot model is loaded from the Robotics System Toolbox, and kinematic corrections are applied to ensure accurate simulation:

UR5e = loadrobot('universalUR5e');

ik = inverseKinematics("RigidBodyTree",UR5e);

ikWeights = [0.25 0.25 0.25 0.1 0.1 0.1];

To move the robot to a specific position, a target transformation is computed, and inverse kinematics is used to derive the corresponding joint configuration:

tform = eul2tform([pi/2, -pi, 0]);

```
tform(1:3,4) = [0.46; -0.07; 0.3]; % Set target position

[configSoln, solnInfo] = ik('tool0', tform, ikWeights, initialIKGuess);
```

The gripper control is achieved by sending goal positions through the corresponding ROS action client:

```
gripPos = 0.515; % Close gripper to grasp

gripGoal = packGripGoal(gripPos, gripGoal);

sendGoal(gripAct, gripGoal);
```

For the vision component, the RGB and depth images are read from ROS topics and processed to identify a green-colored object:

```
rgbSub = rossubscriber('/camera/rgb/image_raw', 'sensor_msgs/Image',
'DataFormat','struct');

depthSub = rossubscriber('/camera/depth/image_raw', 'sensor_msgs/Image',
'DataFormat','struct');

rgbImg = rosReadImage(receive(rgbSub, 10));

depthImg = double(rosReadImage(receive(depthSub, 3)));

hsvImg = rgb2hsv(rgbImg);

mask = (hsvImg(:,:,1) > 0.25 & hsvImg(:,:,1) < 0.45) & ...
    (hsvImg(:,:,2) > 0.4) & (hsvImg(:,:,3) > 0.3);
```

Using the segmented mask, the system estimates the object's 3D position from the depth image using the camera intrinsics:

```
pos3D = compute3DPoint(depthImg, mask, fx, fy, cx, cy);
```

This code structure allows for clear separation of logic between vision and control, while maintaining synchronization through ROS topics and services. The modular design also supports rapid testing and potential future extensions, such as more advanced object recognition models or dynamic planning.

6. Conclusions

This work demonstrates the integration of motion planning and vision-based perception for autonomous object manipulation using the UR5e robotic arm in a simulated environment.

By leveraging ROS, MATLAB, and the Gazebo simulator, a modular and extensible framework was developed for executing pick-and-place operations. The robotic system was capable of identifying a target object using RGB and depth data, estimating its 3D position, and performing a complete manipulation sequence.

Key contributions include the implementation of inverse kinematics-based motion planning, real-time joint state feedback, and a basic but effective color-based object segmentation approach. The solution proved reliable in simulation, highlighting the potential for future deployment in real-world robotic applications.

Future work will focus on extending the system with more advanced object detection algorithms, robust transformation pipelines between vision and robot frames, and introducing dynamic obstacle avoidance during motion execution. Additionally, efforts will be directed toward physical deployment of the system on a real UR5e platform to validate its performance in a non-virtual settings

7. References

[1]. Templates for RoboCup Virtual Robot Manipulation Challenge
[2]. ROS Toolbox

DEVELOPMENT OF A ROBOT FOR MINI SUMO COMPETITIONS

STEFAN Mihnea-Andrei, STATE Gabriel-Marian și IVAN Andrei Mario (Conducător științific)

Faculty of Industrial Engineering and Robotics, Specialization: Robotics, Year of Study: III, II e-mail: mihneastefan502@gmail.com

RESUME:

Mini Sumo competitions are robotics challenges involving autonomous mobile platforms constrained to a maximum weight of 500 grams and dimensions of 10x10 cm, operating within a circular arena. The primary objective is to detect and eject the opponent robot from the ring. Despite their compact form factor, these systems incorporate a variety of complex components, including proximity and line sensors, motor drivers, power regulation modules, and embedded software implementing strategy selection and real-time decision-making algorithms. Participants gain practical experience in mechanical design, embedded programming, sensor integration, and control systems.

KEYWORDS: Autonomous Robotics, Sensor Integration, Real-Time Control, DIP ***switches****.*

1. Introduction

This paper presents the design and development of advanced Mini Sumo robots engineered for high performance in competitive environments. The robots have reached a mature stage of development, demonstrating reliable behavior and adaptability in a wide range of combat scenarios typical of Mini Sumo matches. Through rigorous testing and iterative improvement, the systems are capable of making real-time decisions, maintaining strategic positioning, and reacting effectively to various opponent behaviors.

Each robot features a robust and modular mechanical structure, allowing for quick maintenance, easy upgrades, and configuration flexibility. The architecture adheres strictly to the dimensional and weight constraints imposed by international Mini Sumo regulations, ensuring compatibility with the rules of virtually any competition in this category. The combination of structural durability, smart design, and advanced control systems positions these robots as competitive and resilient platforms in autonomous robotics challenges.

2. Current Status

The project currently includes three high-performance competition-grade Mini Sumo robots. Each robot features a custom-designed steel chassis, precision-machined using CNC technology to ensure durability and structural integrity during matches. While all three share a common mechanical robustness, they differ in key design aspects such as sensor layout, chassis geometry, and component placement—allowing for performance comparisons and strategic diversity in competitive scenarios.

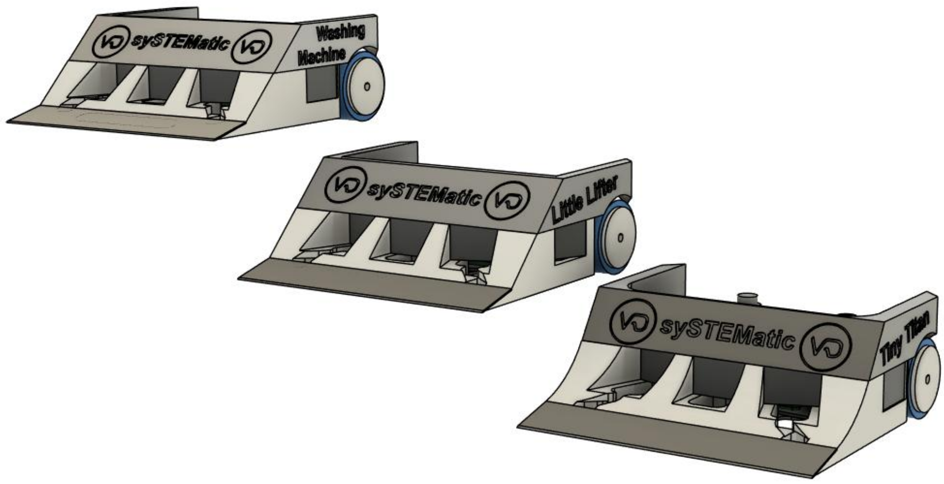

Fig.1

3. Chassis

All three robots feature custom-designed steel chassis, precisely machined using CNC technology to ensure high structural rigidity, durability, and dimensional accuracy—key factors in high-intensity Mini Sumo matches.

Despite sharing the same base material and sensor count (five sensors per robot), each chassis incorporates unique design choices tailored to specific tactical advantages:

- Two of the robots utilize side-mounted sensors positioned at 90 degrees relative to the front center sensor. Of these, one features a curved front section designed to enhance the ability to deflect or lift the opponent upon contact.
- The third robot adopts a more angular design, with a 135-degree front profile. Its lateral sensors are angled forward at approximately 60 degrees from the center sensor, offering improved forward detection coverage and optimized engagement during frontal collisions.

These structural and layout variations enable comparative testing between different geometries and sensing strategies, providing valuable insights into mechanical effectiveness and tactical versatility.

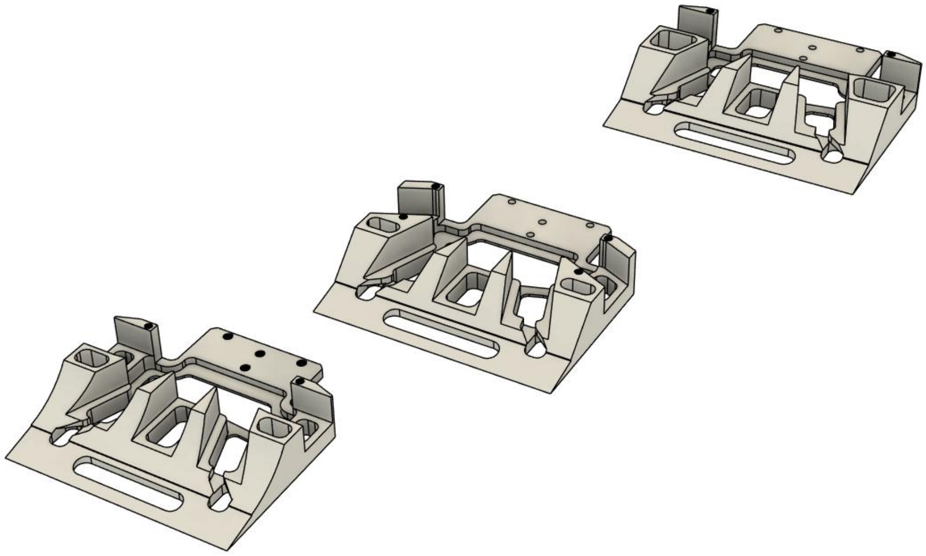

Fig.2

4. Programming

Mini Sumo robots are programmed using a modular architecture, which reflects their physical modular construction. This programming approach allows developers to modify individual components of the code such as motor control, sensor handling, or strategic behaviors without interfering with the overall logic structure. This separation of concerns ensures that updates or improvements can be made quickly, efficiently, and without compromising the core performance of the robot.

The detection system is built around a central algorithm designed to keep the opponent aligned with a mid-positioned sensor. Once an object is detected, the robot calculates the direction and speed needed to engage or reposition strategically. On top of this core, we integrate multiple layers of logic: edge detection using infrared sensors to prevent falling out of the arena, escape strategies when stuck or facing aggressive opponents, and even switchable behavior profiles based on the opponent's style.

Each robot has several predefined modes selected via DIP switches or a small menu in the code, enabling it to adapt to different competitors or tactics without needing a full reprogramming. Modular programming not only increases code reusability and testing efficiency but also mirrors the iterative nature of engineering — allowing for rapid prototyping and continuous optimization before each competition.

```
if (getSensors(0, 0, 0, 0, 0)) {
  search();
}
// Center sensor is triggered, move forward at 30% power
else if (getSensors(0, 0, 1, 0, 0) ) {
  xmotion.Forward(45, 1);
}
// Left sensor is triggered, move left at 30% power
else if (getSensors(1, 0, 0, 0, 0) ) {
  xmotion.Left0(50, 1);
}
// Right sensor is triggered, move right at 30% power
else if (getSensors(0, 0, 0, 0, 1) ) {
  xmotion.Right0(50, 1);  //a fost 35 dupa 1 test, la fel si sus
}
// Diagonal left sensor is triggered, move left at 20% power
else if (getSensors(0, 1, 0, 0, 0) ) {
```

Fig.3 Centering Algorithm

```
void search() {
  if (analogRead(LeftLine) < linevalue && analogRead(RightLine) > linevalue) {
    // Line detected with the left line sensor
    xmotion.Backward(linespeed, 100);
    xmotion.Right0(linespeed, 80);
  }
  else if (analogRead(LeftLine) > linevalue && analogRead(RightLine) < linevalue) {
    // Line detected with the right line sensor
    xmotion.Backward(linespeed, 100);
    xmotion.Left0(linespeed, 80);
  }
  else if (analogRead(LeftLine) < linevalue && analogRead(RightLine) < linevalue) {
    // Line detected with both line sensors
    xmotion.Backward(linespeed, 100);
    xmotion.Right0(linespeed, 100);
  }
  xmotion.Forward(30,0);
}
```

Fig.4 Opponent Search Function

6. Conclusion

In this paper, we have outlined the design, development, and current capabilities of our Mini Sumo robots, focusing on the mechanical structure, sensor integration, and modular programming. The robots are equipped with custom CNC-machined steel chassis, which provide excellent durability and precision. However, it has been observed that the current steel material used for the chassis may be vulnerable to scratches and deformation from contact with opponents. To address this, we plan to enhance the structural integrity by using a stronger, more resilient steel in future iterations. This improvement will ensure that the robots maintain their performance and structural integrity, even in the most intense competitive environments.

LINE FOLLOWER ROBOT

ROȘIORU Gabriel-Sebastian, IVAN Andrei Mario (Conducător științific)

Faculty: Industrial Engineering and Robotics, Specialization: Mechatronics and Robotics, Year of study: I, email: sebirosioru12@gmail.com

ABSTRACT: This paper presents the process of making a line follower robot viable for line follower classic competition and for line follower turbo competition using an ESP32, Bluetooth PID tuning and automatic sensor calibration.

KEY WORDS: Line follower, ESC, ESP32, PID.

1. Introduction

The line follower contest is one of the oldest types of robotics competition. The goal in one of these events is simple, a robot should follow a black line on a white background in the shortest time possible.

There are some restrictions like: the robot should not have any sticky solution on its wheels to improve traction, and the robot should fit in a 25x25cm square, not weighing more than 1kg.

The simplicity of the goal makes this type of competition so hard because it is a battle where every millisecond counts.

The objective of this project was to make a robot that would perform well in this type of challenge and also to be able to compete in the line follower turbo category, where the robot needs to follow the line on the walls and ceiling.

A key feature of the proposed design is the implementation of Bluetooth PID tuning. This approach eliminates the need for continuous code modifications, allowing for rapid iteration and optimization of control parameters. Additionally, the use of analog sensors provides more precise line tracking capabilities, further enhancing the robot's responsiveness.

2. Current status

Modern line follower robots have evolved with advanced features like brushless motors, DShot ESCs, and analog sensor arrays, enhancing precision and speed. Innovations such as Bluetooth PID tuning and real-time calibration facilitate rapid adjustments without reprogramming. Despite these advancements, top-tier performance demands meticulous optimization in weight, power delivery, and sensor accuracy, as even minor inefficiencies can significantly impact competition outcomes.

3. Project implementation

3.1 Hardware & Electronics

The first step was to find a microcontroller that would have built in Bluetooth, so I settled for an ESP32-C3. I chose this board also for its small size and small weight. This type of ESP is rather powerful and makes a great choice for this kind of task where speed is a big factor, if I have chosen a less powerful board, it could have impacted the performance of the robot because the speed that the sensors are read counts very much on the total performance of the robot.

Another key component was the motors. I used BLDC motors due to their high speed and low response time. The specific motors are RS1306B 2700KV, and I also added a 5:1 gear ratio for bigger torque. The ESC used with these motors is a BLHELI 32 compatible with DShot protocol. I could have used the normal communication for BLDC motors using the “Servo” library in Arduino IDE, but this would have meant that the signal length would have been between 1ms and 2ms which at high speeds is slow. By using DShot [1] the information is sent rather quickly to the ESC (around 26,7microseconds/signal sent). The way that this protocol works is shown below (Fig. 1).

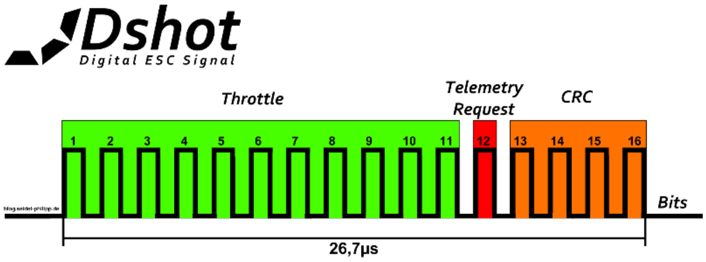

Fig. 1. Dshot communication

The sensor array is a modified version of the XLINE 16 Line Sensor Board - Digital V2 from JSUMO, now capable of transmitting analog signals. This modification allows for more precise detection of the line position, as opposed to the original digital-only output. I chose this sensor board not because of its IR sensors but because of its shape, the curved shape of the PCB and the placement of the IR sensors help much when the robot encounters a 90° turn. Another big advantage of this board is that the sensors are multiplexed, so I need to connect only 7 wires for 16 sensors.

The robot is also equipped with an IR start stop sensor as a safety measure, although I can control the start and stop from Bluetooth, I chose to use a separate sensor.

The chassis of the robot is designed to be aerodynamic and also extremely lightweight, this is why I chose to 3D print it out of carbon fiber PLA.

The end result can be seen in the picture below (Fig. 2).

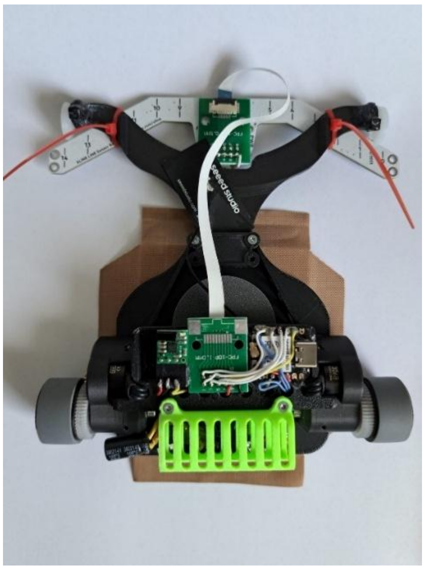

Fig. 2. The final robot

3.2 Software

The software was made using Arduino IDE and was designed to take full advantage of the ESP32, starting with the RMT. The RMT (Remote Control) is a peripheral designed to generate accurate and stable signals to control external devices such as LEDs, motors, and other peripherals. It is well suited for generating the DShot signals in a high-performance and accurate way on the ESP32 platform. I have used a pre-existing library for the control of the motors, but for the BLDC that actuates the turbine, I used the normal PWM method of controlling the motor. The DSHOT protocol consists of transmitting 16-bit packets to the ESCs: 11-bit throttle value, 1-bit to request telemetry and a 4-bit checksum. There are three major protocol speeds: DSHOT150, DSHOT300 and DSHOT600. In my case, I use DSHOT600 because it is the fastest protocol and it suits my purpose of making a fast robot.

I have also implemented a PID controller so that the robot is able to follow the line with a bigger accuracy than with a Bang-Bang type of controller. The code below shows the implementation of the PID algorithm (Fig. 3).

```
void PID() {
  int error=pos-setpoint;
  integral=integral+error;
  int diferencial = error * pdv[0] + pdv[1] * (error-lastError) + KI * integral;
  lastError = error;
  if (diferencial >= pdv[2]) diferencial = pdv[2];
  else if (diferencial <= -pdv[2]) diferencial = -pdv[2];
  if(abs(700-pos)<40)
    diferencial = 0;
  if(diferencial < 0)
  {
      rspeed = max(200,int(pdv[2]+diferencial));
      lspeed = int(pdv[2]);
  }
  else if(diferencial >= 0)
  {
      rspeed = int(pdv[2]);
      lspeed = max(200,int(pdv[2]-diferencial));
  }
  Serial.print(rspeed);
  Serial.print(" ");
  Serial.print(lspeed);
  Serial.print(" ");
  Serial.println(pos);
  if (pos<100){
    rDshot.sendThrottleValue(0);
    lDshot.sendThrottleValue(vit);
  }
    if (pos>1300){
    rDshot.sendThrottleValue(vit);
    lDshot.sendThrottleValue(0);
  }
  else if(pos <= 1300 && pos >=100 ){
  rDshot.sendThrottleValue(rspeed);
  lDshot.sendThrottleValue(lspeed);
  }

}
```

Fig. 3. PID implementation

As you can see I have a specific condition that prevents the full stop of the motors unless the robot left the line, then and only then a motor stops, but in contrary, regardless of the PID gains values, the minimum speed value that a motor could be is 200. I also have implemented a condition that allows the robot to go full speed when the position of the sensors is not perfectly in the middle of the black line.

The auto calibration of the sensors is executed always when the robot starts and works as follows: The robot is placed with all the sensors on the white part of the track, it reads 10 times the values of each sensor finding the maximum read value, after this is adds 50 to this found value and this is the maximum value for white background. In the main code, any value below this threshold is automatically set to 0, leaving only values for the black line. The calibration algorithm is shown in below (Fig. 4).

```
int calib(){
  int max = 0;
  int val = 0;
  for(int i = 0;i<10;i++){
    for(int i = 0;i<15;i++){
      digitalWrite(s0, i & 0x01);
      digitalWrite(s1, i & 0x02);
      digitalWrite(s2, i & 0x04);
      digitalWrite(s3, i & 0x08);
      val = analogRead(AI);
      if (max < val)
      max = val;
    }
  }
  return max+50;

}
```

Fig. 4. Sensor calibration

Finally, the Bluetooth PID and speed tuning. I have decided to only use the proportional and derivative part of the PID controller, and also to be able to change the speed in real time. The advantage of the ESP32 is that the Bluetooth connection does not add any delays. I send via Bluetooth a string that contains the KP, KD and the speed then I store each of those values in a variable that is used in real-time (Fig. 5).

```
class MyCallbacks: public BLECharacteristicCallbacks {
    void onWrite(BLECharacteristic *pCharacteristic) {
      String value = pCharacteristic->getValue();
      char buf[sizeof(value)];
      value.toCharArray(buf, sizeof(buf));
      char *p = buf;
      char *str;
      //Serial.print(value);
      for(int i=0; ((str = strtok_r(p, " ", &p)) != NULL);i++)
        {
          pdv[i] = atof(str);
        }
        Serial.print(pdv[0],4);
        Serial.print(" ");
        Serial.print(pdv[1],4);
        Serial.print(" ");
        Serial.println(pdv[2],4);

    }
};
```

Fig. 5. Receiving Bluetooth data

4. Conclusion

The line follower robot successfully integrates Bluetooth PID tuning and analog sensor calibration, significantly improving control accuracy and ease of parameter adjustment. While the robot performs well in both classic and turbo categories, further enhancements in speed and weight reduction are needed to achieve top-level competitive performance.

5. Resources & Bibliography

[1] https://github.com/derdoktor667/DShotRMT

DEVELOPMENT OF A PROTOTYPE FOR A SIX-AXIS EDUCATIONAL ROBOT ARM

ZAMFIROIU Mihai Alexandru, ȚENESCU Matei Mihai, MIRICĂ Eduard Leonard, GEROGESCU Gabriel, Andrei Mario IVAN (Conducător științific)

Faculty: Industrial Engineering and Robotics, Specialization: Robotics and SIA, Year of Study: II, e-mail: alexzzz2004@gmail.com

ABSTRACT: This article presents the development journey of a six-axis robotic arm prototype, the latest iteration in a series of robotic systems we have designed and built. This robot continues the legacy of two earlier models, integrating lessons learned and new design improvements into a more advanced platform. The fabrication process combined 3D-printed PLA components with precision-cut metal parts, balancing accessibility with structural integrity. The arm is actuated by six NEMA 17 stepper motors—three of which are standard-sized and coupled with planetary gearboxes for increased torque, while the other three are compact pancake variants, optimized for space-saving joints. For motion feedback and precision, the robot is equipped with a hybrid sensing system: three rotary encoders and six AS5600 magnetic encoders provide detailed positional data for closed-loop control. This setup allows the robot to achieve accurate and repeatable movements across all six degrees of freedom. This project marks a significant step forward in our exploration of accessible, modular robotic systems—and demonstrates how iterative design and mixed-material construction can yield capable and scalable solutions.

KEYWORDS: maximum 5, conform subiectului lucrării.

1. Introduction

This article presents the development journey of a six-axis robotic arm prototype, the latest and most advanced iteration in a series of robots we have designed and built. This robot was conceived as a challenge—to test the limits of our fabrication, design, and control capabilities—and serves as a direct upgrade from our previous two robotic models.

Our first prototype featured a four-axis configuration, three of which were numerically controlled. The second version expanded on this foundation with five axes, four of them numerically controlled. This current version completes the progression with six fully numerically controlled axes, offering greater flexibility, range of motion, and control precision.

One of the most significant upgrades is the robot's size. While the first two models reached approximately 30 cm when fully extended, this new prototype boasts a maximum reach of 1.2 meters—making it four times longer and enabling a much wider operational workspace. To handle the increased mechanical load and extended arm length, we incorporated both 3D-printed PLA components and precision-cut metal parts, enhancing its structural rigidity and payload capacity. The robot can currently lift up to 0.8 kilograms.

The actuation system consists of six NEMA 17 stepper motors—three standard size with planetary gearboxes for high-torque applications, and three compact pancake motors for lighter joints. For position feedback and control accuracy, we integrated three rotary encoders and six AS5600 magnetic encoders, allowing smooth, closed-loop movement across all axes.

Compared to its predecessors, this robot offers significantly improved movement precision and far fewer mechanical limitations. It represents a major leap in both capability and ambition, serving as a modular, scalable platform for future experimentation in robotic motion, automation, and control systems.

2. The Current Stage

In recent years, educational robotic arms have become more common in universities and research labs. These systems are used to teach robotics concepts, test algorithms, and develop new technologies. Six-axis robotic arms are especially popular because they can replicate complex, human-like movements. [3]

Commercial robotic arms are often expensive, which makes them hard to access for students. To solve this, many projects use affordable components such as 3D-printed parts made from PLA and widely available stepper motors like the NEMA 17. Planetary gearboxes are often added to increase torque for heavier loads.

To improve precision and control, most systems use encoders. Magnetic encoders, such as the AS5600, and rotary encoders help create closed-loop control systems, which allow the robot to correct its position in real time.

Motion control is usually based on forward and inverse kinematics, most often using the Denavit-Hartenberg method. Many robotic arms also include user interfaces that offer joint-space and Cartesian-space control, as well as features like teach-in programming or voice control.

Modern setups often use modular electronics, such as BIGTREETECH Octopus Pro boards and Raspberry Pi computers, to control the robot. These platforms allow more flexibility, customization, and integration with other systems.

Overall, the field is moving toward making robotic arms more **accessible**, **modular**, and **precise**, while keeping costs low. The prototype developed in this project follows these trends by combining 3D printing, closed-loop control, custom software, and modern electronics.

3. Evolution and Description of the Robot

The six-axis educational robotic arm presented in this project is the result of a structured and iterative development process, spanning three distinct prototype generations. The initial version was a four-axis configuration, three of which were numerically controlled via stepper motors. Although limited in motion capability, this prototype served as a proof of concept for mechanical design and basic control strategies. Building on this foundation, a second prototype introduced five degrees of freedom, with four active joints, enhancing the arm's versatility and allowing for a broader range of experimental tasks.

The current version completes this progression by achieving six fully actuated joints, offering a complete six degrees of freedom (6-DOF) articulated configuration. This advancement enables full spatial manipulation of the end-effector, including complex orientation control in 3D space, suitable for a wide variety of educational, research, and automation tasks, as seen in fig 1.

Structural and Dimensional Enhancements

Compared to its predecessors, the latest prototype exhibits a significant increase in both size and mechanical complexity. While the earlier models reached a maximum extension of approximately 30 cm, the current arm has a fully extended length of 1.2 meters—representing a 4x increase in reach. This expansion dramatically increases the robot's operational workspace, enabling it to handle larger tasks, objects, and work surfaces. To maintain structural stability under increased loading conditions, the mechanical design incorporates a hybrid structure composed of 3D-printed PLA parts and laser-cut aluminum elements. PLA was selected for rapid prototyping and part modularity, while aluminum parts were integrated in high-stress areas to ensure rigidity, minimize flexion, and increase durability.

As a result of these improvements, the robot is capable of lifting payloads up to 0.8 kg, a considerable achievement given its lightweight construction and open-source hardware philosophy.

Actuation and Feedback System

The arm is actuated by six NEMA 17 stepper motors, selected for their wide availability, reliability, and cost-effectiveness in robotic applications. The first three joints—base, shoulder, and elbow—are equipped with standard NEMA 17 motors fitted with planetary gearboxes, significantly increasing output torque for load-bearing axes. The remaining three joints—wrist pitch, wrist yaw, and wrist roll—utilize compact "pancake" NEMA 17 motors to reduce mass and save space in the upper segments of the arm, where inertia and balance become critical.

To enable precise control and closed-loop feedback, the system integrates two types of sensors: three rotary encoders and six AS5600 magnetic encoders. This hybrid encoder setup allows for high-resolution positional monitoring of each joint, which is critical for accurate and repeatable motion. The combination supports real-time correction of positioning errors, especially during dynamic tasks or in the case of skipped steps—a common limitation of open-loop stepper motor systems.

Mechanical Transmission and Joint Architecture

Mechanically, the robot employs a belt-driven transmission system for the first three joints. High-tension, low-elasticity timing belts were selected to minimize backlash and ensure smooth torque transmission while keeping the assembly compact and serviceable. The use of belt drives also improves the synchronization between motor rotation and encoder feedback, reducing the error margin during acceleration and deceleration phases.

Joint 4 (wrist pitch) is driven by a 1:6 gear reduction system, implemented to boost torque without increasing motor size. This setup is especially useful in operations requiring tool inclination or lifting small payloads at a distance. Joints 5 and 6 (wrist yaw and roll) are direct-drive, prioritizing minimal mechanical complexity and response time. Notably, Joint 5 is driven through a mechanical extension rod, which relocates its motor behind Joint 4, preserving a compact form factor in the wrist section while minimizing mass at the end-effector, as seen in fig. 2.

To support these mechanical systems, high-performance bearings and reinforced rotational shafts have been introduced in critical areas. Ball bearings are used at all major rotational points to reduce friction and allow smooth, repeatable movements. In future iterations, more specialized bearings are planned to further enhance load handling and positional accuracy.

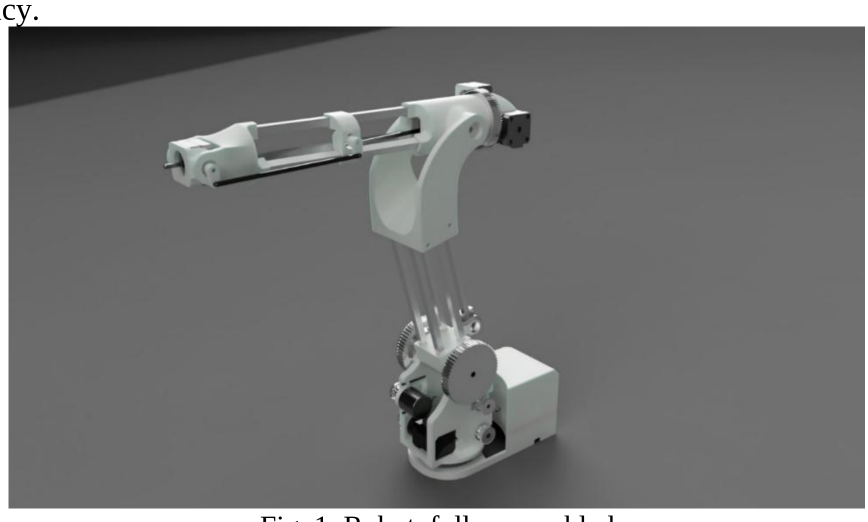

Fig. 1. Robot fully assembled

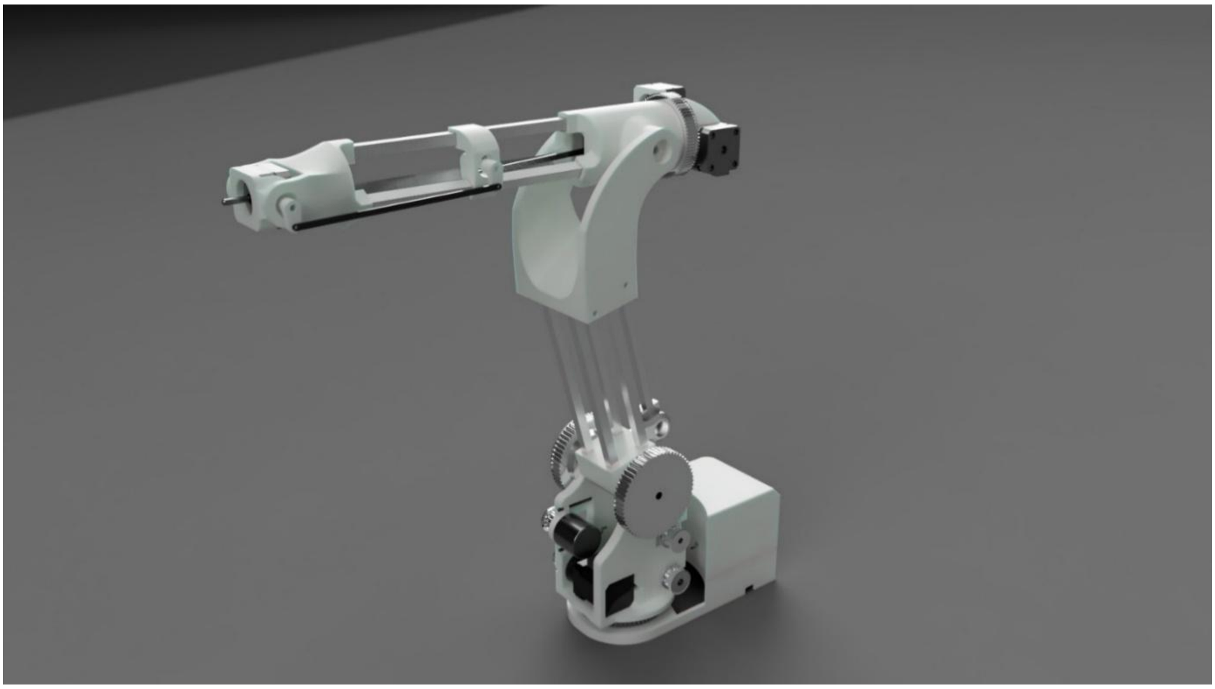

Fig. 2. Axis 4 and 5

4. The development of the Control System

The robot's control system has been developed entirely from the ground up, designed with flexibility, modularity, and scalability in mind. One of its key strengths is its ability to control different robotic configurations. By simply updating the kinematic parameters and specifying the appropriate serial port, the program can interface with and control a variety of robots, not just this six-axis model.

The user interface is divided into three main tabs, each tailored to different control strategies:

1. **Joint Mode Tab**
This tab allows axis-by-axis control of the robot. Each joint is operated through an individual slider accompanied by an incremental input field, allowing precise step-based movement as defined by the user. Additional controls include a speed adjustment slider with incremental input and a configurable gripper control slider for end-effector manipulation.
2. **Cartesian Mode Tab**
Structurally similar to the Joint Mode, the Cartesian Mode adds spatial manipulation by including six sliders—three for linear movement along the X, Y, and Z axes, and three for rotation around those same axes. These controls allow intuitive movement in Cartesian space. The tab uses inverse kinematics to compute joint positions based on the desired tool pose, ensuring that values across tabs remain synchronized. Speed and gripper settings are shared in real time between the Joint and Cartesian tabs for a seamless control experience. [2]
3. **Voice Control Tab**
This tab introduces a layer of accessibility by supporting simple voice commands for core functionalities. The user can switch between tabs, move the robot, adjust speed settings, and control the end-effector using intuitive voice inputs. This feature enhances hands-free operation and improves the human-robot interaction experience.

Teach-In Programming and Advanced Features

The interface also includes a **Teach-In Programming** tab that supports real-time recording and playback of motion sequences. Users can add specific robot configurations, redo or refine movements, save sequences, and upload them for future use. Motion programs are stored in .rld (Robot Learn Data) files, providing a reusable and easily shareable format for robotic routines.

Additionally, the interface allows the robot to be triggered by **external digital inputs**, making it operable in slave mode as part of a larger automated system. This expands the robot’s potential use in industrial or production-line settings.

Finally, the interface offers both dark and light mode themes to suit user preference and improve visibility in different working environments.

5. The Integration of the Forward Kinematics

The robot's forward kinematics are calculated using the Denavit-Hartenberg (D-H), (fig. 4.) matrix method, a standard approach in robotic arm modeling. [1] This mathematical framework allows the system to determine the precise position and orientation of the end effector based on the current joint angles.

A dedicated software module processes encoder inputs and computes the real-time position of the robot in 3D space. This continuous positional feedback is critical not only for monitoring but also for error correction. In the event of missed steps—common in open-loop stepper motor systems—the encoder data is compared against the expected position from the kinematic model, allowing the system to compensate and realign the robot’s movements accordingly.

This integration of D-H-based forward kinematics with live encoder feedback enhances both the precision and reliability of the robot, enabling smooth and consistent operation even under variable load conditions or sudden disturbances.

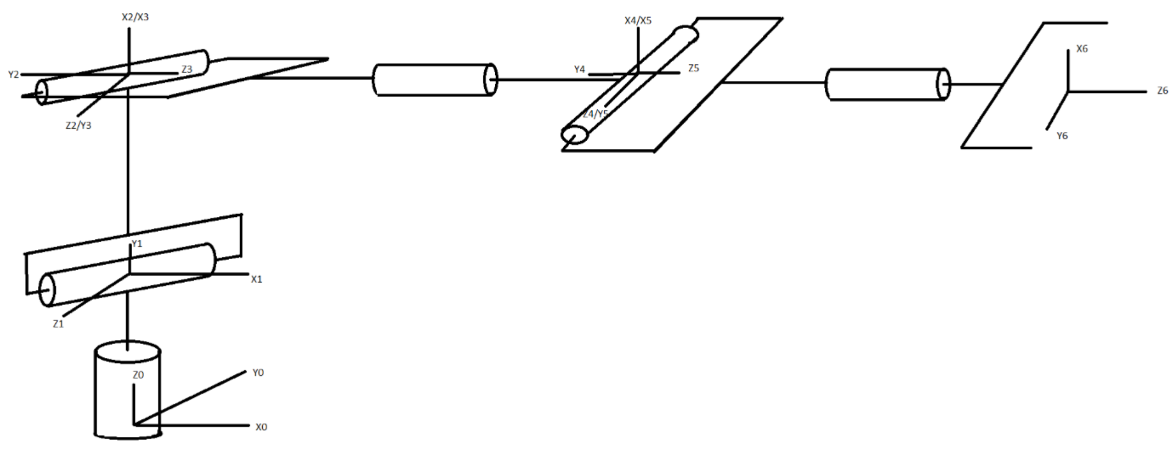

Fig. 3. Simplified Kinematic Diagram

6. The 3D printing of the robot and the parts used

Additively manufactured gears, produced via fused filament fabrication (FFF), were employed as provisional components during the prototyping phase. These served as functional placeholders until the final gear assemblies, machined from high-strength aluminum alloys, could be fabricated to meet the desired mechanical performance and durability specifications.We have printed all of our 3D printed components out of PLA on bambulab printers, with tolerances of 0.15mm.

All polymer-based components utilized during the development phase were fabricated using polylactic acid (PLA) filament on Bambu Lab FFF 3D printers. The printing process was calibrated to maintain dimensional tolerances within ±0.15 mm, ensuring adequate fit and function for preliminary integration and mechanical testing.

Currently, standard deep-groove ball bearings are implemented on the primary rotational axis to facilitate smooth motion and support radial loads. Plans are in place to transition to application-specific bearing solutions in subsequent iterations, in order to accommodate higher load capacities and improve system performance under specialized operating conditions.

7. Conclusions

The development of this six-axis robotic arm marks a significant advancement in our ongoing exploration of robotics design, fabrication, and control systems. Through iterative prototyping and continuous refinement, we have progressed from basic four- and five-axis models to a fully articulated, closed-loop six-axis robotic platform capable of precise and adaptable motion.

By integrating high-torque stepper motors, rotary and magnetic encoders, and advanced mechanical transmission systems, we have achieved a balance between structural rigidity and fine motion control. The use of both 3D-printed PLA components and precision-cut metallic parts provided a versatile and scalable manufacturing approach, allowing rapid prototyping while maintaining the mechanical integrity required for practical use.

The control system was developed entirely in-house, offering modular software that supports multiple control modes—including joint space, Cartesian space, teach-in programming, and voice commands. With a robust GUI and a flexible architecture capable of controlling various robotic configurations, the platform is primed for expansion into more complex applications.

Furthermore, the implementation of Denavit-Hartenberg-based forward kinematics, encoder-based feedback compensation, and real-time position verification establishes a foundation for high-precision robotic behavior, even under dynamically changing conditions.

This project not only demonstrates our ability to build a sophisticated robotic system from scratch but also lays the groundwork for future research and deployment in automation, collaborative robotics, and advanced human-robot interaction. The lessons learned and systems developed here will serve as a strong foundation for further innovation in robotic technology. [4]

8. Bibliography

[1] J. J. Craig, *Introduction to Robotics: Mechanics and Control*, 3rd ed. Pearson Prentice Hall, 2005.
[2] M. W. Spong, S. Hutchinson, and M. Vidyasagar, *Robot Modeling and Control*. Wiley, 2006.
[3] S. B. Niku, *Introduction to Robotics: Analysis, Systems, Applications*, 2nd ed. Wiley, 2010.
[4] M. P. Groover, *Automation, Production Systems, and Computer-Integrated Manufacturing*, 4th ed. Pearson, 2016.

SPIDER ROBOT WITH FACIAL RECOGNITIOn

PETCU Eva-Gabriela și AWAD Sara și IVAN Andrei Mario (Conducător științific)

Facultatea: IIR, Specializarea: MRENG, Anul de studii: I, e-mail: eva.petcu@yahoo.com

ABSTRACT: Arachne is an innovative hexapod robot equipped with eighteen MG996R servo motors, enabling smooth, spider-like locomotion. Each of the six legs is powered by three motors, allowing precise and coordinated movement. The robot integrates a facial recognition system using an ESP32CAM module, which governs its behavior. Upon recognizing a registered face, Arachne advances toward the subject; in the presence of an unrecognized individual, it retreats. This interplay between perception and motion highlights the robot's responsive design. While the facial recognition adds complexity, the primary focus remains on bio-inspired mobility. Arachne exemplifies the synergy between mechanical engineering and artificial intelligence in mobile robotics.

CUVINTE CHEIE: facial recognition, complexity, mobility, hexapod, registered face.

1. Introduction

Arachne is a six-legged robotic prototype developed with the goal of mimicking spider-like movement while incorporating intelligent behavior through facial recognition. This project combines mechanical design, control systems, and basic artificial intelligence to create a robot capable of both mobility and human interaction. The primary aim of Arachne is to explore how robotic systems can respond autonomously to visual stimuli, specifically by identifying familiar faces and adjusting movement accordingly. Beyond its academic relevance, Arachne has potential applications in areas such as security, surveillance, search and rescue, and hazardous environment exploration.

2. Current state

Hexapod robots integrated with facial recognition technology represent a fascinating intersection of mechanical engineering, computer vision, and artificial intelligence. These six-legged machines are designed not just for agile and adaptive locomotion, but also for interactive behavior using real-time visual input. Robots like SpiderPi by Hiwonder and open-source projects like Animabot showcase how facial detection, tracking, and even emotional response can be embedded in mobile platforms. Often powered by lightweight, flexible computing solutions like the Raspberry Pi, they use software libraries such as OpenCV or dlib to interpret human faces and react accordingly, turning their heads, following movement, or initiating responses.

This combination allows for deeper engagement in educational settings, where students can experiment with AI and robotics in an integrated way. In research environments, these robots are testbeds for studying locomotion, human-robot interaction, and vision-based control. Some even go further, incorporating gesture recognition, voice commands, or AR markers for more complex tasks. As components become cheaper and algorithms more efficient, we're seeing a shift toward consumer-friendly kits and robots capable of adapting to their users and surroundings in near-human ways.

A noteable hexapod project is:

-SpiderPi by Hiwonder

- Platform: Raspberry Pi 4B or 5
- Features:
- 120° HD wide-angle camera for facial, color, and tag recognition
- AI vision capabilities using OpenCV
- Inverse kinematic gait for smooth movement
- Wi-Fi control via PC software or mobile app
- Use Cases: Educational purposes, AI vision learning, and interactive demonstrations

3. Mechanical Design and Architecture

The physical structure of Arachne is centered around a hexapod chassis, a design chosen for its mechanical stability and resemblance to arachnid locomotion. Each of the six legs is actuated by three MG996R servo motors, giving the robot a total of eighteen motors. These servo motors are commonly used in robotics due to their high torque and reliable response, making them well-suited for both weight-bearing and rapid movement tasks.

Each leg has three degrees of freedom (3-DoF), which allows it to move in multiple planes:

- The coxa joint enables horizontal rotation, positioning the leg outward or inward.
- The femur joint controls vertical leg lifting and lowering.
- The tibia joint extends or contracts the leg, contributing to stride length and balance.

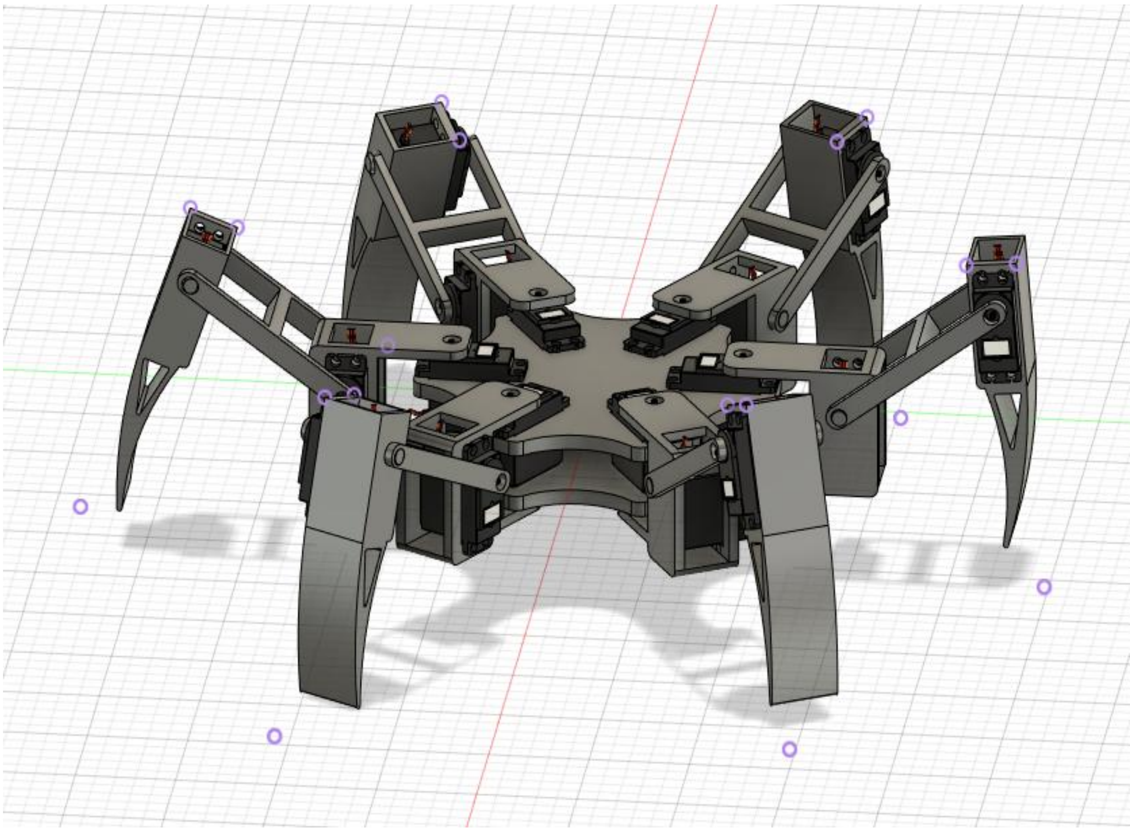

Fig. 1. 3D Design

This configuration (see fig. 1) allows Arachne to use various walking patterns or "gaits," including the tripod gait, which keeps three legs on the ground at any time for optimal stability. The robot's frame was designed with weight distribution in mind to minimize strain on individual servos and to allow it to navigate minor terrain irregularities. The leg design also enhances energy efficiency by supporting forward motion with minimal friction.

4. Control System and Electronics

Arachne is powered by a combination of standard robotics components, with a focus on modularity and accessibility. The robot's brain is an ESP32-CAM, a microcontroller with built-in Wi-Fi capabilities and an integrated camera module. This allows for basic image processing and remote connectivity. The ESP32-CAM is programmed using the Arduino IDE, which facilitates the implementation of both servo control and facial recognition functionality.

Key electronic components (see fig. 2):

- ESP32-CAM module: Controls the camera and runs the facial recognition algorithm.
- MicroSD card: Stores reference images of known users.
- Servo driver board (PCA9685): Controls all 18 servo motors via PWM signals.

- Power supply: Typically a battery pack capable of delivering sufficient current for both logic and motors.
- Wiring and PCB layout: Designed for compactness and minimal signal interference. The robot is wired in such a way that the ESP32 can send movement commands based on recognition results. The servo motors receive timed pulse-width modulation (PWM) signals that dictate the angle of rotation for each joint, thereby coordinating leg movements during gait cycles.

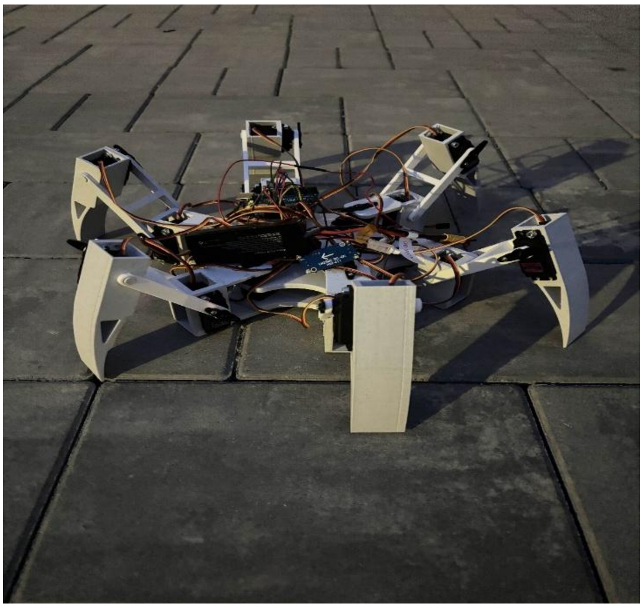

Fig. 2. Arachne in real life

5. Facial Recognition Integration

One of Arachne's distinguishing features is its facial recognition functionality. While many robotic platforms focus solely on movement, Arachne integrates computer vision for interactive behavior. The ESP32-CAM captures an image and compares it with stored images on the microSD card. If a match is found (based on vector similarity or threshold comparison), the robot moves forward. If no match is detected, the robot retreats or remains stationary.

This behavior was designed to simulate familiarity and alertness, similar to how living creatures respond differently to known and unknown individuals. Although the processing capabilities of the ESP32-CAM are limited compared to full AI platforms, it handles lowresolution image comparison efficiently. The face registration process involves capturing an ID-style photo of each user and storing it in a predefined dataset. During runtime, the camera scans continuously and processes each frame for facial features.

This system has real-world analogs in airport security, mobile device unlocking, and surveillance. The concept was inspired in part by the software used by Palantir Technologies, where even partially obscured faces can be identified based on machine learning models.

6. Applications and Future Development

Although Arachne was developed primarily as a research and educational tool, its potential applications are significant:

6.1. Security and Military

By replacing facial recognition with environmental sensors (e.g., thermal, gas, metal detection), Arachne could be deployed in military zones to:

- Detect mines or IEDs.
- Locate enemy positions.
- Enter confined or dangerous areas without risking human lives.

Its quiet, leg-based locomotion makes it less detectable than wheeled or tracked robots, especially in rugged terrain.

6.2. Emergency Response

In civilian contexts, Arachne could be outfitted with smoke detectors, heat sensors, or microphones to:

- Locate people trapped in collapsed buildings.
- Identify the source of fire in enclosed or dangerous spaces.
- Guide firefighters by relaying information about interior conditions.

These scenarios benefit from the robot's autonomous movement and programmable response logic, reducing risk to first responders.

6.3. Educational and Research Tool

Due to its modularity and open-source programming environment, Arachne is also ideal for teaching mechatronics, computer vision, and robotics at undergraduate levels. She combines key concepts from mechatronics, computer vision, and robotics in one hands-on platform. Students learn mechanical design and actuator control through the robot's complex leg movements, explore image processing and facial detection using tools like OpenCV, and apply robotics principles such as inverse kinematics and sensor-based decision-making. This interdisciplinary system encourages practical problem-solving, teamwork, and real-world application of theory, making it highly effective for STEM education. Inverse kinematics (IK) is a fundamental concept in robotics used to calculate the joint angles needed to move a robot's limbs to a specific position in space. In simpler terms, it's the process of figuring out how to move a robot's joints so that the end point—like a foot, hand, or sensor—reaches a desired location. In a hexapod robot, each leg typically has 3 degrees of freedom (joints for hip, knee, and ankle), and inverse kinematics is used to determine the exact angles each joint must take to place the foot at a specific point on the ground. This allows the robot to walk smoothly, balance, or adjust its posture dynamically.

7. Challenges and Limitations

Despite its promising features, Arachne has several limitations:

- Limited processing power: The ESP32-CAM cannot handle complex image analysis or multi-face databases efficiently.
- Servo fatigue: Continuous use can lead to overheating, especially under load.
- Battery constraints: High torque servos draw significant current, requiring a robust power system.
- Recognition sensitivity: Poor lighting or partially visible faces may reduce accuracy. These issues point to areas of future improvement, such as:
- Upgrading to Raspberry Pi or NVIDIA Jetson for AI tasks.
- Integrating LiDAR or ultrasonic sensors for better environmental awareness.
- Using lightweight carbon or 3D-printed materials to improve mobility and endurance.

8. Conclusion

Arachne showcases the integration of biomimetic design and intelligent behavior in a compact, mobile platform. With its spider-like agility and interactive vision system, the robot is not only a proof of concept for future applications but also a model for interdisciplinary collaboration in robotics. The project highlights the feasibility of using accessible components to build complex systems with real-world implications.

By combining motion control, computer vision, and embedded programming, Arachne represents a meaningful step forward in the field of autonomous robots designed for both interaction and exploration.

9. Bibliography

[1] Çavaş, M., & Ahmad, M. B. (2019). A review on spider robotic system. International Journal of New Computer Architectures and Their Applications (IJNCAA) Vol, 9, 19–24. (https://www.zotero.org/google-docs/?QDS2t6)

[2] Sun, C., Yuan, M., Li, F., Yang, Z., & Ding, X. (2019, February). Design and simulation analysis of hexapod bionic spider robot. In Journal of Physics: Conference Series (Vol. 1168, No. 2, p. 022094). IOP Publishing.

[3] Uddin, M. I., Alamgir, M. S., Chakrabarty, J., Hossain, M. I., & Samy, M. A. A. (2019, November). Multitasking spider hexapod robot. In 2019 IEEE international conference on robotics, automation, artificial-intelligence and internet-of-things (RAAICON) (pp. 135-140). IEEE.

[4] Meddeb, H., Abdellaoui, Z., & Houaidi, F. (2023). Development of surveillance robot based on face recognition using Raspberry-PI and IOT. Microprocessors and Microsystems, 96, 104728

[5] Phan, D. K., Tran, P. N., Pham, N. T., Le, T. H. T., & Dang, D. N. M. (2024, February). Innovative Multi-Modal Control for Surveillance Spider Robot: An Integration of Voice and Hand Gesture Recognition. In Proceedings of the 2024 9th International Conference on Intelligent Information Technology (pp. 141-148).

[6] Cruz, C., Sucar, L. E., & Morales, E. F. (2008, September). Real-time face recognition for humanrobot interaction. In 2008 8th IEEE international conference on automatic face & gesture recognition (pp. 1-6). IEEE.

[7] Korkmaz, E. E. (2023). Smart Borders. In Smart Borders, Digital Identity and Big Data (pp. 6886). Bristol University Press.

[8] Youvan, D. C. (2024). Tech Titans and the Surveillance State: Examining Support for Public Surveillance Among US Technology Leaders.

[9] Pele, A., & Mulholland, C. (2023). On Facial Recognition, Regulation, and" Data Necropolitics". Ind. J. Global Legal Stud., 30, 173.

RB2501 – ARTICULATED ARM ROBOT WITH THREE DEGREES OF FREEDOM

DINICĂ Bogdan-Andrei, CÎRJA Rareș, IVAN Andrei Mario (Conducător științific)

Faculty: Industrial Engineering and Robotics, Specialization: Mechatronics and Robotics, Year of study: I, email: bogdandinica2@gmail.com

ABSTRACT: RB25012 is a 3D printed articulated arm robot prototype, based on a closed kinematic chain and an electromagnetic end-effector. Its mechanical structure mimics those of industrial robots used in palletizing applications, meaning that the system integrates a triad linkage ensuring the end-effector maintains parallelism with the base plane, as well as a parallelogram structure used to drive the second link of the arm. This approach simplifies the control while also increasing the load stability. Unlike industrial robots, RB2501 does not have a fourth numerically controlled axis, further simplifying the movement.

KEY WORDS: articulated arm robot, electromagnet, closed kinematic chain, 3D printed.

1. Introduction

The automatization of industrial processes has been quickly developing during the past decades, continuously growing the demand for robotized solutions, due to their reliability and efficiency. This thesis takes the idea of an industrial robot, and simplifies both its mechanical and electronic systems.

The mechanical system is designed using modern CAD software and materialized through additive manufacturing techniques. This methodology enables rapid iteration, quick response to real-world testing, and enhanced customization capabilities.

The control of the robotic system is managed by a Raspberry Pi Pico microcontroller, programmed in Arduino. The microcontroller was chosen due to its higher feasibility than an Arduino Nano board.

Lastly, a graphical user interface has been programmed, as it enables the user to have more intuitive control of the manipulator, while also offering the alternative of teach-in programming.

The purpose of the paper is to apply and expand the knowledge acquired at university, using it in the design and complete realization of a compact automation system.

2. Current state

In modern industry, palletizing robots, often based on closed kinematic chains, represent the pinnacle of automation in logistics and manufacturing. Unlike conventional open-chain manipulators, these industrial robots make use of parallel or hybrid serial-parallel mechanisms to provide higher rigidity, payload capacity and positional accuracy. These particularities make them suitable for efficient and precise palletizing tasks [1].

Recent advancements focus on the implementation of advanced algorithms, including AI-based approaches, used to control the robot and generate real time trajectories. This enables optimal paths, adaptive force control and advanced collision avoidance. Modern robotic cells are equipped with 2D or 3D cameras and LIDAR units to integrate dynamic object detection algorithms into palletizing applications, allowing complex tasks, such as mixed palletizing, to be performed.

Leading manufacturers such as ABB, Kuka, Fanuc and Yaskawa-Motoman are at the forefront of deploying these advanced palletizing solutions.

3. Project implementation

The robot has been assembled and is in functional condition, both with regard to the mechanical construction and with regard to the electronic circuits and the programming of the microcontroller, as well as the graphical interface.

For the robot's mechanical construction, two articulated mechanisms based on parallelograms, specific to palletizing robots, are used. The first is the closed kinematic chain, represented by a parallelogram that drives the second segment and serves to reduce the weight applied to the supporting structure and to facilitate the control of the arm. The second mechanism consists of two parallelograms, which serve to keep the robot's flange parallel to the base plane, which constitutes the fourth degree of freedom, passive, eliminating the need for an additional motor.

The robot's operational capabilities have been enhanced by a simplified, yet effective end-effector, being represented by an electromagnet, which can simulate the action of a vacuum gripping system.

The mechanical system is designed in Autodesk Fusion, realized through FDM 3D printing [2], and the robot is controlled using a Raspberry Pi Pico programmed in Arduino and a graphical user interface (GUI) application developed in Python.

3.1. Mechanical structure

The articulated arm (represented in Fig. 1) is comprised of two links, having a bilateral symmetrical disposal of the joints, and it is placed onto a rotating base. The mechanical system is based on industrial principles, the most important being: the closed kinematic chain and the system based on two parallelograms joined through a triad.

Fig. 1. RB2501

The closed kinematic chain (Fig. 2) implies a mechanism, which allows the third motor to be placed on the rotating platform, with the aim of easing the industrial process through two main advantages. The first advantage is represented by positioning the center of mass at a low height, lightening the arm – facts that contribute to a high stability of the robot. The second important advantage is constituted by the simplified kinematic model, in comparison with the open kinematic chain. This is due to maintaining the inclination of segment 2 relative to the ground when only the second motorized joint is actuated, the third remaining stationary [3].

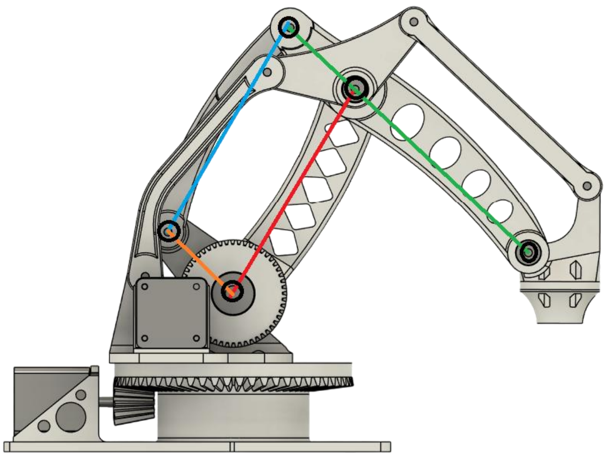

Fig. 2. Closed kinematic chain

The articulated mechanism (Fig. 3), formed by two parallelograms joined by a triad, adds a fourth degree of freedom (pitch orientation), yet without the need for an additional motor, keeping the flange parallel to the base regardless of configuration. This mechanical particularity helps both by simplifying control and the kinematic model, and by lightening the arm. In addition, the absence of the motor also involves an increase in the positioning precision of the end effector, eliminating potential control errors.

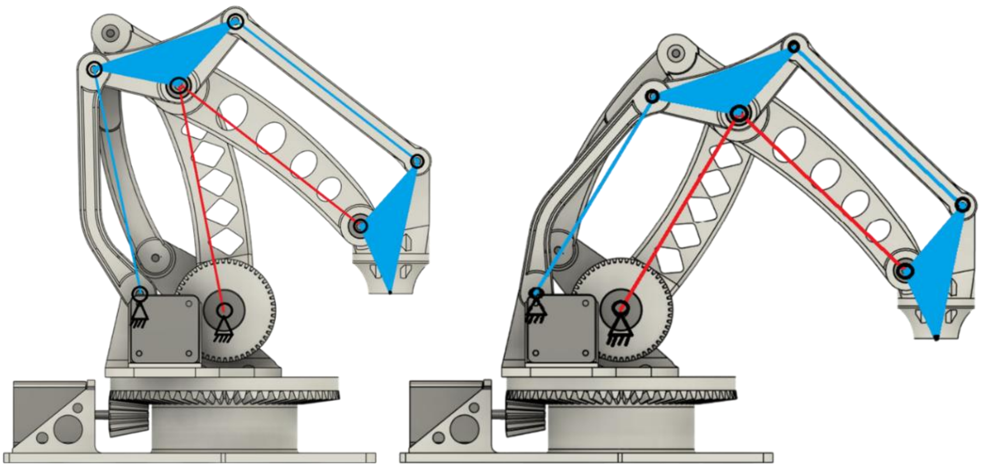

Fig. 3. Parallelogram structure

All active joints are driven by stepper motors, through gearings. The first joint (base rotation) is actuated via a bevel gearing (Fig. 3), the driver gear having 10 teeth and the driven gear having 60 teeth (therefore, a 6:1 ratio). The type of gears was chosen in order to allow the placement of the motor onto the fixed base plate, without further rising the rotative base.

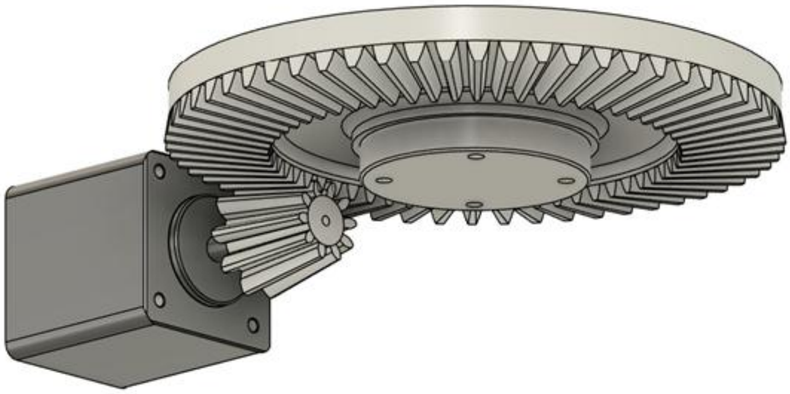

Fig. 4. Bevel gearing

The second and third links are driven through helical gearings (Fig. 4), the driver gear having 13 teeth and the driven gear having 52 teeth (generating a 4:1 ratio). This allows a smoother power transfer between teeth, translating into a quieter transmission, capable of higher loads compared to a similar spur gear.

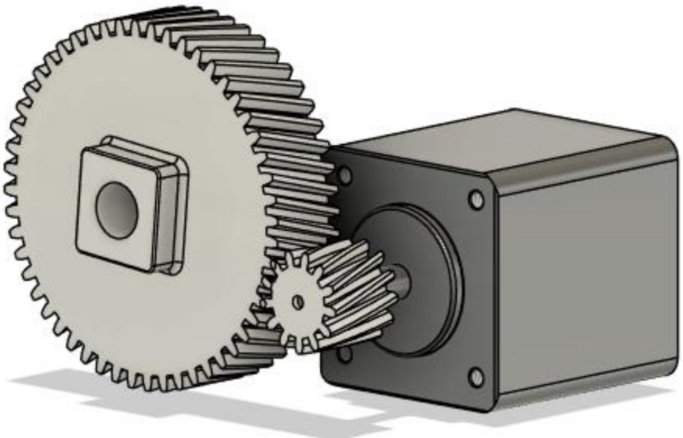

Fig. 5. Helical gearing

3.2. Electronics

The microcontroller chosen for this application is a RaspberryPi Pico, due to its high speed (133MHz) and advanced functions for many of its GPIO pins.

For the actuation system, three NEMA 14 stepper motors are being used, controlled via TMC2209 v3 drivers, featuring silent control and two-way communication. The drivers are attached to the microcontroller through single-wire UART communication (software serial pins on the Pico, as it only has two hardware serial ports).

To close the feedback loop, AS5600 magnetic encoders have been mounted onto the motors, communicating with the RaspberryPi through the I2C bus. As the sensors are hardcoded with the same adress (0x36), a multiplexer (TCA9548A) must be used, in order to switch between the three encoders.

For the electromagnetic end-effector, a generic H bridge DC motor driver has been used, in order to modulate its voltage (through PWM). This is needed because of the high heat produced by the electromagnet at 12V, with the aim of preventing any damage to either itself or surrounding PLA parts.

The entire circuit (Fig.6) is powered by a 12V DC power supply connected to a 220V AC wall outlet. To power the microcontroller and magnetic encoders, a step-down module is being used to provide 5V DC.

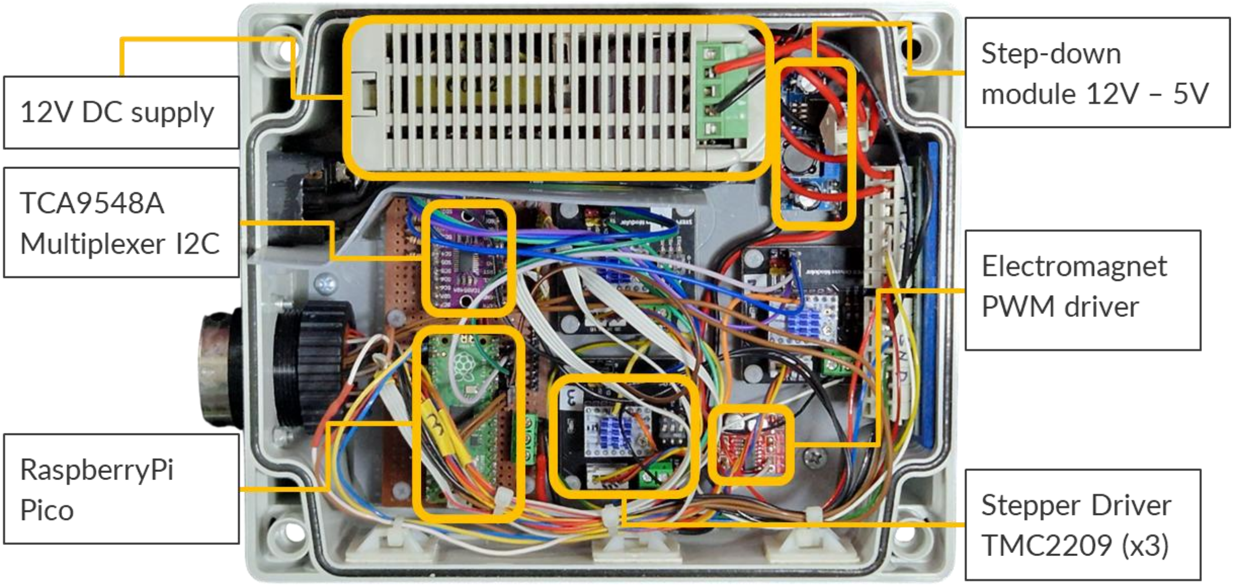

Fig. 6. Electronics

3.3. Programming

The control of the manipulator is done through a graphical user interface (GUI) (Fig. 7), coded in Python and run on a Windows laptop. The application has the task of calculating angles and transmitting them to the microcontroller, through USB serial communication.

The GUI offers two operating modes: *Joint* and *Cartesian*, the latter being achieved by solving inverse kinematics equations. The program also features teach-in programming, via an external window (*Recordings*), with functionalities such as: record, wait instructions, autoplay mode, import/export and direct editing of the program file. When exported, the program is a .bin file that can be later used to import said program into the application.

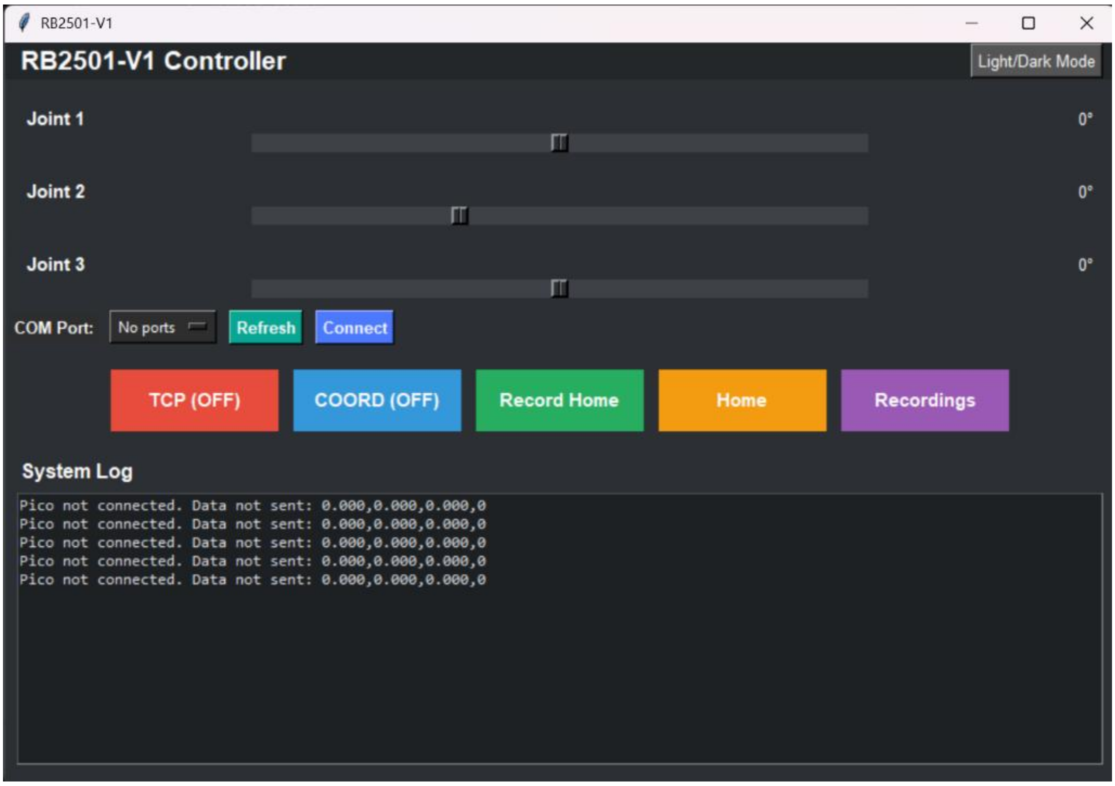

Fig. 7. GUI – main menu

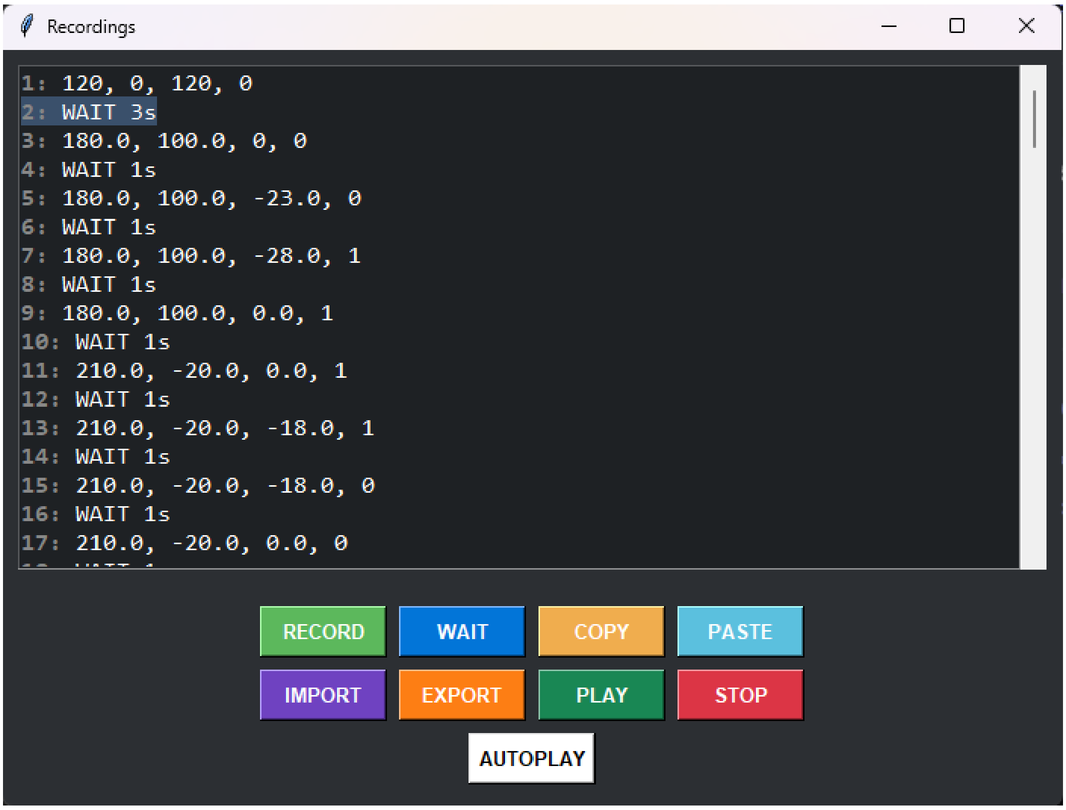

Fig. 7. GUI – Recordings window

The inverse kinematics equations are presented in Fig. 8. Theta1 represents the angle of the first joint (base rotation), theta2 is the inclination of the first link and theta3 is the angle of the second joint, relative to the ground. L1, L2 are the lengths of each link, in this case both equal to 120mm. The function detailed in Fig. 8 converts a cartesian input from the user into a set of three joint values (in degrees), and returns them. [4][5]

```python
def inverse_kinematics(x, y, z):
    theta1 = m.atan2(y, x)
    L = m.sqrt(x ** 2 + y ** 2)
    A = m.sqrt(L ** 2 + z ** 2)
    alpha1 = m.acos((L1 ** 2 + A ** 2 - L2 ** 2) / (2 * L1 * A))
    alpha2 = m.atan2(z, L)
    alpha4 = m.acos((L2 ** 2 + A ** 2 - L1 ** 2) / (2 * L2 * A))
    theta2 = m.pi / 2 - alpha1 - alpha2
    theta3 = alpha4 - alpha2
    return m.degrees(theta1), m.degrees(theta2), m.degrees(-theta3)
```

Fig. 8. IK equations

The Arduino code for the RaspberryPi Pico receives the target angle for each motor from the GUI, via serial bus, and drives the steppers accordingly. To determine their absolute position, the microcontroller commands the I2C multiplexer, which routes the specified sensor, allowing a reading. The code then handles wraparound, counting the total degrees of rotation, and calculates a control signal value (proportional to the motor's speed), based on a PID function (Fig. 9).

```cpp
void calculatePID1()
{
  //Determining the elapsed time
  currentTime1 = micros(); //current time
  deltaTime1 = (currentTime1 - previousTime1) / 1000000.0; //time difference in seconds
  previousTime1 = currentTime1; //save the current time for the next iteration to get the time difference
  //---
  errorValue1 = totalAngle1 - targetDeg1; //Current position - target position (or setpoint)

  edot1 = (errorValue1 - previousError1) / deltaTime1; //edot = de/dt - derivative term

  errorIntegral1 = errorIntegral1 + (errorValue1 * deltaTime1); //integral term - Newton-Leibniz, notice, this is a running sum!

  controlSignal1 = (proportional1 * errorValue1) + (derivative1 * edot1) + (integral1 * errorIntegral1); //final sum, proportional term also calculated here
  controlSignal1 = min(controlSignal1, maxSignal1);
  //Serial.print("Control Signal: "); Serial.println(controlSignal);
  previousError1 = errorValue1; //save the error for the next iteration to get the difference (for edot)
}
```

Fig. 9. PID function

At the beginning of the movement, the PID-generated signal is overwritten by a ramping function, ensuring a smooth movement. The PID controller also ensures that step losses do not influence the robot's precision, as the magnetic encoder tracks real time positions, meaning that even when manually moved out of place, the arm recovers the distance.

4. Conclusions

The RB2501 robot proves the feasibility of creating a small, low cost and reliable robotic arm using 3D printing and open-source electronics. Using a closed kinematic chain and a parallelogram structure, the robot maintains high stability and simplified control without the need for a fourth numerically controlled axis. The use of bevel and helical gearings helps torque transmission and contributes to the smooth and silent operation of the articulated arm.

Regarding the electronics, the use of a RaspberryPi Pico microcontroller, TMC2209 drivers, AS5600 magnetic encoders and TCA9548A multiplexer results in an accurate control system, using feedback-based error correction through PID.

The Python application provides a modular and intuitive experience in both the joint and cartesian modes, also integrating the teach-in method and playback functionality, inspired by industrial robots' programming methods.

This project represents an application of basic knowledge in robotics engineering, combining CAD, mechanical design, electronics and software integration into a functional prototype. Overall, the RB2501 project reached its intended goal: designing and implementing a fully functional robotic arm based on industrial design, using accessible technology and knowledge obtained during the courses and independent research.

In the future, we want to: implement object recognition using a webcam; logical commands into the Recordings window (such as *if*, *while*, *for* statements); the lead-through programming method; improvement of the positioning precision.

5. Bibliography

[1]. Niku, S. B. (2010). Introduction to Robotics: Analysis, Systems, Applications (2nd ed.). Wiley

[2]. Gibson, I., Rosen, D., & Stucker B. (2015) — Additive Manufacturing Technologies: 3D Printing, Rapid Prototyping, and Direct Digital Manufacturing(2nd edition). Springer

[3]. Carbone, G. şi Ceccarelli, M. (2004), "Design Issues for a 3 DOF Spatial Parallel Manipulator", Mechanism and Machine Theory, vol. 39

[4]. Craig, J. J. (2004). Introduction to Robotics: Mechanics and Control (3rd ed.). Pearson Prentice Hall.

[5]. Spong, M.W. şi Vidyasagar, M. (1989), Robot Dynamics and Control, John Wiley & Sons

OBJECT RECOGNITION ALGORITHM BASED ON ARTIFICIAL INTELLIGENCE

Ghinet Andreea Diana, IVAN Andrei Mario(Conducător științific)

Faculty:Industrial Engineering and Robotics, Specialization:RSP, Year of study: IV,
e-mail:ghinet.diana@yahoo.com

ABSTRACT:
This project presents an intelligent pick-and-place system using the xArm5 robotic arm and a 3D IFM O3R222 camera.The system uses artificial intelligence to detect and select the closest object based on 3D depth data.Captured images are processed in Python using the ifm3dpy SDK and OpenCV.A preview of the target object is shown to the user for manual confirmation before the robot executes the action.The control logic is implemented using Python, with optional integration into ROS-based architectures.The OVP800 processing unit streams XYZ and depth buffers for real-time scene analysis.The system uses a vacuum gripper to grasp objects and sort them into appropriate locations.Docker containers were used to isolate the environment and potentially run AI models such as Roboflow or YOLO.The architecture is modular, scalable, and can be extended with full object classification and autonomous decision-making.This work demonstrates the potential of hybrid human–AI collaboration in industrial automation tasks.
KEYWORDS: Roboflow, Python, Object detection, 3D vision, Intelligent robotics.

1. Introduction

In modern industrial environments, the ability to automate object manipulation tasks such as sorting, packaging, or recycling is critical to improving efficiency and reducing human error. Traditional robotic systems often rely on predefined positions or colored markers, which limits their flexibility and adaptability in dynamic environments. As artificial intelligence and 3D vision technologies evolve, there is a growing opportunity to develop smarter, more autonomous systems capable of understanding and interacting with the physical world.

This project was developed to explore and demonstrate an intelligent approach to robotic pick-and-place using real-time depth data and AI logic. The main goal was to build a hybrid system that combines sensor input, automated decision-making, and human-in-the-loop validation to handle unstructured scenarios. By using the xArm5 robotic arm, an IFM O3R222 depth camera, and a modular AI-based control algorithm, the system can detect objects, preview the decision, and execute grasping operations autonomously or semi-autonomously.

I chose this topic because it combines key fields I'm passionate about: robotics, computer vision, and artificial intelligence. It allowed me to learn how to integrate multiple technologies—both hardware and software—and solve real-world challenges in robotic perception, decision-making, and control. The project not only fulfilled academic goals, but also reflected a realistic use case for intelligent automation in logistics or manufacturing.

2. Current status

The object recognition algorithm is currently implemented using a depth-based approach. It processes real-time XYZ and distance data from the IFM O3R222 3D camera and identifies the closest object by analyzing the depth map. The algorithm extracts the minimum Z (depth) value from the scene and computes the corresponding 3D coordinates of the detected object.The selected point is visually marked and previewed using OpenCV. This allows the user to confirm or reject the detection before the robotic action takes place. The algorithm includes logic for preview rendering, coordinate transformation, and command execution for the xArm5 robot.While basic recognition is based on geometric proximity (closest object), the architecture supports future integration of AI-based classification models such as YOLOv8 or Roboflow inference for semantic recognition.

3. Hardware Used

xArm5 robotic arm:

A 5-degrees-of-freedom industrial-grade robotic arm with sub-millimeter precision. Controlled via Python SDK, it is used for grasping and placing objects using a vacuum gripper.

IFM O3R222 3D camera:

A Time-of-Flight camera with 224x172 resolution, capable of capturing accurate depth and XYZ information in real-time (range: 0.3–8m).

OVP800 Processing Unit:

Acts as the main controller for IFM cameras, handling port-to-application assignment, buffer streaming (XYZ, distance), and app configuration (e.g., app1 on port0).

PC with Python + OpenCV + ROS:

Runs the logic: image processing, preview, object selection, robot coordination. Uses ifm3dpy SDK, OpenCV for display, and optionally ROS for more advanced integration.

4. Camera Test Script

To validate the correct configuration and communication with the IFM O3R222 3D depth camera, a dedicated Python script was developed using the ifm3dpy library. The purpose of this script is to initiate a connection to the OVP800 processing unit, request a single frame of 3D image data (XYZ and radial distance), and extract spatial information from the captured frame.

The script begins by creating a connection to the OVP800 device using its IP address (in this case, 192.168.1.235). The connection is established through the O3R object provided by the ifm3dpy.device module. Once the connection is successful, the FrameGrabber is initialized to request specific image buffers: the XYZ coordinate map and the radial distance image. These buffers represent the 3D structure of the scene as seen by the Time-of-Flight camera.

Upon receiving a complete frame via the wait_for_frame().wait() call, the script accesses the raw data using get_buffer(...). Two key pieces of data are extracted:

- the **XYZ buffer**, which contains per-pixel 3D coordinates in meters, and

- the **radial distance image**, which represents the Euclidean distance from the camera to each pixel in the scene.

For test and verification purposes, the script identifies the **central pixel** of the frame and prints its corresponding XYZ coordinates. This allows the developer or operator to assess whether the camera is returning coherent and calibrated spatial data.

```
from ifm3dpy.device import O3R
from ifm3dpy.framegrabber import FrameGrabber, buffer_id
import numpy as np
import cv2

o3r = O3R(ip="192.168.1.235")
fg = FrameGrabber(o3r)
fg.start([buffer_id.XYZ, buffer_id.RADIAL_DISTANCE_IMAGE])
frame = fg.wait_for_frame().wait()

xyz = frame.get_buffer(buffer_id.XYZ)
depth = frame.get_buffer(buffer_id.RADIAL_DISTANCE_IMAGE)

cy, cx = depth.shape[0] // 2, depth.shape[1] // 2
print("Central point coordinates [X, Y, Z]:", xyz[cy, cx, :])
```

5. AI and Docker Usage

One of the key components that enhances the flexibility and scalability of the intelligent pick-and-place system is the use of Docker containers and AI-based object recognition pipelines. These technologies allow the system to be modular, platform-independent, and ready for future upgrades involving advanced artificial intelligence.

Artificial Intelligence Integration

Although the current version of the object recognition algorithm is based on geometric heuristics (e.g., closest object in depth), the architecture is designed to support integration with AI models. Specifically, the system can be extended to include real-time object detection and classification using pretrained deep learning models such as:

- ***YOLOv8*** (You Only Look Once) for real-time object detection
- ***Roboflow API*** for cloud-based or edge-deployed inference
- ***Custom-trained CNN models*** for identifying specific shapes or item categories

Docker Containerization

To ensure compatibility across machines and avoid dependency conflicts, Docker was employed to encapsulate the runtime environment. Docker allows bundling together Python scripts, libraries (such as ifm3dpy, opencv-python, torch), AI models, and network interfaces in a standardized container that can be deployed and run on any host system.

Key advantages of Docker in this context include:

- **Isolation**: The container runs independently of the host system, avoiding version mismatches.
- **Portability**: The environment is easily replicable on different machines (e.g., development laptop, deployment server).
- **Scalability**: Multiple containers can run in parallel, each with specific AI models or camera interfaces.

6. Conclusions

This project demonstrates a functional and scalable intelligent object recognition and pick-and-place system based on real-time 3D perception and modular software architecture. Using the IFM O3R222 3D camera, accurate spatial data was extracted and processed in Python to identify objects in the environment. The xArm5 robotic arm was successfully integrated and controlled to perform autonomous grasping actions based on the processed data.

The algorithm features a hybrid control scheme that combines geometric analysis (based on depth data) with human-in-the-loop decision validation. The preview mechanism allows manual confirmation of the object to be picked, ensuring safety and accuracy in dynamic scenarios. Additionally, the system is prepared for integration with deep learning models such as YOLOv8 or Roboflow, enabling advanced semantic object classification.

Docker containers have been used to isolate and replicate environments, making the system portable and suitable for industrial deployment. Overall, the system provides a solid foundation for future development in intelligent robotic manipulation and can be extended toward fully autonomous sorting platforms.

8. Bibliography

IFM Electronic. (2023). *IFM O3R222 3D Camera Documentation*. Retrieved from https://www.ifm.com

IFM Electronic. (2023). *ifm3dpy Python SDK – API Reference*. Retrieved from https://api.ifm3d.com

UFACTORY. (2022). *xArm5 Robotic Arm Technical Manual*. Retrieved from https://www.ufactory.cc

Roboflow. (2024). *Deploying Object Detection Models with Roboflow Inference Server*. Retrieved from https://docs.roboflow.com

Docker Inc. (2023). *Docker Documentation – Get Started*. Retrieved from https://docs.docker.com

AUTOMATICALLY RELOADED TANK WITH AUTOMATICAL TARGET NEUTRALIZATION (ARTATN)

AGHIANĂ Sebastian-Daniel, COSTEA Dimitris-Mihai, NIȚA Andrei-Cristian, IVAN Andrei Mario (Conducător științific)

Faculty: Industrial Engineering and Robotics, Specialization: Mechatronics and Robotics, Year of study: I, email: dimitriscostea@gmail.com

ABSTRACT: The idea behind this project came from our curiosity about how defense robots could operate autonomously, especially in scenarios requiring constant reloading and targeting. ARTATN—short for Automatically Reloaded Tank with Automatic Target Neutralization—combines multiple robotics domains: a mobile tank base (R1), an intelligent turret (AT1), and a six-axis robotic arm (N2) for reloading. Each subsystem was developed to be modular yet work seamlessly together.

KEY WORDS: efficient, robotic arm, autonomous, 3D printed.

1. Introduction

At the moment, the ammount of threats that directly disrupt important processes happening inside a predefined space is increasing, such that they are uncontrollable by traditional means (systems needing constant manual input), for this problem we have found a solution that can mitigate all the issues presented above, ARTATN. This fully automaticall system is able to defend a predefined space from threats with the help of three components: The mobility system R1, the turret T1, and the reload system which is a multi purpose 6dof robotic arm with the codename N2.

The majority of the parts composing the system has been designed using CAD software and created as a final part through 3D printing. The three components engulf multiple materials: PLA+, PETG, ABS.

The control of the mobile parts, the chassis and the turret, is made posible by the use of an ESP32 microcontroller and a WEMOS D1 R2, while N2 is fully controlled by an ARDUINO UNO R3.

For switching between the running modes of the chassis and turret, and for monitoring the running parameters, the user can connect to the ESP32 microcontroller driving the turret through WIFI, and by using a simple browser window.

Last but not least, the project has had the role of proving not only to other people but to us too that it is possible to create something different that has a simple yet important role contrasting with other automated systems.

2. Current state

In today’s time automatical security solutions for predefined perimeters are limited to phisical objects, electronics, meant to either stop the disturber, or to deter it from interfiering. Unlike these solutions, our resolution has brought us to making a single system that can work in conjunction with the existing ones/or standalone, for more precise and more efficient protection. We want to reduce/eliminate the issue created by the necessity of having multiple elements to a security system, it becoming increasingly large, expensive, and hard to manage, by displacing them with a single set of electronics which single scope is to detect disturbances and through the equipment available, remove or deter them from interfeiring with the space that is defended.

3. Project implementation

At the moment, the project has reached the state of “Functional Prototype”, which we use as a base for studying different use cases and how real world parameters affect the usability and reliability of the whole system.

For reaching this point we have gathered multiple sources of information related to mechanics, electrics, electronics, and security industry such that we can deliver a good finite project that can cover any security need demanded by the user.

For the chassis we have used a complex yet simple design meant to give it great ground clearance for passing over foreign objects and rought terrain. The build is fully modular meaning each component that is structural can be changed for either a different configuration, different electronics or for changing the whole scope of the chassis. The turret that is meant to deter/eliminate the disturbances is directly mounted on the chassis, which encloses the electronics that are necessary for its target seeking and shooting.

The efficient and fast functioning of the system depends on the 6dof arm that reloads it, thus it being tailored to the turret’s necessitiess, having a fast motion sequence that resupplies the turret with ammo.

The different parts of the systems have been designed in different CAD software, R1 in AUTOCAD, T1 and N2 in SHAPR3D, and printed using FDM 3D printing of different materials. As for the programming part of the R1 – T1 system, we used already existing projects which we modified to fit our needs, in the case of R1 implementing autonomous running and colision detection plus data monitoring through the WIFI interface, in the case of T1, the code was changed such that the microcontroller understands different targets [4][5].

3.1. Chassis – R1 :

Serves as the mobile foundation for the defense platform. Designed in AUTOCAD and 3D printed in PLA+ for enhanced structural integrity (tensile strength: 37 MPa), the main structure (represented in Fig. 1) supports a 2.5 kg payload including internal electronics and the turret seen. The modular frame incorporates a two-layer shelf system, mounted on corner rails, allowing the entire electronics bay to slide out as a self-contained unit.

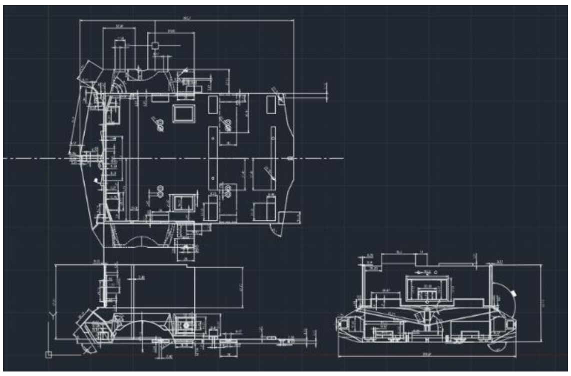

Fig. 1. R1 Main Structure

Propulsion is handled by four 6V DC motors with 1:48 gear reductions, drawing 200 mA each and delivering a combined torque of 2.4 Nm [2]. They are controlled via an L298N dual H-bridge driver, with each side powered through separate channels. Omni-directional wheels mitigate lateral resistance during tank-style turning, preserving gear integrity under load.

An ESP32 microcontroller governs locomotion and user interface. It hosts a Wi-Fi access point (IP 192.168.4.1, port 80) (Fig. 2), serving an HTML-based dashboard with motion controls, speed slider, autonomous mode switch and data monitors. Real-time telemetry from three HC-SR04 ultrasonic sensors is relayed via a logic level converter to adapt their 5V output to the ESP32's 3.3V logic. Power is supplied by an 18V 72 Wh battery feeding multiple LM2596-based step-down converters. These provide dedicated voltages for subsystems: ESP32 and Wemos D1 (5V), turret system (9V), L298N (8V) [1], turret firing (6V), and others. Voltage regulation for level shifting is handled by an AMS1117 [3]. The system is fully operable from any Wi-Fi-enabled browser, requiring only a connection to the onboard SSID and navigating to the ESP32's IP. The interface loads instantly, enabling both manual and autonomous operation. All the wiring connecting the electronics is internal.(represented in Fig. 3).

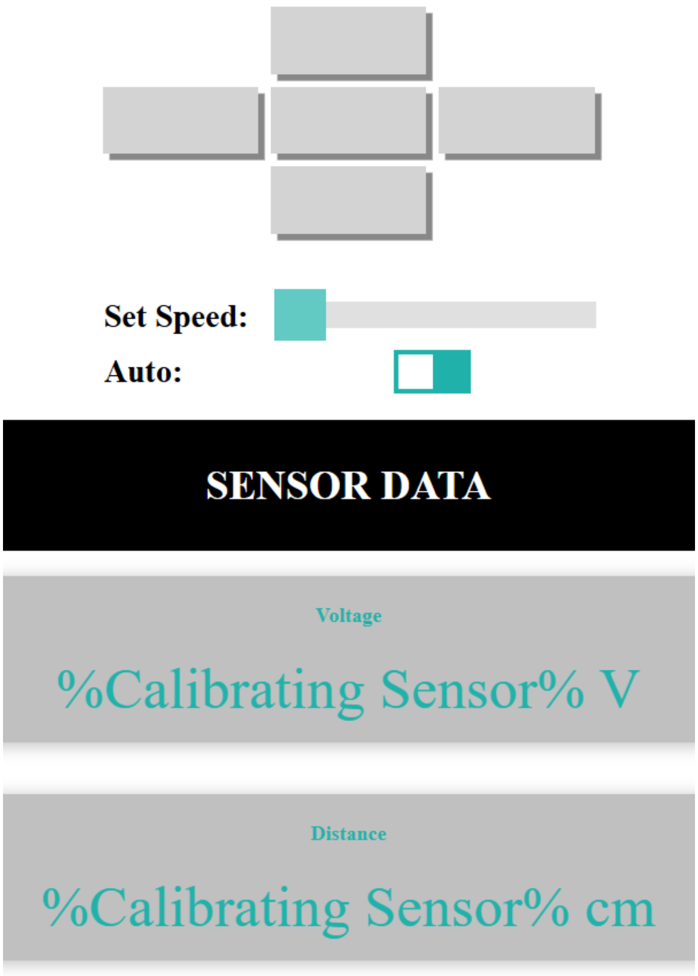

Fig. 2. WIFI Interface

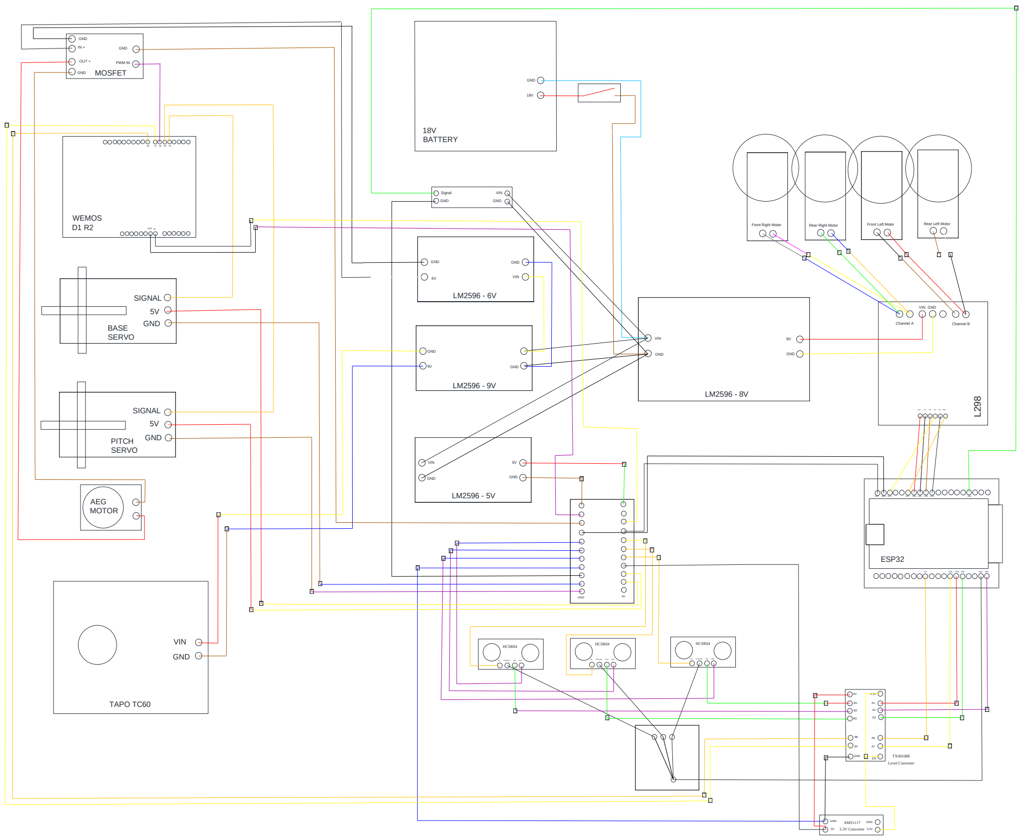

Fig. 3. R1 And T1 Electronics Wiring Diagram

The image above describes all the connections between each component inside the body of R1, on the right we have the driving system formed out of the 4 dc motors and theit driver, commanded by the ESP32 which gets data from the three forward collision detection sensors. The signal from the sensors gets passed through the level converter and fed into the microcontroller. The command pin for their search signal is given by only one pin connected to the ESP and split into three. The center portion mainly consists out of voltage converters feeding each level. The left side consists out of T1's equipment: a laser, two servos, one DC motor for shooting and a mosfet trigger that commands it. Also on the left side, we can find the power source, the 18v battery. All the connections/wire color changes are marked with a rectangle on the diagram so that the user can track each cable accurately.

3.2. Autonomous Turret – T1 :

AT1 is a motorized turret (Fig. 4) mounted on R1(Fig. 5), designed to autonomously detect and neutralize targets (in this case yellow balloons) using computer vision and a projectile-firing AEG mechanism. It is controlled by a Wemos D1 R2 Mini, which receives UDP packets over Wi-Fi and actuates two MG996R [15] servos for yaw and pitch via zig-zag scanning.

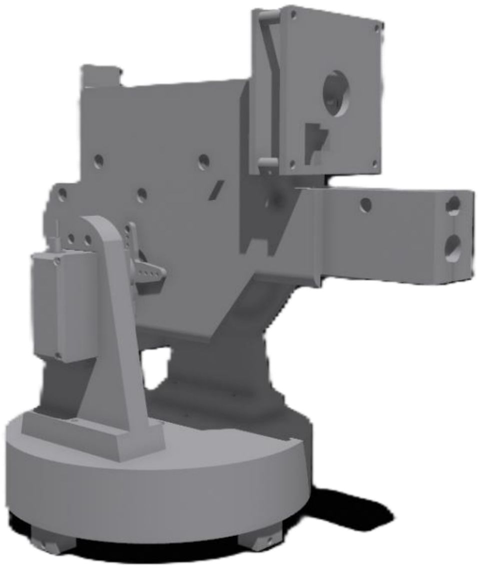

Fig. 4. Autonomous Turret Structure

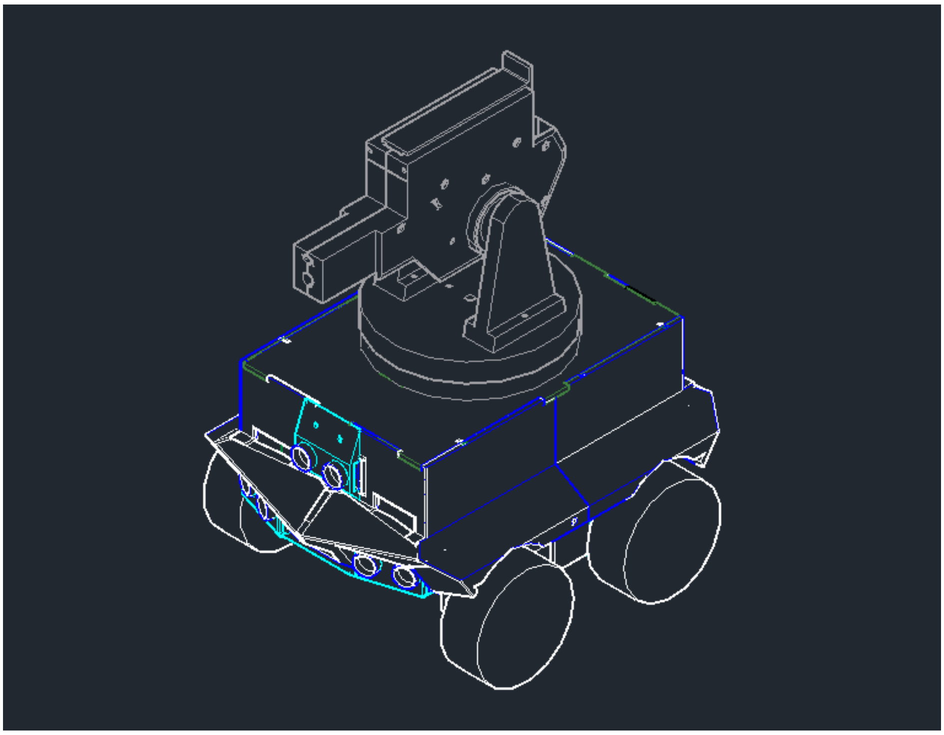

Fig. 5. Autonomous Turret T1 Structure On R1

Target detection is handled by a TP-Link Tapo camera streaming live video to a computer running an OpenCV pipeline. The image is converted to HSV color space, filtered for yellow, and processed to extract balloon contours and positions. A red laser [9] near the barrel provides visual targeting. The system compares the laser dot with the target center, adjusting servo angles frame by frame until alignment is stable, then fires. UDP commands include: yaw(angle), pitch(angle) — aim control, shooter() — trigger AEG motor, stopcar() — stop chassis, laser(on/off), idle() — auxiliary functions

With a frame resolution of 640×480 and 60° FOV, the turret calculates angular offset as: θ_per_pixel ≈ 0.09375°; for a 20-pixel error → ~1.875° correction PID adjustments smooth aiming to within ±5 pixels. The turret's 300 g mass sits ~5 cm from rotation center, requiring ~1.5 kg·cm torque—well within the MG996R's 11 kg·cm capacity, ensuring quick and reliable motion.

3.3. Robotic Arm Reloading System – N2 :

The robotic arm we used in this project, which we named N2, is a custom-built 6-DOF articulated manipulator constructed mainly from PETG filament with 45% infill. It is the successor to our earlier 5-DOF version, nicknamed N1, and features significant upgrades both in mechanical strength and in control flexibility. It uses three NEMA17 stepper motors for the base and upper arm (J1, J2, J3), each with different reduction systems: a cycloidal gearbox [10] [11] (1:10) for J1 and timing belts [12] with 1:18 and 1:6 ratios for J2 and J3 respectively. For the second arm we use one TD8125 for J4 (rotation) at 5v and 3 MG996R at 5V for J5 (pitch) J6 (yaw) and gripper. The arm presents 3 limit switches for the stepper motors to not rotate past certain points,a proximity sensor to detect the tank, a cooling fan for the internals and a purple RGB N2 logo on the back. The complete structure is presented below (Fig. 6).

Fig. 6. N2 Complete Structure

In total, the arm reaches up to 57 cm when fully extended, which is enough to comfortably reach the top-mounted turret and place ammunition inside it. The servos are controlled through a PCA9685 module, while the steppers use DRV8825 drivers connected to an Arduino Uno, with two step-downs, one for 5V and one for 12V powered by a custom built 16V battery, capable of running the entire setup for about 25 minutes. We performed load calculations for the arm to determine its maximum payload under full extension. Based on our simulations, the torque on the second joint (Fig. 7) reaches approximately 3.17 Nm while J3 (Fig. 8) handles around 0.78 Nm. This means the arm can safely carry and maneuver loads up to 200 grams when fully extended without compromising speed or stability. These calculations factored in the distances from joint centers to the centers of mass of each segment, and the cosine law was used in the inverse kinematics solver to determine joint angles needed to reach desired positions in 3D space. The robotic arm's design, while educational in scope, also aligns with real-world practices for industrial robotic control [13] [14].

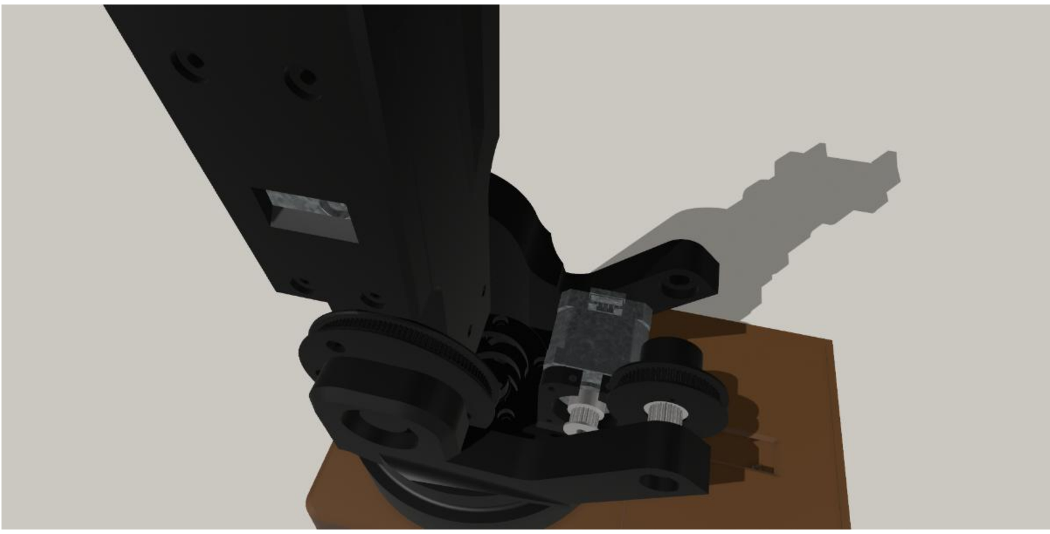

Fig. 7. N2 – Belt System For J2

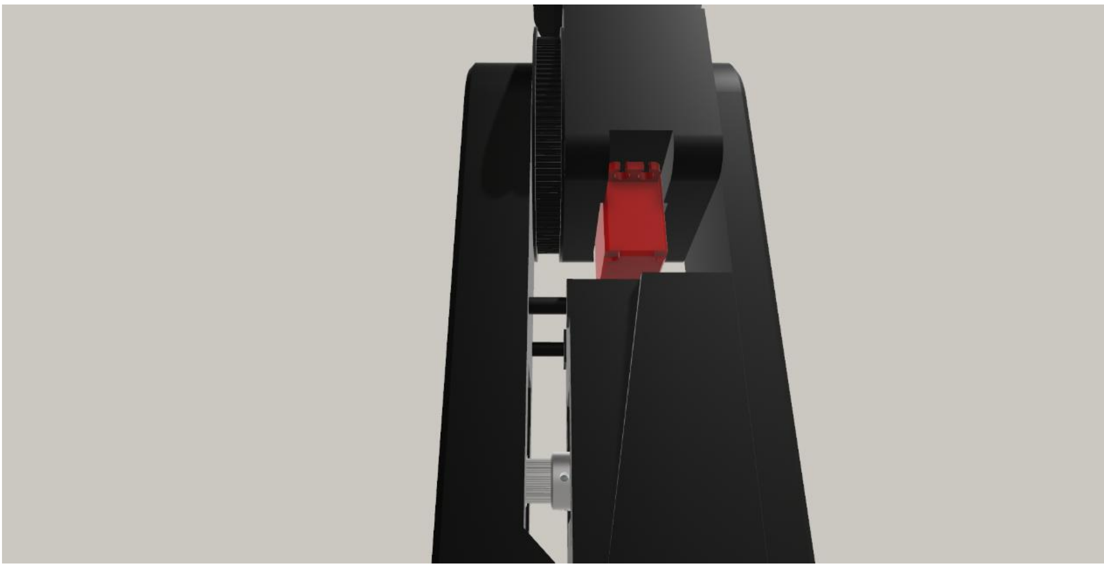

Fig. 8. N2 – Belt System For J3

Geometric dimensions: ground to J1: 5 cm (Fig. 9 and Fig. 10), J1 to J2: 2 cm, J2 to J3: 22 cm, J3 to J4: 0 cm, J4 to J5: 7 cm, J5 to J6: 5 cm, J6 to gripper tip: 8 cm. Movements are computed through inverse kinematics using atan2 and cosine law, enabling precise manipulation, for example [6] [7] [8]:

```
bool inverseKinematics(float x, float y, float z, float &theta1, float &theta2, float &theta3) {
float x_wrist = x - GRIPPER_OFFSET;
float y_wrist = y;
float z_wrist = z;
float r = sqrt(x_wrist * x_wrist + y_wrist * y_wrist);
float s = z_wrist - BASE_HEIGHT;
theta1 = atan2(y_wrist, x_wrist) * 180.0 / M_PI;
float D = (r*r + s*s - L1*L1 - L2*L2) / (2.0 * L1 * L2);
```

```
if (D > 1.0 || D < -1.0) return false; // Out of reach
theta3 = atan2(sqrt(1 - D*D), D) * 180.0 / M_PI;
float phi = atan2(L2*sin(theta3*M_PI/180.0), L1 + L2*cos(theta3*M_PI/180.0));
theta2 = (atan2(s, r) - phi) * 180.0 / M_PI;
return true; }
```

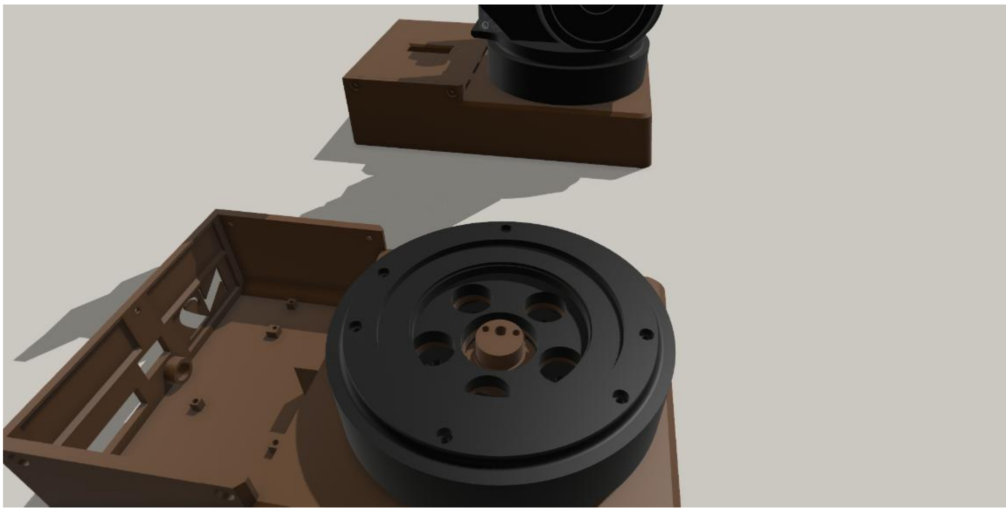

Fig. 9. N2 – Cycloidal Gearbox System (1:10) For J1

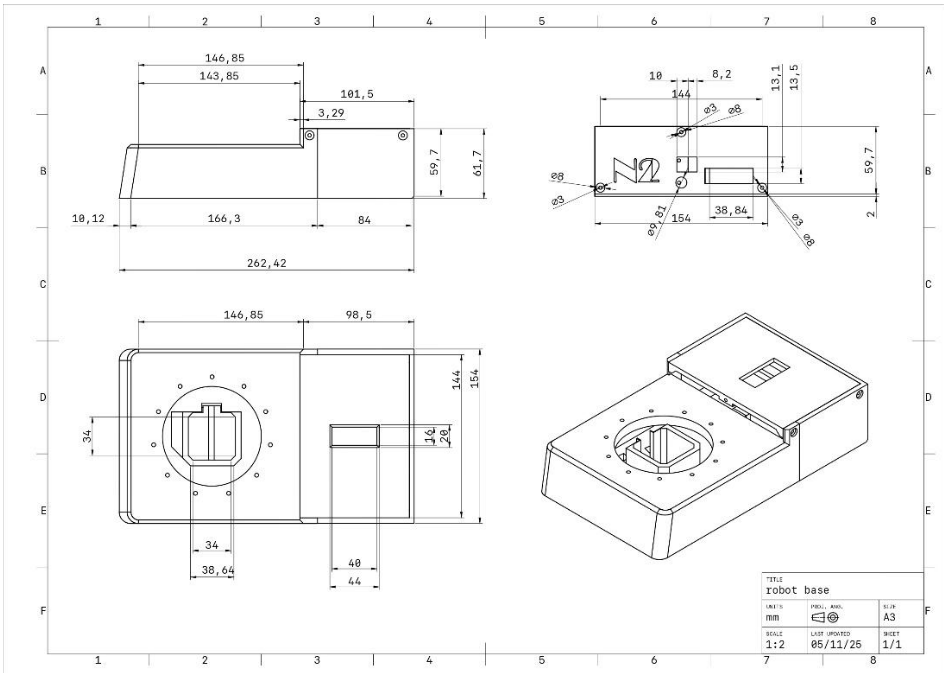

Fig. 10. N2 – Base Structure

4. Equations:

Formula for calculating the power loss of the electronics for defining runtime:

$$P_{dissipated}\,[W] = P_{out} \times \left(\frac{1}{\eta} - 1\right) \quad (1)$$

Formula for calculating the resistance of the main structure for R1:

$$\sigma[N] = \frac{M \times c}{I} \quad (2)$$

Formula for calculating the necessary torque to move the chassis assembly:

$$Necessary\ Torque[N] = (m \times g \times \sin(\theta)) + (m \times g \times \cos(\theta) \times \mu) \times R \quad (3)$$

5. Tables:

Table 1. Calculated Running Parameters

Continuous Power Draw (W)	Continuous Current Draw (A)	Power Draw While Stationary (W)	Current Draw While stationary (A)
47.44	6.88	28.54	4.13

Table 2. Runtime

Battery Parameters	Usage Case	Power Draw(W)	Runtime(min)
72Wh/18V	Continuous	47.44	91
	Stationary	28.54	151
	Stationary + Aim	35.44	122

The tables above decribe the power electronics characteristics in different usage scenarios, first presenting the full instantaneous necessary power and current while running continuously and while stationary, on the other hand, the second one presents how much the TANK will run taking into account those parameters. Aditionally, the last row describes the runtime of the "Shelf" outside the chassis as a standalone unit.

6. Conclusions:

ARTATN is a modular robotics platform that demonstrates how different systems can work together to create a complete solution. With a mobile base, an autonomous turret, and a reloading robotic arm, it mimics real-world automation challenges and solutions.

Looking ahead, we aim to evolve this system into a scalable framework for other robotics applications. Future plans include the development of CNC machining units based on similar motion and control systems, as well as aerial drones equipped with AI modules capable of autonomous navigation and ethical network penetration for security research. These goals represent our desire to contribute to both technical innovation and cybersecurity education.

7. Sources:

[1] https://www.ti.com/lit/ds/symlink/lm2596.pdf
[2] https://media.digikey.com/pdf/Data%20Sheets/Adafruit%20PDFs/3777_Web.pdf

[3] https://www.alldatasheet.com/datasheet-pdf/view/205679/ADMOS/AMS1117.html
[4]https://github.com/un0038998/ElevatingCar/blob/main/Elevating_Car/Elevating_Car.ino
[5]. Tomas H., "Auto Targeting Turret – GitHub Repository", https://github.com/tomash1234/auto-targeting-turret.
[6] J. J. Craig, "Introduction to Robotics: Mechanics and Control," Pearson, 2004.
[7] B. Siciliano, "Robotics: Modelling, Planning and Control," Springer, 2009.
[8] R. N. Jazar, "Theory of Applied Robotics," Springer, 2010.
[9] Adafruit Industries, "Miniature Laser Module Product Sheet," https://www.adafruit.com/product/3777.
[10] What is Cycloidal Drive? Designing, 3D Printing and Testing
How To Mechatronics https://www.youtube.com/watch?v=OsS9-FzKN6s
[11] Cycloidal Drive V3 & Robot Dog Test Leg
James Bruton https://www.youtube.com/watch?v=IVpYtyS5Q-k
[12]https://www.researchgate.net/publication/361301754_Timing_Belts
[13] Inverse Kinematics: a review of existing techniques and introduction of a new fast iterative solver **Andreas Aristidou** **Joan Lasenby** University of Cyprus **University of Cambridge**
[14]https://www.researchgate.net/publication/273166356_Inverse_Kinematics_a_review_of_existing_techniques_and_introduction_of_a_new_fast_iterative_solver
[15] https://www.alldatasheet.com/datasheet-pdf/pdf/1131873/ETC2/MG996R.html

8. Notations:

The following notations have been used:

$P_{dissipated} = Power\ Converted\ To\ Heat\ [W]$;

$P_{out} = Output\ Power\ [W]$;

$\mu = Efficiency\ [\%]$;

$\eta = Coefficient\ Of\ Friction$;

$\sigma = Tensile\ Strenght\ [\frac{N}{m^2}]$;

$M = Bending\ Moment\ [Nm]$;

$c = Distance\ From\ Central\ Axis\ Of\ The\ Plate\ To\ The\ Furthest\ Point[mm]$;

$I = Moment\ Of\ Inertia\ [mm^4]$;

$m = mass\ [kg]$;

$g = Gravitational\ Acceleration\ [\frac{m}{s^2}]$;

$R = Wheel\ Radius\ [m]$;

$\theta = Angle\ [deg]$;

SCARA-Type Robot

STANESCU Razvan, TOMESCU Vlad, ENCULESCU Maria, Andrei Mario IVAN (Conducător științific)

Facultatea: Facultatea de Inginerie Industriala si Robotica, Specializarea: Robotica, Anul de studii: II,
e-mail: razvanstanescu54@gmail.com

We have built a functional model of an industrial SCARA-type robot with an RTRR kinematic configuration, for educational purposes. The project aims to deepen the theoretical knowledge acquired in the studied subjects by applying it in practice.

KEY WORDS: SCARA-Robot, industrial.

1. Introduction

This project presents the development of a functionl model of an industrial SCARA-type robot with RTRR (Rotation – Translation – Rotation – Rotation) kinematic configuration, designed primarily for education purposes. The project was created with the goals of applying theoretical knowledge acquired up to this point for a better understanding of them and later for educational material. The main objective were to understand the operating principles of SCARA robots, to develop skills in designing and assembling component, and to implement an efficient control system, To achieve these goals, we used 3D-printed parts, an Arduino board, a CNC shield, and Nema 17 stepper motors along with a4988 drivers and standardized mechanical elements. For the software we made a GUI application that enables the control of the SCARA robot.

2. Current state

There are already numerous resources and projects available that focus on articulated arm industrial robots that can be used for educational purposes. These include detailed documentation, open-source designs, and programming tutorials. However, SCARA robots, despite being commonly used in high-speed pick-and-place operations and precision assembly tasks, are less documented and explained. While industrial application of SCARA robots are common and well established, accessible information, open-source projects, and educational tools for understanding their specific kinematics and control systems are relatively limited. This lack of resources pushed us to start this project.

3. 3D Printed Parts and Robot Design

The mechanical structure of the SCARA robot was buit usign 3D-printed components, which allowed us to maintain a small overall cost and to iterate through multiple design prototypes. After we decided the axies configuration (RTRR – Rotation, Translation, Rotation, Rotation) and chose the main standardized mechanical elements and the electronics we designed the rest of the parts around them using Autodesk Fusin 360. (Fig. 1) The use of 3D printing not only accelerated the prototyping process but also gave us the flexibility to rapidly implement and test design improvements based on practical constraints.

The robot consists of the following key structural elements: base, rotation joints that features motor mounts and bearing holders to support the each Nema 17 stepper motor, arm that house the gears and transmission belts, and the vertical movement mechanism that consist of a lead screw-driven carriage mounted on linear guide bearings that represents the Z-axis assembly and the gripper.

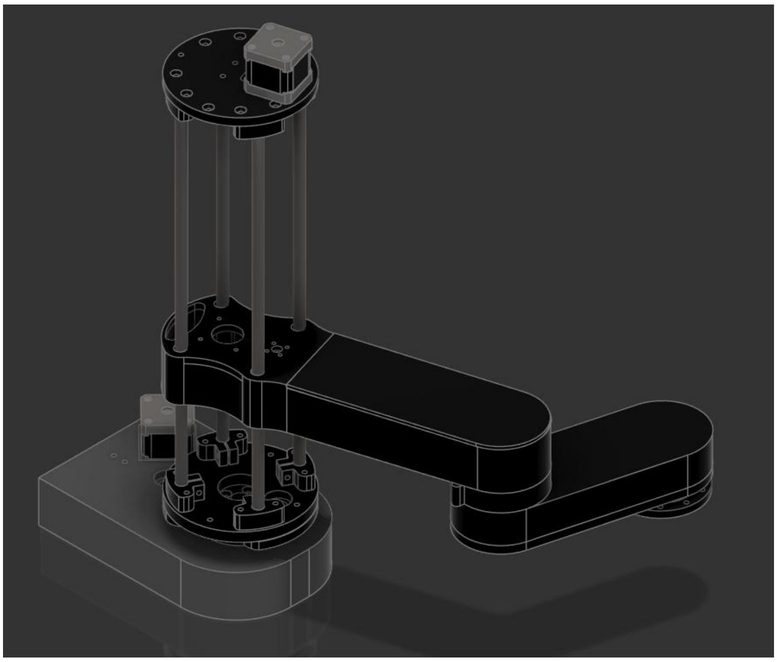

Fig. 1. 3D Model

4. Software

ScaraGUI (fig. 2.) is a Java Swing application made by us that enables control of a SCARA robot through serial communication with an Arduino microcontroller. The toolkit integrates dedicated windows for motor testing, building motion sequences, and monitoring the data exchange.

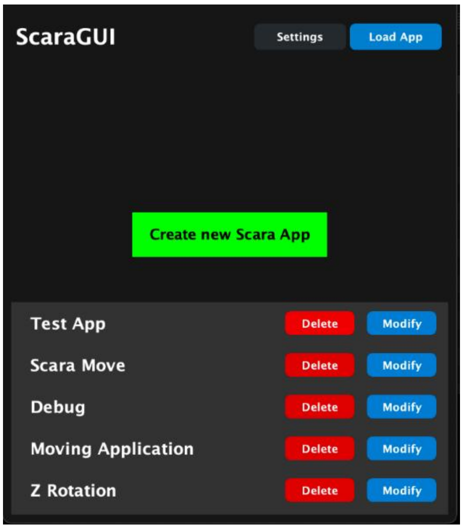

Fig. 2. ScaraGUI landing menu

General architecture main components; scaragui, main window of the application, arduinomanager, handles communication with the arduino, motortestgui, interface for testing individual motors, logviewergui, monitors arduino serial output, and appcreationgui, interface for creating applications (motion sequences); communication with arduino; uses the jserialcomm library for serial communication; communication parameters (defined in serialportparameters): 115200 baud, 8 data bits, 1 stop bit, no parity; and controlled hardware components.

The SCARA robot contains the following controllable components:

Joint1, first stepper motor (stepper1) – base rotation, Joint2, second stepper motor (stepper2) – first arm rotation, Joint3, third stepper motor (stepper3) – second arm rotation, Z, stepper motor for the z axis (stepperz) – vertical movement, and Gripper, servo motor for gripping objects (0–180°).

MotorTestGUI (Fig. 3) allows the user to select a specific motor (joint1, joint2, joint3, z, gripper); control movement (forward/backward direction, number of steps); configure speed and acceleration; homing (calibration) individually or for all motors; keyboard shortcuts (w = forward, s = backward); and safety limit check (e.g., the z axis cannot go below 0).

LogViewerGUI allows the user to displays messages received from arduino in real time; save logs to a text file; optional auto-scroll; and timestamp for every message.

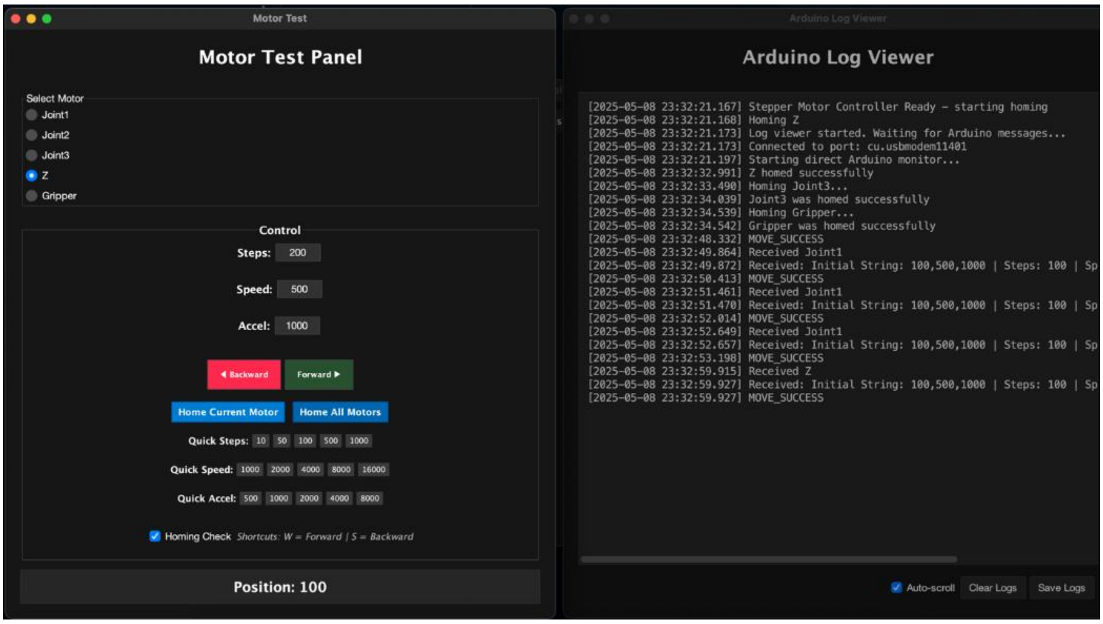

Fig. 3. MotorTestGUI with LogViewerGUI

AppCreationGUI (Fig. 4) allows the user to create and save operation sequences; each operation defines positions for all motors; save/load configurations from yaml files; and sequential execution of operations with visual feedback.

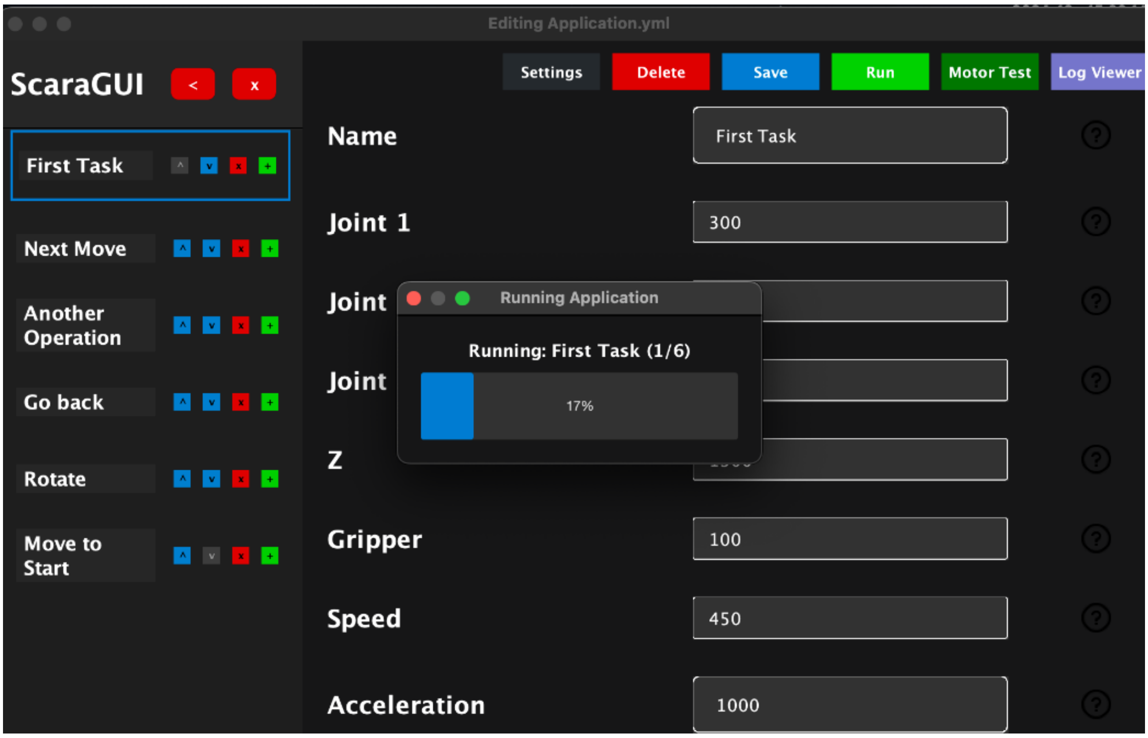

Fig. 4. AppCreationGUI running an application

SettingsGui (Fig. 5) allows the user to discover and list available serial ports; connect/disconnect to the selected arduino device; and save preferred port for future sessions.

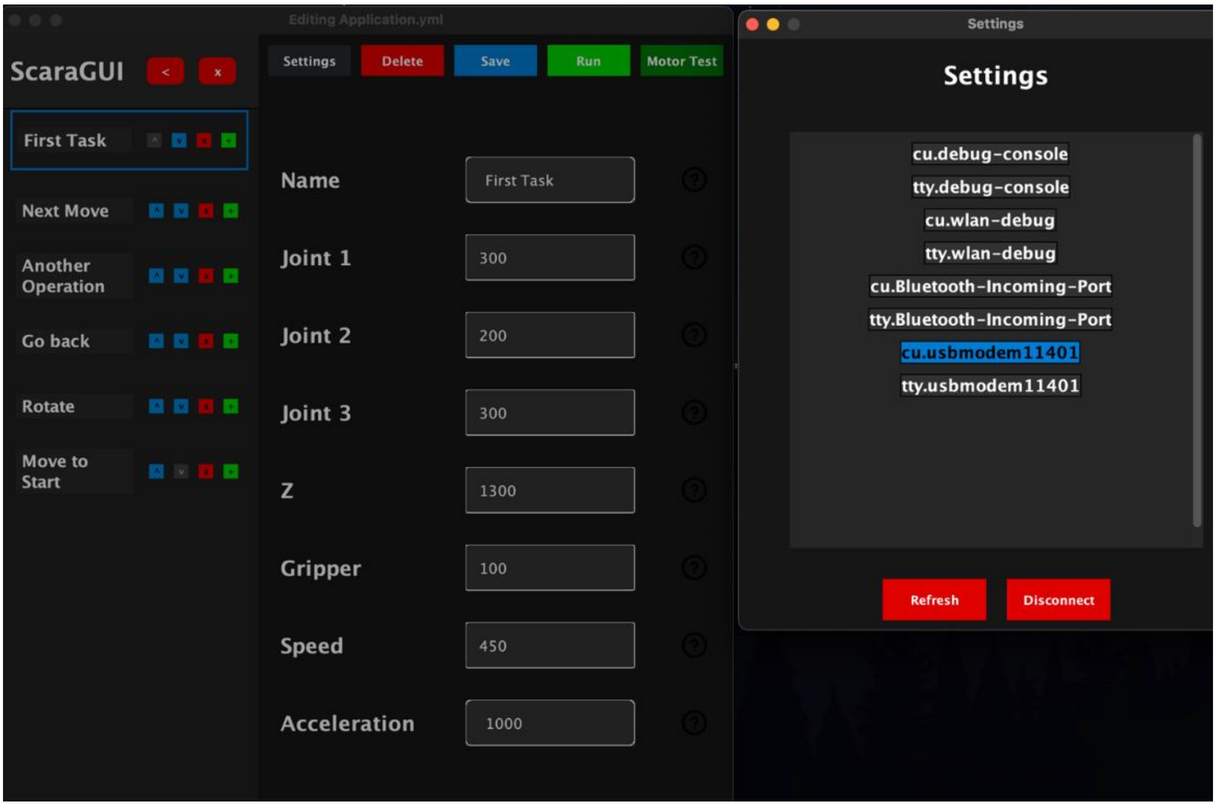

Fig. 5. SettingsGUI with AppCreationGUI together

Commands sent to Arduino direct motor movement:
format: motor:steps,speed,acceleration
example: joint1:100,4000,2000; homing for a specific motor:
format: home:motor
example: home:z; homing for all motors:
format: home; and command for a complete operation:
format: cmd:joint1,joint2,joint3,z,gripper,speed,acceleration
example: cmd:100,200,0,150,180,4000,2000.

Responses from Arduino "MOVE_SUCCESS", the movement was executed successfully, and "MOVE_FAILED", the movement failed (e.g., motor not homed, limit exceeded); informational messages (e.g., "homing z", "z homed successfully")

The Arduino side manages direct control of stepper motors using the accelstepper library; control of the servo motor for the gripper; processing commands received via the serial port; homing operations using limit switches; software limit verification for safety; feedback messages sent back to the java application; and configuration and persistence.

The application uses YAML files for arduinoconfiguration, stores information about the preferred serial port, applicationconfiguration, stores the created applications (operation sequences), and operationmodel, model for individual operations; and running the application.

6. Conclusions

This project focused on the development of a SCARA-type robot with an RTRR kinematic configuration, using accessible components such as 3D-printed parts, Nema 17 stepper motors, A4988 drivers, and an Arduino board. By integrating a custom Java-based graphical interface (ScaraGUI), we achieved a fully functional system capable of executing motion sequences with precise and configurable control.

The software stack of the java project is a compact Maven project written in modern Java 8. Its modular folder structure separates the Swing user interface from the serial-communication layer and from the YAML-based saving system, which makes maintenance and testability more simple.

8. Bibliografie

[1]. https://docs.oracle.com/javase/tutorial/uiswing/index.html
[2]. https://fazecast.github.io/jSerialComm/ - Librarie Conectare Java la Arduino prin Serial.
[3]. https://en.m.wikipedia.org/wiki/SCARA
[4]. https://ro.m.wikipedia.org/wiki/Apache_Maven
[5]. https://forum.arduino.cc/t/using-cnc-shield-v3-directly-with-arduino-ide/1022999/3
[6]. https://docs.arduino.cc/learn/electronics/stepper-motors/

SUKI- THE MAKING OF A ROBOT DOG

1ACSINTE Ana-Maria, 2MIRICĂ Eduard Leonard, 3POSTELNICU Andrei, 4MAHLER Marius-Mihai, IVAN Andrei Mario(Conducător științific)

Facultatea: Inginerie Industrială și Robotică, [1,2]Specializarea: Robotică, [3,4]Specializarea: Robotics, Anul de studii: II, e-mail: ana_maria.acsinte@stud.fiir.upb.ro

Summary: Suki came to life in August 2024 for a competition in China. The initial goal was to assist people with disabilities, including those with visual impairments or mental health issues, by providing support and emotional comfort. It also serves as an ideal companion for individuals allergic to pets, offering a risk-free experience. The project was recently resumed, and we came up with a new purpose for the robot dog, in addition to the previously mentioned ones: to be used in the military, in areas that are difficult for humans to access. We have updated both the programming and the mechanics, including kinematic calculations and electronics.

KEY WORDS: dog, military, service, support, companion

1. Introduction

Suki is a robotic dog developed initially for a competition held in China in August 2024. Its main purpose was to assist people with disabilities, particularly those with visual impairments or mental health conditions. The robot aims to provide emotional support and serve as a safe, hypoallergenic alternative to real pets. More recently, the project was revived and expanded to consider military applications—particularly in environments that are difficult or dangerous for humans to access (Fig. 1).

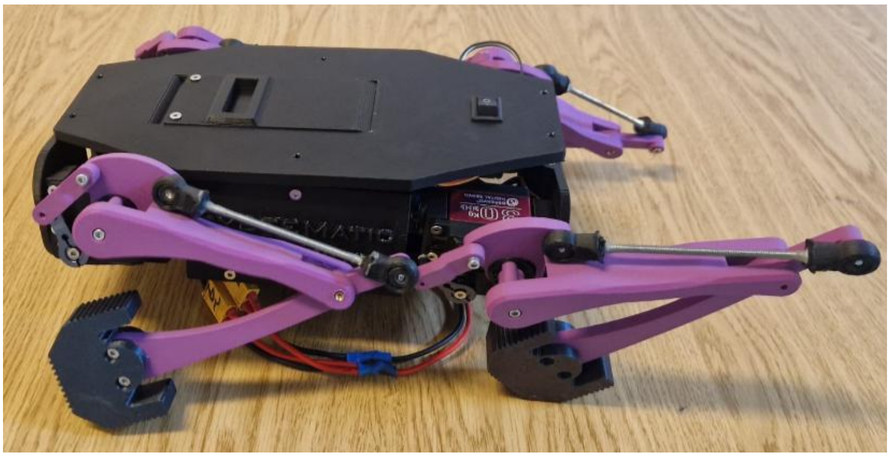

Fig. 1. The robot

2. Development status

Suki's development has involved several technical stages:

- **CAD Design**: The mechanical structure was designed and optimized in Autodesk Inventor and Fusion 360, transforming an initial source of inspiration into a functional, articulated robotic frame (Fig. 2).

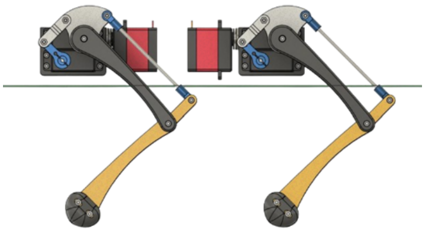

Fig. 2. The legs

- **Hardware Integration**: The robot is powered by 12 DS3218 servo motors, which enable complex leg movements for walking and turning. Control is handled by 2 servocontrollers, and an Arduino UNO who manages sensors and basic logic.

- **Sensors**: Suki is equipped with a pulse sensor (BPM) to interact with the user's biofeedback, and plans exist to integrate more sensors such as cameras, proximity detectors, or facial recognition modules.

- **Structure and Assembly**: Mechanical components were assembled manually using 3D-printed parts and lightweight structural materials (Fig. 3).

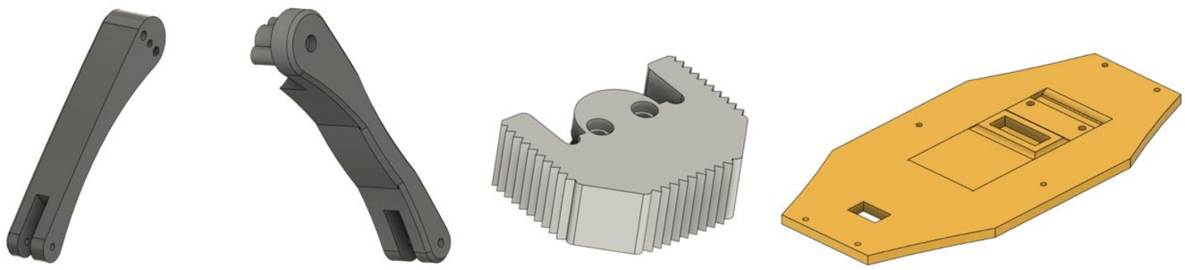

Fig 3. The 3D printed elements

- **Programming**: Suki was programmed in C++, using libraries specific to the servo controllers that we are using (Fig. 3). Currently, there is a program for automatic servo calibration, which also allows for manual position adjustment. Another program detects heartbeats after the user touches the sensors, and there is also a greeting program, which lifts the right front leg and swings it to simulate a wave.

```
#include <SoftwareSerial.h>
#include <CytronServoShield.h>

SoftwareSerial swSerial1(2, 3);
SoftwareSerial swSerial2(10, 11);
CytronServoShield servo1;
CytronServoShield servo2;

// Pozițiile inițiale calibrate pentru stat în picioare
uint16_t pozitii_servo1[9] = {0, 5001, 7001, 7001, 5501, 4001, 6001, 2501, 4001};
uint16_t pozitii_servo2[5] = {0, 5001, 5001, 5001, 5501};
```

Fig. 3. The libraries and the static positions

3. Future improvements

Looking ahead, our primary goal is to make Suki 100% autonomous, capable of acting without any human input. This would involve integrating a broader range of sensors to help it perceive and respond to its environment. For instance, we plan to incorporate color sensors for visual recognition, distance sensors for obstacle avoidance and navigation, and sound modules that allow Suki to bark with emotional context—such as expressing happiness, sadness, or fear, depending on the situation.

To support this increased functionality, we aim to transition from the current Arduino UNO to a Raspberry Pi. While Arduino has been sufficient for basic movement and sensor input, it lacks the processing power, memory, and multitasking capabilities required for more advanced features like real-time sensor fusion, audio processing, and decision-making. The Raspberry Pi would enable the use of machine learning algorithms, complex input/output handling, and a more modular software architecture.

Another major area for improvement is mechanical stability. Currently, the robot's legs place a significant load on the servo motors, especially when attempting to hold a position. This not only consumes more power but also reduces the lifespan of the servos. To address this, we plan to redesign the leg mechanisms by integrating gears and ball bearings, which would distribute mechanical stress more efficiently. This would allow the legs to remain fixed in place without requiring the servos to stay under constant tension, resulting in smoother operation and greater durability.

Finally, we also intend to reuse and optimize the existing sensors—such as the BPM (pulse) sensor—by integrating them more deeply into Suki's interactive behaviors, ensuring that the robot can respond meaningfully to real-time biometric data from its user.

5. Technical Challenges

We encountered a variety of technical issues:

- **Servo Calibration**: Precise movement required extensive manual tuning of angles, and many trial-and-error cycles (Fig. 4).

```
void adjust(int ch, int delta) {
  if (ch >= 1 && ch <= 8) {
    pozitii_servo1[ch] = constrain(pozitii_servo1[ch] + delta, 1000, 9000);
    servo1.position(ch, pozitii_servo1[ch]);
    Serial.print("Adjusted Servo1 "); Serial.print(ch);
    Serial.print(" by "); Serial.print(delta);
    Serial.print(" -> "); Serial.println(pozitii_servo1[ch]);
  } else if (ch >= 9 && ch <= 12) {
    uint8_t c2 = ch - 8;
    pozitii_servo2[c2] = constrain(pozitii_servo2[c2] + delta, 1000, 9000);
    servo2.position(c2, pozitii_servo2[c2]);
    Serial.print("Adjusted Servo2 "); Serial.print(c2);
    Serial.print(" by "); Serial.print(delta);
    Serial.print(" -> "); Serial.println(pozitii_servo2[c2]);
  } else {
    Serial.println("Canal invalid");
  }
}
```

Fig. 4. Manual calibration code

- **Instability**: Achieving consistent balance was difficult, especially when the robot changed direction or shifted weight.

- **Limited Processing Power**: Arduino's limited memory and computational ability created bottlenecks, especially when trying to read sensors while controlling multiple servos simultaneously.

- **Power Management**: Ensuring consistent voltage supply to all 12 servos without overheating or underpowering them was a challenge – In China, for example, due to the high current and voltage required to power all 12 servo motors, we ended up overloading them. As a result, the servos lost precision and their ability to support weight effectively.

- **Code Complexity**: As new features were added (sensor readings, movement sequences, safety conditions), code maintenance became increasingly complex, motivating the transition to a more modular and scalable system on Raspberry Pi.

6. Inverse kinematics

In order to achieve more natural and precise leg movement, the project incorporates inverse kinematic (IK) equations. These equations are essential for calculating the exact angles each servo must reach in order for the robot's leg to move to a specific position in space. The mathematical model was derived using basic geometry and trigonometry, focusing on a 2DOF (degrees of freedom) leg mechanism (Fig. 5).

In the program, these inverse kinematic calculations are used to automate walking cycles. For example, when Suki moves forward, each leg follows a four-step motion sequence:

- Lift the leg up by 40mm

- Move the leg forward by 50mm

- Lower the leg back down by 40mm

- Move the leg back by 50mm

Each leg returns to its original position at the end of the cycle, ensuring balance and repeatability. By adjusting the input coordinates and using the IK equations, we can generate smooth, controlled motion across various terrains. These calculations are essential for synchronizing all four legs and are a key part of our plan to achieve full autonomy in the future.

This approach not only ensures more fluid movement but also allows for real-time adaptation to different walking patterns, such as turning, sidestepping, or climbing over small obstacles. By adjusting the parameters of the step (height, stride length, timing), we can easily customize the gait depending on terrain or user commands. In future iterations, we plan to integrate feedback from IMU sensors (inertial measurement units) and force sensors on the legs, allowing the robot to dynamically adjust its posture and maintain balance even on uneven surfaces. This would mark a major step toward biomimetic locomotion, bringing Suki closer to the natural movement of a real quadruped.

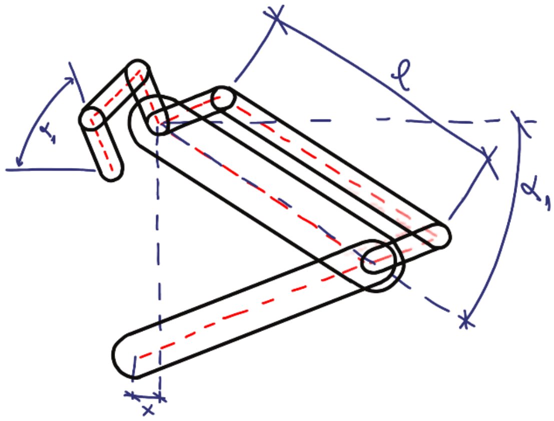

7. Conclusion

Suki is a unique blend of assistive technology and emotional robotics. It aims to provide help and companionship in civilian life while offering real potential for use in search-and-rescue and military operations. The combination of CAD design, robust hardware, and expanding software makes it a strong foundation for future development. While the team faced notable technical obstacles, the project has laid the groundwork for an intelligent, adaptable robotic companion with real-world impact.

7. Bibliografie

[1]. Instructables- 3D Printed Robot Dog

SCANNER 3D

GUȚESCU Robert Andrei, IVAN Andrei Mario(Conducător științific)
Faculty: Industrial Engineering and Robotics, Specialization: Mechatronics and Robotics, Year of study: I, email: gutescur@gmail.com

ABSTRACT: The GRBL OpenScan project is an automated photogrammetry scanning tool, a unique adaptation of the open-source project OpenScan. It stands out for its cost-effective approach, utilizing cheaper components while maintaining the scan quality of the original project.

KEY WORDS: 3D Scanner, Photogrammetry, GRBL, 3D printed.

1. Introduction

Photogrammetry is the science and technology of obtaining reliable information about physical objects and the environment by recording, measuring, and interpreting photographic images and patterns. It is used to extract three-dimensional measurements from two-dimensional data.

This project uses a high-definition webcam mounted on a semicircle that orbits around the object to be scanned and rotates on a revolving plate. Thus, the camera can capture images from any point relative to the object.

The semicircle and revolving plate are driven by 2 NEMA-17 stepper motors, which are controlled by stepper drivers on a GRBL shield mounted on an Arduino Uno.

The paper aims to apply and expand the knowledge on automated photogrammetry and its use cases.

2. Current status

OpenScan, a modular 3D scanning project, is currently actively maintained and has evolved significantly since its inception. OpenScan's firmware, hardware plans, and documentation are publicly available, allowing for modifications and custom builds. Ongoing development includes new firmware updates and hardware integrations, such as the Arducam 16MP camera with focus control. An optional cloud-based processing service, funded by community support, provides users with an automated pipeline for processing scans.

3. Project implementation

3.1. Mechanical structure

The semicircle (represented in Fig. 1) slides through a curved path and is driven by the stepper motor with a cog wheel that drags the teeth on the side of the semicircle.

Fig. 1. Semicircle

The revolving plate (visible in Fig. 2) rotates the object around its yaw axis and is directly connected to the other stepper motor.

Fig. 2. Revolving plate

3.2. Electronics

The microcontroller chosen for this application is an Arduino Uno with a GRBL shield programmed with a modified version of GRBL firmware. This modification allows the CNC machine to execute homing on a single axis.

For the homing system, a microswitch (Fig. 3) is mounted at the maximum travel limit of the semicircle. This prevents the camera module from colliding with the scanner's body and sets the absolute zero position before each scan.

A power supply provides 12V 3A to the Arduino, shield, drivers, and motors. The camera is powered via USB.

The computer software communicates with the Arduino via one USB connection, and another USB connection directly to the webcam for the image stream.

Fig. 3. Limit switch

3.3. Software

GRBL is open-source software or firmware that enables motion control of CNC machines. It uses G-CODE to receive information about movement, destination, speed, etc.

The computer application (Fig. 4) allows the user to select and connect to an Arduino board via serial communication, select and preview the webcam for manual focus, select the desired number of pictures to be taken, and finally click the "Scan" button, which will start generating the positions and sending them to the Arduino as G-CODE. The camera will capture an image for each stopping point and save it in a default location ("[…]/Pictures").

The program computes points on a Fibonacci sphere, giving a uniform distribution of directions in 3D space. Each point on the graphical representation (Fig. 5) represents a desired camera orientation or position relative to the scanned object. Each 3D point is converted to angles using inverse kinematics (IK). Once joint angles are calculated, they are translated into G-code commands (G0 X... Y...) that move each axis to the corresponding angle or position.

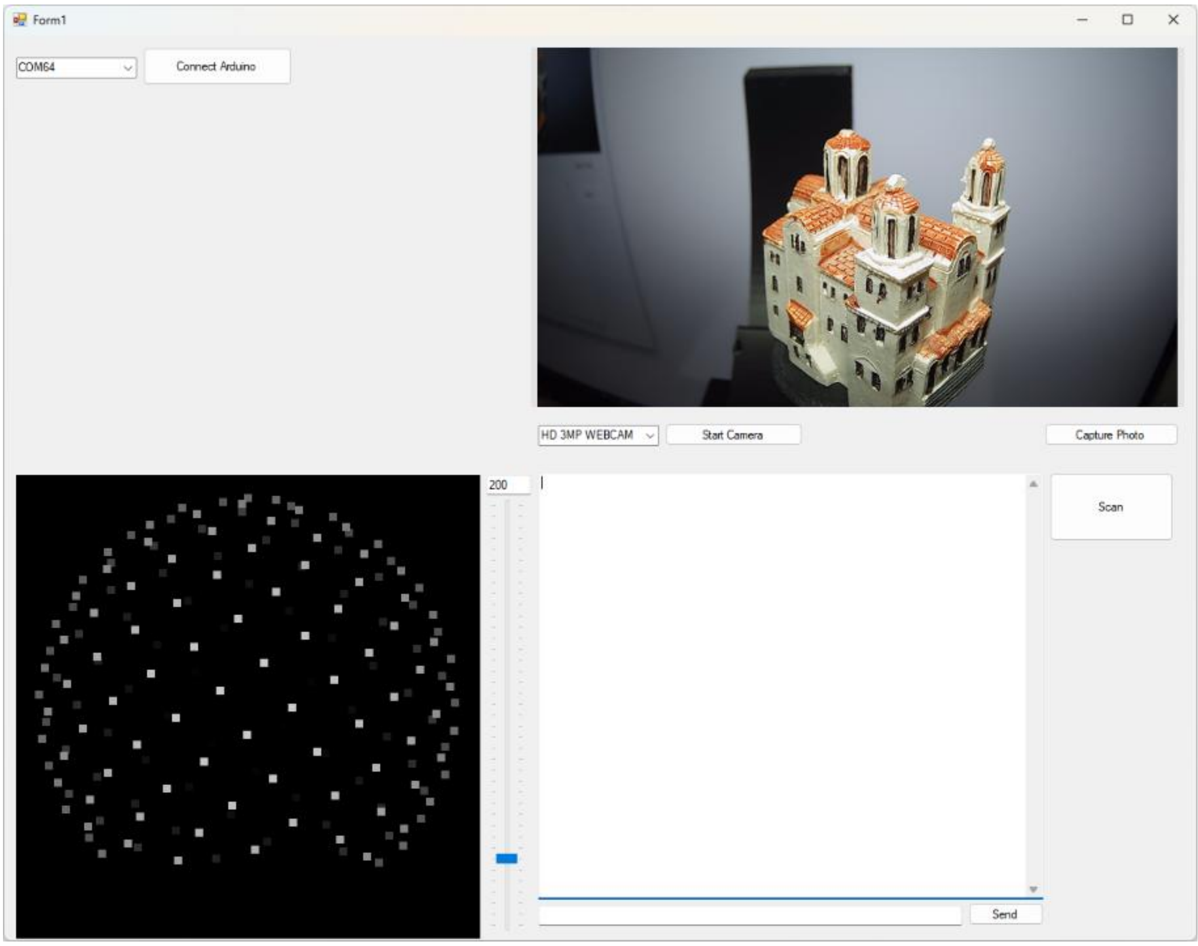

Fig. 4. WinForms Application and GUI

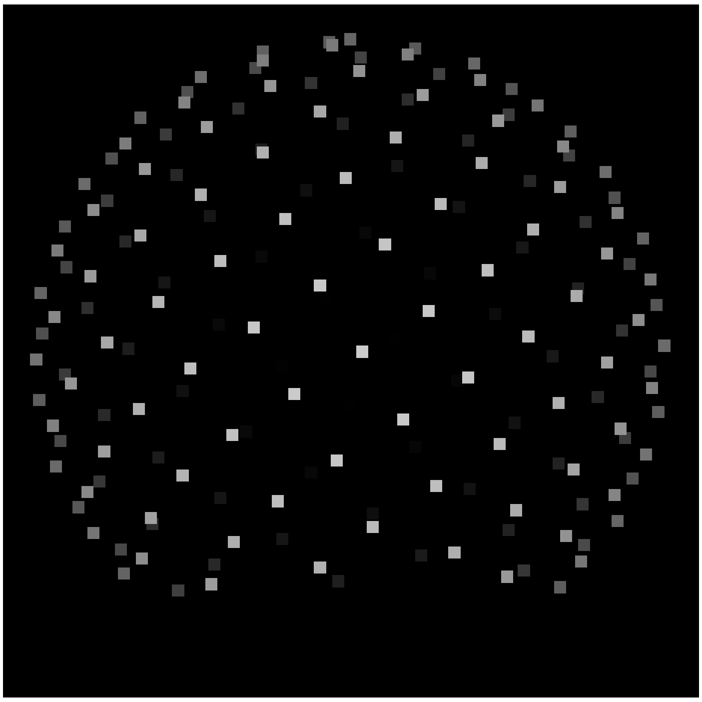

Fig. 5. Graphical Fibonacci Sphere

After capturing all images of an object, third-party software can be used to generate the virtual 3D object as a digital file (Fig. 6).

Fig. 6. Final 3D scan

4. Conclusions

The GRBL OpenScan (Fig. 7) project demonstrates the practicality of creating a small, low-cost, and reliable 3D Scanner using 3D printing and open-source electronics. The scanner achieves high-quality 3D scans using a consumer-grade webcam and a simple structure.

Regarding the electronics, using an Arduino Uno instead of a Raspberry Pi 4B microcontroller and a generic webcam instead of the Arducam IMX519 considerably reduces the price of this scanner.

The WinForms application provides an intuitive experience as simple as plug-and-play, ensuring a user-friendly interaction with the scanner.

This project represents applying basic knowledge in photogrammetry, mathematics, CAD design, electronics, and software integration into a functional prototype. Overall, the Scanner 3D (GRBL OpenScan) project reached its intended goal of designing and implementing a fully functional automated photogrammetry device using accessible technology and knowledge from independent research.

In the future, the GRBL OpenScan project aims to enhance the WinForms application for an even better user experience, reduce the number of I/O from 3 to 2 (one USB and one for power supply), add a white LED ring around the camera, and integrate the software with a 3D scan generation API.

Fig. 7. GRBL OpenScan

5. Bibliography

[1]. https://github.com/OpenScan-org/OpenScan-Design
[2]. https://github.com/grbl/grbl

HUMAN HAND

NEACȘU Lorena-Elena, MORARU Ștefan and IVAN Andrei Mario(Conducător științific)

Faculty of Industrial Engineering and Robotics, Specialization: Robotics, Year of Study: I
E-mail: lorenaneacsu205@gmail.com

Summary: Human hand is a prototype of an interactive humanoid hand, made to do the gesture of shaking hands with a human user, designed with a special support adjusted to the optimal height to achieve physical communication in the most comfortable way. It was first designated for a faculty project but due to its interactivity we discovered many more opportunities.

The hand has a slightly hidden light sensor, a photoresistor, integrated in the lower part of the wrist, such that when you grab the hand it is completely covered, activating the four internal servomotors in the forearm to rotate and grab your hand in return.

In the future we want to extend the mobility and add new degrees of freedom for a more natural effect.

Key Words: humanoid, photoresistor, social, autonomous

1. Introduction

In the last years, technology has been a significant part of every human's life, tough it's still regarded as a foreign presence among us.

We wanted to diminish the barrier between humans and robots by bringing them closer in the most simple and notorious way: the "shaking hands" gesture, widely used around the world, that has a deep social meaning, it makes connections, it transmits trust and partnership.

That was our goal, the merge of robotic interaction into our day-to-day life. Moreover, the realistic design and size offer a familiar feel, and the maximum height of the robot make the grab accessible, being also able to vary due to its mobility. It can be placed on different flat surfaces and it is automatically triggered when the photoresistor is covered, making it completely autonomous.

We will present the evolution of our project from its first steps to the current stage, offering complete detail about the project.

2. Current stage

Just like our project, there are many other focusing on the same purpose, aiming to help children interact with robots via toys, robotic companions, and even AI assistants in anticipation of a future integrated with robotics. For example, the EU funded SHAPE project, as well as Japan's Minamisoma "Robot Town", seeks to engender acceptance of human-robot interactions by introducing socially assistive robots in homes, schools, and public areas so that people can gradually get accustomed to their existence. Equally, community pilot projects with robotic assistants like Pepper and Temi in public libraries, hospitals, and care homes aim to normalize robotic intervention, allowing people to build trust through repeated non-threatening interactions. These initiatives help the populace to acclimatize to the socio-psychological aspects of robotics.

3. The 3d model

The 3D model of the hand is not entirely designed by us, we got inspired by an inventor on-line and decided to use the same 3D model since it fitted our needs completely. Since being quite realistic we couldn't modify it if we wanted to because the model was so detailed it would send our PC's into freeze mode when we tried to open and remodel it. Because of this reason we kept the model as it is and decided to model only the support on which the hand stands. For this reason we will credit the owner of the hand model at the end of this presentation. The model was printed in a faculty laboratoy and then assembled by us. The assembling process was tricky because the arm needed to be put together at the same times as the electronic pieces so they would stay in place. This fact was one of the hardest steps in this project

4. Circuit model

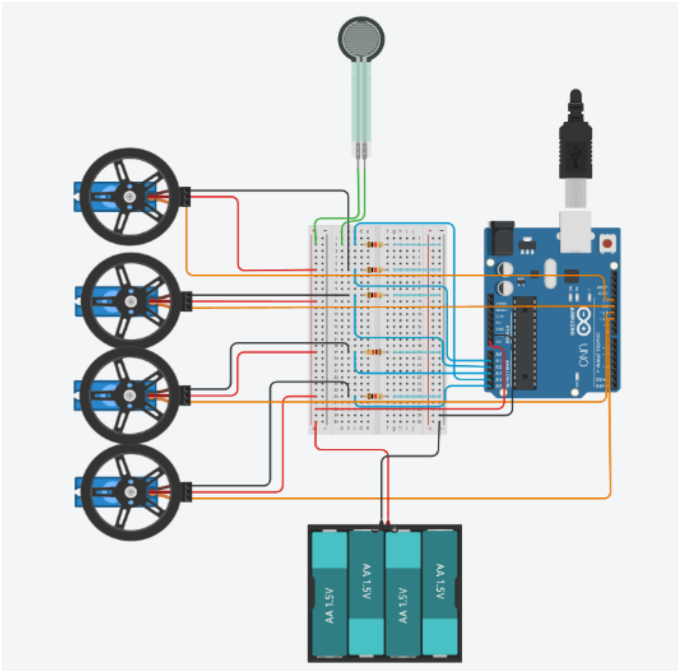

Fig. 1. Circuit model

The circuit model was made in TinkerCad for easy understanding (Fig. 1). You can see the 4 servomotors we used for the fingers, the pinky and the ring fingers are connected to the same motor for simplifying reasons. At the top of the image is the photoresistor connected to the breadboard then to the Arduino Uno board. We used an Arduino because it is a versatile microprocessor board that met our needs. On the breadboard we put some shunt resistors to measure the current that goes through. We powered the motors and the board from four AA type batteries in a special support because the servos are required 6V to function and the board self-regulates the needed tension. The Arduino Uno board is one of the best choices for projects like this due to its accessibility and the user-friendly interface. We left an open-space at the end for better understanding and for easy access to the components (Fig. 2).

Fig. 2. Real life circuit

5. Programming

The programming was done in Arduino IDE (Fig. 3). A portion of the code is presented where it gives the value read by the photoresistor to detect if it's bright or dark. It has a threshold of 15 to decide the light level. If it's under 15 it means it's dark and the cycle begins. If it's above that threshold, the system is on stand-by. It also has protection modes to not engage in the cycle if it is already active and operating. At the end there is a small delay to prevent any unnecessary processing by the photoresistor.

```
void loop() {
  // If the cycle is not active, read the photoresistor value
  if (!isCycleActive) {
    int photoresistorValue = analogRead(photoresistorPin);

    Serial.print("Photoresistor Raw Value: ");
    Serial.println(photoresistorValue);

    // Start servo cycle only if it's dark (low photoresistor value)
    if (photoresistorValue < 15) {
      performServoSequence();
    } else {
      Serial.println("It's too bright. Waiting...");
    }
  } else {
    Serial.println("Servo cycle active. No photoresistor detection.");
    delay(1000);  // A small delay to prevent unnecessary processingA
  }
}
```

Fig. 3. Portion of the code

6. Conclusion

The "Human hand" project has turned out to be a successful one and it has lived up to our standards. We presented it during public events with the faculty and it caught the attention of many people, professors, children and their families and so on. As for future improvements we want to articulate its wrist and extend it up to an elbow to be able to actively shake the user's hand. Another improvement would be to make it even more modular, to be able to take it and rebuild it with ease. About programming, it could be improved to show other gestures when triggered, such as the “okay” sign or the “like” one. To not interfere with the shaking, we would need to add other measures of triggering, such as other type of sensors or even a button.

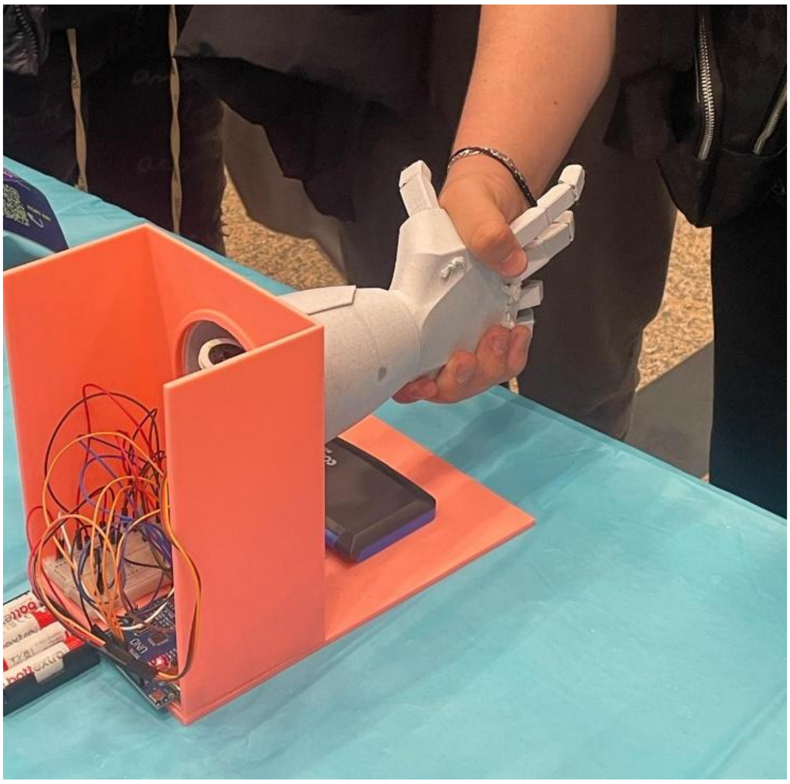

Fig. 4. Human hand at a public event

8. References

[1].https://youtu.be/Fvg-v8FPcjg?si=XCzf1hmi1SCoEuM8
[2].https://www.viralsciencecreativity.com/post/arduino-flex-sensor-controlled-robot-hand
[3].https://www.tinkercad.com/things/5hZSd74Fbg7-sizzling-bruticus/editel?returnTo=https%3A%2F%2Fwww.tinkercad.com%2Fdashboard&sharecode=gwU_1OfGOuB84bed3-Bq-kCbH5fHILWjCzD2E03CacI

CT-7567

POSTELNICU Andrei, MITICA Octavian-Alexandru, MAHLER Marius-Mihai, IVAN Andrei Mario(Conducător științific)

Faculty: Industrial Engineering and Robotics, Specialization: Mechatronics and Robotics, Year of study: II, email: OriginalAndreiposte@yahoo.com

ABSTRACT: This vocal assistant robot is an intelligent device which uses advanced voice recognition and response generating software, while using ChatGPT as its processing engine. It is made to interact in a natural way with its user, being able to answer any question, carry out conversations offering an almost human interaction thanks to the software and hardware components used.

KEY WORDS: Robot, Speech, Servo, Python, Assistant

1. Introduction

CT-7567 is a humanoid head robot (as seen in fig. 1) powered by ChatGPT and real-time speech recognition, designed to interact naturally with people of all ages. Created to support children with disabilities, CT-7567 makes learning more engaging and accessible. It also functions as a music companion, an intelligent hotel concierge offering location and weather updates, and a promotional unit in stores for product and service information.

Smart, interactive, and adaptable — CT-7567 is where human connection meets cutting-edge AI.

Fig. 1. Robot’s Current Appearance

2. Current Status

Similar initiatives, such as the InMoov project [1][2] and TonyGPT [3] have demonstrated the potential of combining ChatGPT with humanoid platforms, showcasing capabilities like multilingual communication, facial recognition, and responsive expressions, thereby enriching user interaction and engagement.

These projects underscore the growing trend of integrating advanced AI models into humanoid robots to facilitate more intuitive and accessible human-robot interactions, aligning with the objectives of CT-7567.

3. System Architecture and Current Development Status

This humanoid robotic head is a custom-built interactive platform designed for natural, expressive interaction. Constructed from white PLA plastic (as seen in fig. 1), the head simulates realistic facial movement, including dynamic eye motion and jaw articulation. The system integrates servo motor control, voice recognition, and conversational AI to create a lifelike robotic experience.

3.1 Eye and Eyelid Mechanism

The robotic head features a total of six SG90 micro servos [4] (as seen in fig. 2) dedicated to controlling the eyes. Two of these servos manage the movement of the eyeballs, one allowing vertical (up and down) motion and the other enabling horizontal (left to right) movement. The remaining four servos are assigned to the eyelids, with individual control over each upper and lower lid. This configuration permits expressive blinking and subtle eye gestures that enhance the robot's emotional realism [5].

3.2 Jaw Movement

For the mouth, the robot uses two MG996R high-torque servo motors [6] (as seen in fig. 2) to control the jaw's up and down movement. These servos operate in tandem to ensure a stable and smooth opening and closing motion. The dual-servo setup provides sufficient torque for consistent performance and synchronizes the movement for more natural speech simulation.

3.3 Servo Driver

All eight servos are controlled by a PCA9685 [7] (as seen in fig. 2) servo motor driver, which communicates directly with the Raspberry Pi. The driver allows for precise pulse-width modulation to each servo channel and is crucial for managing the robot’s coordinated movements. It is connected to the Pi using the TX and RX pins, as well as the SDA and SCL pins for I2C communication, along with 3.3V and ground for power and logic reference.

3.4 Power Supply

The entire mechanical system is powered by an 11.1V Li-Po battery (as seen in fig. 2). This battery feeds a step-down voltage regulator [8] (as seen in fig. 2), which converts the voltage to 6V. This regulated output powers the PCA9685 servo driver and, through it, all connected servos, including the SG90 and MG996R models.

In addition to the servos, a 12V cooling fan (as seen in fig. 2) is connected directly to the Li-Po battery to maintain thermal stability during operation. An on/off switch is integrated into the circuit to control power delivery to the servos and fan, enabling safe power management without the need to disconnect the battery.

The Raspberry Pi 5 [9] (as seen in fig. 2) itself is powered independently using the official Raspberry Pi power brick, which is connected directly to a standard AC wall outlet. This ensures the Pi receives a stable and sufficient power supply separate from the high-drain servo system, preventing voltage drops and ensuring consistent performance during processing and communication tasks.

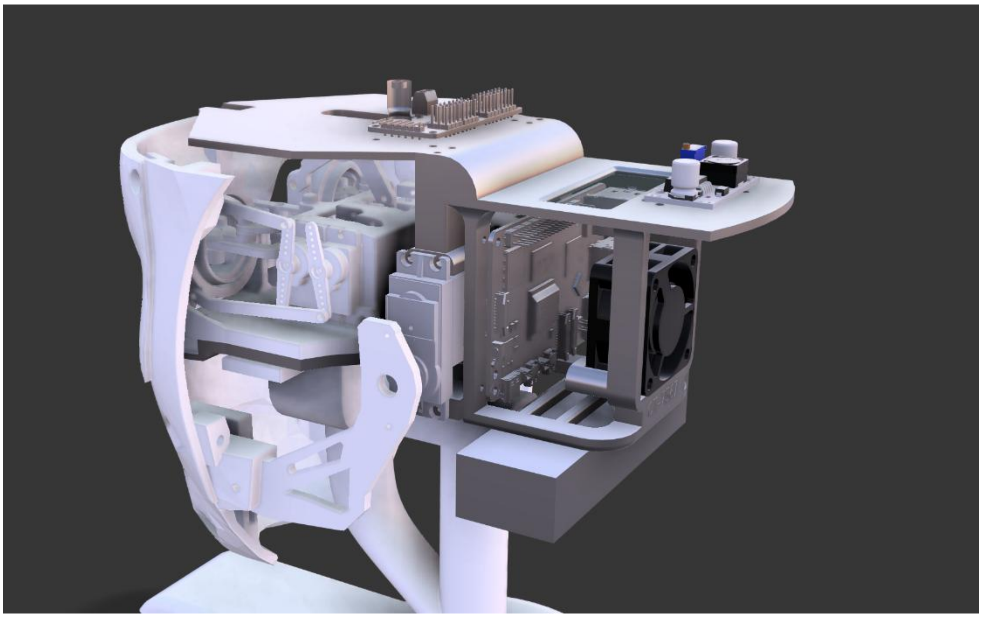

Fig. 2. Robot's Internal Hardware

3.5 Main Controller

The robot is controlled by a Raspberry Pi 5 with 8GB of RAM. The Pi serves as the central processing unit, running a Linux-based operating system. It handles all logic and control tasks, including servo commands, audio processing, and AI communication. Speech is detected through an external USB microphone connected to the Raspberry Pi. This allows the robot to capture voice input in real time, process it using Python-based speech recognition tools, and respond with context-aware dialogue generated by ChatGPT. The speech then gets converted to temporary mp3 file that gets played over a Bluetooth speaker located in the robot's forehead. The conversational AI system enables interactive and intelligent responses tailored to the user's speech.

3.6 User Connection

All programming, configuration, and monitoring are done remotely. The robot is accessed via an SSH (Secure Shell) connection from a mobile phone or laptop. This is done by connecting both the Raspberry Pi and the controlling device to the same Wi-Fi hotspot, allowing remote terminal access for code execution, debugging, and system updates without needing a direct physical connection.

This remote setup provides a flexible and portable development environment, especially useful during testing, mobility, or when deploying the robot in different locations.

3.7 Code

We used Python along with several helpful libraries to create an AI assistant that can understand voice commands, respond with smart answers, and talk back in a natural way.

The speech_recognition library is used to listen to spoken words through a microphone and convert them into text. That text is then sent to OpenAI's servers using the openai library, where ChatGPT processes the message and generates a response. The same OpenAI library is also used for text-to-speech, which means it takes the response from ChatGPT and turns it into voice output, making the assistant sound more human when speaking (as seen in fig. 3).

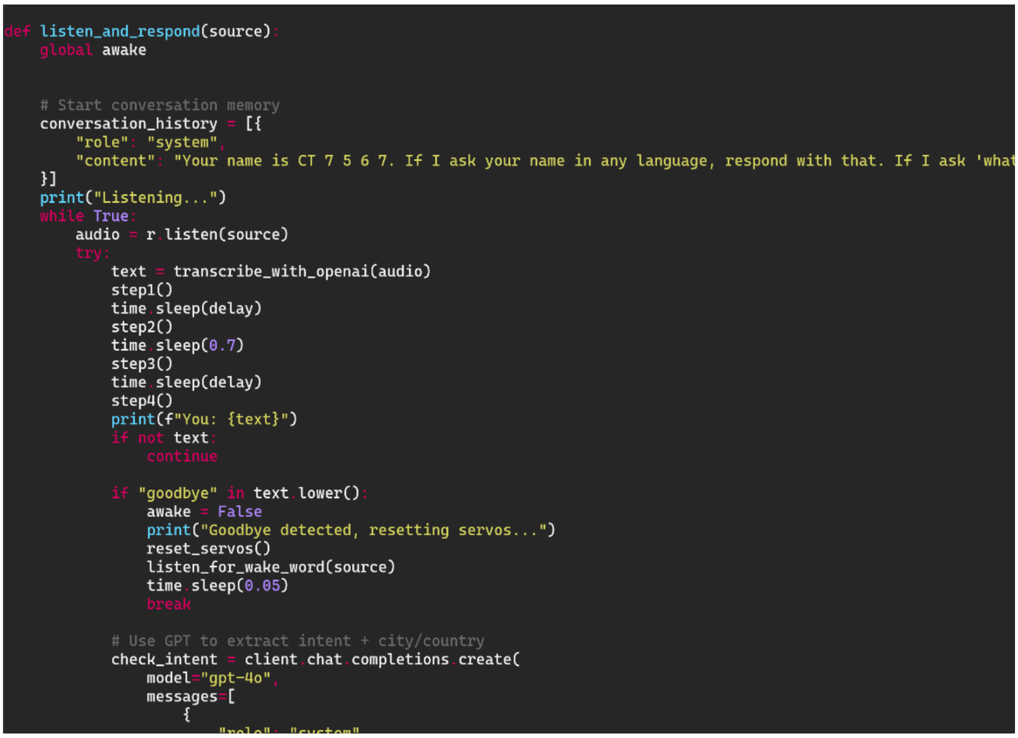

```
def listen_and_respond(source):
    global awake

    # Start conversation memory
    conversation_history = [{
        "role": "system",
        "content": "Your name is CT 7 5 6 7. If I ask your name in any language, respond with that. If I ask 'what
    }]
    print("Listening...")
    while True:
        audio = r.listen(source)
        try:
            text = transcribe_with_openai(audio)
            step1()
            time.sleep(delay)
            step2()
            time.sleep(0.7)
            step3()
            time.sleep(delay)
            step4()
            print(f"You: {text}")
            if not text:
                continue

            if "goodbye" in text.lower():
                awake = False
                print("Goodbye detected, resetting servos...")
                reset_servos()
                listen_for_wake_word(source)
                time.sleep(0.05)
                break

            # Use GPT to extract intent + city/country
            check_intent = client.chat.completions.create(
                model="gpt-4o",
                messages=[
                    {
```

Fig. 3. The OpenAI portion of the code

For physical movements, the assistant uses adafruit_motor and PCA9685 libraries, which control servo motors. This allows it to perform actions like blinking and moving its mouth (as seen in fig. 4).

```python
def close_servo1():
    for angle in range(servo5_max, servo1_min - 1, -step):
        servo1.angle = angle
        time.sleep(0.001)

def open_servo1():
    for angle in range(servo1_min, servo1_max + 1, step):
        servo1.angle = angle
        time.sleep(0.002)

def open_servo2():
    for angle in range(servo2_max, servo2_min - 1, -step):
        servo2.angle = angle
        time.sleep(delay)

def open_servo4():
    for angle in range(servo4_max, servo4_min - 1, -step):
        servo4.angle = angle
        time.sleep(delay)

def open_servo5():
    for angle in range(servo5_min, servo5_max + 1, step):
        servo5.angle = angle
        time.sleep(delay)

def left_servo6():
    for angle in range(servo6_initial, servo6_max + 1, step):
        servo6.angle = angle
        time.sleep(delay)

def right_servo6():
    for angle in range(servo6_max, servo6_min - 1, -step):
        servo6.angle = angle
        time.sleep(delay)
```

Fig. 4. The portion of code controlling the servo motors

The langdetect library helps detect the language being spoken, so the system can handle different languages if needed. The requests library allows the assistant to access real-time data from the internet, such as weather updates (as seen in fig. 5).

```python
import os
import openai
from dotenv import load_dotenv
import time
import speech_recognition as sr
import numpy as np
from adafruit_pca9685 import PCA9685
from adafruit_motor import servo
import busio
import board
import threading
import pygame
from openai import OpenAI
from pathlib import Path
import io
import requests
from langdetect import detect
```

Fig. 5. The portion of code integrating libraries

All of these tools come together to allow the assistant to listen, understand, reply in different languages and even tell us real time information (as seen in fig. 6).

```python
#Weather
OPENWEATHER_API_KEY = "fd77336554407c67ebc28865797cb8e0"

def get_weather_free(city, lang="en"):
    url = f"http://api.openweathermap.org/data/2.5/weather?q={city}&appid={OPENWEATHER_API_KEY}&units=metri
    try:
        res = requests.get(url)
        data = res.json()
        if res.status_code == 200:
            weather = data["weather"][0]["description"]
            temp = round(data["main"]["temp"])
            return f"The weather in {city} is {weather}, around {temp} degrees Celsius."
        else:
            return f"I couldn't get the weather for {city}."
    except Exception:
        return "There was a problem getting the weather."

def get_time_free(city):
    try:
        zones = requests.get("http://worldtimeapi.org/api/timezone").json()
        match = next((z for z in zones if city.lower() in z.lower()), None)
        if not match:
            return f"I couldn't find the time for {city}."
        time_data = requests.get(f"http://worldtimeapi.org/api/timezone/{match}").json()
        current_time = time_data["datetime"][11:16]
        return f"The current time in {city} is {current_time}."
    except Exception:
        return "There was a problem getting the time."
```

Fig. 6. The real time weather module portion of code

3. Conclusions

CT-7567 represents the fusion of robotics, AI, and accessibility, offering a versatile humanoid head capable of lifelike expression, intelligent conversation, and real-time interaction. With a carefully engineered servo system, robust Python-based control, and seamless remote connectivity, it serves as an educational tool, concierge, music assistant, and promotional guide, making advanced technology more personal, engaging, and inclusive.

In the near future, we plan to enhance CT-7567 with a camera system capable of object recognition, facial detection and tracking, as well as depth perception to enable basic object handling. The robot will also be upgraded with a fully articulated neck made of durable metal instead of 3D-printed PLA plastic, improving both the realism and fluidity of its movements. Additionally, we aim to equip CT-7567 with a pair of robotic arms and hands fitted with pressure sensors, allowing it to lift objects, perform hand gestures, communicate using sign language, and carry out a variety of interactive tasks with greater precision and expression.

4. References

[1]. EZ-inMoov Robot Head

https://www.thingiverse.com/thing:6030262

[2]. https://en.wikipedia.org/wiki/InMoov?utm_source=chatgpt.com

[3].https://www.roboticgizmos.com/tonygpt-humanoid-robot-chatgpt/?utm_source=chatgpt.com

[4]. https://www.alldatasheet.com/datasheet-pdf/pdf/1572383/ETC/SG90.html

[5]. How to Build a Simple 3D Printed Arduino Animatronic Eye Mechanism https://www.youtube.com/watch?v=Ftt9e8xnKE4&t

[6]. https://www.alldatasheet.com/datasheet-pdf/pdf/1131873/ETC2/MG996R.html

[7]. https://www.alldatasheet.com/datasheet-pdf/pdf/293576/NXP/PCA9685.html

[8]. https://www.alldatasheet.com/datasheet-pdf/pdf/543794/TI1/LM2596S.html

[9]. https://datasheets.raspberrypi.com/rpi5/raspberry-pi-5-product-brief.pdf

ACCESS KEY STORAGE SYSTEM WITH FINGERPRINT SENSOR

POSTELNICU Andrei, IVAN Andrei Mario(Conducător științific)

Faculty: Industrial Engineering and Robotics, Specialization: Mechatronics and Robotics, Year of study: II, email: OriginalAndreiposte@yahoo.com

ABSTRACT: This biometric security box combines a user-friendly design with functional hardware and software to create a secure and effective access control system. The Arduino Nano manages all logic, while the fingerprint sensor provides personalized authentication and the servo motor enables physical locking and unlocking. The system is compact, autonomous, and customizable.

KEY WORDS: Biometrics, Authentification, Servo, Arduino, Security

1. Introduction

This project features a compact biometric security box designed to safeguard access to a laboratory key. Created with white PETG filament using a 3D printer, the box uses fingerprint authentication to unlock, ensuring that only authorized individuals can access its contents. It is powered by a 7.4V Li-Po battery and integrates a fingerprint sensor, a servo motor, and an Arduino Nano to manage the entire process. The system is designed for portability, low power consumption, and secure access (as seen in fig. 1).

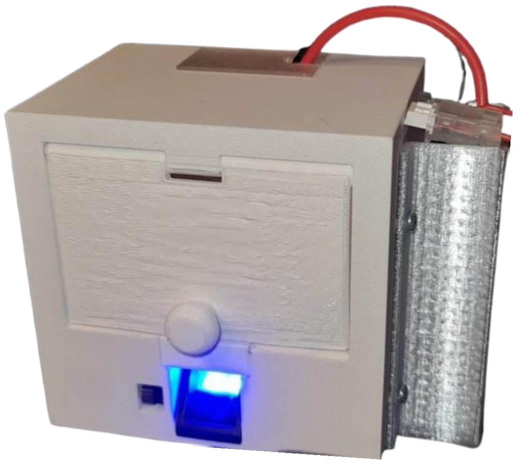

Fig. 1. The box's Current Appearance

2. Current Status

Similar to the Arduino Nano-controlled fingerprint-authenticated servo lock project [1] [2], your design integrates biometric authentication with servo-driven locking mechanisms, enhancing secure access control.

This project aligns with the Portable Biometric Lockable Case initiative, both employing Arduino Nano and fingerprint sensors to create personalized, secure storage solutions.

3. Current Status

3.1 Main Controller

The Arduino Nano [3] functions as the central processing unit of the system. It receives fingerprint data from the sensor and executes the logic needed to control the lock. It processes input, controls the servo motor, and communicates with the fingerprint sensor via serial commands.

3.2 Authentication Module

The fingerprint sensor [4] is responsible for reading and verifying fingerprints. Once the reset button is pressed, the sensor becomes active and waits for a fingerprint scan. If the scan matches a stored template, it signals the Arduino to unlock the box. New fingerprints can be registered by uploading a different sketch via the USB port on top of the box.

3.4 Locking Mechanism

The SG90 servo motor [5] physically locks and unlocks the box. When a valid fingerprint is detected, the Arduino commands the servo to rotate 90 degrees, unlocking the lid. After a one-minute delay, the servo returns to its original position (0 degrees), re-locking the box. This automation ensures security even if the user forgets to relock the system.

3.5 Power Supply

The entire system is powered by a 7.4V Li-Po battery. The battery provides sufficient power to operate the Arduino, fingerprint sensor, and servo motor. To conserve power, an on/off switch disconnects the system when not in use. A reset button is included to initialize the fingerprint reading process after powering on.

3.6 Code Overview

The code is adapted from Adafruit's official fingerprint sensor examples [6] (as seen in fig. 2). It uses the Adafruit_Fingerprint library for fingerprint detection and the Servo library to control the SG90 motor. Upon system startup, the Arduino initializes the fingerprint sensor and waits for a scan. If a valid fingerprint is identified, the servo rotates to unlock the box. The program then pauses for one minute (60000 milliseconds) before automatically returning the servo to the locked position.

```
  // found a match!
  Serial.print("Found ID #"); Serial.print(finger.fingerID);
  Serial.print(" with confidence of "); Serial.println(finger.confidence);

  myServo.write(90);  // Rotate to 90 degrees
  Serial.println("Servo rotated to 90 degrees.");

  delay(60000);      // Wait for 1 minute

  myServo.write(0);   // Return to original position
  Serial.println("Servo returned to 0 degrees.");
  return finger.fingerID;
}

// returns -1 if failed, otherwise returns ID #
int getFingerprintIDez() {
  uint8_t p = finger.getImage();
  if (p != FINGERPRINT_OK)  return -1;

  p = finger.image2Tz();
  if (p != FINGERPRINT_OK)  return -1;

  p = finger.fingerFastSearch();
  if (p != FINGERPRINT_OK)  return -1;

  // found a match!
  Serial.print("Found ID #"); Serial.print(finger.fingerID);
  Serial.print(" with confidence of "); Serial.println(finger.confidence);
  return finger.fingerID;
}
```

Fig. 2. The unlocking portion of code

New fingerprints can be added by uploading a separate enrollment sketch [7] (as seen in fig. 3) to the Arduino, scanning the new fingerprint, and re-uploading the unlocking code.

```
Serial.print("Waiting for valid finger to enroll as #"); Serial.println(id);
while (p != FINGERPRINT_OK) {
  p = finger.getImage();
  switch (p) {
  case FINGERPRINT_OK:
    Serial.println("Image taken");
    break;
  case FINGERPRINT_NOFINGER:
    Serial.print(".");
    break;
  case FINGERPRINT_PACKETRECIEVEERR:
    Serial.println("Communication error");
    break;
  case FINGERPRINT_IMAGEFAIL:
    Serial.println("Imaging error");
    break;
  default:
    Serial.println("Unknown error");
    break;
  }
}

// OK success!

p = finger.image2Tz(1);
switch (p) {
  case FINGERPRINT_OK:
    Serial.println("Image converted");
    break;
  case FINGERPRINT_IMAGEMESS:
    Serial.println("Image too messy");
    return p;
  case FINGERPRINT_PACKETRECIEVEERR:
    Serial.println("Communication error");
    return p;
  case FINGERPRINT_FEATUREFAIL:
    Serial.println("Could not find fingerprint features");
    return p;
  case FINGERPRINT_INVALIDIMAGE:
    Serial.println("Could not find fingerprint features");
```

Fig. 3. The enrollment portion of code

3.7 3D Model

The entire box's design is original, modeled by me (as seen in fig. 4). It's fully custom, optimized to fit all components securely, and includes cutouts for the sensor, reset button and power switch. The design also allows the user to mount the box onto a wall by removing the small wall inside the compartment and drilling a few holes for easy mounting.

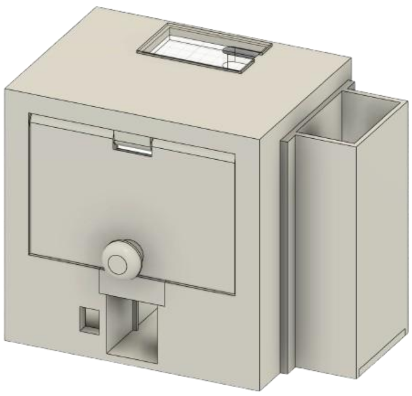

Fig. 4. The 3D Model of the box

3. Conclusions

This project demonstrates how accessible components like a fingerprint sensor, servo motor, and Arduino can be integrated into a robust and practical biometric locking system. With 3D-printed parts and a simple power supply, the security box is an excellent example of DIY innovation applied to real-world needs in access control and secure storage.

In the near future, I plan to upgrade the locking mechanism by replacing the current servo setup with a more secure system that uses a retractable metal rod. This would provide enhanced resistance against tampering or forced entry. Additionally, I intend to redesign the box to better conceal the Li-Po battery inside a hidden compartment. This will not only improve the aesthetic and compactness of the design but also increase security by making power access less obvious to potential intruders.

4. References

[1]. Arduino Nano Controlled Fingerprint-Authenticated Servo Lock:
https://docs.cirkitdesigner.com/project/published/3c7f87d7-91a1-496f-9284-2556ad715f04/arduino-nano-controlled-fingerprint-authenticated-servo-lock?utm_source=chatgpt.com
[2]. Portable Biometric Lockable Case:
https://projecthub.arduino.cc/NZDoug/portable-biometric-lockable-case-c08add?utm_source=chatgpt.com
[3]. Adrduino Nano Datasheet:
https://docs.arduino.cc/resources/datasheets/A000005-datasheet.pdf
[4]. Adafruit Fingerprint Sensor Datasheet:
https://cdn-learn.adafruit.com/downloads/pdf/adafruit-optical-fingerprint-sensor.pdf [5]. Adafruit fingerprint detection example code
[5]. SG90 Servo Motor Datatsheet:
https://www.alldatasheet.com/datasheet-pdf/pdf/1572383/ETC/SG90.html
[6]. Adafruit fingerprint detection example code:
https://github.com/adafruit/Adafruit-Fingerprint-Sensor-Library/blob/master/examples/fingerprint/fingerprint.ino
[7]. Adafruit fingerprint enrollment example code:
https://learn.adafruit.com/adafruit-optical-fingerprint-sensor/enrolling-with-arduino

FLEET TRACKING SYSTEM FOR LOGISTICS

STOICA David-Christian and Scientific Coordinator, Constantin-Adrian POPESCU(Conducător științific)

Faculty of Industrial Engineering and Robotics, Industrial Logistics Specialization, 2nd year, stoicadavid12@gmail.com

ABSTRACT: Studies on fleet logistic tracking system are focused on using GPS, and IoT technology for maintaining business productivity and reducing transportation costs. Positioning vehicles in real-time allows for routing optimization to reduce time and fuel costs. Driver behavior assessment and preventive maintenance enhance safety and extend vehicle life. Enterprises can be more agile and responsive in managing operations due to traffic changes.

1. Introduction

Fleet tracking systems, one of the most widely utilized technologies to maximize operational productivity and minimize cost for companies, has been fundamentally restructuring with the progressive trend toward digitalization. With their live tracking feature enabled by GPS, IoT devices and an advanced data analytics engine, they help you optimize driver performance, optimize routes and plan maintenance needs in advance for the vehicles.

The main purpose of this investigation is to increase the efficiency of a fleet, by reducing delivery times, fuel costs and logistics related hazards. It is at this approach where creative concepts of fleet management are developed, which could be put into action and that are in line with the contemporary civilization's logistic pace.

2. Current Developments in Fleet Logistics Tracking Systems

Recent developments in the fleet tracking system market have ensured that the systems themself are now an integral part of any transportation and logistics operation. These products utilize high-end technologies, which are based on GPS, IoT and AI and which are capable of real time tracking, predictive analytics and, process automation.

Some of these advances include:

- **Vehicle tracking in real-time**: Ensures the accurate location of every vehicle on the fleet. This allows real-time routing decisions and fast reaction in case of events.
- **Route optimization with AI:** With help of AI-algorithms, the accumulated traffic data and road conditions are constantly analyzed in order to propose the most efficient routes, saving fuel and cutting down on delivery lead time.
- **Telematics-based safe driving behavior detection:** unsafe driving behavior pattern detection is used to improve road safety. [1]
- **Automotive prognostics:** Maintenance of vehicles is scheduled according to dynamic vehicle data ahead of failure deviation such that, the vehicle does not experience downtime and can be used for a longer time. [2]

- **System integration:** This software is able to provide compatibility with onboard equipment and back-office software, allowing an easy integration with other (external) systems and delivering a shared management mode.

3. Case Study: Advanced Implementation of a Fleet Management System

In this project we have created a modern fleet logistics monitoring system oriented to enhancing the operational and transport safety along with advanced technology.

The following individual components comprise the system: [3]

- **Real-time GPS tracking:** Provides real-time tracking through all levels of the vehicle unit. It facilitates effective fleet management of routes and immediate response in the event of an incident with a fleet.

- **Proximity sensors and traffic telemetry:** These sensors and controllers are used in obstacle detection and traffic monitoring eventuates dynamic route modifications thus reducing delay and fuel consumption.

- **Route algorithms:** These algorithms analyze the collected data (such as traffic conditions, weather and road restrictions) to determine most efficient routes by fuel consumption and time.
- **Driver behavior monitoring:** Company fleets are controlled by a driving behavior policy, through which high risk driving patterns can be corrected, ultimately saving on insurance.

Findings indicated some positive effects in OTT efficiency, cost saving and customer satisfaction.

4. Introduction to the Tracking System We Developed

At the core of the tracking system is the Arduino Due microcontroller (Fig. 1). It receives coordinates from the UBLOX M9N GPS module and, using the L800 GSM module, sends them via the internet to the main dashboard.

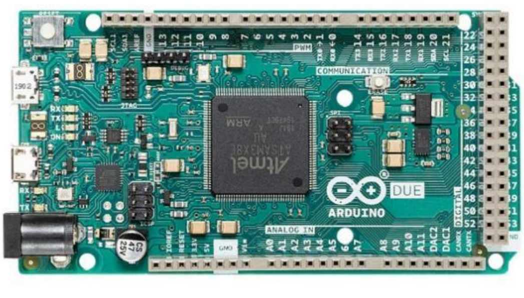

Fig. 1. Microcontroller Arduino Due

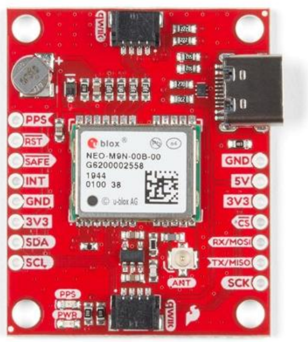

Fig. 2. GPS Module UBLOX M9N

The device was placed in a 3D-printed enclosure that protects the components from external environmental factors (Fig. 3 and Fig. 4).

Fig. 3. Enclosed Tracking System Case

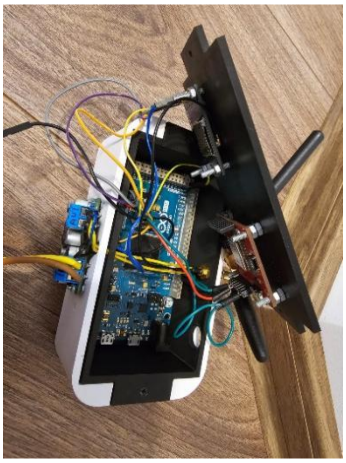

Fig. 4. Open Tracking System Case

There are two types of antennas shown in Fig. 3, because one of them receives satellite signals related to the current latitude and longitude, while the other transmits the data to the database connected to the main dashboard (Fig. 5).

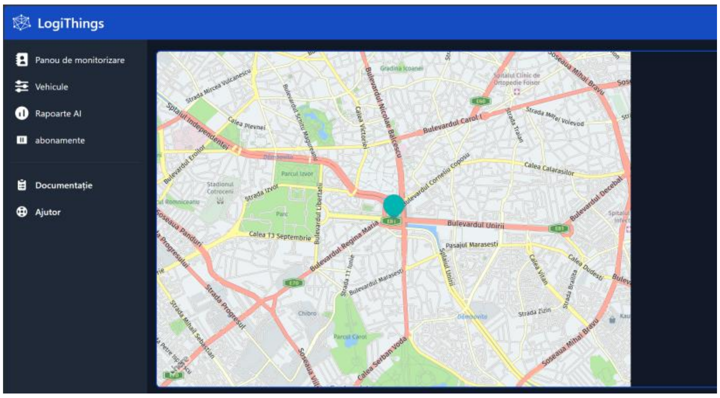

Fig. 5. Dashboard

5. Results Following the Implementation

The implementation of the advanced fleet tracking system led to significant improvements in the company's operations: [3]

- **Up to 15% reduction in fuel consumption:** Route optimization and driver behavior monitoring contributed to substantial fuel savings.
- **Improved driver behavior:** Real-time monitoring enabled the identification and correction of risky behaviors, such as speeding or harsh braking, resulting in fewer incidents and reduced vehicle wear.
- **Proactive vehicle maintenance:** The system generated alerts for preventive maintenance based on mileage and other parameters, helping avoid unexpected breakdowns and extending vehicle lifespan.

- **Increased customer satisfaction:** Faster and more efficient deliveries, made possible through route optimization and real-time tracking, led to higher customer satisfaction and stronger business relationships.

6. Conclusions

The use of a sophisticated tracking system for the logistics fleet has shown to be beneficial in both operational functions and cost optimization. Enablement of vehicle tracking in real-time facilitated optimization of routes, which improved the delivery schedules and energy consumption associated with deliveries.

Analysis of driver conduct also improved safety and accident risk mitigation. Adoption of latest technologies has improved the flexibility and effectiveness of the logistics fleet, which underscores the need for a digital shift within the transport industry.

The findings of the GPS monitoring systems underscore their importance in industrial settings while also highlighting the need for modern industrial logistics.

7. References

[1]. https://www.carolguy.com/cum-poate-revolutiona-monitorizarea-prin-gps-flotele-de-vehicule/

[2]. https://flimogps.ro/blog/solutii-eficiente-de-urmarire-gps-flote/

[3]. https://localizareauto.ro/blog/studiu-de-caz-cum-a-crescut-productivitatea-unei-companii-de-logistica-cu-ajutorul-gps-urilor-de-monitorizare/

[4]. https://docexpress.ro/blog/beneficiile-sistemelor-de-urmarire-gps-in-timp-real/

STATIC ANALYSIS OF A SUBASSEMBLY FROM A PRODUCT GROUPING SYSTEM

BERCEA Crina-Izabella, Tudor-George ALEXANDRU(Conducător științific)

Facultatea: Inginerie Industrială și Robotică, Specializarea: Logistică Industrială, Anul de studii: IV, e-mail: crinaizabella02@yahoo.com

ABSTRACT: The present paper addresses the simulation challenges of an automatic packaging system that groups packaged products into sets for secondary packaging. A subassembly which is responsible for transferring grouped bags to the packaging machine was analyzed. Simulations were completed in ANSYS for verifying the structural integrity through static analysis. A simplified 2D shell model was developed comprising clean room aluminum components (Aleris 55HX). Rigid joints were defined for transferring the load between the analyzed components. The mesh quality was high (0.97), and the loads included gravity, linear acceleration due to the motion, and the pressure induced by the handled products. The results proved minimal displacements and stresses, well below the 120 MPa limit, confirming the adequate design.

KEY WORDS: computer-aided engineering, static analysis, product grouping system, equivalent stresses, equivalent strains;

1. Introducere

The system analyzed is an automated grouping mechanism designed to collect individually packaged products, such as soup pouches, and organize them into predefined sets for secondary packaging into a common batch. Placed above the infeed conveyor of a horizontal packaging machine, it ensures continuous and efficient product handling on the production line. Its integration optimizes the packaging workflow by reducing manual operations, minimizing errors, and increasing throughput, key factors for improving productivity and traceability in logistics processes.

To verify its performance, a static structural simulation was completed by employing ANSYS software. The simulation followed key Computer Aided Engineering (CAE) concepts: preprocessing, where the geometry was imported and simplified into a 2D shell model having the material properties (Aleris 55HX aluminum alloy) assigned; meshing, where a controlled element size of 3 mm was defined for ensuring result accuracy; the definition of boundary conditions and loads (BCs), including contacts, gravity, linear acceleration and pressure induced by the handled products; and post-processing, where nodal displacements and equivalent stresses were evaluated. The results confirmed the structural integrity of the system and its suitability for industrial application.

2. Aspects regarding CAE

A typical CAE project includes the following stages [1].

- **Preprocessing**: the geometry is modeled and the physical properties of the assembly and its components (material properties) are defined, as well as those of the environment in which it works in the form of applied loads and constraints.
- **Solving**: using an appropriate mathematical formulation of physics (classical mechanics, fluid dynamics, laws of thermodynamics, etc.);
- **Postprocessing**: the results are presented graphically, animated and/or saved in text format so that they can be interpreted and validated;
- **Verification and interpretation of the results**: is carried out through analytical calculations, experimentally, or by comparing the results of the simulations with other results from the specialized literature.

Figure 1 illustrates the stages of a CAE project and the relationship between them.

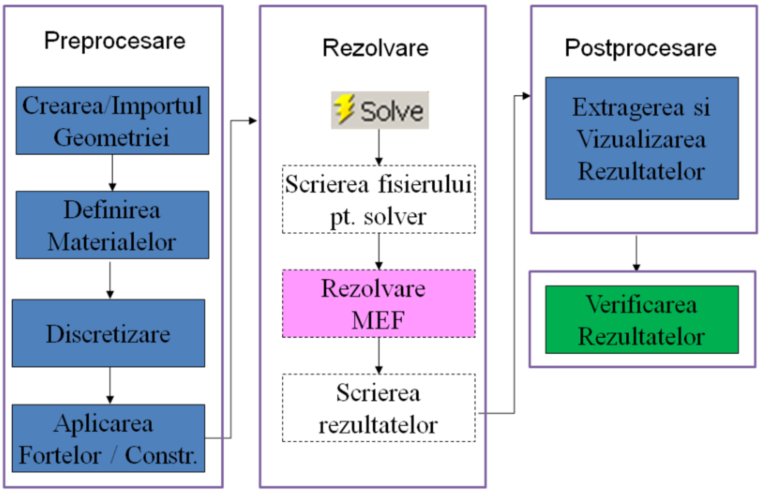

Fig. 1. Stages of a CAE project [1]

2. Literature overview

Over the years, CAE has evolved into a complex field, using advanced structural analysis programs based on the Finite Element Method (FEM), a very general numerical calculation method [2].

Today, reducing the time to market for a product is an important factor for the success of companies. In this case, the use of computer-aided engineering (CAE) helps companies reduce development cycles by simplifying the design process and using virtual testing. This not only shortens the time needed to launch a product to the market, but also reduces development costs by minimizing the need for physical prototyping and extensive testing [3].

According to a study conducted by Market Research Intellect, the global computer-aided engineering (CAE) market has seen significant growth as companies seek to improve their product development processes and maintain their competitive advantage. Additionally, the increasing complexity of engineering projects, the need for innovation in product development, and the growing focus on cost reduction and efficiency improvement are also contributing to the growth of the global computer-aided engineering market. In this case, the global CAE market is estimated to register a compound annual growth rate (CAGR) of over 10% in the coming years, reflecting the growing interest in advanced engineering solutions. [4]

Similar work is depicted in [5]. This paper examines the structural behavior of a conveyor system installed in road cleaning vehicles, focusing on various critical components of the conveyor that transports waste from the road to the vehicle body. The authors develop a finite element model of the belt conveyor system and perform static and dynamic load assessments, including examination of acceleration phases in operation, to identify stress concentrations, displacement fields, and vibration-influenced behavior.

In [6] the authors investigate the structural strength of a forming module used in the food processing of vegetables into minced steaks. A 3D CAD model of the module is created and then subjected to a finite element analysis under several load cases: hydrostatic pressure of the vegetable mixture, forces exerted by pneumatic actuators during blockages, and ejector/die collisions. The materials used are stainless steel (1.4301/304), and safety factors of 1.1 (for the base material) and 1.4 (for the welds) are applied. The results show maximum stresses of approximately 108.6 MPa in the worst case, and displacements of up to 3.45 mm in the case of a pusher blockage; all these factors are within the prescribed safety limits.

3. The studied assembly

The designed system (Fig. 2.) has the role of automatically grouping, in sets, the products packed in envelopes, for the purpose of their secondary packaging in a common package (Fig. 3.). It can be easily integrated into logistic systems and mounted above the input conveyor of a horizontal packaging machine.

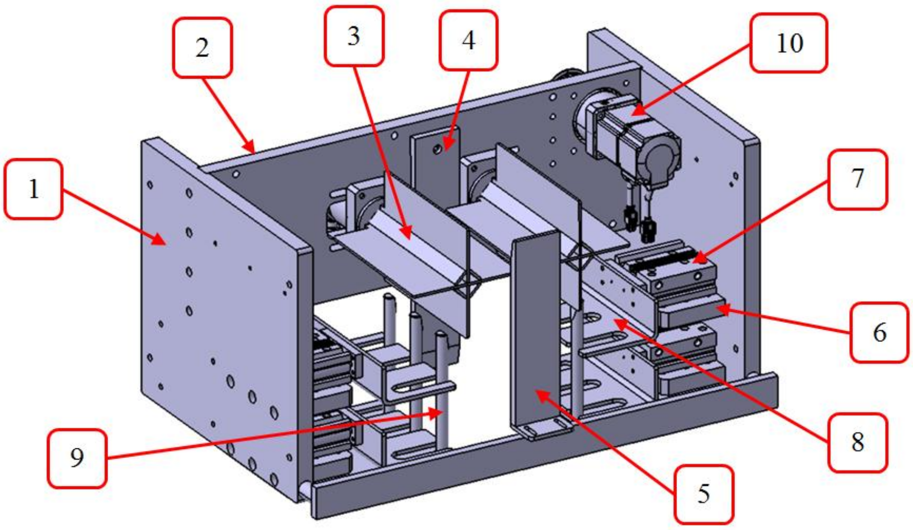

Fig. 2. The assembly of the analyzed system

In accordance with figure 2, the names of the studied components in depicted in Table 1.

Tabel 1. Names of the components

Component number	Component name
1	Side mounting plate
2	Fixing plate
3	Paddles
4	Back stopper
5	Front stopper
6	Pneumatic cylinder support plate
7	Pneumatic cylinder
8	Grouped-product holder
9	Safety pins
10	Gearbox

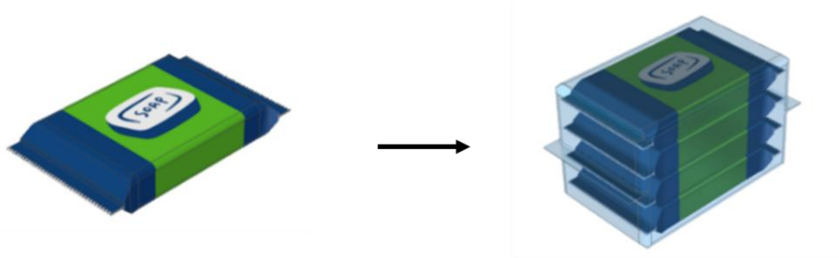

Fig. 3. Examples of packed products [4]

The grouped product holder was chosen for analysis, which has the role of taking over the groups of formed envelopes and transferring them in a controlled manner to the lower levels, until they reach the input conveyor of the packaging machine. In this case, the system will automatically group soup envelopes, each weighing 80 g, resulting in final packages consisting of 5 envelopes.

The subassembly chosen for analysis consists of the following components (Fig. 4.):

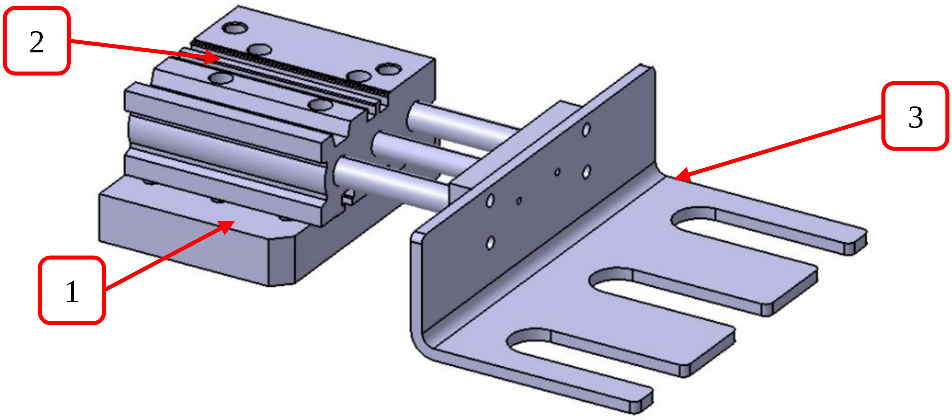

Fig. 4. The studied sub-assembly: *(1) - Pneumatic cylinder support plate; (2) - Pneumatic cylinder and (3) Grouped-product holder*

- **Pneumatic cylinder support plate**

Table 2. Characteristics of the pneumatic cylinder support plate

Specifications	Values
Dimensions (W x H x L)	82 x 20 x 120 mm
Material	Aluminum Alloy

- **Pneumatic cylinder**

Table 3. Pneumatic cylinder specifications

Specifications	Values
Dimensions (W x H x L)	36 x 83 x 103 mm
Stroke	50 mm
Material	Aluminum alloy and structural steel

- **Grouped product holder**

Table 4. Characteristics of the grouped product holder

Characteristics	Values
Dimensions (W x H x L)	100 x 51 x 170 mm
Thickness	5 mm
Material	Aluminum alloy

4. Static analysis

A static analysis will be completed to determine the static response of the analyzed assembly (displacements, stresses, etc.) under the defined pressure. The analysis will be performed using ANSYS software, a finite element analysis program widely used in industry and research to simulate the response of physical systems subjected to mechanical, thermal or electromagnetic loads.

A presentation of how to simulate the behavior of the structure, following the specific steps of the computer-aided engineering process mentioned in Section 1 is depicted below:

➢ **Preprocessing:**

- *Geometry import and mid-surface extraction (Fig. 5.):*

In this stage, the geometry was imported into the ANSYS software. In order to reduce the calculation time and lower the complexity of the analysis, a simplification of the model was completed by employing the 2D Shell modeling approach. In this case, the geometry simplification consisted of:

- Converting from 3D to 2D using the Mid-Surface command;

- Imprinting the faces of the pneumatic cylinder assembly onto the other components to materialize the contact areas and remove the pneumatic cylinder;

- The removal of small entities such as chamfers and holes to facilitate the mesh generation.

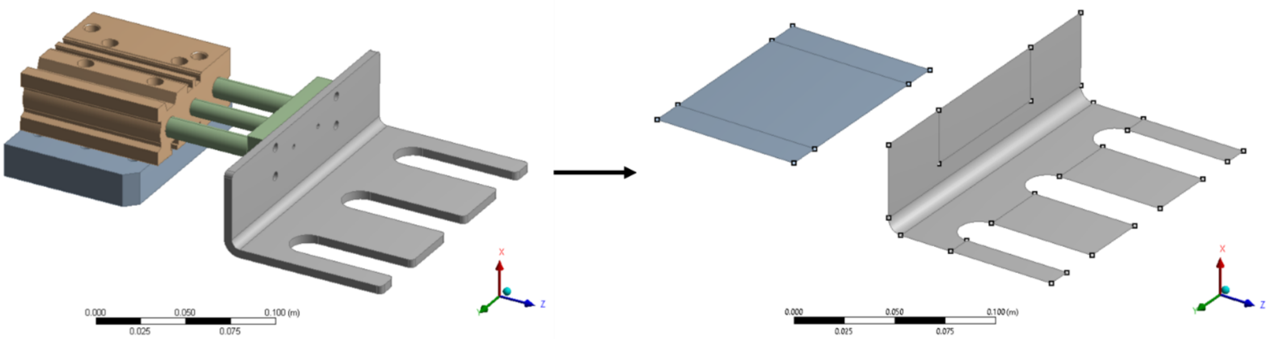

Fig. 5. Geometry import and simplification stages

- *Material definition:*

The analyzed component operates in a clean room environment. Thus, a special class of aluminum alloy is employed for its design – The Aleris 55HX. Its mechanical properties are depicted in table 5. For completing the static analysis, the density, Young's Modulus, Poisson ratio and tensile yield strength characteristics are required.

Tabel 5. Caracteristicile materialului *Aleris 55HX* [6]

Characteristics	Values
Density [g/cm^3]	2.7
Poisson ratio	0.33
Young's Modulus [MPa]	68900
Tensile Yield Strength [MPa]	120

- *The definition of body interactions (Fig. 6.):*

Two types of rigid contact were defined under the form of fixed joints:

- The first type is a *Body-Body* joint between the pneumatic cylinder support plate and the product holder;
- The second is a *Body-Ground joint* for materializing the interaction area between the pneumatic cylinder support plate and the other assembly elements which are not materialized.

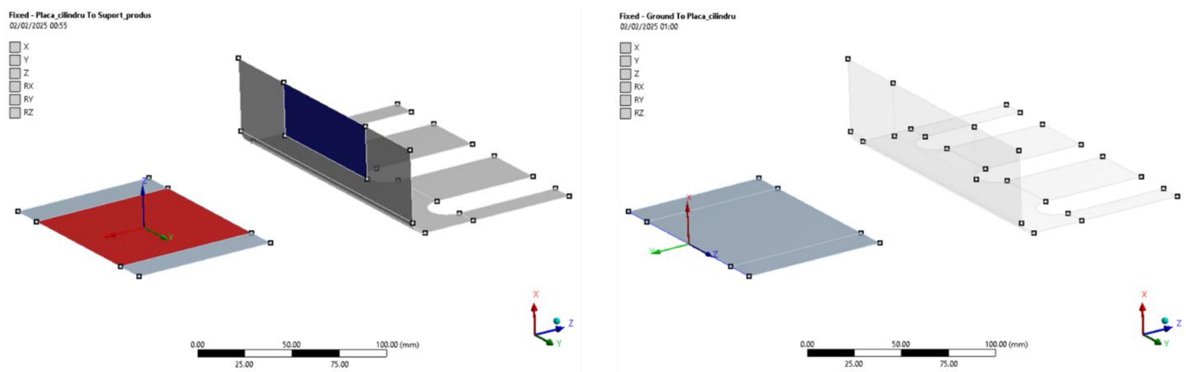

Fig. 6. Contact definition stage

- *Meshing (Fig. 7., Fig. 8.):*

In the next stage, the meshing was defined by controlling the global element size to 3 mm. The face meshing technique was achieved alongside topology operations for delimiting the surfaces of the two studied bodies in groups of 4 edges. Altogether, the applied setting helped achieve a 0.97 element quality.

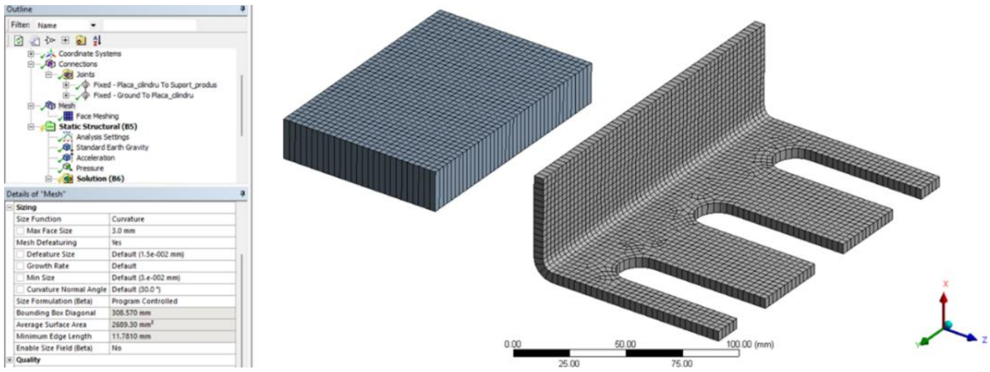

Fig. 7. Mesh generation

- *Loads and boundary conditions (Fig. 9.):*

Two types of loads are considered:

- Interial loads:
  – Standard earth gravity to take into account the gravitational loads - 9806.6 mm/s²;
  – Linear acceleration, given the motion imposed by the pneumatic cylinder. In this case, the stroke of 50 mm is completed in 0.5 seconds. Thus, the velocity can be calculated as:

$$v = \frac{50}{0.5} = 100\ mm/s \tag{1}$$

From (1) the linear acceleration can be calculated as:

$$a = \frac{100}{0.5} = 200\ mm/s^2 \tag{2}$$

- Pressure load is defined under the form of compressive pressure. By knowing the mass of 80 g of each envelope and the maximum number of handled enveloped as 5, the total mass of 0.08 Kg is multiplied the standard earth gravity. Afterwards, the pressure is derived from the surface area of the grouped product holder (6240 mm^2):

$$p = \frac{5 * 0.08 * 9.81}{6240} = \frac{3.924}{6240} = 0.00062885\ MPa \qquad (3)$$

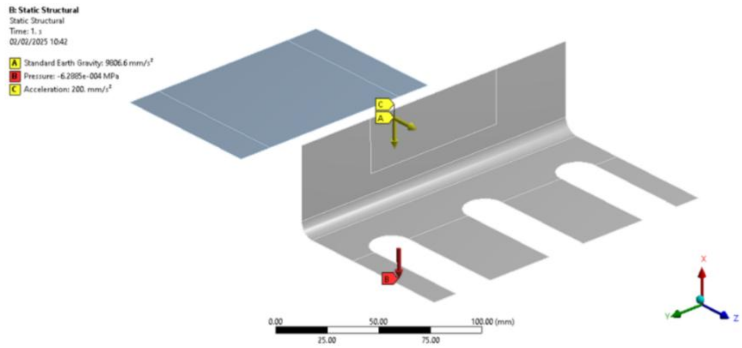

Fig. 9. Definition of loads and boundary conditions

- **Solving, post-processing and result verification:**

In the next stage, the results are processed under the form of fringe plots:

- *Nodal displacement plot depicted in Fig. 10;*

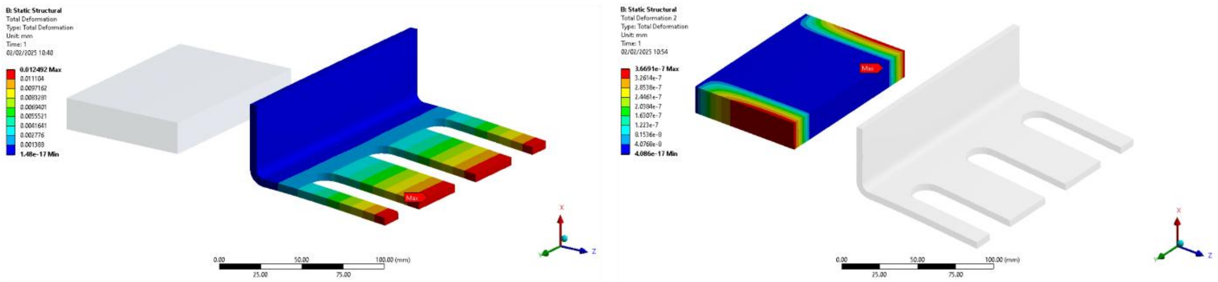

Fig. 10. Nodal displacements (Δ_{max} = 0.01 mm for the grouped product holder)

- *Equivalent stress plot depicted in Fig. 11;*

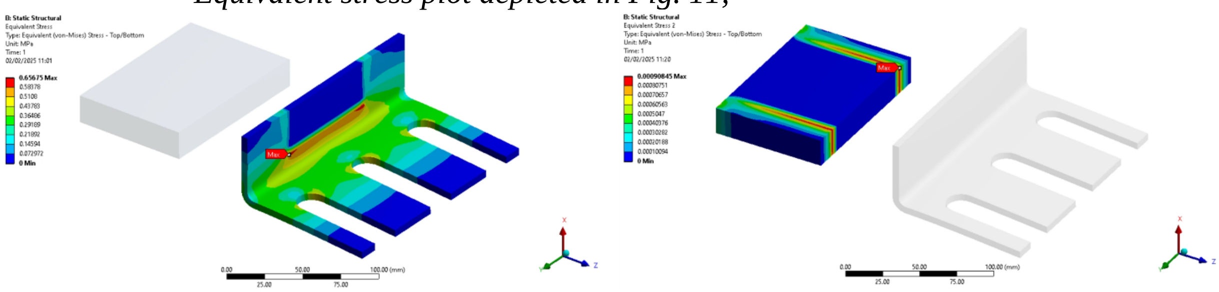

Fig. 11. The equivalent von-Mises stress (σ_{max} = 0.65 MPa for the grouped product holder)

The results processed reveal that:

- The calculated displacement have a magnitude of 10µm, the value does not pose any risk to the positional accuracy of the system
- The calculated stress has a magnitude of 0.65 MPa, far from the elastic limit of the material of 120 MPa. Thus, there is no risk of structural integrity loss.

5. Conclusions

The static analysis performed in ANSYS confirmed that the proposed design solution ensures safe and reliable operation under the applied loads. The simulations demonstrated minimal displacements (Δ_{max} = 0.01 mm) and low equivalent stress magnitude (σ_{max} = 0.65 MPa), well below the yield strength of the Aleris 55HX aluminum alloy. These results validate the structural integrity and stiffness of the grouped product holder and the pneumatic cylinder support plate. The use of CAE methods allowed for rapid and cost-effective verification, without physical prototypes. 2D shell modeling proved effective for accurate and efficient analysis. Therefore, the system can be safely integrated into packaging lines, ensuring stable performance and extended service life. Future work will focus on dynamic and fatigue simulations to more accurately assess durability under cyclic loading conditions.

6. References

[1]. Pupăză C. and Parpală, R.C. (2011), *Modelare şi analiză structurală cu ANSYS Workbenchsuport de curs*, Politehnica Press, București, ISBN 978-606-515-189-5.

[2]. Onica, I. (2016), *Introducere in modelarea cu elemente finite*, UNIVERSITAS Petroșani, Petroșani, ISBN 978-973-741-509-7.

[3]. Hamon, C. L., Green, M. G., Dunlap, B., Camburn, B. A., Crawford, R. H., and Jensen, D. D. (2014), " Virtual or physical prototypes? Development and testing of a prototyping planning tool.", Proceedings, ASEE Annual Conference & Exposition, ASEE Conferences , Indianapolis, 2014.

[4]. *** – https://www.marketresearchintellect.com/product/global-computer-aided-engineering-cae-software-market-size-and-forecast/

[5]. Thomai, M. P., & Sivamani, S. (2025). Structural Analysis of Different Components of a Conveying System Used in Road Cleaning Vehicles. Engineering Proceedings, 93(1), Article no. 1, DOI:10.3390/engproc2025093001

[6]. Ignasiak, Ł., Bieńczak, A., Woźniak, P., Kozłowicz, K., Różyło, R., & Szczepaniak, J. (2021). Finite Element Simulation Tests of the Structural Strength of the Molding Module for Burger Production from Vegetable Outgrades. Materials, 14(22), Article no. 6747, DOI: 10.3390/ma1422674

OPTIMIZING STORAGE AND AUTOMATED RECOVERY

CRACIUN Cristian-Ioan, POPESCU Adrian(Conducător științific)

Faculty of Industrial Engineering and Robotics, Industrial Logistics specialization, 4th year

ABSTRACT: The project proposes the creation of a functional ASRS (Automated Storage and Retrieval System) model on a small scale, with the aim of demonstrating an automated flow of product storage and retrieval. The presented mechanism uses three stepper motors controlled by an Arduino UNO, each coordinating a movement axis (X, Y and Z). Two work orders were created: storing the product on the shelf and retrieving it. The operation is based on synchronized and logical movements of the three axes. The project provides a solid basis for further expansion with different development methods.

KEYWORDS: ASRS, automation, prototype model

1. Introduction

This paper aims on Automated Storage and Retrieval Systems (ASRS), with a particular focus on functional prototypes and their current use in industry. The main objective is to assess the current state of research in this field and to highlight the most relevant technological solutions. The findings are based on the analysis of scientific articles dealing with the development, optimization and integration of ASRS in both industrial and educational settings.

The project involves building a functional ASRS model for demonstration purposes, using Arduino and stepper motors as core components. The aim is to gain a better understanding of how real-world storage systems can be controlled efficiently.

This work brings together elements of mechatronics, automation and programming, and serves as a solid foundation for further development in this area.

2. Current state

Automated Storage and Retrieval Systems (ASRS) have become essential components of modern logistics, significantly contributing to the efficiency of storage processes, space optimization and the reduction of the operational costs. Widely used in industries such as automotive, pharmaceuticals, food and beverage, and e-commerce, these systems provide precise and rapid solutions for the automated handling of load units.

According to an analysis by Kaviani, ASRS technologies are increasingly integrated with emerging technologies like Artificial Intelligence (AI) and the Industrial Internet of Things (IIOT), enhancing inventory management efficiency and operational adaptability within modern supply chains [1]. In the same direction, the study by Alabdulkarim and Noche highlights the advantages of implementing ASRS in large-scale warehouses, particularly in terms of reduced space utilization and improved material flow [2].

In parallel with industrial advancements, the scientific literature includes numerous examples of ASRS prototypes and scale models developed for educational or experimental purposes. For instance, the work of Joseph and Latha describes the design of a scaled-down ASRS model intended for use in educational labs, employing an Arduino-based control system and simplified actuation elements [3]. Similarly, Sharma and Pandey propose an ASRS mock-up that replicates automated motion along three axes and enables real-world operation simulations in a controlled environment [4].

As e-commerce continues to reshape the market, manufacturers and logistics providers must respond to higher consumer demand and an increased variety of stock-keeping units (SKUs). Moreover, industries such as food and beverage and pharmaceuticals are subject to strict regulations that require secure and safe handling of products, often in temperature-sensitive environments [5].

The study referenced in [6] proposes an Arduino-controlled ASRS prototype featuring Bluetooth communication and cloud storage via IoT. The authors emphasize the benefits of such a system in minimizing human error, reducing operational costs, and decreasing labor dependency. The integration of wireless communication and cloud storage allows remote command execution via mobile applications, real-time system data access, and efficient management of storage and retrieval operations.

3. Development of the automated storage solution

3.1. Design and implementation of the prototype:

In the context of warehouse automation and logistics flow optimization, it was decided to build a functional ASRS-type model, meant to simulate the basic principles of automatic product handling. The project aims to offer a concrete representation of how such a system works, in a scaled form, usable both for educational purposes and as a testing base for future developments.

For building the model, mechanical, electronic and software components were used to replicate, on a smaller scale, the functioning of an industrial automated storage system. The goal was to create an educational prototype that can simulate the essential movement of an ASRS on its 3 motion axes.

The main components used were: NEMA 17 stepper motors, perfect for the needs of the model due to their small step and higher torque, DRV8825 motor drivers which are used to allow motor control, 2040 aluminum profiles, toothed wheels, GT2 belts, and V-slot rails form the motion principle of the model.

The construction process took place in several successive stages: The first stage was the design of the structure, where a MINILOAD-type configuration with 3 motion axes was defined. The basic structure was made of aluminum rails, cut and assembled to allow linear movement on X and Y, with V-slot wheels mounted for guiding.

The second step was assembling the transmission system, where GT2 belts were tensioned on the pulleys and mounted together with the stepper motors, ensuring precise movement on the axes. For the Z axis (Fig.2), the same principle was used as for the others, the only difference being its function, which is to extend and retract the sliding tray, not for movement.

Fig.1. Mechanical component fabrication process

Fig.2. The construction process of the extendable tray

The third stage of building the model consisted in installing the electronic components (Fig.3), where each motor was connected to a driver and powered by a 12V 5A power supply. To allow the simultaneous connection and powering of multiple drivers, a CNC Shield compatible with the Arduino UNO was used. This shield supports the direct integration of up to 4 stepper motor drivers and ensures an organized distribution of control signals for each axis. In addition, the CNC Shield allows separate power input for the motors, with a higher voltage than what the Arduino board can handle, thus ensuring stable operation of the stepper motors without overloading the microcontroller.

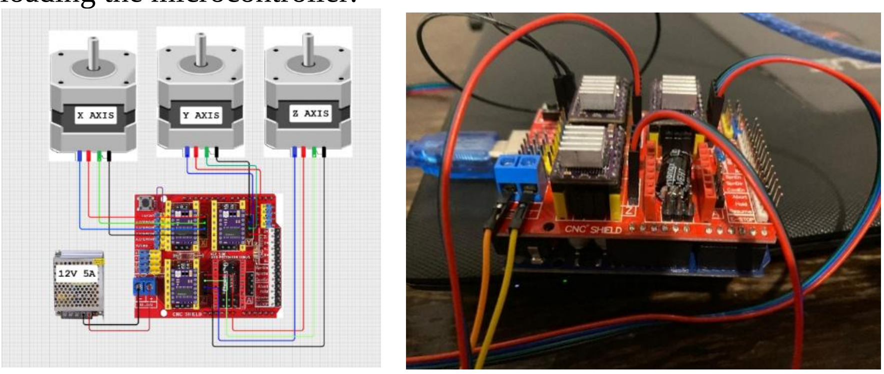

Fig.3. Designing the electrical schematic

Another stage consisted in programming the system, which was controlled using the Arduino board, and the movement sequence were defined. Command R1 is meant to move the system along the X axis by +250mm, Y by +260mm, and once the target position is reached, the Z-axis motor is activated to extend +70mm. Then the Y axis lowers by 20mm, and in the end, all three motors return to their initial position. Command R2 is similar to the first one. After the X and Y motors reach the target position and the Z motor extends the tray, the Y motor moves up by +20mm to lift the desired product. Finally, all three motors return to their initial position.

The system was tested both manually and automatically, verifying the synchronization of movements on each axis.

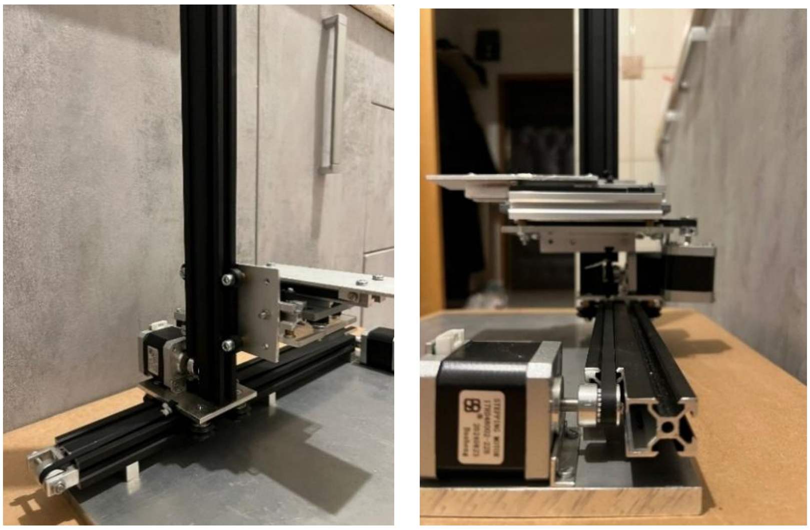

Fig.4. Model construction

3.2. Prototype programming process

For the system to function correctly, it was necessary to determine some basic parameters for controlling the motor axis movements: the number of steps per millimeter, the rotation speed, and the maximum current set through the driver. The calculated values were later implemented in the control program.

- **Steps per mm calculation formula :**

The number of steps required to move one millimeter is determined using the following formula:

$$\text{STEPS\_PER\_MM} = \frac{\boldsymbol{N \times M}}{\boldsymbol{P}} \quad (1)$$

Where the NEMA 17 motor has 200 per revolution (1.8°/step), the microstepping is set to 1/16, the GT2 pulley has 20 teeth, and the belt pitch is 2 mm.

$$\text{STEPS\_PER\_MM} = \frac{\mathbf{200 \times 16}}{\mathbf{20 \times 2}} = 80\text{mm} \quad (2)$$

- **Formula for calculating the motor speed in revolutions per minute (RPM):**

$$\text{RPM} = \frac{\boldsymbol{v \times 60}}{\boldsymbol{P}} \quad (3)$$

- **Formula for the maximum current set on the driver via Vref:**

$$I = \frac{Vref}{8 \times Rsenzor} \tag{4}$$

The code developed for controlling the model was written using the Arduino IDE platform, in the C++ programming language. This code enables precise control of the automated storage system's movements, coordinating the X, Y and Z axes through stepper motors based on a predefined logical sequence of commands.

```
pinMode(ENABLE_PIN, OUTPUT);
digitalWrite(ENABLE_PIN, LOW);
```

This sequence activates the drivers by setting the *ENABLE* pin to *LOW* level.

```
if (inputString == "R1") {
motorX.moveTo(250 * STEPS_PER_MM);
motorY.moveTo(-260 * STEPS_PER_MM);
etapa = R1_MOVE_XY;
```

If the command "R1" is entered in the Serial Monitor, the X motor will move 250 mm, and the Y motor will move 260 mm.

```
if (inputString == "R1") {
  motorX.moveTo(250 * STEPS_PER_MM);
  motorY.moveTo(-260 * STEPS_PER_MM);
  etapa = R1_MOVE_XY;
```

The X and Y motors run until they reach the specified position. Once they arrive, the Y motor moves an additional 20 mm to position the extendable tray at the shelf.

```
else if (etapa == R1_LIFT_Y_20){
    motorY.run();
    if (motorY.distanceToGo() == 0) {
      motorZ.moveTo(70 * STEPS_PER_MM);
      STEPS_PER_MM);
      R1_EXTEND_Z
```

After Y reaches the upper position, the Z motor extends the tray by 70 mm to place the product on the shelf.

```
else if (etapa == R1_DROP_Y_20) {
  motorY.run();
  if (motorY.distanceToGo() == 0) {
    motorZ.moveTo(0);
    etapa = R1_RETRACT_Z;
```

The Z motor retracts the tray back to its initial position.

```
else if (etapa == R1_RETURN_XY) {
```

```
motorX.run(); motorY.run();
if (motorX.distanceToGo() == 0 && motorY.distanceToGo() == 0) {
  etapa = IDLE;
```

This step ends the R1 sequence. The system returns to the *IDLE* state, waiting for a new command.

The R2 sequence is similar to R1, but in reverse order:
- X and Y move to the specific position
- Z extends to get under the product
- Y moves up 20 mm to "lift" the product
- Z retracts with the product
- The system returns to the starting position

4. Conclusions

The project allowed for deeper understanding of both theoretical and practical aspects related to the automation of logistics processes. By using accessible and adaptable components, it successfully simulated the basic movements of an automated storage system, in line with the operating principles of a real industrial installation.

The model demonstrated the feasibility of implementing an educational ASRS prototype capable of executing predefined pick-and-place sequence under the control of an Arduino microcontroller. The tests carried out showed food coordination between the mechanical and electronic components, despite the simplified configuration and the absence of advanced feedback or automatic position detection systems.

However, to improve functionality and expand the system's capabilities, the following development directions are proposed: integrating a real picking platform compatible with standardized objects or containers, adding an LCD screen to display current commands, implementing an RFID module to allow automatic identification of products or storage locations, integrating a Bluetooth communication module to enable system control directly from a phone or tablet.

5. Bibliography

[1]. Zeenat Khan şi Mohsin Bilal Ahmed (2025), „Advancements in Automated Storage and Retrieval Systems: A Comprehensive Review" , Juniper Publishers.

[2]. Alabdulkarim, A., & Noche, B. (2018). „*Automated Storage and Retrieval Systems (AS/RS) in Warehouse Automation: A Review*. In Proceedings of the 5th International Conference on Industrial Engineering and Operations Management".

[3]. Billy Sagara, S.T., Dr. Sugih Sudharma Tjandra, S.T., M.Si., Yansen Theopilus, S.T., M.T. (2019). „Design of a Miniature Automatic Storage and Retrieval System (AS/RS) for Educational Purposes".

[4]. Sharma, A., & Pandey, A. (2020). "*Development of a Small Scale ASRS for Flexible Manufacturing Systems*. ResearchGate".

[5]. SSI Schaefer - „Ce este un sistem automatizat de stocare și recuperare (ASRS)?"

[6]. Manisha Suresh Pingale, Dr. Haripriya H. Kulkarni, INTERNATIONAL JOURNAL OF SCIENTIFIC & TECHNOLOGY RESEARCH VOLUME 8, ISSUE 09, SEPTEMBER 2019, ISSN 2277-8616

6. Notations

N = number of steps per motor revolution

M = microstepping value
P = mechanical perimeter (mm/revolution)
v = movement speed

THE DEVELOPMENT OF THE ANTAGON CONCEPT: ANSYS-BASED ANALYSIS OF A SPECIALIZED RESERVOIR

PETREANU Julia-Cristiana, Alexandru Tudor(Conducător științific)

Faculty of Industrial Engineering and Robotics, Specialization: Industrial Logistics, Year of study: I,
e-mail: juliapetreanu@yahoo.com

ABSTRACT: This paper addresses the innovative concept of ANTAGON, a new brand in the perfumery industry focused on dual-fragrance products and proprietary production systems. The study introduces the structural analysis of a critical reservoir component within the ANTAGON filling system, by employing ANSYS simulation tools. The research focuses on: material selection, model simplification, mesh generation, boundary conditions and the evaluation of the structural behavior under gravitational loading. Results confirm the mechanical integrity and suitability of the reservoir for industrial use, with optimal safety factors ensuring a safe and reliable operation.

KEY WORDS: ANTAGON, Static analysis, Finite element method, logistics

1. Introduction

Stainless steel reservoirs are essential components in the perfume manufacturing process. They serve as storage and transfer units for olfactory bases, essential oils, and solvent blends [1]. Their role goes beyond containment as they ensure product purity, maintain chemical stability, and prevent contamination during logistic operations. Thanks to its excellent corrosion resistance, mechanical strength, and hygienic properties, stainless steel, particularly AISI 304 and 316L grades has become the material of choice in the cosmetics and pharmaceutical industries, where high standards of cleanliness and durability are required [2].

Assessing the structural integrity of these reservoirs is essential to ensure safe operation under various conditions, including static loads from stored liquids, dynamic effects during filling, and external forces due to the industrial environment. Structural failure can result not only in economic losses due to production downtime, but also in product contamination and safety risks. Consequently, predictive validation using finite element analysis (FEA) has become an essential step in the design and certification process, allowing engineers to assess performance prior to manufacturing [3].

In this study, a three-dimensional model of a stainless steel perfume reservoir was developed and analyzed using ANSYS Workbench. The model was simplified using mid-surface commands, to reduce computational costs while preserving key geometric characteristics. Realistic boundary conditions, including gravitational loads and internal liquid pressure, were defined to simulate operational behavior.

The aim of the analysis is to evaluate the total deformation, von Mises stress distribution and safety factor, which collectively describe the tank's ability to withstand the applied loads. These results provide insight into design effectiveness, confirm compliance with industry standards, and support future optimization of fragrance production systems.

2. Literature survey

Papers similar to the present work are depicted in various research studies. For example, in [4], a comprehensive finite element analysis is presented for evaluating the mechanical response of large oil storage tanks subjected to non-uniform foundation settlements. The study developed a high-fidelity ANSYS model to study the stress and strain distribution in the tank shell and bottom plates under various loading conditions and geometry. Critical areas where local plastic deformation can occur were highlighted, emphaszing the importance of accurate finite element modeling in tank and vessel design.

Similarly, the structural strength of a molding module designed for the production of hamburgers from plant waste using ANSYS-based finite element simulations was depicted in [5]. The research focused on evaluating operational and failure load cases, such as hydrostatic pressure and actuator-induced stresses, applied to stainless steel components. The analysis identified stress concentrations and quantified deformations, all within safe limits, thus confirming the design's compliance with sanitary and mechanical requirements.

In [6], a numerical study was completed in ANSYS which explored static, modal, and response spectral analyses of vertical storage tanks subjected to hydrostatic and seismic loads. The authors proposed a 3D model of cylindrical tanks and compared the results of finite element analysis with analytical formulations, identifying stress hotspots and deformation trends under different fluid levels. The paper demonstrated ANSYS's ability to accurately reproduce real-world operating conditions and served as a benchmark for optimizing tank geometry and wall thickness to improve their structural efficiency.

3. Pre-processing

Figure 1 depicts the geometry of the analyzed assembly.

Fig. 1.3D CAD model of the studied assembly

Manufacturing of the stainless steel reservoir is completed by employing roll bending forming manufacturing process. Thus, the resulting sheet metal body can be converted to a 2D surface model by using the mid-surface technique. Topology operations are also employed to facilitate the mesh refinement around the bottom neck of the geometry, given the change in the cross section and the proximity of this area to the fixed support location.

The material properties are extracted from MATWEB library and are depicted in table 1.

Tabel 1. Material properties

Characteristic	Values
Material class	304 Stainless Steel
Modulus of Elasticity	$1.93 \cdot 10^5$ MPa
Poisson Ratio	0.29
Tensile Yield Strength	215 MPa

Meshing is completed by employing 2D Shell elements with a constant wall thickness of 2.5 mm. The mapped face option was used given the multiple surfaces of the geometry which encompass edges (See Fig.2).

Fig. 2. Face meshing and element quality

The element quality criterion was used to verify the quality of the mesh, with an average quality of 0.76.

Loads and boundary conditions are applied in conformity with the operational scenario of the geometry. Fixed support conditions are defined on the exterior edges of the reservoir mounting location. A distributed mass is included to replicate the mass induced by the volume of liquid. The magnitude is calculated as 13.07 Kg. Standard earth gravity is included for taking into account gravitational forces and their impact on the calculated stress and deformation (see Fig.3).

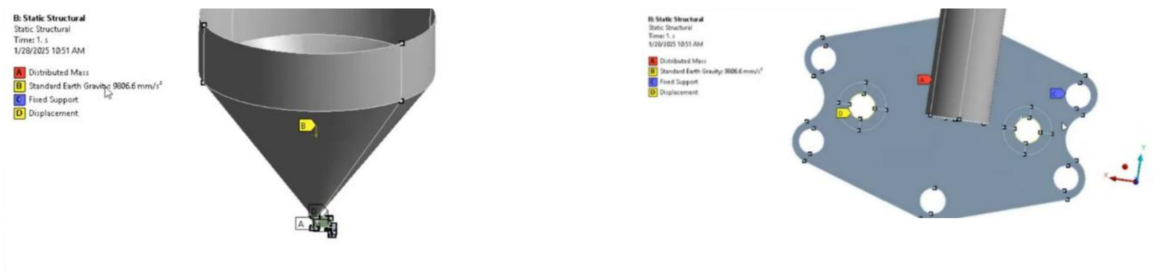

Location of the distributed mass **Location of the fixed support**

Fig. 3. Loads and boundary conditions

4. Solving

In a static structural analysis, ANSYS solves a system of equations describing the balance of forces within a deformable body under static load. These equations are derived from classical continuum mechanics and the finite element method (FEM). No acceleration or damping is considered as the inertial and damping forces are neglected. The continuous domain is divided into finite elements, and the equilibrium equation takes the matrix form [7]:

$$[K]\{u\} = \{F\} \quad (1)$$

Where: K is the global stiffness matrix; u represents the displacement vector and F the exterior forces vector.

The stiffness matrix of each element is obtained from the strain-displacement and stress-strain relationships:

$$\{\varepsilon\} = [B] \cdot \{u\} \quad (2)$$

Where: ε represents the strain and B the strain-displacement vector. The material constitutive matrix depends on Young's modulus and Poisson's ratio.

5. Post-processing

- **The total deformation**

The total deformation plot is depicted in figure 4, having a maximum magnitude of 0.42 mm.

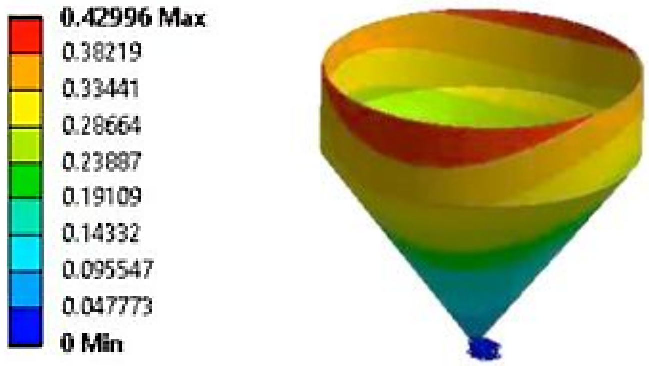

Fig. 4 The total deformation

There is no risk of stability loss during the filling or emptying stage of the reservoir.

- **The equivalent Von-Misses stress**

While the calculated deformation provides an insight into the stability of the reservoir, its structural integrity can only be confirmed by processing the stress magnitude.

Figure 5 depicts the equivalent Von-Misses stress plot.

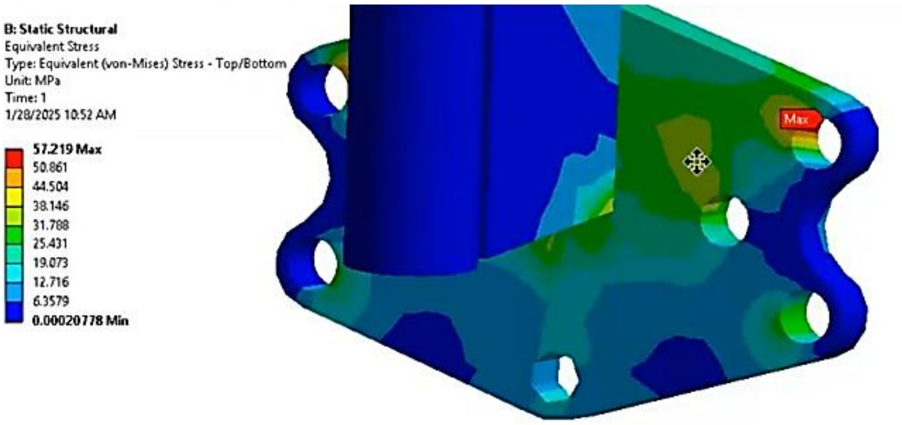

Fig. 5 The equivalent von Mises stress

The maximum stress has a value of 57.2 MPa. Given the tensile yield strength of the material of 215 MPa, there is no risk of structural integrity loss.

Figure 6 depicts the resulting safety factor for the entire structure.

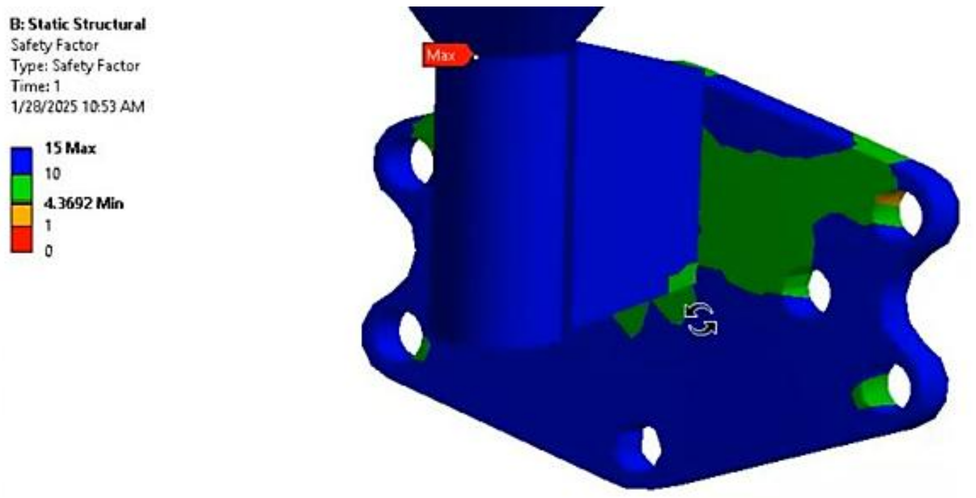

Fig. 6 The equivalent von Mises stress

The most critical value of 4.36 occurs in the location of the mounting flange.

5. Conclusions

This research successfully studied the static structural behavior of a specialized stainless steel tank developed as part of the ANTAGON perfumery concept. By applying finite element analysis via ANSYS Workbench, the study validated the design of the reservoir under realistic operating conditions. The adoption of a 2D shell model proved to be an efficient and reliable simplification technique, significantly reducing computational costs while maintaining geometric fidelity and stress distribution accuracy. The mesh quality, with an average of 0.76, ensured an appropriate result accuracy. Thanks to carefully defined boundary conditions, including gravitational effects and distributed liquid mass, the simulation reproduced the operating environment of the reservoir during the filling and storage cycles. The maximum total deformation of approximately 0.42 mm indicates minimal elastic strain, confirming the stability of the structure under load. Furthermore, the maximum equivalent Von Mises stress, recorded at 57.2 MPa, remains well below the yield strength of 215 MPa for AISI 304 stainless steel.

This results in a safety factor greater than 4.3, demonstrating the ability of the structure to withstand the applied loads without the risk of failure. The analysis also highlights the design's adaptability to industrial implementation, ensuring compliance with the mechanical integrity and hygiene standards required in the cosmetics and perfumery sectors. These results confirm the ANTAGON suitability as a reliable component within a dual-fragrance logistics system.

8. References

[1]. Abambres, M., & Arruda, M. R. (2016). "Finite element analysis of steel structures– a review of useful guidelines", International Journal of Structural Integrity, 7(4), 490-515.
[2]. İrsel, G. (2019). The effect of using shell and solid models in structural stress analysis. Vibroengineering Procedia, 27, 115-120.
[3]. Bucalem, M. L., & Bathe, K. J. (1997). Finite element analysis of shell structures. Archives of Computational Methods in Engineering, 4(1), 3-61.
[4]. Jiao, Y., Wang, Y., Li, J., & Liu, X. (2024). "Finite Element Analysis and Improved Evaluation of Mechanical Response in Large Oil Storage Tanks Subjected to Non-Uniform Foundation Settlement", Processes, 12(12), Article no. 2838.
[5]. Ignasiak, Ł., Bieńczak, A., Woźniak, P., Kozłowicz, K., Różyło, R., & Szczepaniak, J. (2021). "Finite Element Simulation Tests of the Structural Strength of the Molding Module for Burger Production from Vegetable Outgrades", Materials, 14(22), Article no. 6747.
[6]. Pantusheva, M., & Zdravkov, L. "Numerical analysis of vertical steel storage tanks in ansys workbench and ansys mechanical APDL", available online at: https://www.researchgate.net/publication/337136950_Numerical_Analysis_of_Vertical_Steel_Storage_Tanks_in_ANSYS_Workbench_and_ANSYS_Mechanical_APDL
[7]. Onica, I. (2016), *Introducere in modelarea cu elemente finite*, UNIVERSITAS Petroșani, Petroșani, ISBN 978-973-741-509-7.

PREDICTIVE MAINTENANCE IN INDUSTRY 5.0: INTEGRATING SENSORS FOR EFFICIENCY AND SAFETY

STOIAN Bogdan-Nicolae, COSTEA Mihai, NĂSTASE Marian-Sebastian, Emilia-Maria Popescu, Constantin-Adrian POPESCU(Conducător științific)

Faculty of Industrial Engineering and Robotics, Specialization: Industrial Logistics[1)], Safety and Integrity of Structures[2)], Industrial design and innovative products[3)], Academic year: Masters 1st,
e-mail: bogdan.stoian0403@upb.ro

ABSTRACT: Predictive maintenance is essential in Industry 5.0, an era in which advanced technology is deeply integrated into industrial processes. By using IoT (Internet of Things) sensors, companies can monitor the condition of equipment in real time and anticipate potential failures before they affect the production line. This allows for the optimization of operations and the prevention of high costs associated with unplanned equipment downtime.

IoT sensors collect relevant data, such as temperature, vibration, pressure, or other signs of wear, and this information is transmitted to analytics platforms, which use artificial intelligence (AI) algorithms to predict when a component might fail. This proactive approach allows maintenance teams to intervene on a scheduled basis, thereby reducing downtime and maximizing production efficiency.

Within Industry 5.0, predictive maintenance not only optimizes equipment performance, but also contributes to reducing energy consumption and protecting the environment by reducing waste generated by defective parts. In addition, the use of these technologies increases the safety of employees, as the risks associated with uncontrolled machine failures are reduced.

The examples in the industry are already obvious. For example, in the automotive industry, IoT sensors are used to monitor the condition of assembly machines, and the data collected is analyzed to predict failures before they manifest themselves. These solutions are already implemented in many factories, offering a futuristic model for integrating predictive maintenance into industrial processes, thus reinforcing the advantages of Industry 5.0.

KEY WORDS: Industry 5.0, sensors, predictive maintenance

1. Introduction

Defining Industry 5.0: Introducing the concept of Industry 5.0, with a focus on human-machine collaboration. In this era, advanced technologies such as artificial intelligence (AI), collaborative robots (cobots), and IoT are being integrated to support human workers and improve industrial processes.

The importance of maintenance in Industry 5.0: Maintenance plays an essential role in ensuring the continuity of production processes and minimizing downtime. In Industry 5.0, maintenance is not only a repair activity, but also an element of prevention, prediction and optimization.

2. Literature Review

Industry 5.0 introduces a new paradigm where people and advanced technologies, including IoT sensors, work together to optimize industrial processes. A critical component of this ecosystem is the use of smart sensors for **predictive maintenance**, monitoring equipment condition, and reducing downtime. This literature review explores recent advances in the use of IoT sensors for maintenance in Industry 5.0, drawing on 14 relevant scientific sources.

2.1. Integration of IoT sensors in Industry 5.0

a. IoT sensors are essential elements of predictive maintenance, allowing the collection of real-time data on the operation of industrial equipment. According to Zhang et co. (2021), these sensors are interconnected through wireless networks and 5G communications, sending data to cloud systems where they are analyzed by Artificial Intelligence (AI) algorithms [1].

b. IoT sensors enable predictive maintenance by monitoring equipment and analyzing data in real-time. Bibri and Krogstie (2022) explored the impact of these sensors in smart factories [2].

Vibration sensors for detecting mechanical failures

a. Predictive maintenance based on vibration analysis is one of the most effective methods of preventing mechanical defects. Singh & co. (2022) demonstrated that IoT vibration sensors can detect bearing wear before major failures occur [3].

b. According to Mishra et co. (2023), high-precision vibration sensors can identify mechanical imbalances before they lead to major defects [4].

Temperature sensors to prevent equipment from overheating

a. In industrial systems, abnormal temperature fluctuations can indicate serious problems, such as overheating of motors or faulty electrical contacts. Liu et co. (2020) analyzed the impact of IoT temperature sensors, the study showed that implementing thermal monitoring based on IoT sensors can extend the service life of equipment by 20-30% [5].

b. Almeida & co. (2021) demonstrated the efficiency of IoT sensors in thermal monitoring of industrial components, preventing defects caused by high temperatures [6].

Current and voltage sensors for monitoring energy consumption

a. Optimizing energy consumption is a key objective in Industry 5.0. Kumar et co. (2021) demonstrated that IoT current and voltage sensors are able to detect anomalies in the power supply of electrical equipment, thus preventing their damage. This research highlights the role of IoT sensors in identifying abnormal power consumption and preventing overloads [7].

b. A study by Tahir & co. (2022) showed that IoT sensors for measuring current help detect anomalies in energy consumption, reducing energy losses [8].

Acoustic and ultrasonic sensors for defect detection

a. Acoustic sensors can identify mechanical problems based on the analysis of the sound generated by the equipment. Rizzo & co. (2022) investigated the use of ultrasonic sensors for the detection of gas and liquid leaks in industrial plants. This study showed that ultrasonic sensors can detect microcracks in pipes with an accuracy of over 90% [9].

b. Bouchard et co. (2023) analyzed the use of ultrasonic sensors for the detection of gas leaks and mechanical cracks in industrial systems [10].

Optical sensors and thermal imaging cameras for visual inspections

a. Industry 5.0 integrates optical sensors and thermal imaging cameras for automated inspections. Gonzalez & co. (2021) demonstrated that these systems are highly effective in detecting overheating of electrical equipment [11].

b. A study by Torres & co. (2021) showed that optical sensors and thermal imaging cameras are essential for detecting thermal anomalies in industrial equipment [12].

Integration of IoT sensors with Artificial Intelligence for failure prediction

a. Artificial Intelligence plays an essential role in the analysis of data collected by IoT sensors. Gupta & co. (2023) demonstrated that machine learning algorithms can improve the accuracy of failure prediction by 40-50% [13].

b. Huang & co. (2023) demonstrated that AI analysis of IoT data improves fault detection accuracy by more than 50% [14].

2.2. Applications of IoT Sensors in Industry 5.0 for Predictive Maintenance

Industry 5.0 leverages IoT sensors to optimize equipment maintenance by collecting and analyzing data in real time. Here are the main industrial applications for each type of sensor.

Applications of Vibration Sensors

Monitoring of bearings and electric motors, detects premature wear and prevents catastrophic failures.

Ex: The ADXL1002 sensor is used in the automotive industry for assembly engines.

Monitoring of steel structures, detects cracks and loosening of welds in bridges and industrial structures.

Ex: In the aerospace industry, Boeing uses MEMS sensors to detect vibrations in aircraft structures [15].

Applications of Temperature Sensors

Electrical transformer monitoring, detects overheating of coils to prevent fires.

Ex: The LM35 sensor is used in power grids to optimize transformer maintenance.

Industrial furnace monitoring, controls the temperature in metal smelting furnaces.

Ex: The metallurgical industry uses MAX31865 sensors to monitor the temperature in the casting furnaces [16].

Applications of Current and Voltage Sensors

Preventing overloads in factories, detects anomalies in energy consumption to prevent equipment damage.

Ex: ACS758 sensors are used in electronics factories for monitoring production lines.

Optimizing energy consumption, identifies areas with energy loss and optimizes costs.

Ex: In the automotive industry, Tesla uses IoT current sensors to monitor the consumption of industrial robots [17].

Applications of acoustic and ultrasonic sensors

Gas leak detection, identifies natural gas leaks in industrial facilities.

Ex: Chemical plants use ultrasonic sensors to monitor pipelines.

Detection of mechanical defects in production lines, monitors abnormal sounds in gearboxes and compressors.

Ex: In the aeronautical industry, Airbus uses acoustic sensors for turbine wear analysis [18].

Applications of optical sensors and thermal imaging cameras

Automatic weld inspection detects imperfections and cracks in industrial welds.

Ex: Companies in the shipping industry use FLIR thermal cameras for defect detection.

Monitoring of high-power electrical equipment identifies overheating points in electrical panels.
Ex: Energy producing plants use thermal cameras for the inspection of transformer stations [19].

Applications of AI IoT Sensors for Failure Prediction
Predictive maintenance for industrial robots, uses AI to predict assembly robot failures.
E.g. IoT sensors are used in KUKA robots for uptime analysis.

Analysis of the health of equipment in the oil industry, monitors the vibrations and temperature of oil pumps.
Ex: Offshore platforms use machine learning to predict equipment wear [20].

3. Predictive Maintenance

Definition and importance: Predictive maintenance involves using sensors to detect potential failures before they become critical. This reduces the need for emergency interventions and minimizes downtime.

IoT sensors: These sensors collect real-time data from industrial equipment, providing information about its status.

In the context of Industry 5.0, IoT sensors play a critical role in collecting and analyzing the operational data of industrial equipment. These are smart devices capable of measuring essential equipment parameters, such as temperature, vibration, humidity, pressure and energy consumption, sending this data in real time to analytics platforms based on cloud computing and Artificial Intelligence (AI).

3.1. Types of IoT sensors used in maintenance

To ensure an effective predictive maintenance system, different IoT sensors are used depending on the nature of the equipment and the type of defects to be detected:

Table 1. Types of IoT sensors

Vibration sensors [21]		Detects anomalies in the operation of rotating equipment such as motors, pumps, and compressors. Increased vibration may indicate bearing wear or mechanical imbalance of components.
Temperature sensors [22]		It monitors the overheating of electrical and mechanical components, preventing failures caused by high temperatures.
Acoustic and ultrasonic sensors [23]		It analyzes abnormal noises produced by equipment, being used to detect leaks of gases or fluids under pressure.
Pressure sensors [24]		Use in hydraulic and pneumatic systems to detect pressure losses that may indicate leaks or blockages in pipes.

Current and voltage sensors [25]		Analyzes the energy consumption of equipment to identify faults in electric motors or overloads in the grid.
Optical sensors and thermal imaging cameras [26]		They are used for automatic visual inspection of equipment and identification of overheating of electrical components.

Own source

3.2. Architecture of an IoT system for maintenance

An effective IoT system for predictive maintenance includes several interconnected components:

- IoT sensors – collect data on the operation of equipment.
- Communication modules – data is transmitted via Wi-Fi, Bluetooth, Zigbee, LoRaWAN or 5G networks to a centralized server.
- Cloud platform – data is stored and analyzed using Big Data and Machine Learning algorithms.
- Artificial Intelligence (AI) and Predictive Analytics – AI identifies abnormal patterns and can predict when equipment needs maintenance.
- User interface (UI/UX) – operators and engineers can view system parameters in real-time on digital control panels.

3.3. Benefits of Using IoT Sensors in Maintenance

- Reduced downtime – Failures can be anticipated, preventing unplanned equipment downtime.
- Optimization of maintenance costs – Interventions are carried out only when necessary, reducing the costs associated with corrective maintenance.
- Increased equipment life – Minor failures are detected early, preventing complete damage to the equipment.
- Automation of the maintenance process – AI systems can trigger alarms or even command robots for automatic repairs [21].

4. Case study: Implementing IoT Sensors for Predictive Maintenance in an Automotive Factory

4.1. Industry context

AutoTech Manufacturing, an automotive manufacturer in Europe, has experienced frequent problems with unplanned assembly line shutdowns due to unexpected equipment failures. This has resulted in production losses of more than €2 million annually.

To reduce these losses, the company decided to implement a predictive maintenance system based on IoT sensors, integrated with Artificial Intelligence (AI) and Machine Learning (ML).

4.2. IoT Sensor Deployment

The company has installed a network of smart sensors on critical equipment in the assembly plant:

- Vibration sensors (bearing and motor monitoring)
  - Detects vibration variations that indicate mechanical wear.
  - Ex: Mounting on KUKA robotic arms and conveyor belts.
- Temperature sensors (prevention of equipment overheating)
  - Monitors temperatures in electric motors and hydraulic units.
  - Ex: Installation on stamping press and CNC machines.
- Current and voltage sensors (detection of electrical anomalies)
  - Identifies overloads and abnormal fluctuations in energy consumption.
  - E.g.: Use for monitoring the power supply of industrial robots.
- Ultrasonic sensors (leak detection of compressed air and liquids)
  - Detects leaks in pneumatic and hydraulic systems.
  - Ex: Implementation on assembly lines and robots with pneumatic actuators.
- Thermal imaging cameras and optical sensors (weld analysis and part quality)
  - It uses thermal imaging to detect cracks or imperfections in welds.
  - Ex: Use in the robotic welding station.

4.3. Implementation Results

- Downtime reduced by 40%
  - The AI system predicted 85% of failures two weeks in advance
- Maintenance costs reduced by 25%
  - Condition-based maintenance replaced excessive preventive maintenance
- Energy efficiency improved by 15%
  - Consumption optimization based on current sensor data
- Improved product quality
- Thermal cameras detected 30% more defects in body welds [27].

5. Conclusions and future prospects

Predictive maintenance is an essential pillar of Industry 5.0, bringing significant benefits in operational efficiency and reducing maintenance costs. By integrating artificial intelligence, IoT sensors, and real-time data analytics, companies can anticipate equipment failures and optimize industrial processes.

The adoption of this technology not only minimizes unplanned downtime and increases the lifespan of equipment, but also contributes to sustainability by reducing resource consumption and industrial waste. However, the effective implementation of predictive maintenance requires high upfront investments, robust digital infrastructure, and specialized data analytics personnel.

In the future, the development of more accurate predictive models, based on machine learning and advanced artificial intelligence, will lead to continuous improvements in industrial performance. Also, integration with intelligent automation systems and 5G networks will allow for faster and more reliable monitoring of equipment.

Therefore, predictive maintenance is a key element of Industry 5.0, facilitating the transition to smarter, more sustainable and more efficient factories.

6. Bibliography:

[1]. Zhang, Y., & Liu, H. (2021). *IoT-Based Predictive Maintenance for Smart Factories: A Comprehensive Review*. *Journal of Industrial Engineering & Management*, 14(3), 245-260.

[2]. Bibri, S. E., & Krogstie, J. (2022). *The Role of IoT Sensors in Industry 5.0: A Smart Manufacturing Perspective*. *Journal of Future Technology and Smart Systems*, 25(1), 112-130.
[3]. Singh, R., & Gupta, P. (2022**).** *Vibration Sensors for Industrial Predictive Maintenance: An Industry 5.0 Perspective*. *Sensors & Actuators B: Chemical*, 357, 131245.
[4]. Mishra, A., Kumar, R., & Sharma, S. (2023). *Advancements in Vibration Sensing for Predictive Maintenance in Smart Manufacturing*. Mechanical Systems and Signal Processing, 198, 110254.
[5]. Liu, J., & Zhao, W. (2020). *Thermal Monitoring in Industry 5.0: The Role of IoT-Based Temperature Sensors*. *IEEE Transactions on Industrial Informatics*, 16(5), 3321-3334.
[6]. Almeida, P., Costa, J., & Silva, L. (2021). *Temperature Monitoring in Industrial Environments Using IoT-Based Sensors*. IEEE Transactions on Smart Systems, 18(3), 765-780.
[7]. Kumar, V., & Rao, S. (2021). *Energy Monitoring and Fault Detection in Smart Factories using IoT Sensors*. *Journal of Smart Manufacturing and Automation*, 9(2), 145-160.
[8]. Tahir, M., Khan, I., & Yousaf, A. (2022). *Smart Energy Monitoring Using IoT-Based Current Sensors in Industrial Applications*. *Journal of Energy Systems and Efficiency*, 16(4), 421-438.
[9]. Rizzo, F., & Conti, M. (2022). *Acoustic and Ultrasonic Sensors for Predictive Maintenance in Industry 5.0*. *Applied Acoustics*, 190, 108491.
[10]. Bouchard, M., Lefebvre, G., & Tremblay, P. (2023). *Ultrasonic Sensors for Leak Detection in Industry 5.0 Applications*. *Sensors and Actuators A: Physical*, 356, 112576.
[11]. Gonzalez, A., & Martin, D. (2021). *Optical and Thermal Imaging Sensors for Industrial Inspection*. *Machine Vision and Applications*, 32(4), 785-799.
[12]. Torres, J., Martinez, F., & Rodriguez, C. (2021). *Thermal and Optical Imaging for Predictive Maintenance in Smart Factories*. *Machine Vision and Applications*, 36(2), 589-604.
[13]. Gupta, R., & Singh, P. (2023). *Machine Learning for Predictive Maintenance using IoT Sensors*. *IEEE Internet of Things Journal*, 10(3), 1895-1908.
[14]. Huang, Y., Zhang, W., & Li, X. (2023). *AI-Driven Fault Prediction Using IoT Sensors in Industrial Systems*. *IEEE Internet of Things Journal*, 11(1), 251-269.
[15]. Mishra, A., Kumar, R., & Sharma, S. (2023). *Advancements in Vibration Sensing for Predictive Maintenance in Smart Manufacturing*. Mechanical Systems and Signal Processing, 198, 110254.
[16]. Almeida, P., Costa, J., & Silva, L. (2021). *Temperature Monitoring in Industrial Environments Using IoT-Based Sensors*. IEEE Transactions on Smart Systems, 18(3), 765-780.
[17]. Tahir, M., Khan, I., & Yousaf, A. (2022). *Smart Energy Monitoring Using IoT-Based Current Sensors in Industrial Applications*. Journal of Energy Systems and Efficiency, 16(4), 421-438.
[18]. Bouchard, M., Lefebvre, G., & Tremblay, P. (2023). *Ultrasonic Sensors for Leak Detection in Industry 5.0 Applications.* Sensors and Actuators A: Physical, 356, 112576.
[19]. Torres, J., Martinez, F., & Rodriguez, C. (2021). *Thermal and Optical Imaging for Predictive Maintenance in Smart Factories*. Machine Vision and Applications, 36(2), 589-604.

[20]. Huang, Y., Zhang, W., & Li, X. (2023). AI-Driven Fault Prediction Using IoT Sensors in Industrial Systems. IEEE Internet of Things Journal, 11(1), 251-269.

[21]. - https://www.tequipment.net/SKF/CMCP420VT-T2/Vibration-Meter/

[22]. - https://www.romtrade-automation.ro/regulator-de-temperatura-dtk4848r01-in-100-240vac-intrare-sensor-temperatura-platina-rtd-pt100-jtp100-rtu-cu50-ni120-termocuplu-11-tipuri-1-x-out-releu-5a-1-x-alarma-releu-3a-dim-48-x-48.html?gad_source=1&gclid=Cj0KCQiA-5a9BhCBARIsACwMkJ5rj5JeblnF11zfh0mkZVcnMGFdIkXS-VMkmYYa3wXsniiW7r44HRgaAiV5EALw_wcB

[23]. - https://www.meterland.ro/en/gas-leak-detection/1694-flir-si2-ld-industrial-acoustic-imag ing-camera-for-pressurized-leak-detection-and-mechanical-fault-detection.html

[24]. - https://www.tme.eu/no/en/details/mipag1xx010bsaax/pressure-transducers/honey well/

[25].-https://shop.hioki.eu/CT6873-AC-DC-Current-Sensor-Fluxgate-200-A-10-MHz/CT6873?utm_source=google&utm_medium=cpc&utm_campaign=current_sensors_per_max&utm_content=&utm_term=&gad_source=1&gclid=Cj0KCQiA-5a9BhCBARIsACwMkJ6uhgtIWm5gN6HtsaYupaDIrpwhWBPCd7mHyBenYj5htR2vE51IHUkaAgQHEALw_wcB

[26].-https://www.ifm.com/ro/ro/product/O2U540?source=gs&gad_source= 1&gclid=Cj0KCQiAa9BhCBARIsACwMkJ6Gg1zAnonrQPp34MC0ul_bCZzTxiZMWmsTH5yBIO7JGVW7LGJttqcaAkGYEALw_wcB

[27]. Wang, J., Zhang, T., & Li, P. (2023). *Smart Maintenance Strategies in Automotive Manufacturing Using IoT and AI. International Journal of Industrial Engineering and Management*, 22(4), 457-475.

STUDY ON THE IMPACT OF THE IMPLEMENTATION OF VLM IN DISTRIBUTION CENTERS

STOIAN Bogdan-Nicolae, Constantin-Adrian POPESCU(Conducător științific)

Faculty of Industrial Engineering and Robotics, Specialization: Industrial Logistics,
Academic year: Masters 1st,
e-mail: bogdan.stoian0403@upb.ro

Abstract: The paper analyzes the impact of implementing a Vertical Lift Module (VLM) system in distribution centers, with the main purpose of optimizing logistics processes and increasing operational efficiency. The study starts from the identification of the growing need for automation in warehouses, in response to market demands for fast deliveries, increased precision and efficient use of space.

By integrating a VLM system with a warehouse management system (WMS), multiple benefits are highlighted, including: reduced time picking, increased order accuracy, saving storage space and improving the ergonomics of operators' work. The paper also includes a quantitative analysis of the performance before and after the implementation of the VLM, highlighting the improvements made to the logistics flow.

In conclusion, the implementation of automated technologies such as VLM is an essential step for the modernization of distribution centers, contributing significantly to increasing their competitiveness and sustainability.

KEY WORDS: VLM, collection, optimization.

1. Introduction

General context

In the modern logistics industry, the efficiency of the picking process is essential for the success of automated warehouses. Among the innovative solutions for managing this process are **Vertical Lift Modules (VLMs)** (see figure 1), which are automatic storage equipment that uses vertical space to organize products in an efficient way and speed up the collection process.

Fig. 1. Vertical Lift Modules [1]

In this work, the focus is on the analysis and optimization of the collection process in a distribution center where VLM equipment is implemented, using simulations and optimization techniques based on algorithms. Methods for optimizing product locations in a VLM and how these methods influence the overall efficiency of the system will be discussed. Various collection strategies and how to integrate a warehouse management system (WMS) to coordinate the process will also be analyzed.

Objectives of the work

The main purpose of this paper is to analyze how the collection process in a distribution center can be optimized with the help of **the Vertical Lift Module**, taking into account critical factors such as collection time, collection errors and operating costs. More specifically, the impact of optimizing product locations and the implementation of optimization algorithms to reduce collection distances will be analyzed.

2. Current state of play

Lenoble N. & Co. states that in the literature on AS/RS systems, VLM systems have been less studied compared to others, and existing work has mainly focused on determining system efficiency and operator utilization using analytical models and simulations for various VLM configurations [2].

In the article, Nicola M. & Co. proposes a new framework for automating the optimal design of VLM systems, taking into account the types and number of trays, as well as the allocation of items in the tray sectors, based on an inventory list, respecting physical, manufacturing and ergonomic constraints, and the complexity of the calculation is reduced by an exact grouping method [3].

René de K. & Co. points out that the collection activity is the most expensive and labor-intensive in a warehouse, accounting for up to 55% of total operating costs, and rigorous design and optimal process control are essential for its efficiency, including aspects such as layout design, stock allocation methods, routing, order grouping and zoning [4].

André S. & Co. analyzes the Single-Picker Routing Problem (SPRP) which involves determining the optimal route for collecting items in a warehouse and can be modeled as a variant of the classic Traveling Salesman Problem (TSP), but requires a special mathematical formulation that takes into account the specific structure of the warehouse layout (with parallel alleys and transverse alleys); this paper proposes such a formulation for the first time, demonstrating through experiments that it is superior to standard TSP models [5].

Meller, R. & Co. presents analytical models for determining the throughput of vertical lift modules (VLMs) or carousels grouped in bridges, used together with human operators taking orders in batches, highlighting the advantage of eliminating travel times compared to static racking and the usefulness of these models in the design of storage systems [6t].

3. Analysis of the algorithms used to calculate the collection time

3.1. The Bellman-Ford algorithm

To compare the efficiency between a classic distribution center (CDC) and an automated distribution center where VLM equipment is deployed, both scenarios can be modeled (see Table 1) and the Bellman-Ford algorithm can be used to calculate the optimal routes for transporting products (see Table 2). The comparison will be made based on the time elapsed between the warehouse locations.

Table 1. CDC vs. VLM Comparison

Criterion	CDC	VLM
Storage method	Fixed shelving, manually accessed	Automatic vertical systems (trays moved by elevator)

Criterion	CDC	VLM
Product access	Manual – employees move between shelves	Automated – the elevator brings the product to the operator
Handling Time	Variable, e.g.: 20 m at 1 m/s = 20 seconds	Constant, ~3 seconds per operation
Route comparison	The operator travels the distance between 10 shelves	The VLM system optimizes and delivers the product directly
Time difference estimation	~10 seconds per transition between shelves, much larger total	~3 seconds per operation, significantly faster
Operator efficiency	Low – depends on the speed and fatigue of the operator	High – the operator stands still, receives the products automatically
Ergonomics and safety	High physical effort, increased ergonomic risk	Fixed workstation, increased ergonomics
Use of vertical space	Limited to operator or ladder height	Maximum – VLM uses all available height
Upfront Cost	Low – low investment	High – high cost for automatic equipment
Long-term operational cost	High – intense and inefficient manual work	Reduced – less staff, increased efficiency

Tabel 2. Comparison exercise

Step	Parameter	CDC	VLM
1	Number of locations	10 locations	10 locations
2	Number of transitions between locations	9 transitions	10 takeovers
3	Time per transition/pickup	10 seconds / transition	3 seconds / pickup
4	Moving between locations	Yes	No
5	Total Handling Time	9 × 10 = 90 seconds	10 × 3 = 30 seconds

To illustrate the structure of a classic warehouse and the way handling routes can be modeled using the Bellman–Ford algorithm, the following figure presents a directed network in which each arc represents the time required to move between two locations. The model highlights the variability of operational costs in a traditional warehouse and supports the use of a shortest-path algorithm to estimate the total handling time.

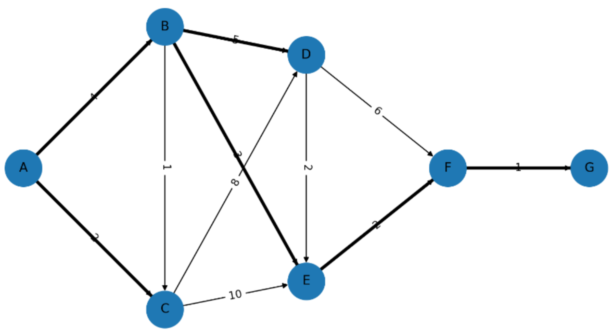

Fig. 2. Directed graph model of a classic distribution center used for Bellman–Ford route optimization

The graph (see figure 2) represents the time-weighted network of a traditional warehouse, where each edge corresponds to the handling time between two storage locations. This structure allows the Bellman–Ford algorithm to compute the minimum-time retrieval route starting from a given node.

3.2. Mathematical model

3.2.1. Classic Warehouse

In a classic warehouse, the total handling time depends on the physical distances between the storage locations. Analyze the case where there are n locations, and each location is connected by a route with a specific handle time rod, where rod is the travel time between locations i and j.

Formulation of the problem for the classic deposit:

Set of locations: Locations are named from L_1, L_2, ... L_n.

Handling time: Each route between locations i and j has a rod handling time, which depends on the distance between the locations and the employee's movement speed.

Objective: Minimizing the total handling time of an employee who needs to collect products from multiple warehouse locations.

Decision variables:

$$x_{ij} = \begin{cases} 1, \text{if you travel the route from , Li. the , Lj.} \\ 0, \text{ otherwise} \end{cases} \quad (1)$$

Objective Function:

Classic Total Time

$$\sum_{i=1}^{n} \sum_{j=1, j\neq i}^{n} t_{ij} * x_{ij} \quad (2)$$

where:

- x_{ij}=1 if there is an active route between the locations Li and Lj, 0 otherwise.
- rod is the handling time between the locations L_i and Lj.

Constraints:

- Each location must be visited exactly once by the employee.

$$\sum_{\substack{j=1 \\ j\neq i}}^{n} x_{ij} = 1, \quad \forall_i = 1, \dots, n \quad \text{(departure)} \quad (3)$$

$$\sum_{\substack{i=1 \\ i\neq j}}^{n} x_{ij} = 1, \quad \forall_j = 1, \dots, n \quad \text{(arrival)} \quad (4)$$

Routing must be carried out optimally, so as to minimize unnecessary travel.

Starting and returning from the same fixed location (e.g. L_1) – if the model is a tour (circuit):

$$x_{n1}=1 \quad \text{(to close the circuit)} \quad (5)$$

Avoiding subcircuits (optional, if a complete TSP solution is desired):

Using Miller–Tucker–Zemlin (MTZ) constraints, to prevent partial cycles:

$$u_i - u_j + n \cdot x_{ij} \leq n - 1, \quad \forall\ i\neq j,\ i, j \in \{2,\dots,n\} \quad (6)$$

where u_i is an auxiliary variable for the order in which locations are visited.

- The employee must start and finish at a fixed location in order to return to the starting point.

$$\sum_{j=1, j\neq i}^{n} x_{ij} = 1, \ \forall_i \in [1, n] \quad (7)$$

This means that the employee will leave each location exactly once.

TSP - Travelling Salesman Problem, i.e. the Salesman's Problem who has to visit a set of locations (cities, shelves, nodes), each once, and return to the starting point, minimizing the distance or total time traveled.

MTZ - Miller–Tucker–Zemlin constraints are used in the mathematical formulation of the TSP problem to prevent the formation of sub-cycles (i.e., smaller cycles that do not include all locations). MTZ uses u_i auxiliary variables, which represent the order in which the locations are visited (not for the starting point, but for the rest of the locations).

3.2.2. Automated Warehouse Model

In an automated distribution center where VLM equipment is implemented, automatic vertical elevator systems bring products directly to the employee. In this case, the handling time is constant for each location, regardless of the distance between locations. VLM systems eliminate the physical movement of employees, and the process becomes much more efficient.

Problem formulation for VLM warehouse:

Set of locations: As in the classic warehouse, locations are named from L1 to Ln.

Handling time: In an automated distribution center where VLM equipment is implemented, the rod handling time is much shorter and constant, as it is determined by the time it takes for the vertical elevator to reach the location and return the product.

Objective: To minimize the total handling time using an automated conveyor system.

Objective Function:

Total VLM Time $$\sum_{i=1}^{n} t_i \quad (8)$$

where:

- t_i is the constant handling time for each L_i location (suppose it is less than the rod in the classic warehouse).

$$t_i \approx t_{fix}, \quad \text{then Total Time VLM} = n \cdot t_{fix} \quad (9)$$

Constraints:

- Each location must be accessed to pick up the products, but it is not necessary to travel between locations, as the elevator brings them all automatically.
- It is assumed that each location is taken once, automatically:

$$t_i = \text{constant}, \quad \forall i \quad (10)$$

4. Analysis of Collection Errors in CDC vs. VLM

In logistics and distribution, the picking activity – i.e. picking items from the warehouse to fulfill customer orders – has a direct impact on operational efficiency and customer satisfaction. In this context, collection errors are critical sources of losses, reshipments, complaints, and decreased productivity. Comparing traditional systems with automated solutions such as Vertical Lift Modules (VLM) is essential for evaluating optimization opportunities.

Types and sources of collection errors:

In classic distribution centers

Traditional distribution centers, based on static racking and manual collection (with carts, handheld terminals or printed lists), are exposed to several types of errors:

- Wrong selection errors: the correct product is confused with a similar one.
- Quantity errors: More or fewer units are picked up than required.
- Location errors: Picking up from the wrong location even though the product is correct.
- Omission errors: Some products aren't picked up at all.
- Batch / FIFO errors: non-compliance with the shipping order according to the validity period.

These errors have as main causes: operator fatigue, incomplete or difficult to read information, long distances to travel, lack of real-time feedback and manual data processing.

In the automated distribution center where VLM equipment is deployed

VLMs are automatic vertical storage systems, which bring items to the operator, on the "goods-to-person" principle. They integrate sensors, barcodes, and intuitive digital interfaces, which significantly reduces the incidence of errors. However, the following types may occur:

- Incorrect confirmation errors: the operator validates the wrong pickup (e.g. scans a barcode without physically picking up the product).
- Calibration/positioning errors: the shelf brought in contains a wrong tray, caused by technical faults.
- Software/configuration errors: The stock-location database is erroneous or incomplete.

Table 3. Comparison of the impact of errors in the two systems

Criterion	CDC	VLM
Estimated collection error rate	1–3% of total orders	<0.2% of total orders
Automatic error detection	Limited	High (sensors, interfaces, logos)
Fix time	High (manual, post-factum)	Low (real-time detection)
Complexity in staff training	Medium – High	Low due to guided interface
Cost per eroare (transport, retur)	High	Low due to better control

5. Impact on the status of inventories

The status of inventories – i.e. the accuracy and timeliness of data relating to existing stocks – is essential for order planning, maintaining an optimal level of supply and preventing out-of-stock or overstock situations. Collection errors directly affect this accuracy, and how the logistics system handles these deviations determines the quality of subsequent decisions.

In classic distribution centers

In traditional systems, inventory updating is usually done:

- manual or semi-automated (with handheld scanners),
- in batches (batch updates) at the end of shifts or days,
- with increased dependence on operators for confirmation of takeovers.
- This approach determines:
- Delays in the actual reflection of movements in the WMS system;

- Inconsistencies between physical and scriptural stock, caused by collection errors not recorded correctly;
- The need for expensive physical periodic inventories (monthly or quarterly cycles);
- The risk of promising deliveries based on inaccurate stocks ("phantom inventory").

In automated distribution centers where VLM equipment is deployed

On the other hand, VLM systems, being fully digitized and integrated with WMS/ERP, offer:

1. Real-time inventory update at each collection or return action;
2. Automatic validation of the quantities taken, through weight sensors or multiple confirmations (scans);
3. Constant monitoring of locations and complete traceability of batches and operators;
4. The possibility of implementing continuous inventory cycles (cycle counting), without interrupting the activity.

Thus, the inventory accuracy in automated distribution centers where VLM equipment is deployed frequently exceeds 99.7%, compared to 90–95% in classic centers.

Table 4. Inventory accuracy

Criterion	CDC	VLM
Updating Inventory	Manual or batch, delayed	Instant, real-time
Inventory accuracy	90–95%	>99,7%
The need for complete physical inventory	High (monthly/quarterly)	Reduced (cycle counting automat)
Traceability	Limited	Complete (by batch, date, operator)
Impact on stock	Major (not immediately noticeable)	Minor (instantly detectable)

6. Conclusions and Further Perspectives

The implementation of Vertical Lift Module (VLM) systems in distribution centers represents a significant step towards automating and optimizing logistics processes, with a direct impact on operational efficiency, cost reduction and increased customer satisfaction. The present paper highlighted the significant benefits of using these advanced technologies, focusing on improving the collection process, a crucial component of distribution center activities.

Following the detailed analysis of the two types of systems – classic warehouses and VLM warehouses – a significant difference was observed in terms of handling time, collection errors and inventory management. In a classic warehouse, the collection process is carried out manually, and the handling time is influenced by the physical distances between the storage locations. Instead, an automated VLM system optimizes these routes, significantly reducing the time needed to access the products and, implicitly, the operating costs. In addition, thanks to the automation of the collection process, selection errors are greatly reduced, which helps to increase the accuracy of deliveries and reduce the costs associated with returns or reshipment of products.

Another essential aspect analyzed in the paper is the impact of collection errors on the status of inventories. In traditional systems, these errors can lead to inconsistencies between physical and scriptural inventory, with negative effects on the order and delivery planning process. On the other hand, VLMs, integrated with warehouse management systems (WMS), allow inventory to be updated in real time, leading to complete inventory traceability and much more precise inventory management. This approach reduces the risk of errors in terms of deliveries and optimizes the flow of products in the warehouse.

As for the further prospects of the implementation of VLM systems in logistics, there are several directions for development and improvement. For example, integrating these systems with emerging technologies such as the Internet of Things (IoT) and Big Data analytics can address the challenges of demand forecasting and real-time inventory optimization. In this context, VLMs will not only be an automated product storage system, but will become an essential element in an intelligent logistics ecosystem, capable of managing freight flows in a dynamic and adaptive way.

Also, tighter integration of VLMs with autonomous transport robots (AMRs) and other robotic solutions could help increase the efficiency of the collection process and further reduce operating costs. In this regard, there is significant potential for the development of hybridized solutions, in which VLMs and AMRs work together in a unitary logistics flow, each responsible for different segments of the product handling process.

Another area where VLMs could have a considerable impact is in the area of sustainability. Although the implementation of these systems involves a high upfront cost, the long-term benefits, such as saving storage space, reducing energy consumption and minimizing errors, can lead to a significant reduction in the environmental impact of distribution centers. In addition, the optimization of the collection process contributes to the reduction of carbon emissions, having a direct impact on the reduction of the ecological footprint of logistics operations.

In conclusion, VLM systems represent a promising solution for the future of logistics, with a significant impact on storage and handling processes. As technologies advance and become more accessible, their implementation will become standard practice in distribution centers around the world. In this context, future research should focus on integrating these systems more effectively with other emerging technologies and developing innovative solutions that meet the ever-changing needs of the logistics industry.

7. Bibliography:

[1]. https://osequip.com/category/vertical-lift-module/

[2]. Lenoble Nicolas, (2018) Frein Yannick, Hammami Ramzi, *Order batching in an automated warehouse with several vertical lift modules: Optimization and experiments with real data*, European Journal of Operational Research, Volume 267, Issue 3, Pages 958-976, ISSN 0377-2217, https://doi.org/10.1016/j.ejor.2017.12.037.

[3]. Mignoni, Nicola & Scarabaggio, Paolo & Carli, Raffaele & Dotoli, Mariagrazia, (2025), *A Framework for the Automated and Optimal Design of Vertical Lift Modules*, IEEE Transactions on Systems, Man, and Cybernetics: Systems., PP. 1-14., https://doi.org/10.1109/TSMC.2025.3547302.

[4]. René de Koster, Tho Le-Duc, Kees Jan Roodbergen, (2007), *Design and control of warehouse order picking: A literature review*, European Journal of Operational Research, Volume 182, Issue 2, Pages 481-501, ISSN 0377-2217, https://doi.org/10.1016/j.ejor.2006.07.009.

[5]. André Scholz, Sebastian Henn, Meike Stuhlmann, Gerhard Wäscher, (2016), *A new mathematical programming formulation for the Single-Picker Routing Problem*, European Journal of Operational Research, Volume 253, Issue 1, Pages 68-84, ISSN 0377-2217, https://doi.org/10.1016/j.ejor.2016.02.018.

[6]. Meller, R. D., & Klote, J. F. (2004). *A throughput model for carousel/VLM pods*. IIE Transactions, Volume36, Issue 8, Pages 725–741, ISSN: 0740-817X, https://doi.org/10.1080/07408170490458472

INTELLIGENT TRACEABILITY AND EFFICIENT AUTOMATION IN INDUSTRIAL LOGISTICS USING QR CODES

ȘUICĂ Cristian și ALEXANDRU Tudor-George (Conducător Științific)

Facultatea: Inginerie Industrială și Robotică, Specializarea: Master Logistică, Anul de studii: I, e-mail: cristian.suica@stud.fiir.upb.ro

ABSTRACT: The present work investigates the use of QR codes to improve traceability and automate decision-making task in industrial logistics. A C++ application is developed to simulate product tracking, while a graph-based algorithm guides autonomous robots with the support of real-time QR data. Adaptive navigation and efficient stock updates are completed by employing dynamic QR codes linked to a database. The study also proposes the use of the Hilbert fractal curve for achieving optimized and collision-free routing in warehouses. A practical solution that combines accessible technology and intelligent algorithms is included to enhance efficiency and reduce errors in modern logistics operations.

1. Introduction

Industrial logistics is undergoing an accelerated transformation, driven by the Industry 4.0 paradigm, which promotes the interconnection of equipment, the digitalization of flows and the automation of operational decisions. In this context, companies are under pressure to optimize their supply chain to respond quickly to market fluctuations, reduce labor costs and increase product traceability from raw materials to the final customer [1]. An essential element of this transformation is the introduction of unique identifiers, easily readable by cyber systems, capable of instantly providing relevant data about the handled item.

QR (Quick Response) codes are thus at the intersection of the requirements of computerization and automation. As two-dimensional codes with a high information density, they can be generated quickly, printed cheaply and scanned by mobile devices or fixed readers installed on robots or conveyor belts. Compared to linear barcodes, QR codes offer increased data storage capacity and tolerance to damage, allowing the integration of metadata (expiration date, batch, destination, handling instructions, etc.) in a compact graphic space. Moreover, if the codes are associated with dynamic URLs, they can be updated in real time in a centralized database, without modifying the physical label [2].

In parallel with the evolution of identification means, mobile robotics has moved beyond the experimental stage to become an integral part of modern warehouses. Autonomous vehicles guided by navigation graphs or visual landmarks (QR codes, AprilTags, etc.) can pick up and deliver products without human intervention, reducing waiting times and the risk of error. However, the performance of these systems depends on the quality of the data provided at each pick-up/delivery point and the ability of routing algorithms to react to changes (blockages, changing priorities, variation in demand) [3].

This paper addresses this dual challenge – intelligent traceability and efficient automation – by proposing an integrated framework based on dynamic QR codes and routing algorithms. The main contributions are: developing a C++ application that simulates the scanning flow and makes autonomous decisions (delivery, verification, recycling) based on the information encoded in the QR; logically modeling a warehouse as a directed graph, from which the minimum distance matrix is derived; demonstrating how a mobile robot uses these distances and QR codes to adjust its route in real time, ensuring a continuous and collision-free flow;

exploring the potential of Hilbert curves, a self-similar fractal algorithm, as a sequential location traversal strategy designed to minimize intersections and increase system scalability.

In addition to the practical implementation, the paper highlights the economic and operational benefits of the solution: reducing the number of labels needed, instant stock updates, reducing picking time and increasing inventory accuracy. Compared to traditional methods (linear barcodes, static labels, manual routing), the proposed approach significantly reduces maintenance effort and facilitates warehouse expansion without a major infrastructure redesign.

The remainder of this paper is organized as follows: Section 2 presents the state of research in the field of traceability and mobile robots; Section 3 describes the C++ application and decision rules; Section 4 details the graphical warehouse model and navigation logic; Section 5 introduces the Hilbert fractal algorithm and discusses expansion scenarios; Section 6 summarizes the conclusions and future directions. Thus, it provides a practical and scalable guide for implementing smart traceability in warehouses, supporting companies' transition to Industry 4.0 and, implicitly, to more resilient and data-driven supply chains.

2. Literature overview

In logistics systems, QR codes are used for automatic identification and sorting of products. They facilitate real-time tracking and data retrieval during operations such as warehousing, transportation, and delivery.

Traceability in logistics refers to the ability to track and monitor the movement, location, and condition of products or materials throughout the supply chain, from their origin (such as raw materials or production) to their final destination (the end consumer). Each item or batch is assigned a unique identifier (such as a QR code, barcode, or RFID tag) that links it to relevant data. The real-time location of goods is monitored as they move through various stages - production, warehousing, transportation, and delivery. A record is kept of all actions performed on the product, including manufacturing stages, handling, storage conditions, and shipping details.

In [4], the authors present a C++-based software application for generating and managing QR codes, designed to support logistics and supply chain management systems. The program follows an object-oriented structure, encoding data into QR codes using an alphanumeric module. Error correction mechanisms for QR codes are implemented to ensure robustness during scanning. The approach can be integrated into logistics IT systems to automate the labeling and tracking of packages. A similar approach is presented in [5]. The goal of the implemented program is to enable real-time tracking and monitoring of logistics flows by using QR code scanning in multiple areas of interest. Information about packages is captured, and the scanned data is converted into geographic locations for displaying and visualizing the current position of shipments. This improves traceability, reducing sources of human error

3. C++ Program

To demonstrate how QR codes can improve traceability in a warehouse, a C++ application was developed that simulates the scanning and decision-making process. The application automatically retrieves a product's data after scanning the QR code and, depending on what that code contains, decisions are made, such as: transfer to delivery, verification or withdrawal from the circuit (see figure 1).

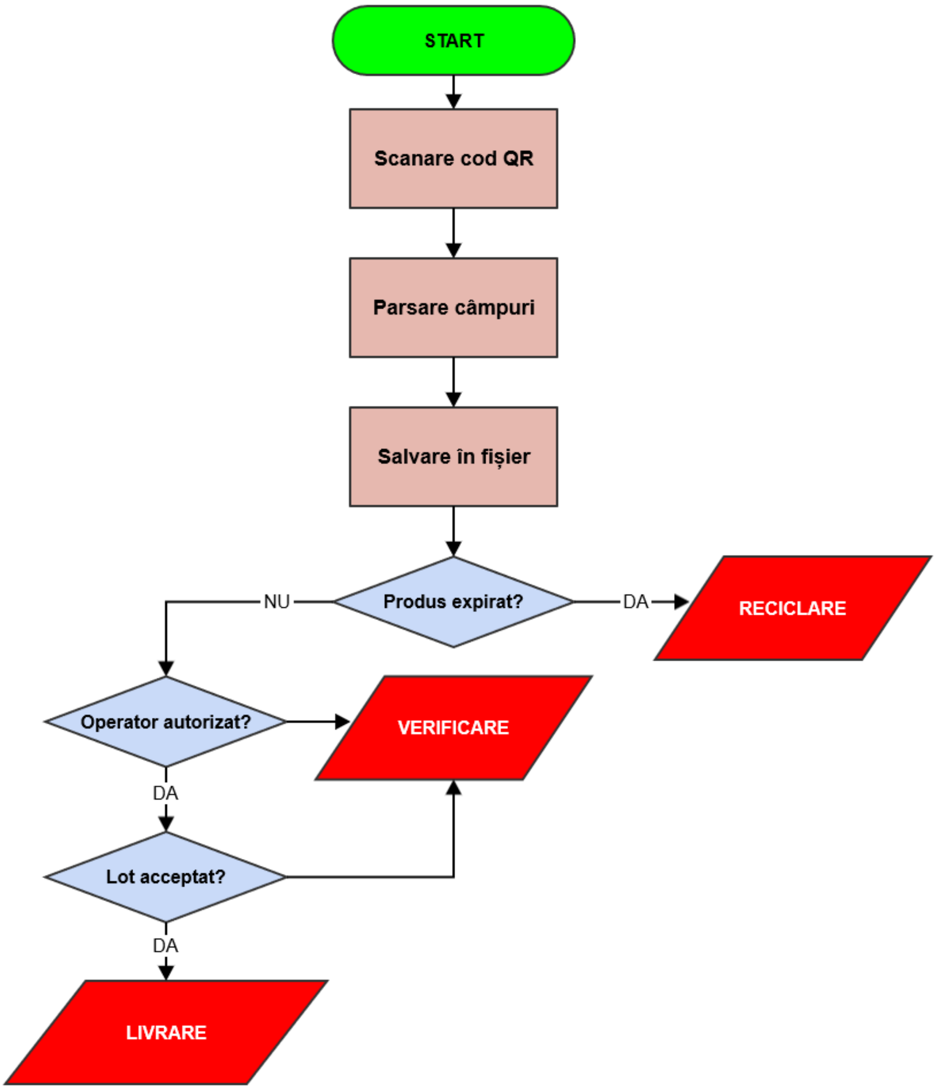

Fig. 1 The workflow of the project

The QR code contains all the important data about a product, grouped into a single string - for example, 123#2025-05-09#LOT45#Ion means that the product has the ID 123, expires on 09.05.2025, is part of the lot 45 and was processed by the operator Ion.

After scanning (simulated by keyboard input), the application automatically extracts this information, saves it in a CSV file (for traceability) and applies a series of simple checks. Based on these checks, the program decides what happens to the product. Checks are made whether the product is expired, whether the operator is authorized and whether the lot is valid. Depending on these rules, the program decides whether the product goes for delivery, verification or return. The result is displayed in the console. The flow is automatic, being easy to follow. The conditions are detailed below:

• "RECYCLE" - if the product is expired (in which case it must be removed from the circuit and returned/destroyed),

• "VERIFY" - if the operator is not authorized or the batch is not recognized (in which case the product must be manually verified before continuing the flow),

• "DELIVERY" - if all information is compliant (valid product, authorized operator, approved batch), and can be sent on for delivery.

Figure 2 details the complete code of the C++ program with the related comments.

```cpp
#include <iostream>    // stream pentru pentru afișare și citire
#include <fstream>     // pentru scriere în fișier
#include <sstream>     // pentru a împărți codul QR în bucăți
#include <ctime>       // pentru a obține data curentă
using namespace std;   // ca să nu mai scriem std:: la fiecare linie, avem biblioteca std
int main()
{
    string qr, id, data, lot, operatorNume;       // declarăm variabilele pentru codul QR și câmpurile lui
    cout << "Introdu codul QR (ID#Data#Lot#Operator): ";      // mesaj
    getline(cin, qr);                                         // citim tot codul QR de la tastatură (ne imagină că îl scanăm)
    istringstream ss(qr);                                       // transformăm șirul QR într-un flux de citire
    getline(ss, id, '#');                                       // extragem ID-ul (până la primul #)
    getline(ss, data, '#');                                     // extragem data expirării
    getline(ss, lot, '#');                                      // extragem lotul
    getline(ss, operatorNume);                                  // extragem numele operatorului
    ofstream out("data.csv", ios::app);                   // deschidem fișierul CSV pentru adăugare la final
    out << id << ',' << data << ',' << lot << ',' << operatorNume << '\n';        // scriem datele separate
    out.close();                                                // închidem fișierul
    time_t t = time(nullptr);                                   // obținem timpul actual în format brut
    tm* now = localtime(&t);                                    // îl convertim într-o dată calendaristică locală
    char today[11];                                             // pregătim un șir în care vom pune data formatată
    strftime(today, sizeof(today), "%Y-%m-%d", now);       // scriem data curentă
    string destinatie;                                          // variabilă unde salvăm decizia finală
    if (data < today)                                     // dacă produsul este expirat (data < azi)
        destinatie = "RETUR";                                   // îl trimitem la retur
    else if (!(operatorNume == "Ion" || operatorNume == "Maria" || operatorNume == "Ana") ||
// dacă operatorul nu e autorizat
        !(lot == "LOT45" || lot == "LOT46" || lot == "LOT47"))
 // sau dacă lotul nu e aprobat
        destinatie = "VERIFICARE";                              // trimitem produsul la verificare
    else
        destinatie = "LIVRARE";                                 // altfel, totul e OK → produsul se livrează
    cout << "Destinație: " << destinatie << endl;               // afișăm decizia finală în consolă
    return 0;                                                   // terminăm programul
}
```

Fig. 2. The complete C++ code

4. Trajectory planning of an autonomous robot

In an automated warehouse, a mobile ground robot navigates aisles with shelves marked A, B, C, D, E, F and special areas: R (recycling), I (inspection/verification) and S (shipping). Dynamic QR codes containing important product information (type: perishable, fragile or standard; destination: delivery, return, verification; status: OK, damaged, expired) are placed on the shelves. Figure 3 represents the proposed warehouse map.

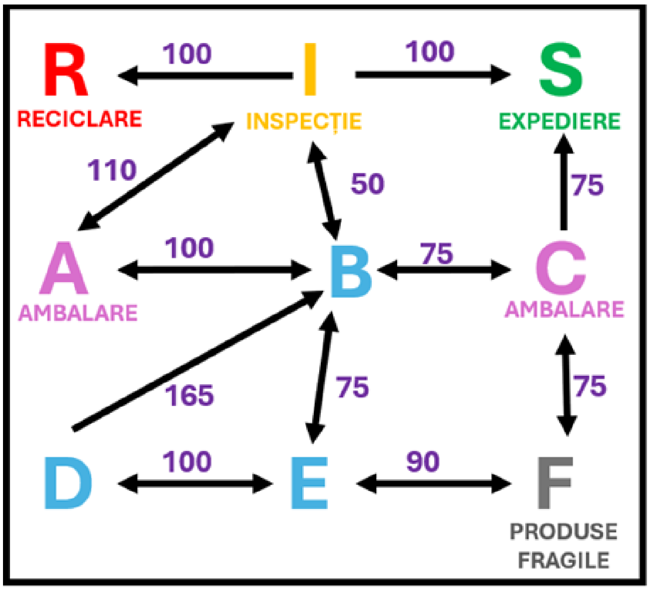

Fig. 3. Logical workflow

The robot scans the codes in real time and dynamically adjusts its route. QR codes allow for precise localization and efficient routing of the robot in the warehouse, being connected to a database that is frequently updated depending on how many times this code is scanned.

When navigating the warehouse, the robot orients itself according to the QR codes mounted in each location. The data in these codes allows the classification of the location and the object, and the robot follows the QR labels to determine its position and context. Thus, when scanning the QR codes, the robot knows exactly what task must be performed at each point.

The novelty lies in the fact that these QR codes are dynamic, that is, they contain a link to a database that is updated each time the robot scans it. When the robot scans the QR, the connection to the database is established, the product status, expiration date, whether the product is fragile, etc. are checked, thus calculating the minimum distance that the robot must travel and where to move.

For path planning, we calculate the distances between the nodes of the graph {R, I, S, A, B, C, D, E, F}. The graph is directed, the robot is restricted in terms of movements. For example, the minimum distance from A to S is 210 (A→I→S) and from E to S is 225 (E→B→C→S). The complete matrix of minimum distances is:

	R	I	S	A	B	C	D	E	F
R	0	∞	∞	∞	∞	∞	∞	∞	∞
I	100	0	100	110	50	125	225	125	200
S	∞	∞	0	∞	∞	∞	∞	∞	∞
A	210	110	210	0	100	175	275	175	250
B	150	50	150	100	0	75	175	75	150
C	225	125	75	175	75	0	250	150	75
D	315	215	315	265	165	240	0	100	190
E	225	125	225	175	75	150	100	0	90
F	300	200	150	250	150	75	190	90	0

(1)

Let's assume that there are 5 food products on shelf B.

A single QR code is stuck on the shelf with the following link to a database:

https://wms.depozit.ro/raft/B1. When the robot scans that QR code, the link to the database (WMS) is accessed, the ACTIVE product on shelf B is searched for at position 1, and the Database returns the data for the product at position 1.

Example of data about a product: id: BX-233, type: fragile, destination: S, status: OK

After the robot picks up the product, it sends a confirmation message to the WMS, such as "I picked up product BX-233 from shelf B", and the WMS updates its database for that shelf, as follows: removes product BX-233 from the list; marks the next product as "first".

The QR code does not physically change, but the next time the robot scans it again, the WMS will send the updated information about the new active product.

Such an approach allows for a unique QR code to be placed on each shelf, regardless of how many products there are, and the code does not need to be changed. Each decision made was based on the information in the QR code and the distance matrix: perishable products are quickly directed to shipping, damaged products to inspection/recycling, and fragile products avoid zone F.

Examples of scans of different QR codes

Scan 1 – Shelf D

QR code:

Type: FRAGILE (so we will avoid zone F), Status: OK, Destination: S

Rule: Packing – Inspection – Delivery, in this order.

Decision: The robot chooses the shortest route, namely D – B – C - B - I – S (distance = 465 m).

Scan 2 – Shelf E

QR Code:

Type: standard, Status: expired, Destination: R,

Rule: If the product status is 'expired', then go to R immediately.

Decision: E → B → I → R (distance = 225m).
Expired product sent for recycling.
The paths for the 2 scenarios are shown in figure 4.

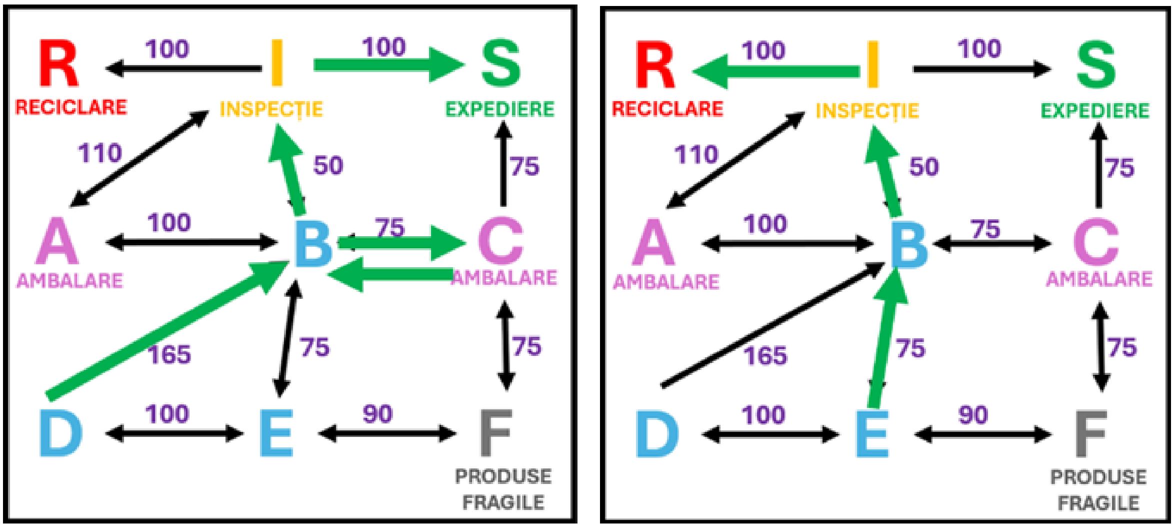

Fig. 4 Traseele aferente celor 2 scenarii.

5. Perspective privind utilizarea algoritmilor fractali

The proposed approach based on graphs and dynamic QR codes allows the use of QR codes in warehouses in a much more efficient way, considerably reducing the number of codes needed for a set of products. Also, by combining these QR codes with graphs, mobile robots can move directly to the appropriate locations, thus shortening the total transit time between trips. The proposed concept can be extended by applying unconventional algorithms, such as those based on fractal algorithms.

A fractal is a fragmented or broken geometric figure that can be divided into smaller parts, each of which is (at least approximately) a reduced copy of the whole. The term was introduced by the mathematician Benoît Mandelbrot in 1975 and is derived from the word fractus, meaning "broken" or "fractured" [6].

Fractals are, basically, a set of complex points that fulfill a certain mathematical condition and that have the following characteristics:

• They present a very detailed structure, visible even at the smallest scales
• They are too irregular to be described by classical Euclidean geometry
• They are self-similar – each fragment reflects, at a different scale, the shape of the whole.
• They have a simple and recursive definition.

The Hilbert curve is a two-dimensional (2-dimensional) geometric fractal that traverses each cell of a square grid (e.g. 4×4, 8×8, 16×16) in a logical, continuous order, without returns or intersections. Each location in the grid is visited exactly once, and the distances between consecutive points are minimal. Due to the property of self-similarity, the path is easily extended and scalable by increasing the order of the curve (see figure 5) [9].

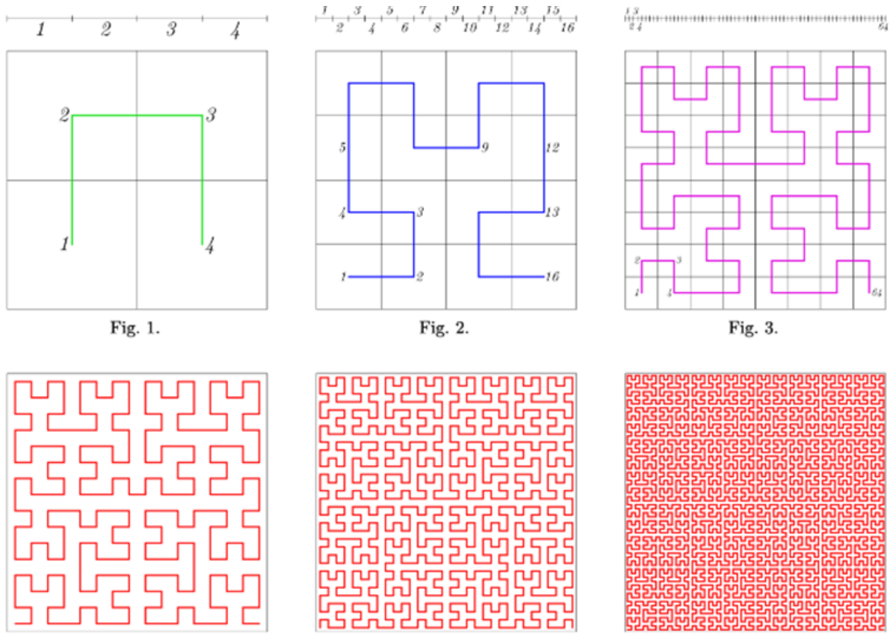

Fig. 5 Algoritmul matematic pur al Curbei

A concrete example is shown in figure 5: for a 4x4 warehouse, the 16 locations are numbered according to the Hilbert path (note that the path is a modified one, it is not the purely mathematical Hilbert Curve). Suppose we want to perform a verification operation, one by one, of the 16 locations of the warehouse. If the robot starts at location 1 (0,0), it goes through the locations in fractal order: (0,0) → (0,1) → (1,1) → (1,0) → ... → (3,3), without repeating or returning. Each move is of a single unit, optimal, without crossings (see figure 6).

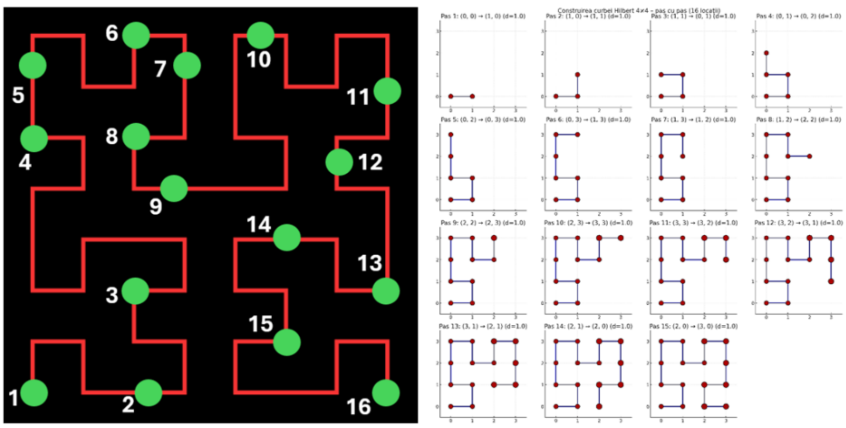

Fig. 6 Algoritmul matematic pur al Curbei Hilbert cu 3 iterații și cele 16 locații și algoritmul Curbei Hilbert modificat și simplificat pentru exemplul ales

QR codes include both the logical position and the action to be performed, and the robot acts sequentially, autonomously. If a certain location cannot be accessed, then the Hilbert algorithm will simply bypass that location, moving to the next point, without changing its route. The model can be expanded simply by increasing the number of iterations, keeping the same rules. In each case, the fractal curve can be visualized step by step and physically implemented in real logistics systems. This method does not require GPS navigation or access to cloud resources, but only QR codes, making it scalable.

6. Conclusions

This work demonstrated how the integration of dynamic QR codes and intelligent algorithms can radically transform the traceability and automation of industrial logistics processes. The use of a C++ application to simulate QR code scanning highlighted the system's ability to make automatic, fast decisions, in accordance with product-specific parameters. By connecting QR codes to a centralized database, real-time traceability was achieved, with a significant reduction in human errors. Also, by modeling the warehouse as a graph and using minimum distances between nodes, it was demonstrated how an autonomous mobile robot can plan optimal routes depending on the conditions and status of the products. The innovation brought by the use of dynamic QR codes allowed for rapid adaptation of decisions without requiring physical changes in the warehouse infrastructure. In addition, the fractal approach through the Hilbert curve provided an elegant and scalable solution for the systematic verification of locations in a warehouse, avoiding collisions and overlaps. This method has the potential to replace classic routing systems, being independent of complex technologies such as GPS or cloud networks. Therefore, the proposed solution brings together accessible technologies with intelligent algorithms to support the digital transformation of industrial logistics, being applicable in numerous practical scenarios and adaptable to the requirements of Industry 4.0.

7. References

[1]. Richnák, P. (2022), „Current trend of industry 4.0 in logistics and transformation of logistics processes using digital technologies: an empirical study in the Slovak republic", Logistics, 6(4), 79, ISSN: 2305-6290

[2]. Reddy, P., Kurnia, S., & Tortorella, G. L. (2022), "Digital Food Supply Chain Traceability Framework", în Proceedings (Vol. 82, No. 1, p. 9). MDPI.

[3]. Lin, H. Y., Chang, K. L., & Huang, H. Y. (2024), „Development of unmanned aerial vehicle navigation and warehouse inventory system based on reinforcement learning", Drones, 8(6), 220, ISSN: 2504-446

[4]. Zhi-Hai, L. (2010), "Realization of QR Code Barcode Programming Based on VC", Journal of Shandong University of Science and Technology, 29(6), 80-84, ISSN: 1672-3767

[5]. Udvaros, J., Forman, N., Tašić, J., & Szabó, L. (2024), „The application of qr codes in the field of e-business in the case of order tracking and logistics. engineering management and competitiveness", (EMC 2024), 275.

[6]. Soltani, M., & Bardsiri, A. K. (2018), „Designing A Novel Hybrid Algorithm for QR-Code Images Encryption and Steganography", J. Comput., 13(9), 1075-1088.

OPTIMIZATION OF STRATEGIC LOGISTICS NETWORKS: ANALYSIS OF LOGISTICS ROUTES UNDER HYBRID THREATS USING DIJKSTRA'S ALGORITHM

PETREANU Julia-Cristiana, Gabriel JIGA(Conducător științific)

Faculty of Industrial Engineering and Robotics, Specialization: Industrial Logistics, Year of study: I,
e-mail: juliapetreanu@yahoo.com

ABSTRACT: In the face of escalating hybrid warfare, where logistical infrastructures become both strategic assets and vulnerable targets, the need for intelligent, adaptive, and risk-aware transport planning has never been more urgent. This paper proposes an advanced optimization of strategic logistic routes using a weighted Dijkstra algorithm that incorporates not only traditional parameters such as distance and cost, but also quantifiable geopolitical risk. Set in the context of the ongoing conflict in Eastern Europe, the case study focuses on identifying the most efficient transport path for critical supplies—such as military-grade drones, encrypted communication equipment, and medical logistics—between the Port of Constanța (Romania) and Kyiv (Ukraine). Each logistic node is evaluated for its geopolitical exposure, risk of interference, and strategic value. The findings demonstrate how compound optimization models can support resilient decision-making in real-time crisis scenarios, ensuring rapid, cost-effective, and secure movement of goods in volatile environments.

KEY WORDS: National Security, Threats, Dijkstra, Technology, Logistics

1. Introduction

Strategic logistics is the backbone of national defense, emergency response, and industrial continuity. As adversaries increasingly deploy hybrid strategies that target infrastructure asymmetrically, the optimization of logistic pathways must evolve beyond classical cost minimization. Hybrid warfare, which includes information disruption, cyber intrusion, kinetic sabotage, and signal interference—demands a new paradigm in operational planning.

This study introduces an approach to logistic route optimization that integrates classical shortest-path computation with dynamic threat analysis. The proposed model is anchored in Dijkstra's algorithm, but extends it by modifying edge weights in response to evolving threat intensities, making it suitable for environments where real-time adaptability is critical.

The paper's primary contributions are:

•A framework for modeling hybrid threat intensities in supply chain routes.

•An enhanced version of Dijkstra's algorithm for weighted threat-aware pathfinding.

•Use-case applications across military, industrial, and humanitarian logistics.

2. State of art

2.1. Logistics under hybrid threats

In an era of hybrid threats involving cyber warfare, electronic surveillance, misinformation, drone incursions, and paramilitary disruptions, strategic supply routes are prime targets. Hybrid warfare blurs the lines between military and civilian spaces, rendering logistical infrastructures not just passive conduits, but contested zones.

NATO documents and EU resilience strategies increasingly emphasize the critical role of Supply Chain Resilience (SCR) under hybrid conditions. Traditional logistic planning based on static cost-distance matrices is now insufficient; instead, planners must incorporate dynamic risk layers that reflect fluctuating security conditions in real time.

2.2. Optimization through graph theory

The use of graph theory, particularly Dijkstra's algorithm, is standard in route optimization. However, in the context of hybrid threats, the classical cost function must be adapted. Recent research in military logistics and supply chain risk management suggests that a compound weighting function, combining distance, financial cost, and risk exposure, yields more realistic and operationally relevant paths.

A growing body of work focuses on "Risk-Aware Shortest Paths" (RASP) and "Multi-Criteria Dijkstra" algorithms, applying them in domains ranging from humanitarian aid logistics to secure communications routing. In these models, risk is assigned not abstractly but as a measurable value—whether through geospatial threat indicators, cyberattack frequency, or conflict zone proximity.

2.3. Application in modern strategic transport

In 2025, the logistical corridor between NATO-aligned countries and Ukraine has become one of the most actively contested supply networks in the world. Transport routes from Romania, Moldova, and southern Ukraine are under constant pressure from cyber-interference, drone surveillance, sabotage operations, and destabilization campaigns. Technologies such as autonomous trucks, AI-enabled risk monitoring, and satellite-linked route diagnostics are being explored, but decisions on ground mobility still rely on robust models that integrate geopolitics into transport equations.

This paper integrates that approach. We model the eastern European logistics corridor as an undirected graph, with each node (city) and edge (route) weighted by a compound function:

$$w = \alpha \cdot \text{distance} + \beta \cdot \text{cost} + \gamma \cdot \text{risk} \qquad (1)$$

Where $\alpha = 0.5$ - distance, $\beta = 0.3$ - cost, and $\gamma = 0.2$ - risk, reflecting the strategic priority of minimizing distance while accounting for cost-efficiency and operational threat levels.

3. Development

3.1. Strategic relevance of the route

The route from Constanța to Kyiv is not merely a geographic connection—it is a vital artery for the transfer of high-value, mission-critical equipment from NATO territory into the heart of Ukraine. Given the ongoing regional conflict, this corridor represents one of the few viable paths for secure transport of sensitive materials including encrypted communication gear, tactical UAVs, and emergency medical supplies.

The selection of nodes—Constanța, Galați, Chișinău, Odesa, Tiraspol, Liov, and finally Kyiv—was not accidental. These cities are either key logistical hubs, border crossings, or geopolitical flashpoints. Evaluating each point with respect to potential hybrid threats is essential in understanding why the compound optimization model produces not just a theoretically short path, but the most resilient one.

3.2. Hybrid threat analysis per node

Constanța (Romania)
Strategic Role: Black Sea port and NATO logistics hub.
Threat Profile:
• Moderate cyber-attack frequency targeting port infrastructure.
• Low physical threat due to NATO protection and stable governance.
• Occasional drone surveillance attempts reported over harbor areas.
Logistical Status: Safe launch point for operations. High transport costs due to port fees, but minimal risk exposure.

Galați (Romania)
Strategic Role: Danube River logistics node with rail and road links to Moldova and Ukraine.
Threat Profile:
• Digital espionage attempts on cross-border cargo manifests.
• Slightly elevated cyber risk due to proximity to Moldovan border.
• Low military threat; Romanian internal security is stable.
Logistical Status: Efficient transfer point with multimodal capabilities. Moderate costs and low-medium risk.

Chișinău (Moldova)
Strategic Role: Capital city, potential bridge to both western Ukraine and Transnistrian region.
Threat Profile:
• Elevated risk of internal destabilization due to political fragmentation.
• Known surveillance activities by foreign intelligence services.
• High interference potential from actors operating through Transnistria.
Logistical Status: Politically delicate node. Cheap transport costs but offset by significant operational risk.

Odesa (Ukraine)
Strategic Role: Coastal Ukrainian port, historically vital but now exposed to constant surveillance.
Threat Profile:
• Regular drone incursions and electronic jamming activities.
• High strategic value makes it a frequent target for kinetic attacks.
• Maritime access increases exposure to hybrid sabotage (mines, drones).
Logistical Status: Route through Odesa remains feasible but high-risk. Critical to weigh threat versus speed of access inland.

Tiraspol (Transnistria)
Strategic Role: Breakaway region under de facto Russian influence.
Threat Profile:
• Highest risk node in the network due to foreign paramilitary presence.
• Limited legal oversight, high smuggling and sabotage potential.
• Surveillance and GPS spoofing incidents reported.
Logistical Status: Volatile but geographically strategic. The model routes through it due to its connectivity benefits, but exposure is severe.

Liov (Ukraine)
Strategic Role: Main western hub for internal Ukrainian logistics; near Poland border.
Threat Profile:

• Occasional sabotage attempts on critical infrastructure.
• Significant cyber defense improvements in 2024–2025.
• Drone interference localized but manageable.
Logistical Status: Stable node with strong defense mechanisms. Slightly elevated transport costs due to demand pressure, but low risk compared to other Ukrainian cities.

Kiev (Ukraine)
Strategic Role: Final destination. Political, military, and economic nerve center of Ukraine.
Threat Profile:
•High surveillance environment.
•Constant cyber-intrusion attempts on inbound logistics data.
• Civilian and military convergence increases complexity.
Logistical Status: Must be reached quickly and securely. All operations converge here, making optimization essential for mission success.

So, the problem has only one type of optimization, but that type is a composed function that reflects all three criteria. The reason why I made this composed function is:

Because in a real situation (like in war logistics):

• A shorter route is not automatically better if it is too risky (e.g. controlled by hostile groups)
• A cheaper route can be circuitous and slow
• A safe route can be very long and expensive

Table 1 Nodes (logistics cities)

City	Description
Constanța (Romania)	strategic port on the Black Sea
Galați (Romania)	Danube logistics hub
Chișinău (Moldavia)	capital with access to Ukraine
Odesa (Ukraine)	port exposed to geopolitical risk
Tiraspol (Transnistria)	area with disputed control
Cernăuți (Ukraine)	western entry point
Liov (Ukraine)	major logistics center in the west
Kiev (Ukraine)	capital, final destination

Table 2 Edges (proposed roads)

Route	Distance (km)	Cost (€)	Risk (0–10)	Composed cost $w = 0.5d + 0.3c + 0.2*r$
Constanța–Galați	230	700	2	325.4
Constanța–Odesa	400	1100	4	530.8

Galați–Chișinău	180	600	3	270.6
Chișinău–Tiraspol	140	500	5	221.0
Tiraspol–Cernăuți	150	600	4	255.8
Cernăuți–Liov	250	900	3	395.6
Liov–Kiev	540	1200	2	630.4
Odesa–Cernăuți	300	1000	4	450.8
Galați–Odesa	260	800	4	370.8
Chișinău–Cernăuți	350	900	5	446.0
Tiraspol–Liov	450	1000	5	526.0
Odesa–Tiraspol	150	500	4	225.8

Figure 1. Road

1. Constanța → Galați = 325.4 → updating Galați (2)
2. Constanța → Odesa = 530.8 → updating Odesa (3)
3. Galați → Chișinău = 325.4 + 270.6 = 596.0 → updating Chișinău (4)
4. Galați → Odesa = 325.4 + 370.8 = 696.2 (does not represend reliable route) (it is grater than 530.8) (5)

5. Odesa → Tiraspol = 530.8 + 225.8 = 756.6 → updating Tiraspol (6)
6. Odesa → Cernăuți = 530.8 + 450.8 = 981.6 → updating Cernăuți (7)
7. Chișinău → Tiraspol = 596.0 + 221.0 = 817.0 (does not represend reliable route) (it is grater than 756.6) (8)
8. Chișinău → Cernăuți = 596.0 + 446.0 = 1042.0 (does not represend reliable route) (it is grater than 981.6) (9)
9. Tiraspol → Liov = 756.6 + 526.0 = 1282.6 → updating Liov (10)
10. Cernăuți → Liov = 981.6 + 395.6 = 1377.2 (does not represend reliable route) (it is grater than 1282.6) (11)
11. Liov → Kiev = 1282.6 + 630.4 = 1913.0 → updating Kiev (12)

Optimum route: Constanța → Galați → Chișinău → Odesa → Tiraspol → Liov → Kiev

Composed function: $w=1913.0$.

4. Advantages and limitations

4.1. Advantages

Multi-criteria resilience
Unlike classical Dijkstra implementations that focus solely on minimizing physical distance or cost, this adapted approach incorporates a composite weight formula:

$$w = \alpha\cdot distance + \beta\cdot cost + \gamma\cdot risk \quad (13)$$

This enables more realistic and mission-relevant routing, especially when dealing with hybrid threat environments.

Dynamic adaptability
The model can be updated in real-time to reflect changing operational risks (e.g., a cyberattack detected on a hub, or a drone strike disabling a highway route). Adjusting the “risk” component allows for rapid recalibration without rebuilding the full graph.

Operational clarity for command
By reducing strategic ambiguity into a quantified, rankable pathing solution, this model supports quick command-level decisions, particularly when time-sensitive delivery of aid or equipment is involved.

Feasibility in hybrid warfare logistics
Given the complexity of modern threats—including signal jamming, satellite spoofing, and misinformation campaigns—the model encapsulates non-traditional risk metrics that are becoming increasingly important for NATO-level logistical planning.

4.2. Limitations

Static risk assumptions

The “risk” values used are pre-assigned and based on qualitative analysis. In reality, threat levels fluctuate rapidly and unpredictably. A more advanced version of the model would integrate live feeds from intelligence sources to update the graph dynamically.

Lack of redundancy mapping
The current model optimizes for a single path. However, in wartime logistics, fallback routes and alternative contingencies are crucial. Extending the model to generate “backup paths” with only slightly higher total costs would enhance robustness.

Not accounting for cargo specificity
Different goods have different sensitivities to delay, damage, or interception. Currently, the algorithm treats all cargo types equally. Future iterations could introduce cargo weightings (e.g., medical supplies prioritized over electronics).

Logistical infrastructure not modeled in full detail
Although nodes and edges abstract key cities and connections, detailed local infrastructure (e.g., warehouse capacity, bridge integrity, fuel access) is not currently modeled—this may affect final delivery feasibility in extreme scenarios.

6. Conclusion

In an era dominated by hybrid threats, where warfare transcends traditional battlefield dynamics and spills into digital, economic, and logistical spheres, the strategic value of optimized supply chains becomes paramount. This research has demonstrated that by enhancing classical graph theory through a compound weighting mechanism—integrating distance, cost, and risk—logistical decisions can be elevated from heuristic approximations to rigorous, scenario-adapted strategy models.

Using a simulated conflict scenario focused on delivering critical equipment from the Port of Constanța to Kyiv, this model proved its utility in isolating not only the fastest or cheapest route, but the most balanced one under current threat conditions. Each node—be it Galați, Chișinău, Tiraspol, or Liov—represents more than a city; it stands as a dynamic asset or liability within a volatile geopolitical landscape. The ability to quantify those variables and incorporate them into route selection enables defense alliances, NGOs, and governmental logistic centers to operate with clarity and foresight.

Moreover, the application of Dijkstra’s algorithm in this compound formulation bridges computational rigor with operational relevance. It accounts for the uncertainties introduced by cyberattacks, surveillance operations, and paramilitary disruptions—realities often omitted in peacetime supply chain models. This methodology can be integrated into existing military-grade planning tools or augmented into enterprise software solutions for dual-use readiness.

Ultimately, the integration of such an algorithm within the wider decision-making process transforms logistics from a background support function into a central pillar of national resilience and strategic agility. In the ongoing context of the Ukraine conflict and broader Eastern European instability, such innovations are not optional—they are essential.

8. References

[1]. Bandura, Romina, Janina Staguhn, and Benjamin Jensen. "Modernizing Ukraine's Transport and Logistics Infrastructure." *Center for Strategic and International Studies (CSIS)*, 2022.
[2]. Grizold, Anton. "The Concept of National Security in the Contemporary World." *International Journal on World Peace* 11, no. 3 (1994): 37–53.

[3]. Katsoulas, Takis, Ioanna Fergadiotou, and Pat O'Sullivan. "Towards a Shared European Logistics Intelligent Information Space." In *Digital Supply Chain Transformation: Emerging Technologies for Sustainable Growth*, edited by Yingli Wang and Stephen Pettit, 99–120. Cardiff University Press, 2022.
[4]. Kusa, Iliya. "Russia-Ukraine War: Harbinger of a Global Shift A Perspective from Ukraine." *Policy Perspectives* 19, no. 1 (2022): 7–12.
[5]. Leffler, Melvyn P. "National Security." *The Journal of American History* 77, no. 1 (1990): 143–52.
[6]. MOLNAR, ISTVAN. "SIMULATION AND OPTIMISATION." *Society and Economy* 27, no. 2 (2005): 213–26.
[7]. Nalbandov, Robert. "DEMOCRATIZATION AND INSTABILITY IN UKRAINE, GEORGIA, AND BELARUS." *Strategic Studies Institute, US Army War College*, 2014.
[8]. Popescu, Nicu. "Ukraine: Four Crises, One Country." *European Union Institute for Security Studies (EUISS)*, 2014.

STUDY ON THE ADAPTATION OF SUPPORT FRAMES FOR VISUALLY IMPAIRED PERSONS

Bocăneț I. Gabriela, Claudiu Bișu(Conducător științific)

Facultatea de Inginerie Industrială și Robotică, Specializarea: Echipamente Tehnice de Recuperare, Anul de studii: II master, e-mail: gabrielabocanet65@gmail.com

ABSTRACT: People with visual impairments face mobility and safety challenges, and adapted walking frames are essential to improve their autonomy. These devices are equipped with advanced technologies, such as sensors and accelerometers, which help detect obstacles and guide users. Compared to standard walking frames, smart ones provide additional safety, haptic feedback, and integration with external devices for health monitoring. Experimental tests have demonstrated the effectiveness of ultrasonic sensors and cameras in improving users' mobility and safety. Research highlights the importance of developing accessible and customizable solutions, in collaboration with specialists and users. The integration of new technologies, such as artificial intelligence and augmented reality, is recommended to support the social and professional integration of people with visual impairments.

KEYWORDS: **Walker frame for the visually impaired with sensors**

1. Introduction

People with visual impairments face numerous challenges in daily life, especially regarding mobility and safety. In this context, assistive devices such as walking frames play a crucial role in improving the quality of life for these individuals.

Unlike walking frames used by sighted individuals—which are designed primarily to support balance and mobility—those intended for the visually impaired must also provide additional safety and orientation features. For a young person with visual impairment, independent mobility is essential for both daily activities and social integration. In such cases, a white cane is not always sufficient, as it does not offer balance support or the ability to carry personal items. Traditionally, walking frames provide physical support and stability; however, recent technological developments have made it possible to integrate sensors that help visually impaired users navigate more easily in their environment.

2. Comparative Analysis Between a Standard Walker and a Sensor-Equipped Walker for Visually Impaired Individuals

The traditional walker, is a mechanical device without sensors or alert systems. It is lighter and more affordable, but lacks the ability to monitor activity or connect to other devices.

The sensor-equipped walker, can include balance sensors and accelerometers to detect movement and potential falls. It monitors steps, distance traveled, walking speed, and other physical activity data. It integrates an alert system capable of sending messages or signals in case of emergency (e.g., a fall). It requires a power supply, with batteries that need to be recharged periodically. It is heavier due to the added electronic components (sensors, batteries, etc.). It is more expensive because of the integrated technologies (sensor systems, monitoring software). It offers customization options through mobile applications designed for health tracking. It can be connected to smartphones, smartwatches, or other monitoring devices. It provides significant advantages in terms of user safety and health monitoring [1].

3. Primary and Secondary Sensors Used in Creating a Smart Walker for the

The sensors used in assistive equipment are divided into two categories: primary sensors and secondary sensors. The primary sensors include ultrasonic sensors, infrared sensors, proximity sensors, laser sensors, and LiDAR sensors, while the secondary sensors consist of artificial intelligence cameras, vibration sensors, haptic sensors, digital compasses, and GPS sensors.

3.1. Senzori Primary Sensors and Their Functions

Ultrasonic Sensors

Functions and Operations: Ultrasonic sensors release sound waves and measure the time it takes for the echo to return in order to detect nearby objects. The time interval between sending and receiving the signal is used to calculate the distance to the object. These functions are effective in identifying solid obstacles and are particularly useful for short-range detection. Thus, the ultrasonic sensor helps to prevent collisions by emitting sound waves. It can also be used to navigate safely in unknown or crowded environments [3].

Infrared (IR) Sensors

Functions and Operations: Infrared sensors release infrared or thermal radiation, which is reflected by nearby objects and then detected by the sensor's receivers. They measure the distance to objects based on the reflected radiation and are effective in detecting differences in the objects' temperature. Although they are less effective in identifying highly reflective or transparent surfaces, infrared sensors are essential for nighttime navigation or in low-visibility conditions. Operating on a principle similar to laser sensors, they use infrared radiation instead of visible light, enhancing user safety by providing information about obstacles in the environment and generating useful thermal images in low light conditions [4].

Proximity Sensors

Functions and Operations: Proximity sensors detect the presence of objects in close proximity to the user, using techniques such as electromagnetic fields or acoustic waves, without direct contact with the objects. These sensors operate through ultrasonic or infrared technology to measure short distances between the walker frame and nearby obstacles. By detecting very close objects, they provide essential and constant information about proximity, by activating warnings through vibrations or visual signals. Effective in crowded environments or situations that require quick detection, proximity sensors help to prevent collisions and support safely navigation in confined spaces. These sensors are ideal for detecting moving obstacles and assisting navigation in constantly changing environments [5].

Laser Sensor

Functions and Operations: The laser sensor detects objects at long distances and generates a detailed mapping of surfaces, providing precise information about obstacles. It contributes to creating a safer environment, facilitating safe navigation by creating 3D maps of the environment. Operating by emitting a laser beam and measuring the time it takes to reach the object and return, the laser sensor delivers accurate distance measurements. In this way, it supports user orientation and helps avoid collisions, providing essential data for high-precision navigation [5].

LiDAR Sensor (*Light Detection and Ranging*)

Functions and Operations: LiDAR sensors use a laser beam to measure distances and create a detailed 3D map of the surrounding environment. These high-precision sensors identify essential details of the environment, facilitating navigation in complex and unknown spaces. By generating an accurate 3D image of obstacles and the surrounding space, LiDAR sensors contribute to safer and more efficient navigation. They operate by emitting a laser beam, which reflects off nearby objects; the time it takes for the signal to return is measured to calculate the distance. These functions are essential for creating 3D maps and supporting autonomous navigation, widely used in autonomous vehicles and drones [6].

Mounting Location:

The primary sensors can be strategically mounted on the frame of the walker to ensure complete coverage of the surrounding environment. Ultrasonic and proximity sensors can be placed on all four sides of the frame, providing efficient detection of obstacles from any direction, including laterally and in front. Infrared sensors can be integrated into the upper or lower part of the frame to detect obstacles at knee, torso, or ground level. The LiDAR sensor, mounted on the upper part of the frame or integrated into glasses, provides a detailed scan of the area in front of the user. Additionally, haptic sensors can be mounted on belts or wristbands, providing tactile warnings, while visual or auditory sensors can be placed on the upper part of the frame to assist with user orientation.

3.2. Integration of Primary and Secondary Functions

The primary sensors (proximity, laser, infrared, ultrasonic, LiDAR) and secondary sensors (AI camera, vibration, haptic, GPS, digital compass) work together to:

- **Detect and avoid obstacles**: Proximity, laser, and LiDAR sensors identify risks in real time, while the user receives haptic notifications.
- **Monitor and analyze the environment**: AI cameras and ultrasonic sensors map the surrounding spaces, providing the user with increased safety.
- **Provide personalized guidance**: GPS and digital compass indicate directions and track the user's position in space.
- **Increase comfort and safety**: Vibration sensors analyze ground stability, preventing loss of balance.

4. Role of Each Sensor Type in the Operation of the Device

In the operation of the smart walker, each category of sensors contributes specifically to improving the user's mobility, safety, and independence.

Ultrasonic sensors, are used to detect nearby obstacles through sound waves. They are particularly effective in crowded or narrow spaces, where precision and rapid response are essential. Through immediate alerts, the system provides the user with enough time to react and avoid collisions.

Infrared (IR) sensors, mounted on the walker frame, play a crucial role in detecting obstacles in low-light conditions or complete darkness. They operate by identifying temperature differences and reflective or transparent surfaces, which may be more difficult for other sensors to detect. Thus, they complement the ultrasonic sensors in situations where they are less efficient, contributing to more complete and safer detection in various usage environments.

Proximity sensors, integrated into the walker frame, enable the detection of objects in close proximity without the need for physical contact. They are essential for preventing collisions in confined spaces, providing a quick response when the user is very close to an obstacle. Through this functionality, the sensors contribute to increased safety and smoother navigation, especially in indoor or crowded environments.

Laser sensors, integrated into the walker frame, provide highly accurate distance measurements to obstacles located at a greater distance. They enable the creation of a detailed 2D mapping of the surrounding environment, which contributes to clearer orientation and safer route planning. Due to their accuracy, these sensors can assist the user in avoiding obstacles outside the immediate detection range of other sensors, thus complementing the assistive system with essential information for autonomous movement.

LiDAR sensors, when integrated into the walker frame, can build precise 3D maps of the surrounding environment, providing a detailed understanding of the space. They support autonomous navigation in complex and dynamic environments by adapting the route in real-time. Due to their ability to quickly detect changes in the surroundings, they enable dynamic obstacle avoidance, contributing to safe and predictable movement for the user.

Artificial Intelligence (AI) cameras, mounted on the walker frame, have the ability to recognize objects, people, signs, and changes in the surrounding environment. They integrate visual data with information provided by other sensors, giving the user a clearer perception of potential risks around them. Thanks to this advanced technology, the system can offer complex visual assistance, helping the user navigate more efficiently and safely in various environments.

Vibration sensors, mounted on the walker frame, are essential for monitoring the quality of the walking surface. They detect unevenness or irregularities in the terrain, quickly signaling the need for an adjustment in the user's walking mode. In this way, they provide continuous feedback, contributing to safer and more comfortable navigation on varied terrain.

Haptic sensors, integrated into the walker frame, provide intuitive tactile feedback through vibrations or pressure. They translate obstacle warnings into physical signals, directly felt by the user, offering an efficient and rapid way to react to obstacles in their path.

GPS sensors, integrated into the walker frame allow the precise localization of the user on a map, thus facilitating the generation of safe routes. They also contribute to monitoring the user's movements, providing accurate information about their position and supporting navigation in unfamiliar or complex environments.

Digital compasses, integrated into the walker frame, maintain the user's correct orientation, providing clear directions. In combination with GPS sensors, they ensure smooth and precise navigation, guiding the user in the right direction to avoid confusion in unfamiliar or complex environments.

5. Synergy of the Multi-Sensor System

By combining these types of sensors, complete environmental detection is achieved (near and distant obstacles, ground conditions, direction of movement). Personalized guidance is provided through haptic signals, vibrations, sound or visual indications. Overall safety and user autonomy are increased, allowing the user to navigate unknown or challenging environments with confidence. A concrete example of how two sensors collaborate (e.g., LiDAR sensor + AI camera in detecting a transparent obstacle) [7].

Table 1: ***The Technology Behind Smart Walkers***

SENSOR TYPE	*TYPE OF FEEDBACK PROVIDED*	*ASSOCIATED COMPONENTS IN THE SYSTEM*
Ultrasonic Sensor	Auditory and tactile feedback for warning	Integration with GPS and AI cameras
Infrared Sensor	Tactile feedback upon object detection	Integration with AI cameras and digital compass
Proximity Sensor	Tactile feedback for quick interaction	Integration with GPS and AI cameras

Laser Sensor	Auditory and visual feedback for critical distances	Integration with digital compass and AI cameras
LiDAR Sensor	Auditory feedback for proximity alerts and generated maps	GPS, AI cameras, and digital compass

According to: **[10.11.12].**

Table 2: ***How Each Sensor Type Functions in Integration with Other Sensors***

SENSOR TYPE	HOW IT WORKS	INTEGRATION WITH OTHER SENSORS
Ultrasonic Sensor	Emits sound waves and measures the time until they reflect off an object.	Complementary with optical sensors for precision in low light conditions.
Infrared Sensor	Detects variations in infrared radiation reflected by surfaces.	Integrates with proximity sensors for close-range detection.
Proximity Sensor	Detects the presence of objects at very short distances via an electromagnetic field.	Useful with LiDAR sensors for fine movement detection at close range.
Laser Sensor	Emits laser beams and calculates distance based on the return time.	Works well with infrared sensors for obstacle avoidance at long distances.
LiDAR Sensor	Uses laser and rotation to create a detailed 3D map by measuring distances.	Perfect for integration with ultrasonic sensors for precise mapping.

Processing according to: **[13.14.9].**

6. Experimental Testing of the Two-Wheeled Walking Frame with Sensors for the Visually Impaired

Steps for Experimental Testing: Initial setup of the walking frame. Static obstacle detection test. Moving obstacle detection test.

Parameters to be Evaluated: Obstacle detection accuracy. The results expected were obtained. The tests included the detection of both static and moving obstacles, and the parameters evaluated were sensor accuracy and response time.

7. Case Study

Testing the Smart Walking Frame

Testing Location: In an indoor room, simulating a real indoor environment.
Tested Device: Walking frame with an ultrasonic sensor mounted on the front (on the middle bar).
Tested Obstacles: Door, tables, chairs, moving people.
Goal: Rapid and accurate detection of static and dynamic obstacles.
Observations: The sensor correctly detected objects at 18-22 cm. The feedback was consistent and coherent. The response time was accurate in relation to changes in the environment.

7.1. Description of the Walking Frame

CLS → Left Lateral Frame / fixed frame;
CLD → Right Lateral Frame / fixed frame;
R1 and **R2** → The two pivoting wheels or front wheels;
D1 and **D2** → Rubber stoppers / on the back legs;
BP → Folding Bar with lateral edge folding system;
BB → Locking Button / folding;
SRF → Central Medial Stabilizing Bar / fixing;
→ Front Rigidizing Support.

Fig. 1.: ***Experimental Model*** **[15].**

7.2. Experimental Model - System Validation

To validate the functionality of the smart walking frame designed for visually impaired individuals, experimental tests were conducted in the laboratory using a standard frame, purchased from the market. It was adapted to integrate the necessary electronic components, transforming it into an assistive device.

7.3. Assistive Equipment Model

In this phase, a functional prototype was built using a classic walker frame, which was adapted to integrate electronic components. Thus, an ultrasonic sensor was mounted on the central, medial bar of the walker frame, powered by its own battery system. The sensor is connected to a control module and is activated through a power on/off switch.

7.4. Description of the Assistive Walker Frame

In our proposal, the entire assembly is fixed to the central medial bar of the walker using screws to ensure stability and proper functioning.
The ultrasonic sensor consists of an emission component and a reception component, both mounted on a supporting base. The system also includes a control module (an electronic board), a power supply system with two batteries, and a switch to turn the equipment on/off. When the sensor detects an obstacle within its range, it emits an audible alert.

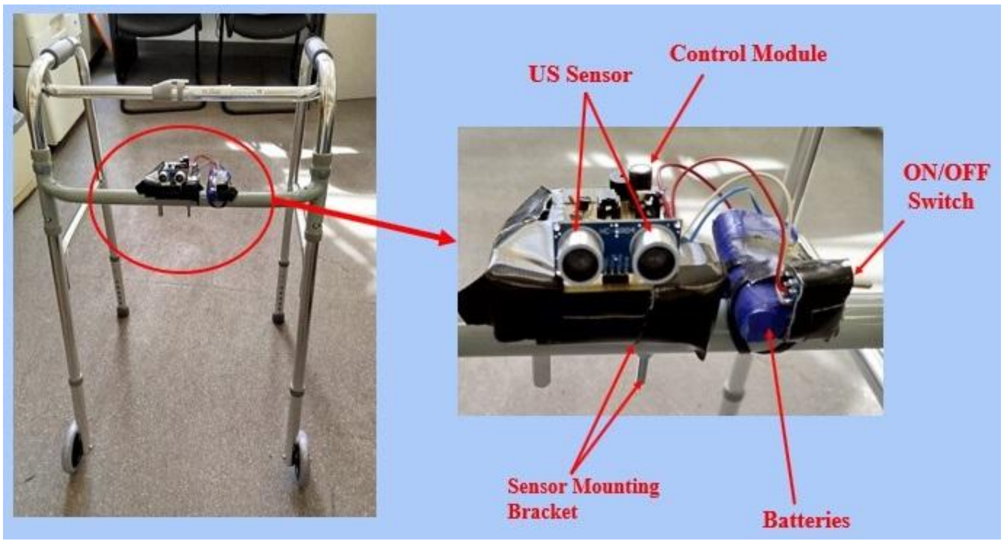

Fig. 2.: ***Description of the Assistive Walker Frame and the Sensor.***

7.5. Aim of Validation

The tests were designed to determine:

- The accuracy of obstacle detection at various distances;
- The system's response upon facing objects of varying heights;
- The optimal positioning of the sensor;
- The distances at which the user receives warnings and where the obstacle validation occurs.

7.6. Validation Methods

The validation method was carried out as follows:

1. The system is powered on using the switch.
2. Upon activation, the LED on the sensor lights up green (indicating the system is functioning without any obstacles).
3. When approaching an obstacle (such as a wall, door, chair, etc.), the LED turns red, and the system emits an audible alert.
4. As the obstacle is removed, the LED returns to green, and the sound signal stops.

This functionality provides the user with intuitive and immediate feedback about the surrounding environment, contributing to increased safety during movement.

7.7. Validation Test Analysis

Table 3: ***Validation Test Results for the Ultrasonic Sensor Mounted on the Walking Frame***

No.	**Tested Obstacle**	**Alarm Trigger Distance (cm)**	**Validation Distance (cm)**	**Observations**
1	Door	19	109	Effective detection at a large distance
2	Chair (Round 1)	25	60	Correct detection; validation at a medium distance
3	Chair (Round 2)	22	78	Improved feedback in round 2
4	Desk with equipment on top	22	112	Tall obstacle, effective detection and validation
5	Door corner / door frame	18 (frame), 7 (wall)	50 (frame), 40 (wall)	Narrow obstacles, but well detected
6	Wall	26	112	Stable and precise response
7	Tall electronic furniture	21	108	Good detection, quick response

7.8. Observations

The tests revealed that the sensor effectively detects large and tall obstacles but has difficulty detecting low-lying objects, such as small furniture or items on the ground. This limitation is due to the sensor's placement on the upper bar of the walker, which is why repositioning it to a lower height is recommended to ensure more complete coverage of the area in front of the user.

Additionally, it was observed that the alarm and validation distances can vary depending on the type and material of the obstacle; however, the system provides consistent and timely feedback, thereby supporting user orientation in controlled environments.

8. Conclusions

Following the conducted research, we have found that adapting walking frames for visually impaired individuals is an essential step toward improving their accessibility and autonomy in various aspects of daily life. Although technological advancements and innovations in assistive devices have significantly contributed to supporting people with visual impairments, many challenges still need to be addressed. Particularly, the design and implementation of accessible, durable, and customizable solutions for various environments—such as homes, public spaces, or workplaces—require closer collaboration between technology specialists, authorities, non-governmental organizations, and users.

Case studies and analysis of various existing solutions in this field highlight the importance of an approach centered on the real needs of visually impaired individuals, considering that each person may have a different degree of visually impaired individuals, considering that each person may have a different degree of visual ability or personal preferences.

Additionally, the accessibility and adaptability of support frames must be constantly evaluated in light of technological developments, and changing social and economic requirements.

In conclusion, although there are innovative solutions that help visually impaired individuals integrate more easily into society, there are still significant steps to be taken to ensure full and sustainable accessibility. Creating a truly inclusive environment depends not only on the development of advanced technologies, but also on changing mindsets and promoting a culture of empathy and solidarity. The continuous integration of emerging technologies will transform the smart walking frame from a simple physical aid into a true digital partner for people with visual impairments.

8.1. Perspectives

1. Optimization of alert distance (red light and sound alarm) = 25 cm;
2. Reactivation distance when no obstacle is present (green light and sound stops) = 50 cm;
3. Addition of two supplementary sensors at the lower part of the walking frame for detecting smaller obstacles;
4. Use of an AI-integrated camera.

Future directions and change in perspective

The future of assistive devices lies in the integration of artificial intelligence and emerging technologies, alongside the promotion of an inclusive and supportive culture that fosters the full social integration of individuals with visual impairments.

9. Bibliography

[1] **Hu, Z., & Li, Z.** "Application of Ultrasonic Sensors in Assistive Devices for Visually Impaired." *Journal of Assistive Technology*, 15(2), 90-105. 2020.

[2] **Johnson, L., & Carter, A.** "Infrared and Proximity Sensors in Navigation Aids." *Technology and Disability*, 31(4), 230-240., 2019.

[3] **Vanderbilt, T., & Millard, B**. *Assistive Technologies for the Visually Impaired: Advances in*

Sensory Substitution. Journal of Visual Impairment & Blindness, 113(3), 229-240. 2019.

[4] **Stief, F. *et al.*** Impact of subject-specific step width modification on the knee and hip adduction moments during gait. *Gait Posture* 89, 161–168 2021.

[5] **He, H., & Lee, J.** *Infrared Sensing Technologies for the Visually Impaired: A Review*. International Journal of Human-Computer Interaction, 36(4), 310-322. 2020.

[6] **Smith, R., & Bennett, C.** *Proximity Sensors in Assistive Devices for the Visually Impaired*. IEEE Transactions on Systems, Man, and Cybernetics, 51(6), 1124-1132. 2021.

[7] **Miller, G., & Davis, R.** *Lidar Systems for Blind Navigation: A Review of Laser-Based Technologies*. Journal of Assistive Technology, 32(4), 179-192. 2018.

[8] **Watson, F. D.**, & **Ali, M. A.** "Artificial Intelligence for the Visually Impaired: An Overview." *Journal of Assistive Technology and Research*, 14(2), 121-138. 2020.

[9] **Thomas, R. K.**, & **Goldstein, D. G.** "Vibration and Haptic Feedback for Navigation Systems in the Visually Impaired." *Journal of Rehabilitation Research and Development*, 245-262. 2018.

[10] **Liu, F., & Zhang, X.** *Haptic Feedback Technologies for Blind and Visually Impaired Individuals*. Journal of Assistive Technology, 34(2), 137-145. 2020.

[11] **Kumar, N., & Patel, R.** *GPS and Digital Compass in Navigation Systems for the Visually Impaired*. Journal of Navigation and Positioning, 18(3), 251-262. 2023.

[12] **Bălan, R.**, & **Ionescu, I.** "Utilizarea tehnologiilor avansate în asistența pentru persoanele cu deficiențe de vedere: O revizuire." *Revista Română de Asistență Socială*, 34(2), 221-235. 2018.

[13] **Niculae, C., & Constantin, A.** *Tehnologii asistive pentru persoane cu dizabilități vizuale*. Revista Științifică de Cercetare Tehnologică și Inginerie, 40(3), 112-121., 2017.

[14] **Lewis, R.,** "Integration of Proximity and Haptic Feedback in Assistive Technologies," *International Journal of Assistive Technologies*, vol. 15, pp. 77-89, 2022.

[15] ***https://echipamenteortopedice.ro/cadru-de-mers/54-cadru-de-mers-cu-rotile.html?srsltid=AfmBOorUtkwBdz37b0p_auEFzPEmToZ5rcNwO3ByCdOVFhBujXjs_Vu0***

EVALUATING THE MAXIMUM VOLUNTARY ISOMETRIC CONTRACTION BETWEEN TRADITION AND INNOVATION. APPLICATIONS OF SEMG, TMG AND LDV

PREDICA Gabriela, BÎȘU Claudiu Florinel, DRAGOMIR Andrei(Conducători științifici)

Faculty of Engineering and Robotics, Master's Program in Equipment for Recovery Therapies, Year of Studies:II, e-mail: gabrielabainiceanu@gmail.com

ABSTRACT: SEMG and TMG are widely used testing methods in the evaluation of MVIC, which cannot be said about LDV. In this article, we propose measurements of CIVM for the purpose of observing data, comparing the recorded parameters, determining the values of the rate of increase of muscle electrical activity following SEMG and TMG testing, as well as using LDV technology in addition, which can be used to create a new type of investigation, to constitute a new medical imaging procedure.
Keywords: SEMG, TMG, LDV, MVIC evaluation.

1. Introduction

In the broader context of the unprecedented development of technology, an approach that is relatively easy to implement and supports the inclusion of people with disabilities is assistive technology. Surface Electromyography (sEMG) and Tensiomyography (TMG) are widely used testing methods for evaluating maximal voluntary isometric contraction (MVIC), which cannot yet be said for Laser Doppler Vibrometry (LDV).

Hypothesis: Through electrical stimulation and data acquisition using sEMG, benchmarks can be established for a new imaging-based investigation technique.

The choice of this topic is motivated by its high relevance: nowadays, rehabilitation engineering complements physical medicine and rehabilitation, physiotherapy, occupational therapy, and sports, as well as rehabilitation programs for individuals with temporary or permanent disabilities. This is achieved by creating assistive equipment and devices; the use of technology enables the analysis of the biological response of skeletal muscles during maximal voluntary isometric contraction (MVIC), involving—depending on the case—monitoring, rehabilitation, and evaluation through assistive equipment, which is the focus of this research.

2. Description of the Evaluation Procedure

2.1.Tensiomiography (TMG) is a method used to monitor the properties of skeletal muscles [1] [2] starting from the evaluation of the transverse displacement of the central area of the muscle (the muscle belly) during an induced muscle contraction, when the muscle belly expands perpendicularly to the direction of force exerted during contraction. It is a non-invasive measurement method that precisely measures muscle contraction velocity under isometric conditions. The data obtained from this evaluation can be used to: determine the type of muscle fiber; determine the muscular state/condition (e.g., level of fatigue, potentiation, inhibition, stress); diagnose functional muscle symmetry, whether temporal or morphological; assess muscle synchronization; rapidly detect (in under 5 minutes) subclinical muscle injuries. [3] It is considered that the method reflects the stiffness of the muscle belly [1], and it has been shown to be affected by muscle fatigue and aging [4]. Additionally, it has been demonstrated that Dm (maximum radial displacement) and Tr (contraction time) increase with the rise in muscle fatigue [5]. By identifying the values of these parameters, the interpretation of the test can provide information about lateral symmetry and functional symmetry. Lateral symmetry refers to the symmetry between muscle groups on the right and left sides of the body. It provides information on imbalances in muscle group development, muscle fatigue, and the risk of muscle tears. Functional symmetry offers information about imbalances at the joint level, specifically between flexor and extensor muscle groups. Significant imbalances at these levels can increase the risk of joint injuries.

Application Method of TMG. The method is based on bipolar neuromuscular stimulation, using two electrodes applied distally and proximally, while signal acquisition is performed with the help of a fiber optic sensor that transmits the signal to a computer equipped with dedicated software for this method. The sensor that measures displacement is positioned tangentially on the largest area of the muscle (the belly of the investigated muscle). The displacement of the muscle belly during contraction is observed, monitored, and recorded. It has been demonstrated that the tensiomyographic method provides valuable data regarding the contractile properties of striated muscle [6] [7].

2.2. Electromiography (EMG) is a method for the graphical recording of muscle biopotentials and the study of their characteristics using surface (cutaneous) electrodes (SEMG). The signal acquisition sensors have built-in: triaxial accelerometers, which record, in addition to muscle contraction force, the accelerations on the XYZ axes (see Fig. 1a); parallel silver bars (see Fig. 1b) for detecting the EMG signal from the surface of the skin. The transmission range is 20 meters; the EMG signal bandwidth is between 20–450 Hz; and the signal sampling rate is 1000 Hz. For maximum signal amplitude, it is important that the sensors are oriented with the silver bars perpendicular to the muscle fiber direction. The arrow located on the upper surface of the sensor should be aligned along the length of the muscle fibers. The sensors must be placed on the muscle belly, away from tendons or muscle heads (see Fig. 2) [8].

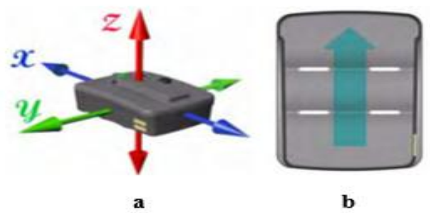

Fig. 1. Inertial detection axes (a); EMG electrode (b) [8]

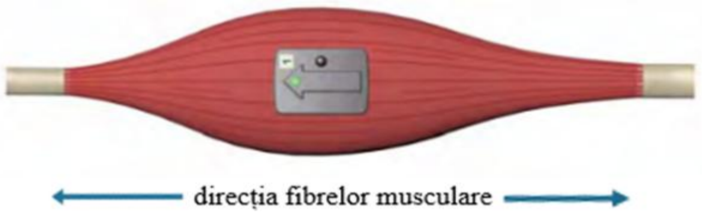

Fig. 2. Direction of EMG sensor placement relative to the orientation of muscle fiber length [8]

The use of sensors is contraindicated in patients with any type of implanted electronic devices (e.g., pacemakers, electronic infusion pumps), irritated or wounded skin, or allergy to silver [8].

2.3. Laser Doppler Vibrometry (LDV) is a technique for non-contact measurement of surface vibrations in various fields: mechanical engineering, civil structures, automotive, industrial and aerospace engineering, manufacturing, and biomedical engineering. The "sensor" used in LDV for measuring vibrations is not physically attached to the measurement surface; a laser beam is directed at a target location on the surface, and the displacement and/or velocity of that surface along the direction of the laser beam is measured using the Doppler effect and principles of interferometry [9] [10] [11].

3. Testing

3.1. Description of the testing protocol using SEMG and TMG techniques. The tests for evaluating the muscular response of the rectus femoris muscle (RF) following electrical stimulation and electrical activity of the muscle during maximum voluntary isometric contraction (MVIC) were carried out at the National Institute for Sport Research (INCS) (see Fig. 3).

Fig.3. sEMG Testing

The equipment used during testing includes the Trigno electromyograph and the electrical stimulation sensors associated with TMG. Before starting the experimental procedure, the subject was provided with information regarding the testing method, the data acquisition procedure, the objectives of the test, and safety warnings concerning their own well-being. The area where action potentials will be acquired is identified, shaved, and cleaned with rubbing alcohol to ensure maximum electrode adhesion. The hardware and test setup are configured in the Delsys "Signal Acquisition" program. The software is programmed for acquisition according to the number of muscles being investigated, determining how many channels will be used, how many seconds each acquisition will last, and how many repetitions will be performed. Bioelectric signal acquisition is carried out in real time and can be visualized on the computer screen while the subject performs the required movement, with electrodes collecting the signal from the target area. The data acquired through "Signal Acquisition" is stored and processed using the "Analysis Software" application. The signal is scaled and filtered first at 100 Hz and then at 10 Hz to remove interference. Exporting the data to Excel enables multiple signals to be displayed in a single graph, which facilitates data correlation and interpretation. The data filtering procedure included: zeroing the signal by centering the isoelectric line using the "Remove Mean" operator, converting the signal's negative values to positive using the "abs" operator from the "Simple Math" mathematical processing library in the EMGANA program, developed by Delsys.

The subject is seated on a chair, with the right lower limb secured at the ankle using a strap to prevent movement during testing.

After applying the EMG electrode, a test was conducted to verify electrode-skin contact and data recording accuracy. Three electrical stimulations were applied at 30 mV, 40 mV, and again 40 mV. The subject was then asked to perform three maximum voluntary isometric contractions (MVICs) as quickly as possible, each lasting between three to five seconds.

3.2. Description of the testing protocol using the LDV technique. At the National University of Science and Technology Politehnica Bucharest, Faculty of Engineering and Robotics, Master's Program in Equipment for Recovery Therapies, experimental applications were conducted to evaluate muscle contraction using Laser Doppler Vibrometry (LDV). Before the experiment, the subject was informed about the experimental components and safety warnings concerning their own protection. While seated on a chair, the subject had two adhesive electrodes (5x5 cm) applied to the posterior forearm, after the skin had been degreased with rubbing alcohol to improve electrode adhesion. The electrodes were then connected to a transcutaneous electrical nerve stimulation (TENS) device, which was used to stimulate the wrist extensor muscles (see Fig. 4).

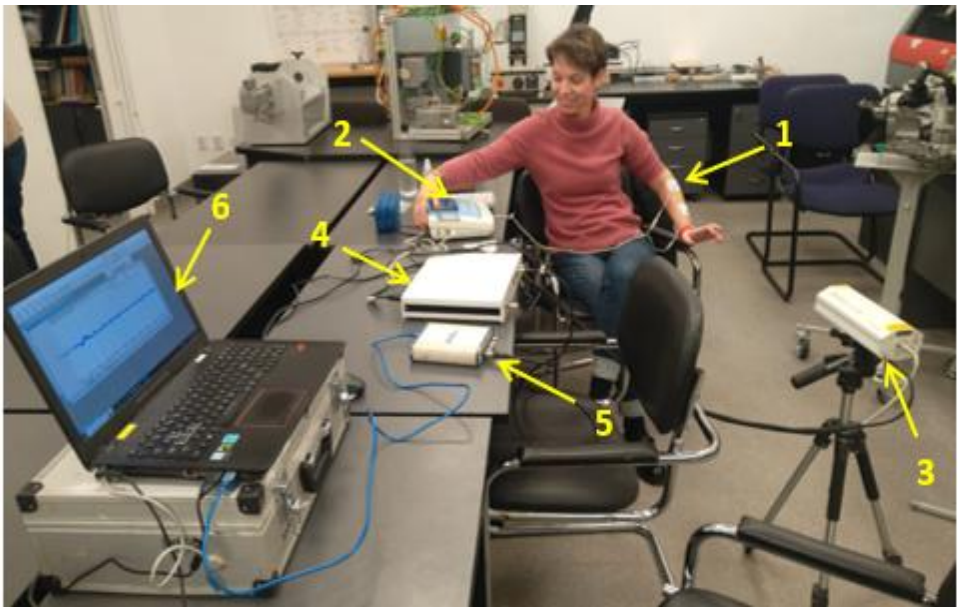

Fig. 4. LDV Testing Protocol: 1 – Adhesive electrodes; 2 – TENS device; 3 – LDV laser; 4 – LDV source; 5 – Signal acquisition module (National Instruments USB-4431); 6 – Fastview Software

The LDV evaluation was based on the use of a Metrolaser Vibrometer 500V, with the following specifications: Velocity range: 5 µm/s to 1000 mm/s; Frequency range of vibrations: DC to >20 kHz; Working distance: 1 cm to 5 m; Displacement range: 0.1 nm to 10 mm; Optics: Collimated or variable focus (1 m – 5 m); Output signal: Analog, demodulated and FM at 10.7 MHz. The tests were performed under preliminary conditions, requiring a quantitative calibration check of the LDV equipment.

4. Results of the Testing and Discussions

4.1. MVIC and Electrical Stimulation of the Rectus Femoris Muscle. During the first contraction, electrical stimulation was applied with a current of 30 mV, resulting in a maximum amplitude of the rectus femoris muscle (RF) of 0.8 mV. After a five-second pause, a second contraction was induced using a current of 40 mV, which resulted in an amplitude of 0.92 mV. After four more seconds, a third stimulation was applied, again with a current of 40 mV, and this produced an amplitude of 0.79 mV (see Fig. 5, Table 1).

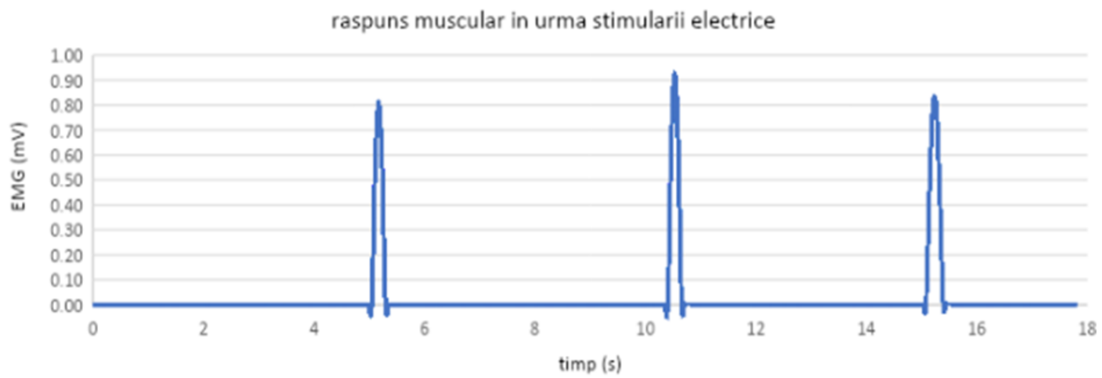

Fig. 5. Muscle response following electrical stimulation

Table 1. Values obtained following electrical stimulation of the rectus femoris muscle

Order of Stimulation	Electrical Stimulation Amperage (mV)	Maximum Amplitude of Rectus Femoris Muscle (mV)
1	30	0.8
2	40	0.92
3	40	0.79

Following each maximum voluntary isometric contraction (MVIC), the following values were obtained: for the first MVIC, a maximum amplitude of 0.19 mV was observed, with a duration of 3.30 seconds and a rate of voltage increase of 0.57 mV/s. For the second MVIC, a maximum amplitude of 0.14 mV was recorded, with a duration of 3.12 seconds and a rate of voltage increase of 0.33 mV/s. For the third MVIC, the maximum amplitude was 0.21 mV, with a duration of 1.68 seconds and a rate of increase of 0.45 mV/s (see Fig. 6, Table 2).

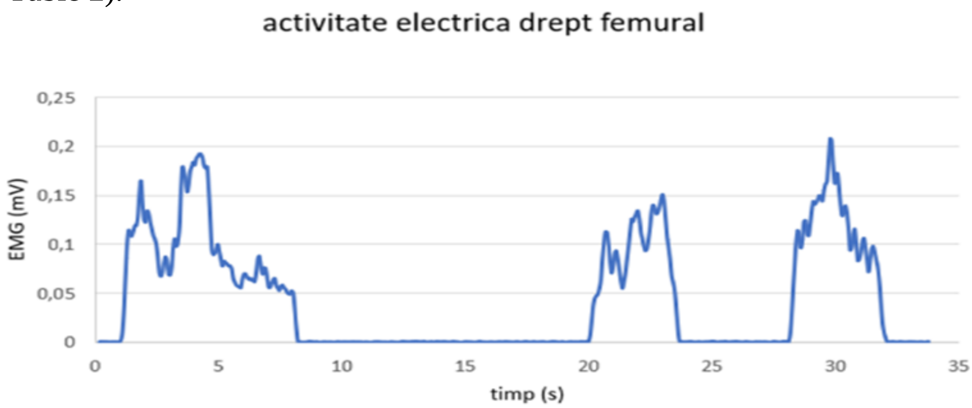

Fig. 6. Electrical Activity of the rectus femoris muscle

Table 2. Values obtained following MVIC of the rectus femoris muscle

MVIC Order	Maximum Amplitude (mV)		MVIC Time to Amplitude (s)	Maximum Rate of Electrical Voltage Increase (mV/s)
1	0.19		3.30	0.57
2	0.14		3.12	0.33
3	0.21		1.68	0.45

From the above values, it appears that the last MVIC had the highest maximum amplitude, namely 0.21 mV, the fastest response time – 1.68 seconds (see Fig. 7), and a voltage rise rate of 0.45 mV/s (see Fig. 8).

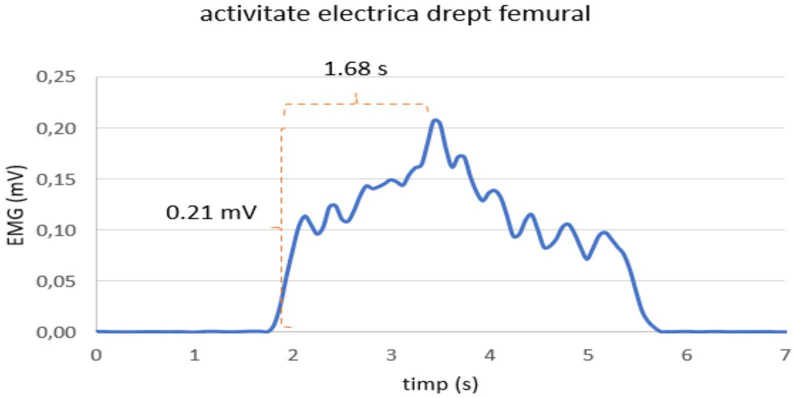

Fig. 7. MVIC 3 – Response time to maximum amplitude

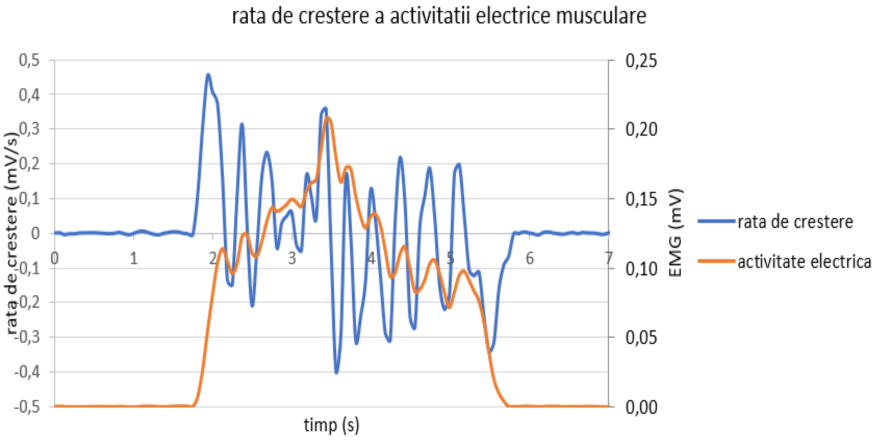

Fig. 8. Rate of increase in electrical muscle activity

The valies obtained using TMG are: Tc – 20.2 ms; Td –22.8 ms; Tr – 53.3 ms. (see Table 3).

Table 3. Parameters obtained from TMG evaluation of the rectus femoris muscle

Muscle	Laterality	Tc (ms)	Td (ms)	Tr (ms)
RF muscle	Right	20.2	22.8	53.3

4.2. LDV Evaluation is based on the use of a Metrolaser Vibrometer 500V. The tests were conducted in preliminary conditions, and a quantitative calibration verification of the LDV equipment is still needed.

To evaluate muscle contraction, LDV technology was employed, a laser-based technique for dynamic characterization with multiple applications. Measurements before and after electrical stimulation represent a key aspect in tracking treatment progress during various stages of recovery. In the figure below (Fig. 9), the laser signal waveform is shown: amplitude (in V) as a function of time (ms). By applying the Fast Fourier Transform (FFT), a frequency spectrum is obtained, corresponding to the frequency response to the stimul during TENS stimulation.

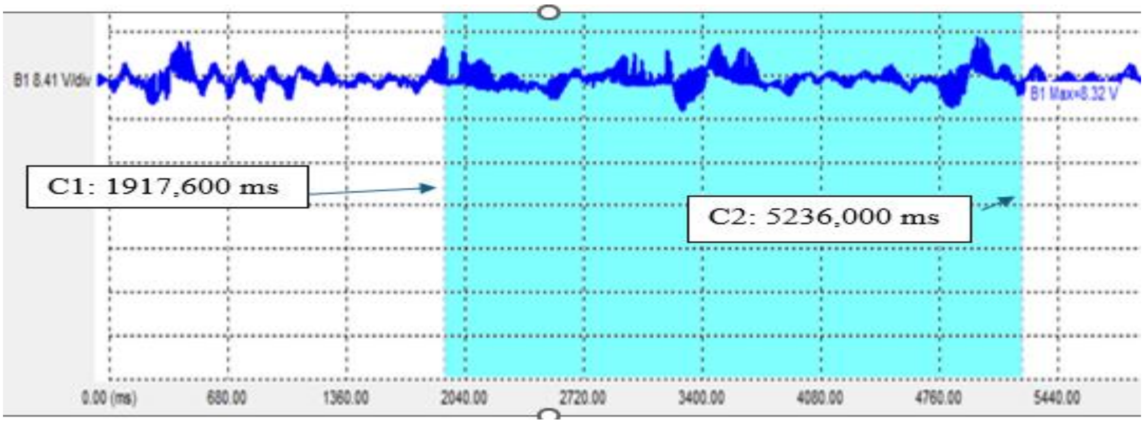

Fig.9. Analgesic Test 8 – Laser Signal: Wave form of Amplitude (V) over time (s)

In the next figure (see Fig. 10), the frequency spectrum during TENS excitation is displayed, highlighting a 5.95 Hz component, characteristic of muscle excitation. As the LDV Vibrometer 500V still requires calibration for determining specific speed values, this work proposes only a qualitative preliminary observation. In other words, the goal is to initiate LDV use in patient evaluations during various recovery stages.

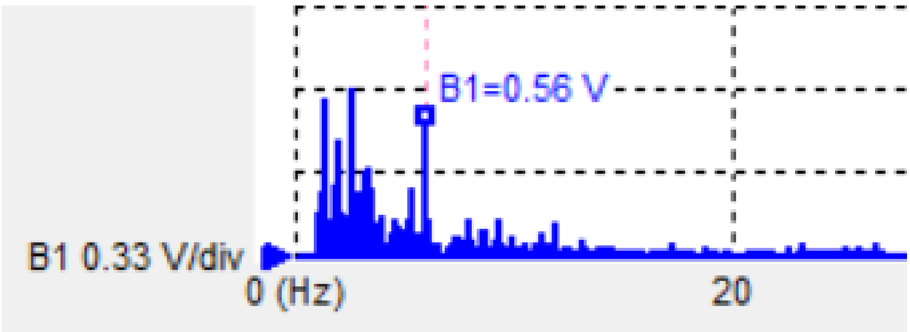

Fig. 10. Frequency spectrum: Analgesic Test 8

A broader visualization of these results is shown below (see Fig. 11), noting that amplitude is in voltage, not speed. Calibration is not yet finalized; the current version is provisional.

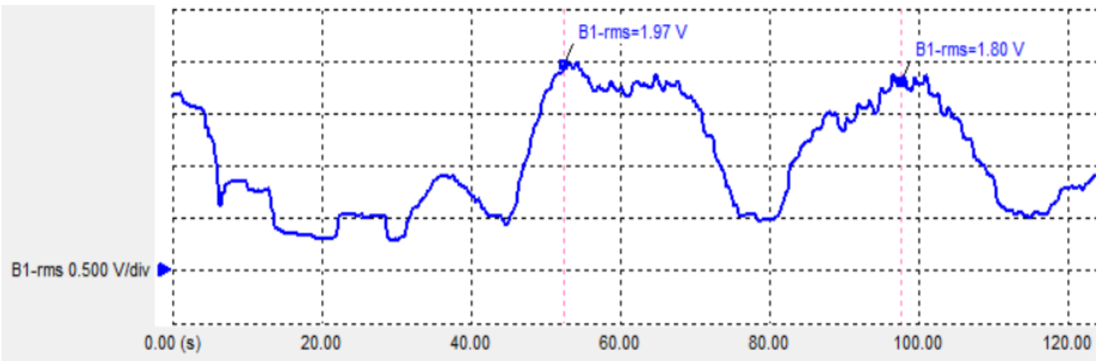

Fig. 11. LDV Evolution Analgesic Test 8

In conclusion, it can be highlighted that LDV technology represents a sustainable proposal for evaluating muscle contraction as a result of rehabilitation procedures. The specific evaluation characteristic is the muscle tension, reflected through its frequency.

5. Conclusions

Functional explorations require solid knowledge of anatomy and physiology, not only from rehabilitation medicine specialists, but also from engineers, researchers, physical therapists, and potentially even occupational therapists and other professionals.

It is important to highlight that the data obtained through sEMG and TMG represent standard references for developing a new type of imaging-based investigation. The capability of LDV and SLDV to accurately convert vibrations into images, across a wide frequency range, is a crucial factor that can contribute to the development of new types of medical imaging procedures, which are also valuable in evaluation/rehabilitation of individuals with disabilities. The fact that measurements can be taken remotely (non-contact) adds another benefit, making this approach even more promising.

Based on these data, members of the interdisciplinary team can adjust recovery programs and frequently adapt the load (volume and intensity) in accordance with muscular responses. Therefore, functional assessments play a crucial role in accurately observing neuromuscular responses, monitoring recovery stages, and adjusting the recovery plan accordingly.

Preliminary tests were carried out to observe data and correlate the recorded parameters. It is proposed that MVIC measurements using SEMG, TMG, and LDV provide complementary and novel insights. We aim to continue research in the upcoming weeks as part of the dissertation work, focusing on tracking these parameters in subjects with disabilities.

6. References

[1] D. D.-U. G. &. G.-M. C. Fernández-Baeza, „Contractile and Mechanical Properties of Quadriceps Muscles Measured by the Method of Tensiomyography (TMG) in Professional Soccer Players: A Systematic Review, Meta-Analysis, and Meta-Regression,” *Bioengineering,* vol. 11, nr. 12, p. 1295, 2024.

[2] B. Šimunič, Model of longitudinal contractions and transverse deformations in skeletal muscles, Ljubljana, 2003.

[3] R. e. a. Dahmane, „Spatial fiber type distribution in normal human muscle: Histochemical and tensiomyographical evaluation,” *Journal of biomechanics,* vol. 38, nr. 12, pp. 2451-2459, 2005.

[4] J. M. R.-R. D. R.-M. D. d. S. Y. S. S. &. Q. M. García-Manso, „Assessment of muscle fatigue after an ultra-endurance triathlon using tensiomyography (TMG),” *Journal of sports sciences,* vol. 29, nr. 6, pp. 619-625, (2011).

[5] K. S. K. A. T. W. C. L. M. E. C. H. W. J. H. A. J. W. D. H. F. J. S. a. M. S. S. J. P. Beausejour, „Innovations in the Assessment of Skeletal Muscle Health: A Glimpse into the Future,”.

[6] A. H. P. a. B. Š. K. Pus, „The use of tensiomyography in older adults: a systematic review,” *Frontiers in physiology,* vol. 14, p. 1213993, 2023.

[7] L. J. D. M. S. I. J. F. M. M. &. H. A. M. Macgregor, „Reduced radial displacement of the gastrocnemius medialis muscle after electrically elicited fatigue,” *Journal of sport rehabilitation,* vol. 25, nr. 3, pp. 241-247., 2016.

[8] https://fcc.report/FCC-ID/W4P-SP-W05/1835396.pdf.

[9] H. M. G. L. Kirsner R. S., „ „Margin assessment of selected basal cell carcinomas utilizing laser doppler velocimetry,”,” *nternational Journal of Dermatology,* vol. 32, nr. 4, pp. 290-292, 1993.

[10] H. O. D. R. J. e. a. Tabatabai, „Novel Applications of Laser Doppler Vibration Measurements to Medical Imaging,” *Sensing and Imaging: An International Journal,* vol. 14, pp. 13-28, 2013.

[11] N. S. L. &. T. E. P. Paone, „Laser doppler velocimetry,” în *An Introduction to Optoelectronic Sensors,* World Scientific, 2009, pp. 230-256.

BALANCE ASSESSMENT TECHNOLOGIES: INTEGRATION OF A TRIAXIAL SYSTEM ON THE BOSU BALL PLATFORM

STANCIU Denise Ioana, Claudiu BÎȘU(Conducător științific)

Faculty: Industrial Engineering and Robotics, Specialization: Industrial Engineering, Year: I, e-mail: denise_ioana.chircu@stud.fiir.upb.ro

ABSTRACT: The paper titled "Balance Assessment Technologies: Integrating a Triaxial System on the BOSU Ball Platform" aims to explore an innovative solution for monitoring and analyzing balance in the context of neurorehabilitation, by combining an unstable platform with triaxial accelerometers. The proposed system incorporates two diametrically opposed accelerometers capable of capturing fine deviations of the center of gravity in the frontal and sagittal planes in real time. The application has the ability to provide objective quantitative data, thus supporting both more accurate diagnosis of functional deficits and tracking of therapeutic progress. The study includes a comparative analysis with existing devices on the market, highlighting advantages related to portability, low cost, and customization potential.

KEYWORDS: postural balance, neurorehabilitation, triaxial accelerometer, BOSU platform, objective assessment

1. Introduction

General aspects regarding balance in neurorehabilitation

Balance is an essential component for nearly all human physical activities, including basic actions such as walking, standing, sitting, or transitioning between postures. However, for most individuals with neurological conditions, maintaining balance becomes a challenge. Stroke, traumatic brain injury, Parkinson's disease, multiple sclerosis, cerebral palsy, and other neurological disorders often lead to deficits in the mechanisms that control balance: the vestibular system (inner ear), the visual system (eyes), the proprioceptive system (receptors in muscles, joints, and skin), the central nervous system (brain and spinal cord), and the musculoskeletal system [1]. All these mechanisms work together to enable balance in both static (standing) and dynamic (walking, running, changing direction) positions. These patients are at increased risk of falls, which can lead to further disabilities, loss of independence, and a decreased quality of life [2].

In neurorehabilitation, the main goal is to help patients recover lost functions. This can be achieved by improving postural control. Restoring balance is one of the most important objectives of the recovery process, as it directly influences the patient's safety and autonomy. Balance training has been shown to activate the neural networks involved in postural control, thus becoming an essential component of rehabilitation therapy.

The Role of Balance Assessment in Neurorehabilitation

An effective and objective balance assessment is essential in the rehabilitation process, providing measurable data that can guide treatment plans, monitor patient progress, and predict fall risk [3]. Traditional methods of balance assessment are based on observation and, although useful, are often limited by subjectivity and the inability to detect subtle changes in the patient's condition. The most commonly used clinical tests include the Romberg Test, Single-Leg Stance

Test, Postural Stress Test, Berg Balance Scale (BBS), Balance Evaluation Systems Test (BESTest), Timed Up and Go Test (TUG), Tinetti Balance Test, and the Gait Assessment Scale [4].

With the advancement of technology and the increasing use of wearable sensors focused on physical rehabilitation programs, new perspectives have emerged for a more accurate and objective assessment of balance [5]. Inertial Measurement Units (IMUs) allow the recording of kinematic data during dynamic movements, providing insights into the complex interactions between postural control systems [6]. By integrating these sensors into various rehabilitation devices (even simple ones), specialists can gain a deeper understanding of patients' specific impairments [7].

In the past decade, the BOSU Balance platform has become one of the most widely used and widespread exercise devices globally [8], [9], being found in more fitness and rehabilitation centers around the world than any other individual piece of equipment that does not involve the use of weights. The BOSU Balance platform has a unique design both structurally and functionally. It consists of a rigid base attached to an inflated rubber hemisphere, resembling half of a stability ball.

The Motivation for Using the BOSU Balance Platform and the Triaxial System

Traditional balance testing methods often focus on static tasks or stable surfaces and do not capture subtle variations in balance changes. In contrast to the stable surfaces commonly used in rehabilitation clinics (such as rigid balance boards), the BOSU Balance platform actively engages the vestibular, proprioceptive, visual, and musculoskeletal systems [10] by introducing dynamic perturbations. This instability requires the user to perform continuous postural adjustments, involving the trunk and lower limb muscles, as well as anticipatory and reactive mechanisms [11].

Integrating a triaxial accelerometer system into the BOSU platform allows for precise measurement of movements in three dimensions, thereby enabling the retraining of complex neurophysiological mechanisms often impaired by central or peripheral nervous system injuries [12].

A triaxial accelerometer is a sensor that measures the acceleration of body movements along three axes (X, Y, and Z). In the context of balance:

- • The X-axis measures lateral (mediolateral) oscillations;
- • The Y-axis tracks anteroposterior movements;
- • The Z-axis captures vertical components and sudden changes in position.

In this context, a series of biomechanical parameters can be calculated, with this paper focusing on the oscillation amplitude.

Integrating the BOSU Ball platform with a triaxial accelerometer provides a hybrid platform that combines the physical challenge and instability required for balance retraining with the capability of digital measurement of postural performance. This combination offers multiple benefits:

- *Portability*: The system can be used in the clinic or even at the patient's home.
- *Cost- efficiency*: Compared to other similar devices currently available, both the BOSU Ball platform and the accelerometers are affordable and easy to implement.
- *Real-time feedback*: The data can be displayed and analyzed immediately, increasing the patient's motivation and the effectiveness of the therapeutic program.

The objective of the paper

This paper aims to explore the integration of a triaxial accelerometer system with a BOSU Ball platform for the objective assessment of balance in the context of neurorehabilitation. The application described in this study was designed to support both the functional diagnostic process and the monitoring of therapeutic progress, providing quantitative and real-time information about the patient's balance performance.

2. Design of the Integrated BOSU–Accelerometer System

Current status

In the current market of technologies dedicated to balance assessment and training, there is a variety of equipment and platforms used for both clinical and sports purposes. These vary in terms of complexity, cost, portability, and the accuracy of the data provided. Below are some examples:

Biodex Balance System SD and Biodex BioSway

Precision: Very high / high: Advanced measurements of force and postural movement, used in research and detailed clinical evaluations [13].

Portability: While the Biodex Balance System SD has low portability—the platform is bulky and intended for use in clinics or hospitals—the Biodex BioSway offers very good portability, allowing it to be used at the patient's home and making it easier to transport [14].

Estimated cost: Both have relatively high costs (~$18,500 / ~$13,000 for new equipment) [15].

Clinical applicability: Stroke, Parkinson's disease, multiple sclerosis, spinal cord injuries [13].

Real-time feedback: It provides visual and auditory real-time feedback for posture and balance adjustment [14].

Contraindications: Severe osteoporosis, non-united fractures, patients weighing >181 kg or <27 kg, acute conditions (pulmonary embolism, acute myocardial infarction, thrombosis), blood pressure >180/110 mmHg. [15].

Relevant observations: Ideal for clinics, hospitals, and research centers, with a high cost and requiring expertise in usage. [13].

Neurocom SMART EquiTest

Precision: Very high – an advanced platform used for balance assessment and for monitoring forces and subtle body movements [16].

Portability: low – it's a larger system that requires a dedicated space [16].

Estimated cost: very high (~$20,000–$30,000 USD for the complete equipment)[17].

Clinical applicability: vestibular disorders, stroke (CVA), spinal cord injuries [16].

Real-time feedback: It provides real-time visual and auditory feedback for dynamic balance adjustmentc [17].

Contraindications: severe cognitive impairments, cardiac instability, acute vestibular disorders [16].

Relevant observations: Premium system for balance assessment, used for diagnostic purposes and research studies. It is costly and requires specialized training [17].

BOSU Ball Platform

Precision: low – does not provide quantitative or objective measurements; response assessment is done visually and subjectively [18].

Portability: excellent – lightweight, compact, and can be transported and used anywhere (home, clinic, gym) [18].

Estimated cost: low – ~$100–150 USD, making it extremely accessible compared to medical platforms [18].

Clinical applicability: Post-stroke rehabilitation, proprioceptive training [19].

Real-time feedback: It does not provide automatic feedback. The therapist must visually assess the patient [19].

Contraindications: Recent lower limb injuries, severe vestibular disorders, severe balance impairments. [19]

Relevant observations: Useful for stabilization exercises, proprioception, and postural muscle strengthening. Requires therapeutic supervision in moderate or severe neurological cases. Does not allow standardized progress evaluation, being intended more for functional intervention than diagnosis [18].

In neurological rehabilitation, the choice of platform depends on the specific needs of the patient and the resources available. The Biodex Balance System SD and Neurocom SMART EquiTest are top-tier solutions for advanced assessments and diagnostics, making them ideal for clinics and hospitals. The BOSU Ball with a triaxial accelerometer can be an economical and portable solution for functional rehabilitation exercises and preliminary balance evaluations [19].

Application Description:

In this study, we analyzed the performance of an experimental application using a BOSU Ball platform in an inverted position – with the rigid side facing up and the unstable spherical side in contact with the ground. This configuration increases the difficulty of balance exercises and provides an additional challenge for the neuromuscular system. Two triaxial accelerometers were mounted on this platform, positioned 180 degrees apart, to cover movements in the frontal (left-right) and sagittal (front-back) planes.

System Components

- BOSU Ball Platform: An unstable hemispherical device frequently used in balance training and rehabilitation.
- Bruel&Kjaer Triaxial Accelerometers: Two sensors capable of measuring acceleration along the three spatial axes (X, Y, Z).
- Signal Analyzer: DIGITLINE DSA-550: A device for processing and transmitting data from the accelerometers to a computer

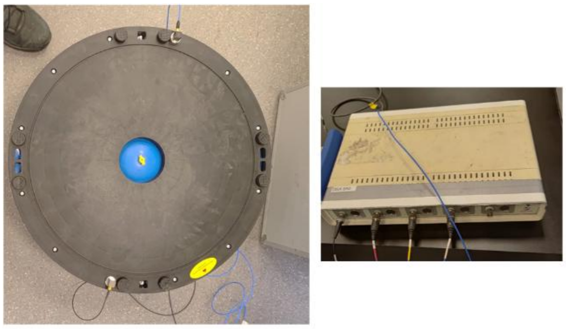

Fig. 1. BOSU Ball platform with triaxial accelerometer
(Personal archive)

Testing Protocol

The subject performs two types of movements on the BOSU platform:

- Lateral voluntary balance movements (left-right): For 30 seconds, the subject moves in a controlled manner in the frontal plane, maintaining balance on the platform.
- Anterior-Posterior movements (front-back): For 30 seconds, the subject moves in a controlled manner in the sagittal plane, maintaining balance on the platform.

The accelerometers record acceleration data along the three axes, of which, in this study, only the data recorded on the X and Y axes are analyzed.

Fig. 2. The subject's position on the platform during exercises
(Personal archive)

Data Analysis

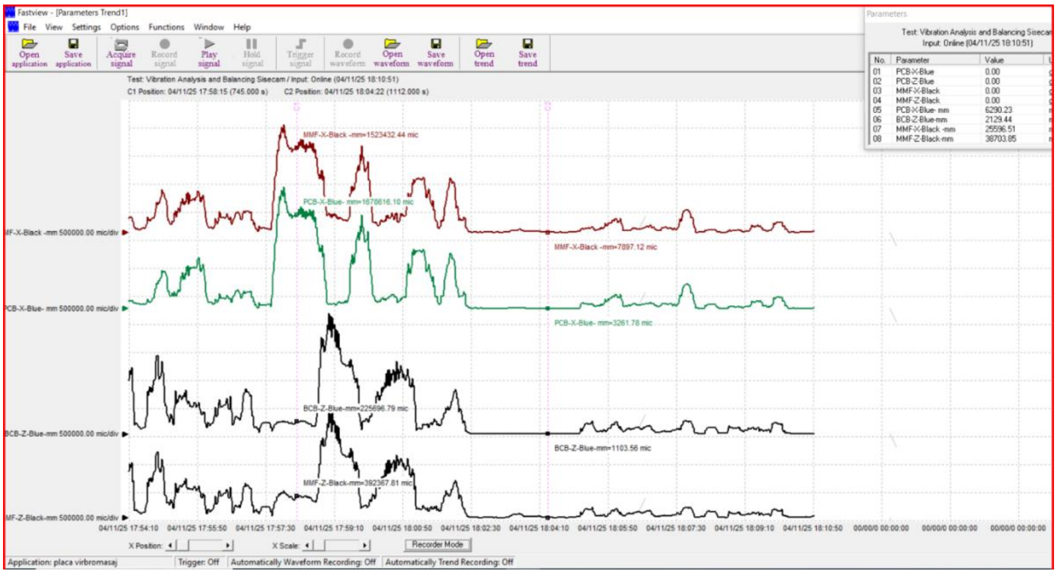

Fig. 3. Data recorded by the triaxial accelerometer during the exercise
(Personal archive)

The analysis of the collected data demonstrated a high correlation between the movements performed by the subject and the signals recorded by the sensors. The detected deviations exactly match the direction and amplitude of the movements, confirming both the high sensitivity of the accelerometers and the platform's ability to accurately transmit postural variations.

The measurements indicated greater deviations during left-right movements than during front-back movements. This observation is consistent across all test sessions and can be explained by a series of anatomical and biomechanical considerations.

Additionally, higher values are recorded during movements in the frontal plane throughout the test. This can be explained by analyzing the support base and postural biodynamics: in the orthostatic position, the human body benefits from a longer support base in the sagittal plane, due to the natural positioning of the feet. Thus, front-back movements can be compensated more efficiently, while in the frontal plane, the base is narrower, making balance maintenance more difficult and demanding for the neuromuscular system.

Stabilization in the frontal plane depends on the activation of the muscles gluteus medius, gluteus minimus, tensor fascia latae, as well as the abdominal obliques. These muscles have a different architecture compared to those involved in anteroposterior balance, which leads to a more complex and often less efficient activation in patients with neurological deficits.

Another reason for the variations in the data is that the central nervous system integrates proprioceptive information more efficiently in the sagittal plane, due to the constant involvement of these movements in daily activities (walking, running, bending). In contrast, lateral balance is not trained as frequently, which may lead to a reduced reactivity in this plane.

Thus, in the case of a loss of balance, the body develops more efficient automatic postural reflexes in the anteroposterior plane (e.g., ankle and knee extension) than in the lateral plane, where adjustments are more complex and involve a greater intersegmental coordination.

Absolute medical contraindications:

- Severe orthostatic instability: Severe orthostatic hypotension, which can lead to dizziness or syncope.
- Uncontrolled epilepsy: Motor and postural stimuli may trigger seizures, especially in sensory-demanding environments.
- Acute muscular or joint injuries: Sprains, dislocations, recent fractures of the lower limbs or spine.
- Active deep vein thrombosis (DVT): Risk of dislodging blood clots during exercise.
- Unstable heart disease: Unstable angina, decompensated heart failure, severe arrhythmias.
- Severe vestibular disorders: Significantly impairs balance and coordination.

Relative contraindications / Major precautions:

- Severe spasticity (Ashworth > 3): Can lead to uncontrolled movements or rigid postures, increasing the risk of falls.
- Severe ataxia: Loss of fine motor control can compromise safety on an unstable surface.
- Cognitive impairments affecting the understanding of instructions: Patients with dementia or severe receptive aphasia may be unable to understand or follow the therapist’s instructions.
- Severe visual disorders: Affects postural control and balance.

- Morbid obesity: May exceed the mechanical support capacity of the equipment and increase the risk of imbalance.

In neurological rehabilitation, each patient must be evaluated individually, and the use of this device should be introduced progressively and only under safe conditions, with specialized medical or therapeutic supervision.

3. Conclusions

Following the implementation and analysis of the BOSU Ball platform equipped with triaxial sensors, the following essential conclusions can be drawn, directly relevant to the field of neurological rehabilitation:

1. The accuracy and sensitivity of the data provided by the integrated sensor system

The most valuable conclusion derived from this study is that the triaxial sensor system mounted on the unstable platform provides sensitive and precise data, capable of capturing subtle variations in postural movements. This fine detection ability allows for the development of personalized rehabilitation plans that are better suited to the clinical specifics of each patient. Thus, interventions can be more accurately targeted based on functional deficits, significantly contributing to the effectiveness of the therapeutic process.

2. Accessibility and Portability

Another important conclusion is related to the practical and economic nature of this solution. The combination of a BOSU platform – already widely recognized and used in functional training – with lightweight and easy-to-install triaxial sensors leads to a balance assessment and training tool that is considerably more financially accessible compared to the sophisticated equipment available in clinical rehabilitation. The portability of the system makes it suitable not only for use in clinics but also for home use or in outpatient therapies, facilitating broader access to modern and effective rehabilitation methods.

3. Potential for further development

Additionally, the significant potential for expansion and enhancement of this application must also be emphasized. The integration of additional features – such as audio-visual feedback or the expansion of the number of sensors to analyze the entire body – could transform this system into a highly useful tool in the recovery process.

Bibliography

[1].Shumway-Cook, A. şi Woollacott, M. H. (2007), Motor Control: Translating Research into Clinical Practice, Lippincott Williams & Wilkins, Philadelphia, ISBN 9780781766913.

[2]. Fay B. Horak, Postural orientation and equilibrium: what do we need to know about neural control of balance to prevent falls?, Age and Ageing, Volume 35, Issue suppl_2, September 2006, Pages ii7–ii11, https://doi.org/10.1093/ageing/afl077

[3]. Sturnieks, D. L., St George, R., şi Lord, S. R. (2008), "Balance disorders in the elderly", Neurophysiologie Clinique, 38(6), pp. 467–478, ISSN 0987-7053.

[4]. Blum, L., şi Korner-Bitensky, N. (2008), "Usefulness of the Berg Balance Scale in stroke rehabilitation: a systematic review", Physical Therapy, 88(5), pp. 559–566, ISSN 0031-9023.

[5]. Patel, S., Park, H., Bonato, P., Chan, L., şi Rodgers, M. (2012), "A review of wearable sensors and systems with application in rehabilitation", Journal of NeuroEngineering and Rehabilitation, 9(1), pp. 21, ISSN 1743-0003.

[6]. Bonnet, V., Mazza, C., Fraisse, P., şi Azevedo Coste, C. (2014), "A review of control strategies for lower-limb exoskeletons to assist gait", Computer Methods in Biomechanics and Biomedical Engineering, 17(1), pp. 1–15, ISSN 1025-5842.

[7]. Mancini, M., şi Horak, F. B. (2010), “The relevance of clinical balance assessment tools to differentiate balance deficits”, European Journal of Physical and Rehabilitation Medicine, 46(2), pp. 239–248, ISSN 1973-9087.
[8]. Riewald, S. T. și Rodeo, S. A. (2015), *Science of Strength Training and Conditioning in Sport*, Human Kinetics, Champaign, IL, ISBN 9781492505710.
[9]. Anderson, K. G. și Behm, D. G. (2005), “The impact of instability resistance training on balance and stability”, *Sports Medicine*, 35(1), pp. 43–53, ISSN 0112-1642.
[10]. Behm, D. G., Colado, J. C., și Giles, L. (2012), “Instability resistance training: Research and practical applications”, Strength and Conditioning Journal, 34(3), pp. 33–48, ISSN 1524-1602.
[11]. Anderson, K. G., și Behm, D. G. (2004), “Maintenance of EMG activity and loss of force output with instability”, Journal of Strength and Conditioning Research, 18(3), pp. 637–640, ISSN 1064-8011.
[12]. Lee, B. C., McGrath, D., și Fraser, S. (2016), “Development of a real-time feedback system for balance training using inertial measurement units”, Sensors, 16(11), 1904, ISSN 1424-8220.
[13]. Wadsworth, C. T., et al. (2007), “Validity and reliability of the Biodex Balance System SD”, Journal of Neurologic Physical Therapy, 31(3), pp. 161–167, ISSN 1557-0576.
[14]. Clark, R. A., et al. (2010), “Validity and reliability of the Nintendo Wii Balance Board for assessment of standing balance”, Gait & Posture, 31(3), pp. 307–310, ISSN 0966-6362.
[15]. Biodex Medical Systems Inc. (2023), Product Manual: Balance System SD & BioSway, Biodex, New York, ISBN 978-0-9796181-2-5.
[16]. Nashner, L. M. (1997), “Computerized dynamic posturography”, The Handbook of Balance Function Testing, Singular Publishing Group, pp. 280–307, ISBN 978-1565936784.
[17]. NeuroCom International (2022), SMART EquiTest Clinical Manual, Natus Medical Incorporated, ISBN 978-1-60427-435-9.
[18]. Behm, D. G., et al. (2010), “Effectiveness of instability resistance training for core strength and balance”, Journal of Strength and Conditioning Research, 24(3), pp. 679–685, ISSN 1064-8011.

ACCESSIBLE SPA CONCEPT FOR WHEELCHAIR USER REHABILITATION THROUGH ASSISTIVE TECHNOLOGIES

PICA Eduard-Ștefan, MOHORA Cristina(Conducător științific)

Faculty of Industrial Engineering and Robotics, Master: Equipment for Recovery Therapies,
Year of study: 1st, e-mail: eduard_stefan.pica@stud.fiir.upb.ro

ABSTRACT: The paper presents accessibility barriers faced by wheelchair users identified by Dr. Eleni M. in SPA contexts, forming the theoretical basis for our future study in Romania. The original contribution lies in a design concept for an adapted sunbed and beach access pathway made from recycled wind turbine blades, inspired by the work of J.J. Joustra and B. Flipsen. These elements are intended for integration within SPA centers and coastal recovery areas, addressing specific mobility needs such as continuous surfaces for wheelchair use. Due to space constraints, this document outlines only part of a broader project. A detailed proposal, including the therapeutic potential of aquatic environments and a fully accessible SPA complex will be presented in extended research. The main objective is to promote barrier-free tourism and rehabilitation.

KEYWORDS: Accessibility, Motor Disability, Assistive Equipment, Inclusive Tourism

1. Introduction

Aquatic rehabilitation is a therapeutic method with significant benefits for people with disabilities, offering a comprehensive approach that combines hydrokinetotherapy and balneophysiokinetotherapy. Water, through its physical properties, creates an optimal and safe environment for recovery by reducing the impact of gravity and facilitating movement, which contributes to improved mobility and reduced pain. The aquatic environment allows the adjustment of movement intensity, making it possible to tailor exercises to individual needs. Water supports muscle toning, increases stability and balance, and improves coordination, flexibility, and range of motion. It reduces joint stress, facilitating post-traumatic or post-surgical recovery. Safe and dignified access to a swimming pool is essential to ensure that everyone can participate in aquatic activities that promote health and social inclusion. Studying this field is crucial for improving the quality of life for wheelchair users and for integrating the most effective methods and assistive equipment into the rehabilitation process. Accessibility to aquatic services for wheelchair users remains a challenge, which highlights the need to analyze existing barriers and identify optimal solutions for integrating these individuals into an effective therapeutic framework. Among its objectives, the study aims to evaluate essential assistive equipment for recovery, suggesting their efficient integration into a specialized SPA. In Romania, many of these technologies are not well known, which explains the public's reluctance to access modern aquatic therapies.

Another objective of this study is to analyze the barriers that prevent wheelchair users from participating in SPA experiences. These obstacles may include inadequate infrastructure, lack of accessible pathways, poor signage, or insufficient ergonomic facilities. Proposed solutions include the use of adapted equipment such as special sunbeds and pathways made from recycled fiberglass for beach or slippery SPA areas, accessible changing rooms and toilets, properly equipped pools, and access lifts. Disability refers to any impairment of physiological, psychological, or anatomical functions. Through proper awareness and improved accessibility to these solutions, the recovery experience of individuals can be significantly enhanced. This study focuses on motor impairments (mobility limitations) and all the specific needs of wheelchair users.

The origin of the term “SPA” is disputed; one popular explanation links it to the Latin phrase “Sanitas Per Aquam, " which translates as “Health Through Water”, while another ties it to the Belgian town of Spa, renowned since Roman times for its therapeutic springs [5]. SPA visits are ideal for disabled people. The proposed center will ensure maximum accessibility and independence in a safe and relaxing environment focused on the treatment, recovery, and maintenance of joint, muscle, and bone health. The project is designed for wheelchair users who can use their upper limbs to operate equipment or perform transfers. The facilities are intended for independent use but can be adapted for caregiver assistance if necessary. Targeted diagnostics include: paraplegia (impairment of the lower limbs while retaining arm functionality), muscular dystrophy (forms that allow upper limb use), multiple sclerosis (limited leg mobility with upper body control), stroke (partial paralysis requiring transfer support), amputations (requiring accessible and safe environments), severe arthritis and degenerative diseases (causing stiffness and pain that limit mobility), and spinal cord injuries (resulting in lower limb weakness). Before engaging in any physical activity, individuals must undergo a thorough medical evaluation. Their physical condition and type of disability must be assessed to determine the most suitable rehabilitation approaches and any necessary precautions to prevent injuries. The rehabilitation program should be progressive, allowing beneficiaries to gradually build their skills without overexertion. [7].

2. State of art

Dr. Eleni M. inspired me through her study [2], which highlights previously overlooked barriers faced by wheelchair users in the SPA industry. Existing research on accessibility in this setting is extremely limited, which motivated me to apply her methods to a Romanian audience (motor disabilities). The study demonstrates the SPA sector’s potential to enhance the physical, mental, and social well-being of wheelchair users, promoting barrier-free tourism. This type of research is increasingly relevant, especially with aging populations and rising life expectancy. Her research involved nine individuals with varying mobility levels (from limited walking to full wheelchair dependence) due to neurological conditions or aging. Participants were selected based on their experience with SPA facilities. The questions addressed their full journey: searching for accessible locations, staff interaction, arrival. Those without SPA experience explained their reasons, while others provided detailed accounts. The analysis helped identify the obstacles they encountered. Perceptions of these barriers vary by country, culture, values, and personal factors such as wheelchair, mobility level, and expectations from the experience. Although the demand for accessible tourism services is growing, many destinations and facilities are still not equipped to meet the specific needs of this consumer segment. Since the desire to travel is universal, wheelchair users face additional obstacles during their journeys, which can limit activity choices and diminish their sense of freedom and relaxation. Negative travel experiences can create psychological barriers, leading individuals to avoid travel altogether due to the stress and challenges involved. The United Nations Convention on the rights of people with disabilities emphasizes the importance of “accessible tourism”, the idea that people with disabilities should be able to use tourism facilities independently, without relying on external assistance or being perceived as recipients of charity. This applies not only to individuals with permanent mobility impairments but also to those with temporary disabilities or other specific needs. One essential aspect of tourism is enjoying the experience. If accessibility is not ensured and travelers face constant barriers, the purpose of recreation and relaxation is undermined.

Informational barriers limit the participation of wheelchair users in sectors such as transportation, healthcare (including SPA services), tourism, and leisure. The lack of clear information regarding accessibility and safety (whether on websites or due to inaccurate responses from staff) makes it difficult to make informed decisions and plan activities effectively. In the transportation sector, airline companies (crucial for long-distance travel) often fail to provide clear information about services available to people with disabilities. Details about necessary procedures or available support are hard to find both on their websites and via customer service lines. In cases of delays or schedule changes, the lack of accurate and timely updates only worsens the situation, adding unnecessary stress. In the healthcare sector, information about accessibility in dental clinics or SPA centers is often incomplete or misleading, complicating the process of selecting an appropriate facility and sometimes leading to unpleasant surprises upon arrival. The hospitality industry faces similar issues. Hotels often advertise as being accessible, yet adapted entrances are poorly marked, accessible toilets are hard to find, and signage for elevators, special entrances, or other accessible features is inadequate. Moreover, staff are not always fully aware of the facility's actual level of accessibility. Many users reported having to make many phone calls for clarification, only to receive vague answers, causing them to cancel their visit.

Environmental (physical) barriers are among the most restrictive for wheelchair users, as they limit access to various spaces and prevent full participation in activities. These obstacles include both architectural and design-related features [3], as well as natural elements. Common issues involve stairs and the lack of essential amenities such as accessible changing rooms. In hotel rooms, beds and showers are often placed at impractical heights for wheelchair users, and cramped furniture makes maneuvering difficult. Outdoors, uneven gravel paths, tall grass, or exposed roots can severely hinder mobility [6]. In some cases, the only solution is to leave the wheelchair, an experience that can be painful, humiliating, or even impossible. The tourism, leisure, and recreation industries are significantly affected by these challenges: poorly placed furniture, heavy or narrow doors, thick rugs, a lack of ramps or overly steep ones, uneven pathways, and insufficient accessible parking spots. Toilets are frequently inaccessible, forcing wheelchair users to enter through back doors or service entrances. The absence of elevators and limited turning space further exacerbate difficulties, turning basic activities into exhausting efforts and contributing to social exclusion.

Social Barriers – negative attitudes, lack of empathy, and inadequate interactions are frequently encountered in sectors such as transportation, healthcare, hospitality, and leisure. In the aviation industry, airline staff are often untrained in assisting passengers with reduced mobility, resulting in discomfort, accidents, and humiliating experiences. Poor communication worsens the issue, as crew members tend to address accompanying people instead of the passenger directly, or use an inappropriate tone, as if speaking to someone with a cognitive disability. What should be an accessible experience becomes instead a stressful one, underlining the need for better staff training. In healthcare, lack of training in patient transfer techniques can lead to injuries, discomfort, or even refusal of treatment. In dental offices, wheelchair users often face reluctance, unjustified delays, and are treated as lower priority. Reception staff frequently prioritize non-disabled patients, while professionals may lack both the preparation and willingness to provide adequate support. In the hospitality sector, staff are often not properly trained, some employees are either overly protective or unsure how to assist appropriately, leading to awkward interactions. In some cases, guests are perceived as a burden, and staff body language reveals discomfort or irritation. Several study participants reported feeling unwelcome at the outset when they initially requested accessibility information from various SPA centers.

Intrinsic barriers, directly related to an individual's physical, psychological/cognitive condition, as opposed to external barriers such as chronic pain, can make participation impossible. Total dependence on caregivers becomes a critical issue for individuals with progressive neurological diseases or severe spinal cord injuries. Without adequate support, autonomy is unattainable. Many wheelchair users feel restricted by their own health conditions, which affect not only their physical ability but also their willingness to visit a SPA. Study participants highlighted specific difficulties: individuals with advanced multiple sclerosis expressed concern about needing specialized assistance; an elderly participant, unable to walk or stand without support, found the environment inaccessible; and another, dealing with fluctuating conditions, feared that staff would not understand their specific needs. Each of these barriers is challenging on its own, but their combined impact can be significantly more limiting and restrictive.

3. Theoretical foundation

I analyzed another case study [1] that focused on the development of functional prototypes from wind turbine blades, using a research-through-design approach. The authors' chosen prototype (a picnic table) enabled material assessment and the identification of key limitations. The blades were cut into structural beams, and waterjet cutting provided precision, but also exposed the material to UV and moisture, an issue relevant to my own project (a sun lounger and access walkway), which will require protective treatments to ensure durability in outdoor environments. In the study mentioned, public acceptance of the reused materials was tested by exhibiting the prototype at a design event with over 25,000 visitors. The feedback was positive: once the origin of the materials was explained, the blade's form was perceived as valuable, and visitors even suggested new applications. This feedback confirms that reuse carries emotional, aesthetic, and commercial impact. The concept I propose, which I will further detail below, also aims to create an emotional connection between user and product (reuse must be anticipated from the design stage). Projects based on wind turbine blades can be standardized by developing reusable beams. The picnic table was one example, but the range of applications is wide. My project follows this direction, minimizing processing, while preserving functionality, and aesthetic value.

Composite materials, especially those reinforced with fiberglass, are widely used in industries where the stiffness-to-weight ratio is critical, making them ideal for applications that require structural efficiency, design flexibility, and durability. These properties are essential to my project, which proposes the reuse of decommissioned wind turbine blades (Fig. 1) to develop an adaptive sun lounger, and an access walkway designed for people with reduced mobility. The sun lounger (Fig. 2), intended for use on the beach or in SPA centers, will be equipped with an automated lift/lower system and adjustable forward/backward tilt (Fig. 3), based on a hydraulic mechanism, remote control, adjustable side bars, and a transfer board for independent access. Constructed from fiberglass, a highly durable material resistant to corrosion, weather, saltwater, sand, and extreme temperatures, the lounger is ideal for outdoor use (beach/SPA center).

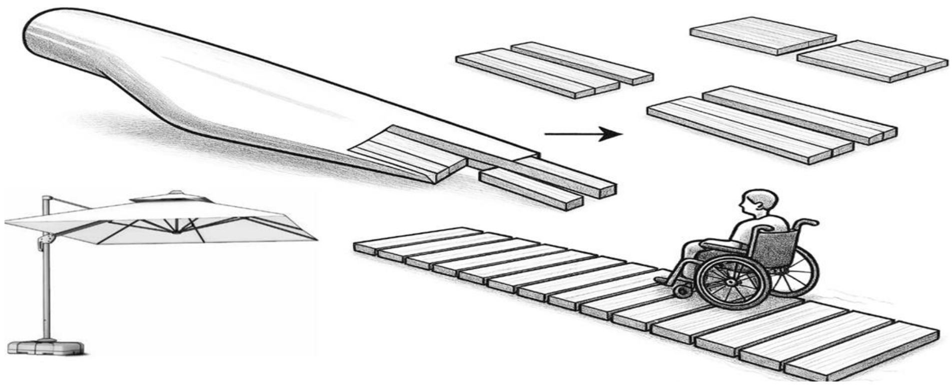

Fig. 1. Concept for reusing decommissioned wind turbine blade to create an access pathway

The access walkway, also made from recycled wind turbine blade material, will be non-slip and stable, with no large gaps between beams, ensuring smooth access for wheelchair users and uninterrupted continuity from the parking lot, across the sand, and to the relaxation area (Fig. 1).

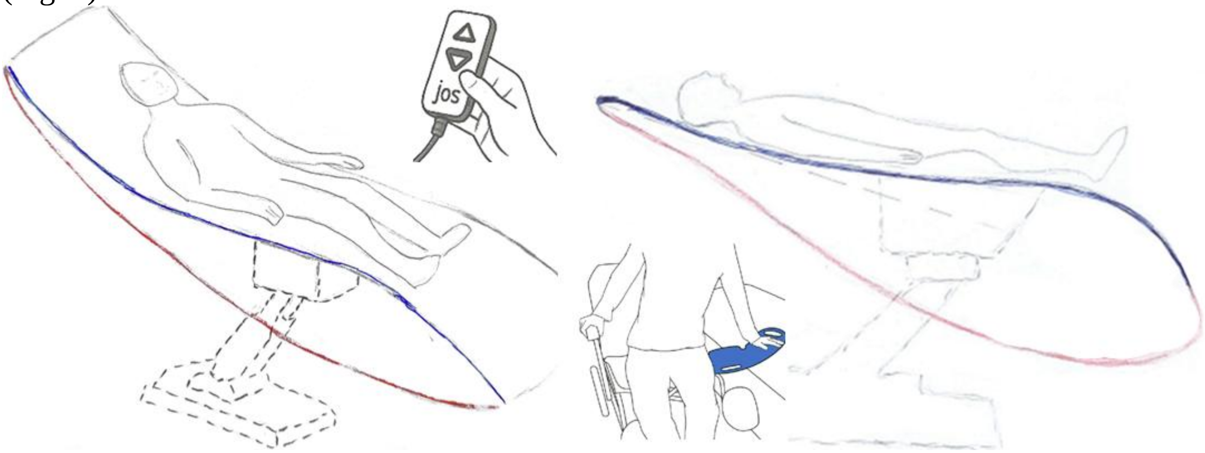

Fig. 2. Lounger/Sunbed concept made from recycled wind turbine blade

Although composites perform well in use, they pose major challenges at the end of their life cycle. Composites are difficult to recycle through standard methods, often being shredded or incinerated, which is unsustainable. Our project promotes circular economy principles through structural reuse, keeping components close to their original form and preserving material value. In this way, the proposed lounge chair becomes a sustainable intervention.

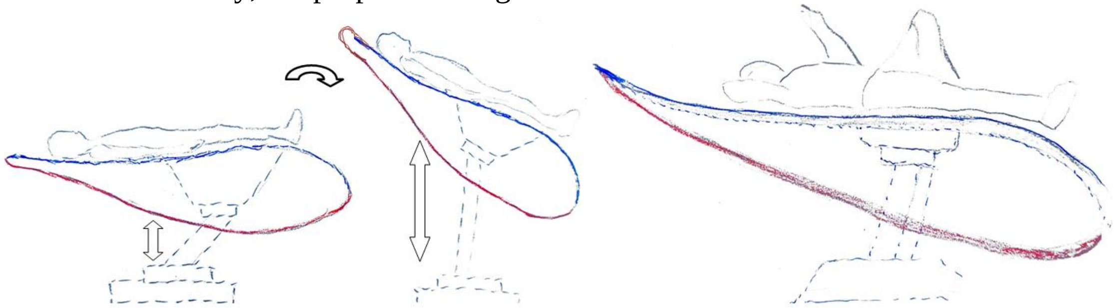

Fig. 3. Lounger with adjustable height and backrest tilt

Wind energy uses large amounts of composites (~150k t in Europe, 2017), with over 2 Mt of blades expected to be decommissioned annually by 2050. Properly treated, worn components can be structurally reused to resist fiber exposure and UV damage. The platform, side rails, and walkway beams will be built from recovered blade segments, adapted to meet the needs of individuals with mobility impairments. The blade's natural curvature, like physiological curves (Fig. 4), offers ergonomic spinal support and reduces pressure.

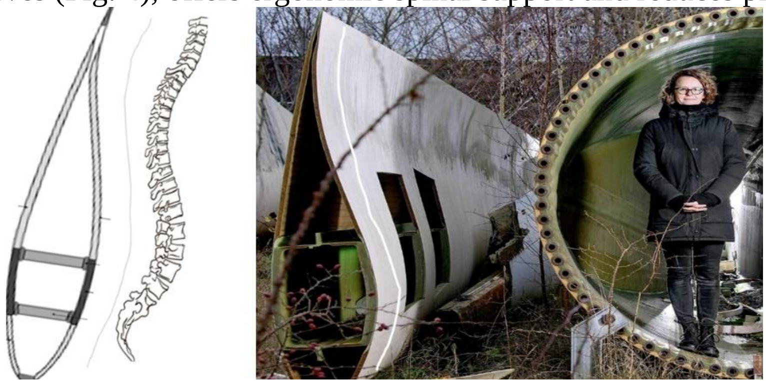

Fig. 4 – Blade shape that reminds of the physiological curvatures of the human spine

Medical studies [4] show that the weight of wheelchair users ranges between 70-100 kg, depending on factors such as age, sex, medical condition, degree of mobility, diet, and lifestyle. An active adult male typically weighs 80–90 kg, an active adult female between 65–75 kg, while passive users may weigh 90–120 kg. In special cases (obesity), body weight can reach 120–160 kg.

$$F = 260\ kg \times 9{,}81\ m/s^2 = 1\ 962\ N;\ \text{safety factor of } 1{,}25 \rightarrow F_{total} = 2\ 452\ N \qquad (1)$$

For safety reasons, a reference value of 160 kg is used as the maximum user weight. Adding the weight of the equipment (~100 kg), the total mass reaches 260 kg.

Conclusions

This study highlights the adaptability of wind turbine blades as a reusable material in inclusive product design, demonstrating that, despite the lack of access to original technical data (often confidential), the observable form (Fig. 4) and structural quality enable effective reuse. The proposed project leverages these qualities while adding a social dimension by increasing accessibility for wheelchair users. Thus, it offers a sustainable and inclusive alternative to conventional SPA experiences, which often remain inaccessible due to various barriers. In the context of an aging population and increasing accessibility needs, adopting inclusive practices will be essential. The project is theoretically grounded in the works of Joustra, Flipsen, Balkenende, and Eleni M., and it shows that materials considered waste can support the development of products with minimal environmental impact. My personal contribution includes creating most of the drawings (except for the umbrella in Fig. 1, the transfer board user in Fig. 2, and Fig. 4), as well as formulating the observation that the physiological curves of the human spine resemble the shape of a wind turbine blade. Based on this insight, I composed the image in Fig. 4, visually juxtaposing a spine, a sectioned blade, and a photograph of a person next to a decommissioned blade, to emphasize the concept of recycling. Future research directions include integrating adjustable handles and umbrellas, applying Eleni M.'s study to a Romanian sample (via an extended questionnaire), and exploring additional ways to recycle wind turbine blades, this topic representing just one possible example. Cutting fiberglass produces fine, irritating dust, so strict safety measures are required. Segmentation allows for varied shapes (curves, flat zones) useful for ergonomic purposes; finishing the edges prevents cuts, and the blade's weight requires stabilization to prevent overturning. Power supply will be provided via connection to an electrical source.

Bibliography

[1]. J.J.Joustra, Bas Flipsen, Ruud Balkenende (2021), „Structural reuse of high end composite products: A design case study on wind turbine blades” – ResearchGate.
[2]. Eleni Michopoulou (2021), „Accessibility to Spa Experiences” – ResearchGate.
[3]. Normative regarding the adaptation of civil buildings and urban space to the individual needs of people with disabilities, indicative NP 051-2012 - NP 051/2000.
[4]. Cooper, R.A., Boninger, M.L., & Rentschler, A.J. (2009). Engineering Better Mobility: Wheelchair Design and Access Technology. CRC Press.
[5]. A van Tubergen, S van der Linden (2002), ,, A brief history of spa therapy”.
[6]. Alina Petruta (2016), ,,Saturn versus Mangalia, for people with disabilities” – author's personal blog (https://alinapetruta.wordpress.com/).
[7]. Maya A. Jones (2021) ,,Paralympian Alana Nichols on turning doubt into motivation and inspiring others” – ESPN.
[8]. Scientific Coordinator Ing.Cristina MOHORA – Internal Course Summary (2025)